

**The Chemoselective, Enantiospecific Cross-Coupling of Secondary  
Boronic Esters and the Stability of Mesoporous Silica Supports for Pd  
Catalysis**

by

Ben William Glasspoole

A thesis submitted to the Department of Chemistry

In conformity with the requirements for  
the degree of Doctor of Philosophy

Queen's University

Kingston, Ontario, Canada

September 2011

Copyright © Ben William Glasspoole, 2011

## Abstract

The Suzuki-Miyaura Cross-Coupling of aryl halides and aryl boronic esters has become one of the most important and oft used C-C bond forming reactions in industry and academia alike. Recently, substantial effort has been invested in expanding this reaction to include alkyl boronic esters as coupling partners, though until recently, success has been limited to primary alkyl boronic esters. Secondary alkyl boronic esters, with the inherent possibility of being chiral, have proven to be more difficult to couple. As a means of expanding our program on the *enantio*- and *regio*selective hydroboration of styrene derivatives, we sought to develop conditions that could couple benzylic (secondary) boronic esters. Not only was the coupling to aryl iodides achieved in moderate to good yield with a commercially available (and relatively cheap) catalyst system and phosphine, but the coupling reaction proceeds with almost complete retention of the stereochemistry installed during the hydroboration reaction. Interestingly, these conditions leave primary (linear) alkyl boronic esters completely untouched. Further examination of the chemoselectivity of the reaction revealed that, despite being unable to cross-couple strictly aliphatic secondary boronic esters, our silver-mediated protocol was able to effectively cross-couple chiral *allylic* boronic esters in high yield and good regioselectivity.

The asymmetric syntheses of novel secondary boronic esters have also been developed to overcome the substrate limitations of the hydroboration reaction. Together with our effective cross coupling strategy, these novel chiral boronic esters have led to

the synthesis of exciting new classes of molecules, most notably, the asymmetric triarylmethanes.

Finally, the stability of mesoporous silica supports used in Pd catalysis was assessed. Though silica supports effectively reduce Pd-contamination in reaction mixtures to sub-ppm levels, their long-term reusability is hindered by material degradation caused by harsh reaction conditions. It was found that aqueous base, required for the Suzuki-Miyaura reaction, is responsible for silica degradation and the collapse of mesostructure. Interestingly, it was determined that the reaction itself had a protective effect on the material, with the boric acid side-product mitigating the deleterious effect of the base.

## Acknowledgements

The five years I've spent in Kingston have been both formative and very enjoyable. I now find myself in the fortunate position of being able to acknowledge not just those who have made my time at Queen's such a positive experience, but the people who have supported me along the way as well.

I would be remiss not to start by thanking Prof. Cathleen Crudden. Cathy, your influence on me as a chemist is obvious, but I am especially grateful for the opportunities you have provided to me while working in your lab. I feel fortunate to have been given the chance to present my work to so many visiting professors, attend good conferences (specifically those within walking distance to the beach) and to work abroad, all with your encouragement.

Working in the Crudden group has also afforded me the opportunity to work along side some very talented people. The old guard of Dave Edwards, Yonek Hleba and Kevin McEleney were helpful in getting me started and setting the tone of what was expected of a Crudden group member. I am also the last surviving member of the best bay in Chernoff, which somehow remained intact from my arrival in 2006 until Steve Dickson's departure in 2011. Jenny, Jon and Steve (and honorary member Jer): I hope you enjoyed our years together as much as I did. I am also indebted to Daisuke Imao, who not only did most of the grunt work to get the coupling project off the ground, but was always up for a late night chat in lab. Daisuke: I will remember you by the "secret reaction" I found in your lab book to help a floundering undergrad student.

I also owe a debt of gratitude to Prof. Varinder Aggarwal at the University of Bristol for agreeing to take me on as a visiting researcher. My time in England was amazing on all counts. I must also thank Dr. and Mrs. Harry McAdie, CMC, OGS and NSERC for making this venture financially viable.

Outside of lab, I have shared good times with a whole host of colourful characters: Jason Hanthorn, Jeremy Praetorius, Steve Dickson, Ben Partridge, and more recently, the inseparable tandem of Fraser & Fowler, to name a few. It's been fun! And, of course, my constant companion and best friend Viv! My time in Kingston would not have been the same had you not agreed to come to Chem Banquet in 2007. Special thanks to Steve, Barbara, Lynsey and Heather Yates for welcoming me into their family and for keeping me well-fed on Sundays.

Lastly, and most importantly, thanks to my family: Mom, Dad, Kellen and Gram. This thesis is a culmination of an education that started by being raised on PBS. It is for Erin, who would have done something important, and done it well.

## **Statement of Originality**

I hereby certify that all of the work described within this thesis is the original work of the author. Any published (or unpublished) ideas and/or techniques from the work of others are fully acknowledged in accordance with the standard referencing practices.

Ben William Glasspoole

September 2011

## Table of Contents

Abstract.....	ii
Acknowledgements.....	iv
Statement of Originality.....	vi
Table of Contents.....	vii
List of Figures.....	xiii
List of Tables.....	xv
List of Schemes.....	xvi
List of Abbreviations.....	xxiii
Chapter 1 General Introduction: The Suzuki-Miyaura Reaction.....	1
1.1 Introduction.....	1
1.2 Transition-Metal Catalysis of Organometallic Reagents.....	2
1.2.1 Grignard reagents make way for Organozinc Reagents.....	2
1.2.2 The Emergence of Boron.....	5
1.3 Basic Mechanism of the Suzuki-Miyaura Reaction.....	6
1.3.1 General Catalytic Cycle.....	6
1.3.2 Generation of an Active Pd catalyst.....	7
1.3.3 Oxidative Addition.....	9
1.3.4 Transmetalation and the Role of Base.....	11
1.3.5 Reductive Elimination to Generate Cross-Coupling Product.....	13
1.4 Suzuki-Miyaura Reactions of sp <sup>3</sup> -hybridized Organoboron Coupling Partners.....	15
1.4.1 Cross-Coupling of Primary Boronic Acid Derivatives.....	15
1.4.2 Cross-Coupling of Secondary Boronic Acids.....	20
1.4.3 Cross-Coupling of Secondary Trifluoroboronate salts.....	22
1.4.4 Cross-Coupling of Secondary Boronic Esters.....	25
1.5 Suzuki-Miyaura Coupling of Primary sp <sup>3</sup> -hybridized Electrophiles.....	26
1.5.1 Primary Alkyl Electrophiles.....	26
1.5.2 Suzuki-Miyaura Coupling of Secondary sp <sup>3</sup> -hybridized Electrophiles.....	29
1.6 General Summary and Outlook.....	31

1.7 References .....	32
Chapter 2 The Cross-Coupling of Secondary Boronic Esters with Retention of Stereochemistry.....	42
2.1 Introduction .....	42
2.1.1 Hydroboration of Styrene Derivatives.....	42
2.1.2 Elaboration of Hydroboration Products .....	46
2.2 Cross-Coupling of Hydroborated Styrene Derivatives with Aryl Halides.....	49
2.2.1 Initial Reaction Development: From Zero to Sixty .....	49
2.2.2 Ligand Effects on the Reaction .....	51
2.2.3 Effect and Role of Silver Salts on the Reaction .....	54
2.2.4 Attempted Cross-Coupling with a Potassium Trifluoroborate Analogue .....	58
2.2.5 Effect of Solvent and Adventitious Water on the Reaction .....	60
2.2.6 Reaction Profile .....	61
2.3 Scope of the Stereoretentive Cross-Coupling of Secondary Boronic Esters .....	63
2.3.1 Stereoretentive Cross-Coupling of a Secondary Boronic Ester .....	63
2.3.2 Scope of the reaction and Effect of Exogenous Base.....	64
2.3.3 Aryl Bromides as Competent Coupling Partners .....	66
2.4 The Remarkable Chemoselectivity of the Reaction.....	68
2.4.1 Suzuki-Miyaura vs. Mizoroki-Heck Protocols.....	68
2.4.2 Branched vs. Linear Cross-Coupling .....	70
2.5 Towards a Mechanistic Understanding of the Reaction.....	72
2.5.1 The Nature of the Secondary Boronic Ester .....	72
2.5.2 <sup>31</sup> P NMR Studies of the Reaction .....	74
2.5.3 The Unexpected Effect of [PPh <sub>3</sub> ] on Stereoretention.....	81
2.5.4 Role of Ligand Excess and Proposed Mechanistic Cycle.....	84
2.6 Conclusions .....	91
2.7 References .....	92
Chapter 3 Lithiation-Borylation to Synthesize Novel Asymmetric Boronic Ester Cross-Coupling Partners.....	97
3.1 Introduction .....	97



3.1.1	<i>Known Methods: Asymmetric Syntheses of Organoborons</i> .....	98
3.1.2	<i>Matteson Chemistry</i> .....	99
3.1.3	<i>Lithiated Carbamates</i> .....	102
3.1.4	<i>Lithiated Carbamates Used in Boronic Ester Homologation</i> .....	104
3.2	The Synthesis and Cross-Coupling of Secondary Allylic Boronic Esters .....	106
3.2.1	<i>Precedence for Allylic Cross-Coupling: Allyl Silanes</i> .....	106
3.2.2	<i>Precedence for Allylic Cross-Coupling: Allyl Boronic Acids and Trifluoroboronates</i> .....	110
3.2.3	<i>The Synthesis and Cross-Coupling of Secondary Allylic Boronic Esters</i> .....	112
3.2.4	<i>Synthesis and Cross-Coupling of Non-Racemic Secondary Allylic Boronic Esters</i> .....	119
3.3	Triarylmethanes.....	121
3.3.1	<i>Triarylmethanes: From Unsymmetrical to Enantiomerically Enriched</i> .....	122
3.4	Asymmetric Triarylmethanes from Dibenzyl Boronic Esters.....	126
3.4.1	<i>Retrosynthetic Analysis</i> .....	126
3.4.2	<i>Racemic Synthesis of Symmetrical and Unsymmetrical Triarylmethanes</i> .....	127
3.4.3	<i>Synthesis of Non-Racemic Dibenzyl Boronic Esters by Matteson Chemistry</i> .....	129
3.4.4	<i>Synthesis of Asymmetric Dibenzyl Boronic Esters via Lithiated Carbamates</i> .....	133
3.4.5	<i>Higher Yielding Syntheses of Non-Racemic Dibenzyl Boronic Esters</i> .....	141
3.5	Lithiation-Borylation for the Synthesis of Asymmetric Allyl Silanes .....	146
3.6	Conclusions .....	149
3.7	References .....	150
Chapter 4	Introduction to Mesoporous Silica Materials.....	156
4.1	Introduction .....	156
4.2	Material Synthesis .....	159
4.2.1	<i>Micelle Formation</i> .....	159
4.2.2	<i>Bulk Morphology of Materials</i> .....	167
4.3	Hydrothermal Stability of Mesoporous Silica.....	169

4.3.1 <i>Improved Material Stability</i> .....	169
4.4 Applications of Functionalized Mesoporous Silica .....	172
4.5 The Beginnings of Our Involvement.....	174
4.6 References .....	175
Chapter 5 Material Stability and the Protective Effect of the Suzuki-Miyaura Reaction	181
5.1 Introduction .....	181
5.1.1 <i>Supported Metal as Catalyst</i> .....	181
5.1.2 <i>Heterogeneity of Pd-loaded SBA-15</i> .....	182
5.2 Effect of Suzuki-Miyaura Reaction on Material Support .....	183
5.2.1 <i>A New Paradigm for Material Stability</i> .....	183
5.2.2 <i>Effect of Aqueous Base on Material Structure</i> .....	185
5.2.3 <i>An Unforeseen Protective Effect of the Reaction</i> .....	189
5.2.4 <i>Elucidation of the Mechanism of Boric Acid Protection</i> .....	192
5.3 Alumina-Doped Mesoporous Silicas .....	194
5.3.1 <i>Stabilizing Effect of Alumina</i> .....	194
5.3.2 <i>Stability of Alumina-Doped Silica to Reaction Conditions</i> .....	196
5.4 Pd Catalysis on Mesoporous Supports .....	198
5.4.1 <i>MCM-41 Pd Catalysts</i> .....	199
5.4.2 <i>SBA-15 Pd Catalysts</i> .....	201
5.4.3 <i>Al-SBA-15 Pd Catalysts</i> .....	202
5.4.4 <i>Pd Leaching with Al-SBA-15 Catalysts</i> .....	206
5.5 Conclusions .....	206
5.6 References .....	207
Chapter 6 Experimental Procedures.....	211
6.1 Cross-Coupling of Benzylic Boronic Esters .....	211
6.1.1 <i>General Experimental Considerations</i> .....	211
6.1.2 <i>Synthesis of benzylic boronic ester cross-coupling partners</i> .....	212
6.1.3 <i>Synthesis of Enantioenriched 1,1-diarylethanes with Aryl Iodides</i> .....	215
6.1.4 <i>Synthesis of Enantioenriched 1,1-diarylethanes with Aryl Bromides</i> .....	221
6.1.5 <i>The Remarkable Chemoselectivity of the Reaction</i> .....	224

6.1.6 Scope of Reactive Boronic Esters under Silver-Mediated Protocol.....	229
6.1.7 <sup>31</sup> P NMR Studies of the Reaction .....	238
6.1.8 The Unexpected Effect of [PPh <sub>3</sub> ] on Stereoretention.....	241
6.1.9 Towards a Mechanistic Understanding of the Reaction .....	245
6.2 Lithiation-Borylation to Synthesize Novel Asymmetric Boronic Ester Cross-Coupling Partners.....	247
6.2.1 Synthesis of Racemic Secondary Allylic Boronic Esters .....	247
6.2.2 Cross-Coupling of Racemic Secondary Allylic Boronic Esters.....	253
6.2.3 Attempted Ligand-based Regioselectivity Switch for Allyl Coupling.....	260
6.2.4 Synthesis of Non-Racemic Secondary Allylic Boronic Esters .....	261
6.2.5 Cross-Coupling of Non-Racemic Secondary Allylic Boronic Esters.....	263
6.2.6 Synthesis of Symmetrical Triarylmethanes by Suzuki-Miyaura Cross-Coupling .....	267
6.2.7 Synthesis of Unsymmetrical Triarylmethanes by Suzuki-Miyaura Cross-Coupling .....	270
6.2.8 Synthesis of Enantiomerically Enriched Dibenzyl boronic esters by Matteson Homologation .....	273
6.2.9 Synthesis of Asymmetric Dibenzyl boronic esters by Lithiation-Borylation ..	280
6.2.10 Transesterification of (2,2-dimethyl-1,3-propanediol) boronic esters to their pinacolate analogues.....	302
6.2.11 Synthesis of Unsymmetrical Triarylmethanes .....	306
6.2.12 The Synthesis of Non-Racemic $\alpha$ -Silyl Boronic Esters as Intermediates for Chiral Allyl Silanes.....	310
6.3 Material Stability and the Protective Effect of the Suzuki-Miyaura Reaction.....	311
6.3.1 Material Synthesis .....	311
6.3.2 Pseudo Studies on Mesoporous Supports.....	315
6.3.3 Effect of base on Mesoporous Silica Stability .....	317
6.3.4 Protective Effect of the Suzuki-Miyaura Reaction on Material Stability .....	318
6.3.5 Effect of B(OH) <sub>3</sub> on the pH of the Reaction Solution .....	319
6.3.6 Thiol-functionalization of Mesoporous Silica and Pd Loading .....	321

6.3.7 <i>Catalysis with Pd-Loaded Thiol-Functionalized Mesoporous Silica</i> .....	322
6.4 References .....	324
Chapter 7 Conclusions and Perspectives .....	325

## List of Figures

Figure 2-1: Proposed method of activation of benzylic boronic esters by Ag <sub>2</sub> O. ....	56
Figure 2-2: Time course for the silver-mediated cross-coupling of a secondary boronic ester and an aryl iodide. Standard reaction conditions (as in Table 2-4) were used. ....	62
Figure 2-3: <sup>31</sup> P NMR of a crude cross-coupling reaction mixture using PCy <sub>3</sub> . The main peak at 46.6 ppm has been assigned to OPCy <sub>3</sub> . ....	75
Figure 2-4: <sup>31</sup> P NMR after 16 h of cross-coupling with PPh <sub>3</sub> . ....	76
Figure 2-5: <sup>31</sup> P NMR for cross-coupling reaction run under standard conditions, stopped after 8 h at 70 °C. ....	77
Figure 2-6: <sup>31</sup> P NMR of Pd <sub>2</sub> dba <sub>3</sub> and 8 equivalents of PPh <sub>3</sub> (with respect to Pd), heated to 80 °C in THF for 8 h. ....	78
Figure 2-7: <sup>31</sup> P NMR of Pd <sub>2</sub> dba <sub>3</sub> , 8 equivalents of PPh <sub>3</sub> (with respect to Pd) and 4-iodoacetophenone after heating at 80 °C for 8 h in THF. ....	79
Figure 2-8: <sup>31</sup> P NMR of Pd <sub>2</sub> dba <sub>3</sub> , PPh <sub>3</sub> , aryl iodide and Ag <sub>2</sub> O after 8 h heating at 70 °C. ....	80
Figure 2-9: Effect of PPh <sub>3</sub> :Pd ratio on reaction yield (blue) and stereoretention (red) in anhydrous DME. ....	82
Figure 2-10: Dramatic effect of H <sub>2</sub> O on reaction yield (red) and stereoretention (blue). ....	83
Figure 2-11: Effect of PPh <sub>3</sub> loading on yield (red) and stereoretention (blue) in the range of 6500-8500 ppm of H <sub>2</sub> O. ....	84
Figure 4-1: Two early hypotheses of cationic surfactant self assembly. The routes initially proposed by Beck (Route A) and the 'folded sheet' mechanism proposed by Stucky (Route B) building off of Kuroda's work with kanemite. ....	161
Figure 4-2: Stucky's Cooperative Micelle Formation Mechanism. Surfactant molecules congregate about silica polyanions (A), eventually forming the geometry favored by the Packing Parameter, <i>g</i> (B). Image adapted from ref. 17. ....	164
Figure 4-4: Reconstructed TEM image of single-crystalline mesoporous resulting from polyimide rubbing treatment of silica glass wafer. The rubbing direction is indicated by the inset arrow. Image taken from ref 23. ....	168

Figure 5-1: Isotherms of pristine SBA-15 (A), SBA-15 after 8 h of Suzuki-Miyaura recycles (B) and SBA-15 after 8 h of <i>pseudo</i> -reaction conditions (C). .....	186
Figure 5-2: Effect of base on the structure of an ordered mesoporous silica. (a) SBA-15- NaCl (b) SBA-15-NaCl heated in 20:1 DMF: H <sub>2</sub> O, 8 h (c) SBA-15-NaCl heated with base. Note that plots (b) and (c) are offset vertically to facilitate viewing. ....	188
Figure 5-3: Effect of Reaction side-products on mesoporous silica. (a) SBA-15-NaCl. Under <i>pseudo</i> -reaction conditions with (b) B(OH) <sub>3</sub> (c) KBr and (d) No additive.....	191
Figure 5-4: X-Ray Diffraction (XRD) to determine long range order. SBA-15-NaCl (a) and after <i>pseudo</i> -conditions in the presence of (b) B(OH) <sub>3</sub> and (c) KBr.....	191
Figure 5-5: N <sub>2</sub> isotherms of SBA-15-NaCl subjected to <i>pseudo</i> -reaction conditions and increasing amounts of B(OH) <sub>3</sub> .....	195
Figure 5-6: Al-SBA-15 (top) subjected to <i>pseudo</i> -reaction conditions for 4 h (middle) and 8 h (bottom).....	198
Figure 5-7: Yields (left) and corresponding N <sub>2</sub> isotherms (right) of pristine catalyst (a), and after one (b) and three (c) uses. ....	200
Figure 5-8: Yield and corresponding N <sub>2</sub> isotherms for (a) SBA-15-SH Pd and three consecutive uses (b-d) in the Suzuki-Miyaura reaction. ....	202
Figure 5-9: Yield (left) and N <sub>2</sub> isotherms (right) for pristine Al-SBA-15-SH Pd catalyst (a) and four consecutive uses (b-e). ....	203
Figure 5-10: XRD pattern of pristine Al-SBA-15-SH-Pd and (b) after 3 uses totalling 15 h reaction time.....	203
Figure 5-11: TEM images of pristine Al-SBA-15-SH Pd catalyst prior to use. ....	205
Figure 5-12: TEM images of Al-SBA-15-SH Pd catalyst after four recycles totaling 20 h of use. Note the maintained ordered mesoporsity and the Pd nanoparticles. ....	205

## List of Tables

Table 2-1: Development of Successful Cross Coupling Conditions. ....	51
Table 2-2: Ligand screen for the cross coupling of an aryl iodide with a benzylic boronic esters. ....	52
Table 2-3: Development of Successful Cross Coupling Conditions. ....	54
Table 2-4: Effect of stoichiometry and the nature of the boronic acid derivative for a standard coupling. ....	58
Table 2-5: Effect of solvent, temperature and additives on the standard reaction (as in Table 2-4). ....	60
Table 2-6: The scope of the stereoretentive cross-coupling of asymmetric secondary boronic esters and aryl iodides. ....	65
Table 2-7: Substrate scope for aryl bromides. Yields reported are based on NMR with internal standard, isolated yield in parentheses. ....	66
Table 2-8: Effect of various ligands on the cross-coupling of 4-bromoacetophenone to benzylic boronic ester 2-5. ....	67
Table 3-1: Yields and selectivities for secondary allylic boronic ester couplings. ....	115
Table 3-2: Cross-Coupling of non-racemic allylic boronic esters. ....	120
Table 5-1: pH of solution during <i>pseudo</i> -reaction (left) and in the presence of B(OH) <sub>3</sub> (centre). The material from the latter experiment was re-subjected to <i>pseudo</i> -conditions and the pH was recorded (right). ....	193

## List of Schemes

Scheme 1-1: The Suzuki-Miyaura cross-coupling of an aryl organoboron with an aryl halide to form an unsymmetrical biaryl. Aryl boranes, boronic acids and boronic esters are all efficient coupling partners. ....	1
Scheme 1-2: Ni-catalyzed cross-coupling of aryl bromides and Grignard reagents. ....	3
Scheme 1-3: Negishi's Pd catalyzed cross-coupling of a vinyl iodide and vinyl aluminate resulting from the hydroalumination of a terminal alkyne. R = <i>i</i> -Bu. ....	4
Scheme 1-4: Generally accepted catalytic cycle for the Suzuki-Miyaura reaction. Isomerization events and the role of base are omitted for clarity. ....	6
Scheme 1-5: Retention of stereochemistry of a chiral ligand on Pd precludes hydroxide attack at the phosphorous centre during ligand exchange. ....	8
Scheme 1-6: Examples of electron-rich alkylphosphine ligands developed by Fu, Buchwald and Hartwig for Suzuki-Miyaura cross-coupling .....	10
Scheme 1-7: Low temperature oxidative addition of an aryl bromide to a monoligated Pd complex. L = P( <i>o</i> -tol) <sub>3</sub> .....	11
Scheme 1-8: Two proposed transmetalation mechanisms that require exogenous base. .	13
Scheme 1-9: The non-innocent nature of dba with respect to reductive elimination. ....	14
Scheme 1-10: The Pd catalyzed cross-coupling of iodobenzene and <i>B</i> -octyl-9-BBN, a primary organoborane. ....	16
Scheme 1-11: Successful cross-coupling of alkyl boronic ester with Thallium salts. ....	17
Scheme 1-12: The cross-coupling of primary boronic acids, as reported by Falck in 2001. ....	18
Scheme 1-13: The <i>Tedicyp</i> and <i>Q-Phos</i> ligands developed by the Doucet and Hartwig groups, respectively. ....	19
Scheme 1-14: Successful protocols for the cross-coupling of both cyclopropyl (top) and cyclopentyl (bottom) boronic acids. ....	21
Scheme 1-15: Optimized conditions for branched selectivity in secondary alkyl trifluoroborate salt cross-coupling. ....	23



Scheme 1-16: Evidence of ring-walking, even under optimized conditions for secondary Molanderates. ....	25
Scheme 1-17: The activation of alkyl boronic esters by <i>s</i> -BuLi and the demonstration of exclusive transmetalation of the primary alkyl chain. ....	26
Scheme 1-18: Alkyl-Alkyl cross-coupling between alkyl iodides and primary organoboranes. ....	27
Scheme 1-19: Cross-coupling of both aryl- and alkyl boronic acids to primary alkyl bromides. ....	28
Scheme 1-20: Ni-catalyzed cross-coupling of <i>sec</i> -alkyl chloride with phenylboronic acid. ....	30
Scheme 1-21: Stereoconvergent cross-coupling of a racemic homobenzylic secondary bromide and a primary organoborane. ....	30
Scheme 2-1: Chemoselectivity of the Rh-catalyzed hydroboration reaction. ....	43
Scheme 2-2: Regioselectivity of the Rh-catalyzed hydroboration reaction as demonstrated by Evans. ....	44
Scheme 2-3: Branched selectivity achieved with the bidentate phosphine-ligated Rh-catalyzed hydroboration reaction. ....	45
Scheme 2-4: Illustration of the regio- and enantioselectivity of the metal catalyzed hydroboration of styrene. ....	46
Scheme 2-5: Reductive hydroarylation coupling (top) and fluoride-mediated silicon coupling (bottom) to 1,1-diarylethanes. ....	48
Scheme 2-6: Recent work from the groups of Suginome (top) and Molander (bottom) on the enantiospecific cross-coupling of secondary boronic ester derivatives. ....	49
Scheme 2-7: Mechanism proposed by Aggarwal to account for stereospecific protodeboronation of boronic esters. ....	57
Scheme 2-8: Chemoselectivity of the cross-coupling reaction even in presence of large excess of styrene derivative. ....	69
Scheme 2-9: The intramolecular chemoselectivity of the Suzuki-Miyaura process over a potential Mizoroki-Heck reaction. ....	70
Scheme 2-10: Chemical inertness of linear boronic esters to reaction conditions. ....	71

Scheme 2-11: Illustration of the importance of an adjacent olefin to ensure successful cross-coupling. Conditions = 1.0 eq. 4-iodoacetophenone, Pd(PPh <sub>3</sub> ) <sub>4</sub> 8 mol %, 1.5 eq Ag <sub>2</sub> O, 1.5 eq K <sub>2</sub> CO <sub>3</sub> , DME, 85 °C, 24 h. NMR yields, unless otherwise indicated. ....	72
Scheme 2-12: Assigned <sup>31</sup> P NMR chemical shifts for components of cross-coupling reaction mixture. ....	81
Scheme 2-13: Proposed basic catalytic cycle for the cross-coupling of secondary boronic esters. Note that the effects of base and Ag <sub>2</sub> O have been omitted for clarity.....	85
Scheme 2-14: Possible fates of the β-hydride elimination product <i>i</i> and their effects on stereoretention.....	87
Scheme 2-15: Attempted cross-over experiment to verify occurrence of olefin decomplexation from Pd. ....	89
Scheme 3-1: The asymmetric borylation of α,β-unsaturated esters as reported by Yun and co-workers.....	98
Scheme 3-2: Asymmetric alkylation of vinyl boronic esters as an alternative to hydroboration.....	99
Scheme 3-3: Homologation of boronic esters by lithiated dichloromethane followed by nucleophilic displacement of a chloride. ....	100
Scheme 3-4: Diastereoselective variant of Matteson-type homologation using chiral auxilliary on boron (in this case, pinanediol).....	100
Scheme 3-5: Synthesis of (R,R)-DICHD for use as chiral auxilliary on boron for Matteson Homologation. Sharpless Asymmetric Dihydroxylation is used to create the critical 1,2-diol motif. ....	101
Scheme 3-6: The enantioselective deprotonation of alkyl carbamates with <i>s</i> -BuLi and the chiral ligand (-)-sparteine. The enantioselectivity of the lithiation is determined by stereodifferentiation in the deprotonation <i>and</i> the configurational stability of the resulting lithium/carbanion pair. In the example given, the lithiated carbamate is configurationally stable and does not undergo a significant amount of inversion <i>via</i> the planar intermediate. ....	102
Scheme 3-7: Dynamic thermodynamic resolution to achieve enantioselective lithiation of benzyl group. TMS= trimethylsilyl. ....	103

Scheme 3-8: Relative configurational stabilities of lithiated carbamates used throughout this work.....	104
Scheme 3-9: Enantioselective synthesis of secondary boronic esters by Aggarwal's method.....	105
Scheme 3-10: Lithiation-borylation with enantioenriched secondary carbamates to yield non-racemic tertiary alcohols.....	105
Scheme 3-11: Gamma-selectivity for the fluoride-promoted, Pd-catalyzed cross-coupling of allyl silanes. ....	107
Scheme 3-12: Stereochemical consequences of a <i>anti</i> -S <sub>E</sub> ' mechanism (top) favored by polar solvents and the <i>syn</i> -S <sub>E</sub> ' mechanism (bottom) at play in THF.....	108
Scheme 3-13: Ligand-based regioselectivity for the cross-coupling of primary allyl silanes.....	109
Scheme 3-14: The effect of olefin geometry on the stereochemical outcome of the cross-coupling of allyl silanoate salts with aryl bromides. The favored conformer (top) dominates as the allylic proton eclipses the double bond and not the bulky <i>iso</i> -butyl group (bottom).....	110
Scheme 3-15: Mechanism proposed by Szábo for the $\gamma$ -regioselectivity for primary allylic boronic acids. ....	111
Scheme 3-16: Solitary example of a racemic secondary allylic trifluoroboronate cross-coupling, as reported by Miyaura. High $\gamma$ -selectivity is observed.....	112
Scheme 3-17: Synthesis of racemic secondary allylic boronic ester <i>via</i> Matteson chemistry.....	113
Scheme 3-18: Poor-yielding synthesis of a conjugated allylic boronic ester by way of a lithiation-borylation approach. The multiple chromatography steps required to isolate the product from unconsumed alkyl boronic ester deflate the yield substantially.....	114
Scheme 3-19: Attempted alteration of the regioselectivity for the cross-coupling of allylic boronic esters based on a ligand strategy.....	116
Scheme 3-20: Two possible pathways leading to $\alpha$ -arylation in aryl systems. Path A proceeds through a direct transmetalation at the $\alpha$ -site. In Path B, transmetalation occurs	

by way of the more typical S <sub>E</sub> ' mechanism, but rapid isomerization occurs to restore conjugation.....	117
Scheme 3-21: Pd-catalyzed decarbonylative coupling. The regioselectivity is dictated by the creation of conjugation in the non-aromatic ring.....	118
Scheme 3-22: Proposed route to asymmetric triarylmethanes by way of a Suzuki-Miyaura cross-coupling strategy. ....	122
Scheme 3-23: Brønsted Acid catalyzed synthesis of symmetrical triarylmethanes from arenes and aromatic aldehydes.....	123
Scheme 3-24: Lewis Acid catalyzed synthesis of unsymmetrical triarylmethanes in two steps. Ar = <i>p</i> -tolyl, Cbz = carboxybenzyl. ....	124
Scheme 3-25: The synthesis of asymmetric triarylmethanes by way of enantioselective C-H activation and cross-coupling.....	125
Scheme 3-26: The asymmetric synthesis of triarylmethanes <i>via</i> chiral Brønsted Acid catalysis. Np = 1-naphthyl, Ts = tosyl. ....	126
Scheme 3-27: Retrosynthetic analysis of an asymmetric triarylmethane through a lithiation-borylation (1) / Suzuki-Miyaura (2) strategy. ....	127
Scheme 3-28: The borylation of a lithiated carbamate to synthesize a dibenzylic boronic ester. TMEDA = tetramethylethylenediamine.....	127
Scheme 3-29: The first synthesis of a symmetrical triarylmethane by Suzuki-Miyaura cross-coupling approach. ....	128
Scheme 3-30: The synthesis of an unsymmetrical dibenzylic boronic ester to synthesize the first unsymmetrical triarylmethane by a Suzuki-Miyaura cross-coupling approach. The reaction is performed in a vial with Teflon-coated cap to prevent loss of solvent at temperatures above its boiling point. ....	129
Scheme 3-31: Chosen approach to non-racemic dibenzylic boronic esters. dished = ( <i>R,R</i> )-dicyclohexyl ethylenediol. ....	130
Scheme 3-32: Unsuccessful approach to non-racemic <i>alpha</i> -chlorobenzylic boronic esters. ....	130
Scheme 3-33: Formation of an unexpected product during homologation of PhBpin with lithium dichloromethane. ....	131

Scheme 3-34: One pot, enantioselective synthesis of dibenzylic boronic ester. ....	132
Scheme 3-35: Enantioselective synthesis of dibenzylic boronic ester with (-)-sparteine and subsequent, stereoloyal cross-coupling to asymmetric triarylmethane.....	134
Scheme 3-36: Dynamic thermodynamic resolution of the lithiated benzyl carbamate with chiral bis(oxazoline) ligands. ....	135
Scheme 3-37: The four step synthesis of a chiral bis(oxazoline) from the natural amino acid, L-leucine.....	136
Scheme 3-38: Non-enantiospecific synthesis of dibenzylic boronic ester (and subsequent oxidation to secondary alcohol) with bis(oxazoline) ligand 3-25.....	137
Scheme 3-39: Aggarwal's strategy of quenching lithiated carbamates resulting from decomplexation of the boronic ester prior to racemization. ....	138
Scheme 3-40: Modest improvement in enantioselectivity in the synthesis of dibenzylic boronic esters by addition of MeOH after borylation. ....	139
Scheme 3-41: Enantioselective synthesis of a dibenzylic boronic ester and subsequent cross-coupling to yield an asymmetric triarylmethane. ....	140
Scheme 3-42: Low yielding cross-coupling reactions of <i>p</i> -methoxy- neopentyl boronic ester (top) and transesterification to the analogous, and unreactive, potassium trifluoroborate (bottom). ....	142
Scheme 3-43: Transesterification of boronic esters. A: Suginome's hydrolysis and pinacol quench of alpha-amido benzylic boronic esters. B: Similar approach with dibenzylic boronic esters leading to over oxidation. ....	143
Scheme 3-44: One-pot synthesis of dibenzylic pinacolate ester from neopentyl analogue followed by cross-coupling with aryl iodide to yield trisubstituted triarylmethane. ....	144
Scheme 3-45: Methodology to obtain both dibenzylic boronic ester and triarylmethane in high yield. ....	145
Scheme 3-46: Initial approach to the synthesis of asymmetric $\alpha$ -silyl boronate esters. The configurational lability of the lithiated silyl methyl carbamate led to a racemic mixture in the product. ....	147
Scheme 3-47: Successful route to tertiary allyl silanes in high yield and er and dr, by way of a non-racemic $\alpha$ -silyl boronate ester.....	148

Scheme 3-48: Quaternary allyl silanes synthesized in high yield and er from lithiated alkyl carbamates.....	149
Scheme 5-1: Unsymmetrical biaryl synthesized <i>via</i> mesoporous silica supported, Pd-catalyzed Suzuki-Miyaura cross-coupling reaction. The side-products, B(OH) <sub>3</sub> , KBr and pinacol are also noted.....	190

## List of Abbreviations

9-BBN = 9-borabicyclo[3.3.1] nonane

Ac = Acetyl

Ad = Adamantyl

Alk = Alkyl

Ar = Aryl

BINAP = 2,2'-bis(diphenylphosphino)-1,1'-binaphthyl

B:L = branched to linear ratio

BQ = benzoquinone

Bu = Butyl

Cb = Carbamoyl (often *N,N*-diisopropylcarbamoyl)

Cbz = Carboxybenzyl

CMC = critical micelle concentration

CMT = critical micelle temperature

COD = 1,5- cyclooctadiene

Cp = Cyclopentadienyl

CTAB = cetyl trimethylammonium bromide

Cy = Cyclohexyl

dba = dibenzylidene acetone

diched = 1,2-dicyclohexyl-1,2-ethanediol

DME = dimethoxyethane

DMF = *N,N*-dimethylformamide

dr = diastereomeric ratio

ee = enantiomeric excess

EISA = evaporation induced self-assembly

EPR = electron paramagnetic resonance

er = enantiomeric ratio

dppb = 1,4-bis(diphenylphosphino)butane

dppe = 1,2-bis(diphenylphosphino)ethane

dppp = 1,3-bis(diphenylphosphino)propane

dpppent = 1,5-bis(diphenylphosphino)pentane

GC-MS = gas chromatography – mass spectrometry

HBCat = catecholborane

HBpin = pinacolborane

HPLC = high-performance liquid chromatography

Iso. = isolated (yield)

L = ligand

LDA = lithium diisopropylamide

Me = methyl

PEO = poly(ethylene oxide)

Ph = phenyl

PPO = poly(propylene oxide)

MPTMS = mercaptopropyltrimethoxysilane

NHC = *N*-heterocyclic carbene

NMR = nuclear magnetic resonance



Nu = nucleophile

R = proton or variable organic group

RDS = rate determining step

TBAF = tetrabutylammonium fluoride

TEM = tunneling electron microscopy

THF = tetrahydrofuran

TMB = trimethylbenzene (mesitylene)

TMEDA = *N,N,N,N*-tetramethylethylene diamine

TMS = trimethylsilyl

TOF = time of flight

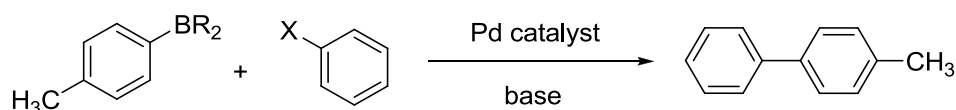
XRD = X-Ray Diffraction

# Chapter 1

## General Introduction: The Suzuki-Miyaura Reaction

### 1.1 Introduction

The Pd-catalyzed cross-coupling of aryl or alkyl halides with boranes or boronic acid derivatives, commonly known as the Suzuki-Miyaura reaction, currently stands as one of the most important and oft used C-C bond forming protocols available to the organic chemist,<sup>1</sup> a fact recognized by a share of the 2010 Nobel Prize in Chemistry.<sup>2</sup> Though initially used mainly to form biaryl, and other  $sp^2$ - $sp^2$  type bonds (Scheme 1-1), progress made especially in the last decade has rendered the coupling of most  $sp^3$ -hybridized coupling partners possible.<sup>3, 4</sup> Indeed, after a generation of advances based mostly on ligand development for oxidative addition and transmetalation facilitating additives, successful cross-couplings of alkyl electrophiles and primary alkyl boronic acid derivatives are now commonplace.<sup>5</sup>



**Scheme 1-1:** The Suzuki-Miyaura cross-coupling of an aryl organoboron with an aryl halide to form an unsymmetrical biaryl. Aryl boranes, boronic acids and boronic esters are all efficient coupling partners.

In spite of the ubiquity of the Suzuki-Miyaura reaction, and even with the extended footprint given to it by a generation of modification and improvement,<sup>6, 7</sup> some

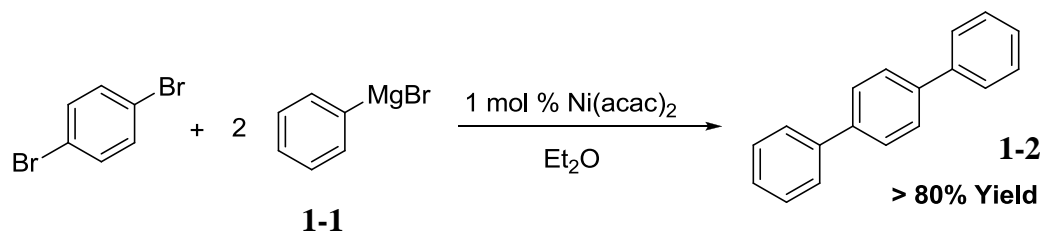
major shortcomings still remain. In terms of reaction scope, a general protocol for the cross-coupling of *secondary* boronic acid derivatives is still lacking. Given that secondary boronic esters may be chiral, and that there is no shortage of ways to synthesize them asymmetrically,<sup>8-10</sup> our inability to create non-racemic carbon frameworks from them needs to be addressed. Furthermore, as the Suzuki-Miyaura reaction is often used in the synthesis of molecules destined for human consumption, a costly and time-consuming Pd-scavenging step is required.<sup>11</sup> Advances made in the field of recyclable, supported catalysts have greatly lowered the amount of Pd that is ultimately leached into solution, though their mode of action needs to be better understood to allow for further improvement. Our forays into these last two issues, ones of reaction scope<sup>12</sup> and Pd contamination,<sup>13</sup> will be the subject of this thesis.

## **1.2 Transition-Metal Catalysis of Organometallic Reagents**

### *1.2.1 Grignard reagents make way for Organozinc Reagents*

Organometallic species of electropositive metals such as magnesium and lithium have been known for well over a century.<sup>14</sup> After inserting magnesium metal into an organohalide bond to form a Grignard reagent, or performing a metal-halide exchange to obtain an organolithium, these reactive species have historically been used as carbon-based nucleophiles in additions to carbonyls.<sup>15</sup> It is precisely this high reactivity, though, that plagues the chemoselectivity and functional group tolerance of the process.

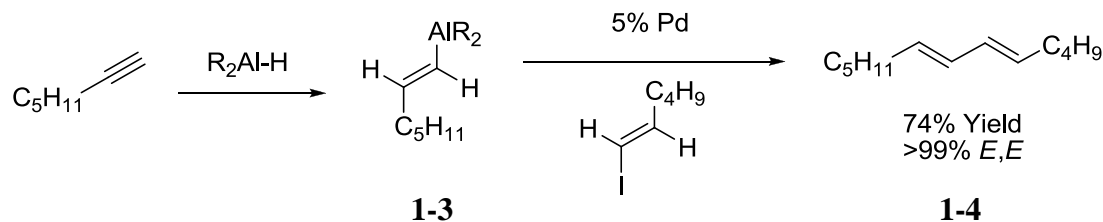
In the 1970s, organometallics started to find application, not just as highly nucleophilic carbon-based reagents, but as candidates for metal-catalyzed cross-coupling reactions. Indeed, in 1972, Corriu<sup>16</sup> and Kumada<sup>17</sup> simultaneously and independently published the first nickel-catalyzed cross-couplings of Grignard reagents **1-1** to aryl and vinyl halides (Scheme 1-2). Considering the possibility of other, undesired processes owing to the high reactivity of the phenylmagnesium bromide used, the decent conversion to cross-coupled products was noteworthy. That said, the high instance of homocoupling, limited functional group tolerance and high sensitivity to moisture caused other researchers to pursue other, milder, organometallic species as cross-coupling partners.



**Scheme 1-2:** Ni-catalyzed cross-coupling of aryl bromides and Grignard reagents.

Negishi recognized that a whole variety of organometallics were accessible *via* hydrometalation reactions across C-C double and triple bonds, including ones where the metal was much less electropositive than magnesium and lithium. Zn, Cd, Sn, Zr, B, Al, and Si were all considered prime candidates, with the latter four metals all having the advantage of known protocols for regio- and stereodefined syntheses.<sup>18</sup> With this in mind, Negishi published the first example of the cross-coupling of an alkenyl aluminum

nucleophile to an aryl bromide electrophile using catalytic amounts of either Ni or Pd.<sup>19</sup> The alkenyl aluminum species **1-3** was easily synthesized, with defined *E*-stereochemistry, by way of a hydroalumination reaction. Gratifyingly, the stereochemistry of the double bond was maintained during the C-C bond forming event (**1-4**, Scheme 1-3). In an interesting twist of fate, Negishi also attempted the Pd-catalyzed cross-coupling of the analogous alkenyl boron resulting from the hydroboration of a terminal alkyne with no success.<sup>19</sup> Had he added a stoichiometric amount of base to activate the boron towards transmetalation, this surely would have constituted the first example of an organoboron based cross-coupling, coming a full three years prior to the seminal publication by Miyaura, Yamada and Suzuki.<sup>20</sup>



**Scheme 1-3:** Negishi's Pd catalyzed cross-coupling of a vinyl iodide and vinyl aluminate resulting from the hydroalumination of a terminal alkyne.<sup>19</sup> R = *i*-Bu.

The following year, Negishi tested phenyl-lithium, magnesium, zinc and aluminum species for the Pd-catalyzed cross-coupling with *p*-iodoanisole to ascertain which organometallic reagent was best suited for Pd-catalysis. Not only did the organozinc species provide the highest yield in terms of product, but compared to the other organometallics, the organozinc species also had the highest functional group

tolerance and produced the lowest amount of homocoupling product.<sup>21</sup> These factors, together with the ease of synthesis of organozincs, led to the proliferation of the so-called Negishi reaction, ultimately leading to a share of the 2010 Nobel Prize in chemistry for Negishi. Though this thesis focuses almost exclusively on the cross-coupling of organoboron reagents, it is important to stress that advances in the Suzuki-Miyaura reaction are often predicated on similar work on the Negishi reaction.

### 1.2.2 *The Emergence of Boron*

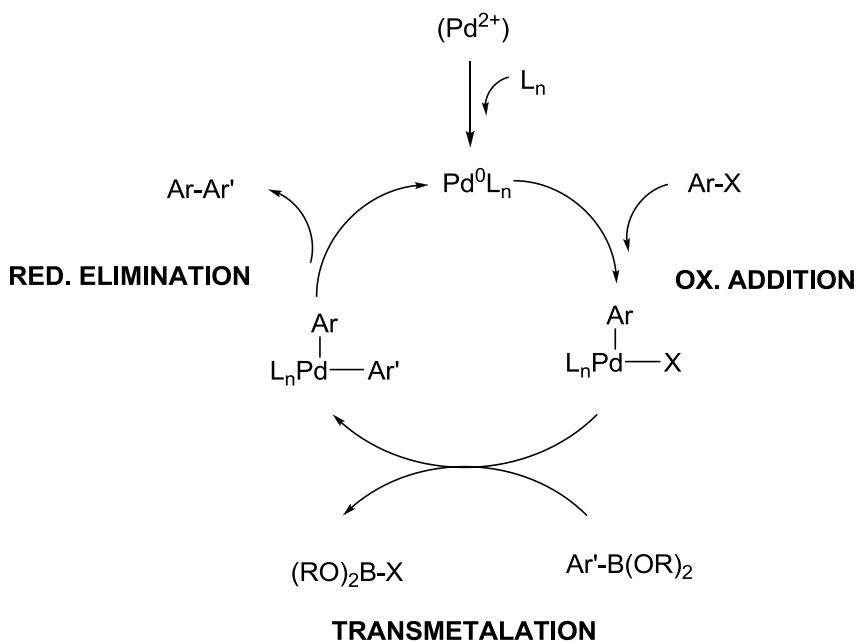
Despite the remarkable success of the organozinc coupling, impetus remained for the development of a boron-based protocol, since organoboron reagents should hold all the positive attributes of organozincs with the added advantage of having known asymmetric syntheses and being less air and moisture sensitive.<sup>22</sup>

In 1979, Miyaura, Yamada and Suzuki reported the successful cross-coupling of alkenyl boronic esters and vinyl bromides with a catalytic amount of Pd(PPh<sub>3</sub>)<sub>4</sub> and a stoichiometric amount of inorganic base, critical to achieve turnover.<sup>20</sup> Interestingly, in outlining the reaction mechanism in a subsequent publication,<sup>23</sup> Suzuki *et al.* accurately depict the role of base as replacing the halide on the Pd-centre, a step that is necessary to enable successful transmetalation from boron to palladium. Of course, it would be the Suzuki-Miyaura reaction's need for base (*vide infra*) that would have substantial consequences on our group's pursuit of reusable, leach-proof catalysts thirty years later.

## 1.3 Basic Mechanism of the Suzuki-Miyaura Reaction

### 1.3.1 General Catalytic Cycle

The basic catalytic cycle postulated for the Suzuki-Miyaura reaction, common to most transition-metal cross-coupling reactions, is outlined in Scheme 1-4.<sup>6</sup> In the case of an aryl-aryl coupling, oxidative addition of a ligated, electron-rich Pd<sup>0</sup> to an aryl halide is followed by transmetalation of the arylboron species. The diarylated Pd then undergoes a reductive elimination, effectively forming the new biaryl C-C bond and regenerating the active Pd<sup>0</sup> catalyst.



**Scheme 1-4:** Generally accepted catalytic cycle for the Suzuki-Miyaura reaction.

Isomerization events and the role of base are omitted for clarity.

What seems, on the whole, to be a fairly straight-forward process actually results from a series of intricate events, some that still aren't fully understood. Indeed, the major steps of the catalytic cycle and contentious points, like the generation of the active Pd catalyst and the critical role of base, warrant further comment.

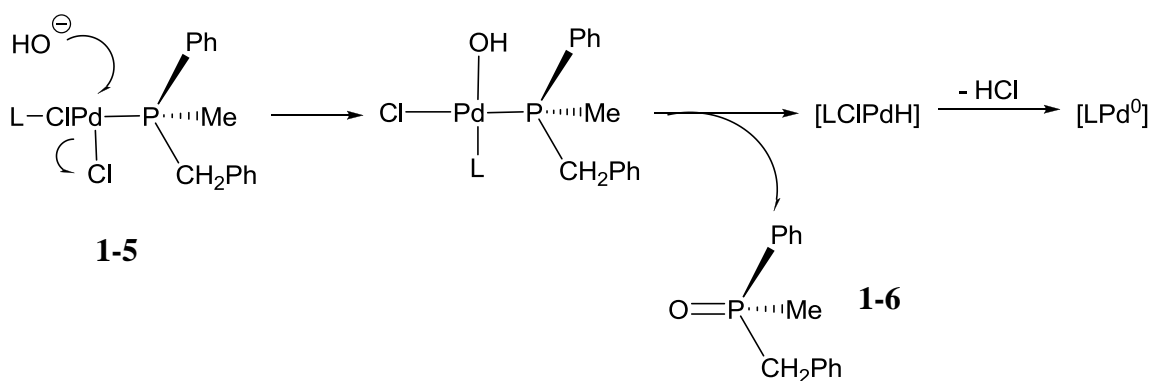
### 1.3.2 Generation of an Active Pd catalyst

As outlined in Scheme 1-4, zero-valent Pd is the active catalyst for the Suzuki-Miyaura reaction. Pd<sup>2+</sup>/Pd<sup>4+</sup> cycles for C-C bond formation are known, though only under strongly oxidative conditions.<sup>24, 25</sup> The conditions for a typical Suzuki-Miyaura coupling are not oxidizing enough to allow access to Pd<sup>4+</sup> and therefore limit the process to the more common Pd<sup>0</sup>/Pd<sup>2+</sup> cycle. It is perhaps somewhat surprising then that, along with their Pd<sup>0</sup> counterparts, Pd<sup>2+</sup> pre-catalysts are also effective at catalyzing the Suzuki-Miyaura reaction. In fact, it is precisely this resistance to oxidation which renders Pd<sup>2+</sup> complexes air-stable, easily handled and, therefore, widely used pre-catalysts.

Several rationales have been reported for the *in situ* reduction of divalent Pd<sup>2+</sup> to the catalytically active Pd<sup>0</sup>. Grushin and Alper were the first to examine this phenomenon in detail.<sup>26</sup> Although initial reports attributed the reduction of Pd<sup>2+</sup> during the Heck reaction to the triethylamine base, they noticed that, when mixed with rigorously dried NEt<sub>3</sub>, PdCl<sub>2</sub>(PPh<sub>3</sub>)<sub>2</sub> remained unperturbed. Exposing the divalent Pd complex to aqueous hydroxide, however, resulted in a complete reduction to zero-valent Pd black. Grushin



and Alper argued that the hydroxide formed in equilibrium by exogenous base and even *trace* amounts of water is sufficient to affect the reduction on a catalytic amount of Pd<sup>2+</sup>. Triphenylphosphine is oxidized to triphenylphosphine oxide in the process. When a resolved chiral phosphine ligand was used instead of PPh<sub>3</sub> (as in **1-5**), the resulting phosphine oxide **1-6** retained its configuration, suggesting that hydroxide attacks Pd directly and that an S<sub>N</sub>2-type process at the phosphine centre is not occurring (Scheme 1-5).



**Scheme 1-5:** Retention of stereochemistry of a chiral ligand on Pd precludes hydroxide attack at the phosphorous centre during ligand exchange.<sup>26</sup>

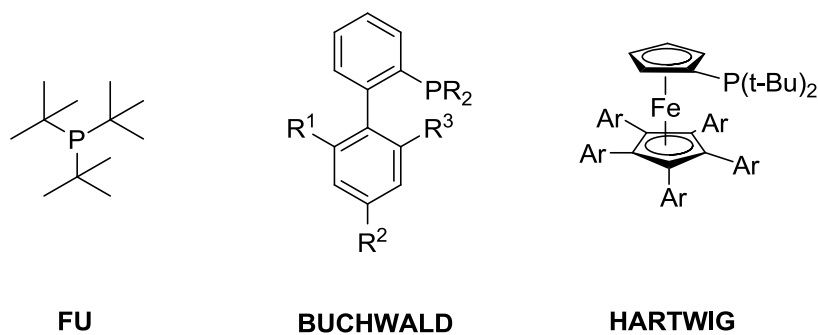
Subsequently, Amatore and Jutand disclosed their findings on the *in situ* reduction of the analogous compound Pd(OAc)<sub>2</sub>(PPh<sub>3</sub>)<sub>2</sub>, formed by the facile reaction of excess PPh<sub>3</sub> with the ubiquitous palladium acetate. They were able to use kinetic data acquired by cyclic voltammetry measurements to demonstrate the spontaneous, if slow, reductive elimination of an acetate and phosphine ligand to yield palladium(0).<sup>27</sup> Indeed, this validates the findings of Grushin and Alper, as their proposed mechanism differed only

by X-type ligand exchange (from  $\text{Cl}^-$  to  $\text{HO}^-$ ) prior to reductive elimination. In any case, reduction of divalent Pd(II) to Pd(0) is definitely feasible under typical reaction conditions. For this reason, of the two Pd complexes most often used in the Suzuki-Miyaura reaction, one is zero-valent ( $\text{Pd}(\text{PPh}_3)_4$ ) and the other ( $\text{Pd}(\text{dppf})\text{Cl}_2$ ) is divalent.<sup>5</sup>

### 1.3.3 Oxidative Addition

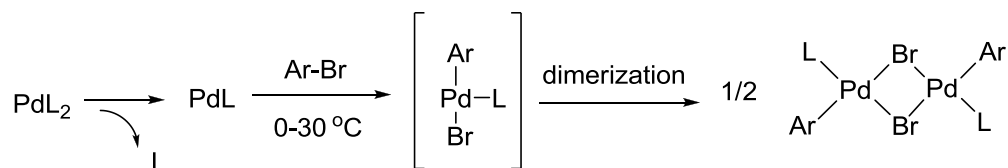
Following the generation of the active Pd(0) catalyst system, the next step is oxidative addition of the aryl, alkenyl or even alkyl halide to the Pd centre in what is often the rate limiting step of the process. As noted by Suzuki in 1995,<sup>6</sup> the Pd insertion into the organohalide is favored when the C-heteroatom bond is weak, leading to an observed reactivity trend that follows  $\text{I} > \text{Br} \gg \text{Cl}$ . A higher propensity for electron deficient aryl halides to undergo oxidative addition is explained by similar reckoning.

Interestingly, a strongly electron-withdrawing group on the organic portion of the electrophile can adequately activate an aryl chloride bond towards oxidative addition, though initially a general protocol for non-activated aryl chlorides remained elusive. To confront this problem, the groups of Buchwald,<sup>28</sup> Fu<sup>29</sup> and Hartwig<sup>30</sup> designed highly active Pd complexes ligated by bulky, electron rich alkylphosphine ligands (Scheme 1-6). Under this paradigm, unactivated aryl chlorides are suitable cross-coupling partners, even at room temperature.



**Scheme 1-6:** Examples of electron-rich alkylphosphine ligands developed by Fu, Buchwald and Hartwig for Suzuki-Miyaura cross-coupling

For the better part of the last fifteen years, the challenge facing the oxidative addition step has not been one necessarily of practice, but of understanding. Indeed, the ligated nature of the catalytically competent Pd complex continues to be hotly contested. In 1995, Hartwig reported that an aryl bromide could oxidatively add to a diphosphine Pd complex ( $\text{Pd}[\text{P}(o\text{-tol})_3]_2$ ) at room temperature, whereas the comparative tetraphosphine,  $\text{Pd}(\text{PPh}_3)_4$ , required prolonged heating at  $80\text{ }^\circ\text{C}$ .<sup>31</sup> The isolated oxidative addition product was a monoligated dimer, which was initially believed to result from aryl bromide oxidative addition to the  $\text{PdL}_2$  complex, followed by ligand dissociation and reversible dimerization. In actual fact, the kinetic data pointed to a ligand dissociation step to form a monophosphine complex,  $\text{PdL}$ , which *preceded* the actual oxidative addition event (Scheme 1-7).<sup>31</sup>



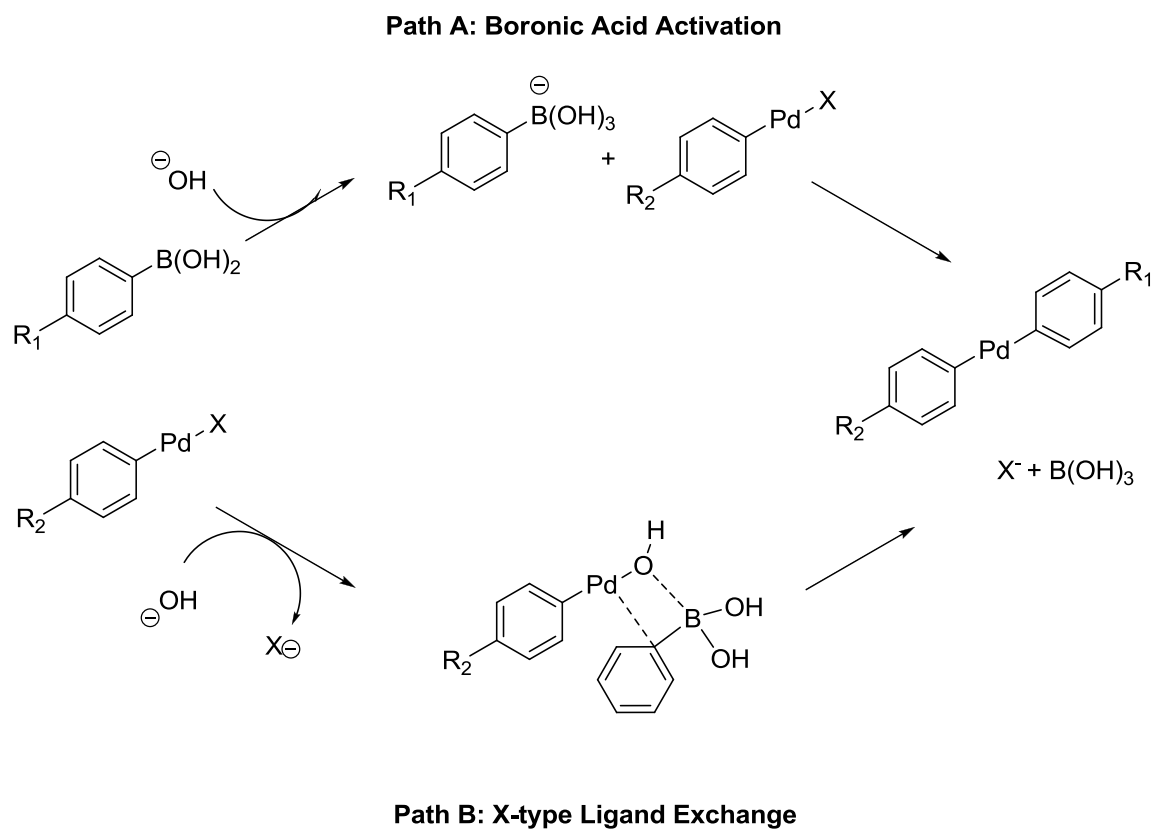
**Scheme 1-7:** Low temperature oxidative addition of an aryl bromide to a monoligated Pd complex. L = P(*o*-tol)<sub>3</sub>

Subsequent work showed that, when using a bulky, electron-rich ferrocenyl ligand (as in Scheme 1-6), the oxidative addition to aryl- iodides, bromides and chlorides all proceeded *via* unique mechanistic pathways, though the transformation invariably proceeded through the highly coordinatively unsaturated [PdL] species.<sup>32</sup> Of course, the bulky ferrocenyl ligand biases the coordination geometry of the catalytically competent complex towards a lower ligated form. More recent computational work has shown that less bulky ligands can lead to active [PdL<sub>2</sub>] catalysts, especially in the case of aryl iodides whose low barrier to oxidative addition may blur the energetic differences between the pathways.<sup>33</sup>

#### 1.3.4 Transmetalation and the Role of Base

Following the oxidative addition step, the transmetalation of organic groups from boron to the Pd centre occurs. Unlike other common Pd-catalyzed reactions such as the Sonogashira or Mizoroki-Heck reaction (which can activate the nucleophilic coupling partner *via* Cu-metal insertion to an alkyne and Pd ligation to an alkene, respectively) the Suzuki-Miyaura reaction relies on the addition of exogenous base to facilitate the

transmetalation of the boronic acid derivative to the metal centre.<sup>34</sup> Initial computational investigations by Maseras and co-workers<sup>35</sup> suggested that exogenous hydroxide was necessary to form a more active borate complex which could undergo transmetalation to Pd much more quickly (Scheme 1-8, **Path A**). More recent experimental work by Amatore and Jutand<sup>36</sup> contradicts this notion, suggesting instead that the borate complex is actually inactive to transmetalation and that aqueous base serves to replace to the Pd-X bond with a Pd-OH bond following the oxidative addition of Pd to an aryl halide. This, of course, is consistent with Alper's proposed mechanism for the reduction of Pd<sup>2+</sup>, initiated by a ligand exchange on Pd. In the case of transmetalations, the hydroxylated Pd species does not reductively eliminate with PPh<sub>3</sub>, but rather takes advantage of the oxophilicity of boron to easily transmetalate with a boronic acid (Scheme 1-8, **Path B**). In any case, both Jutand's experimental findings and Maseras' computational studies agree that the transmetalation *cannot* proceed between the Pd-X and ArB(OH)<sub>2</sub> species and that the addition of base is necessary. This requirement for base is what ultimately foiled Negishi's initial attempts at cross-coupling alkenylboranes in 1976,<sup>19</sup> leading him to turn instead to organozincs.



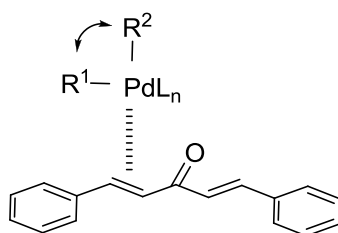
**Scheme 1-8:** Two proposed transmetalation mechanisms that require exogenous base.

### 1.3.5 Reductive Elimination to Generate Cross-Coupling Product

In what is essentially the reverse of an oxidative addition, the reductive elimination step combines the two distinct organic functionalities to complete the cross-coupling and regenerate the active catalyst. Just as the oxidative addition is thought to typically proceed through a monoligated [PdL] complex, Stille proposed that reductive elimination also proceeds through this highly unsaturated complex; the understandable requirement that the organic groups be *cis* is also noted.<sup>37</sup>

This is not to say that reductive elimination cannot proceed through a diligated complex. In fact, the rate of reductive elimination can be enhanced by using bidentate ligands with large bite angles.<sup>38, 39</sup> These large bite angles serve to effectively decrease the distance between the organic groups occupying the other two coordination sites which, ultimately, facilitates the eventual reductive elimination.

Electronics can also have a significant effect on reductive elimination. Given that electron rich metal centres are known to undergo facile oxidative addition events, it is not surprising then that the reductive elimination step, purportedly the opposite of an oxidative addition, should be favored from electron *poor* metal centres. Indeed, Knochel has shown that having a remote site of unsaturation on the organic group capable of back-binding to the metal centre was required to ensure successful reductive elimination from Ni in his work with alkyl Negishi variants.<sup>40</sup> The  $\pi$ -acidic ligand dibenzylidene acetone (dba) is also known to facilitate reductive elimination by coordinating to the Pd<sup>2+</sup> metal centre and pulling electron density into the  $\pi$ -system (Scheme 1-9).<sup>41</sup>



**Scheme 1-9:** The non-innocent nature of dba with respect to reductive elimination.

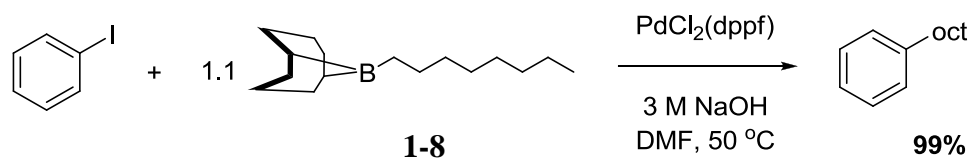
## 1.4 Suzuki-Miyaura Reactions of $sp^3$ -hybridized Organoboron Coupling Partners

### 1.4.1 Cross-Coupling of Primary Boronic Acid Derivatives

The cross-coupling of  $sp^3$ -type organoboron species to haloarenes is typically more difficult than with their  $sp^2$ -hybridized analogues, owing to a much slower transmetalation step.<sup>42</sup> As with other organometallic species, alkyl boron nucleophiles are also very susceptible to  $\beta$ -hydride elimination from the Pd complex after transmetalation, an eventuality that is even more likely with secondary alkyl borons. These problems have mostly been addressed (typically in the form of transmetalation accelerating additives) for primary organoboron coupling partners, but that said, the field of *secondary* boronic ester cross-coupling is still in its infancy.

Indeed, primary alkylboranes have been useful coupling partners for over twenty years.<sup>42</sup> In 1989, Suzuki was able to demonstrate that *B*-octyl-9-borabicyclo[3.3.1]nonane (**1-8**, *B*-octyl-9-BBN) cross-coupled smoothly and in high yield with iodobenzene in the presence of a catalytic amount of Pd and fairly innocuous bases such as NaOH,  $K_3PO_4$  and  $K_2CO_3$  (Scheme 1-10).<sup>42</sup> Following Kishi's lead on facilitating difficult transmetalations to boron,<sup>43</sup> Suzuki also showed that the reaction could be performed at room temperature when TIOH was used as base.<sup>44</sup> As expected, no reaction was observed in the absence of exogenous base.



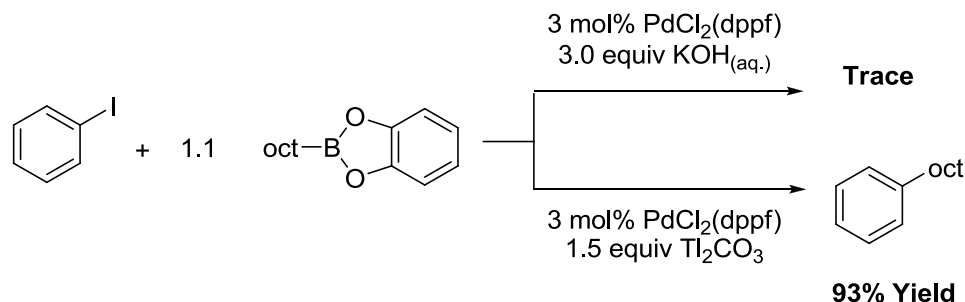


**Scheme 1-10:** The Pd catalyzed cross-coupling of iodobenzene and *B*-octyl-9-BBN, a primary organoborane.

Though a substantial development, there are serious limitations to using alkylboranes as coupling partners. For one, they are notoriously unstable and are almost always used *in situ*, without purification, following the hydroboration of an alkene. The second pitfall most often associated with the cross-coupling of *B*-alkylated-9-BBN derivatives is the poor atom economy of the process. Though it is true that the stoichiometric amount of resultant cyclooctane moiety tarnishes the atom-economy of the process, the uncatalyzed hydroboration reaction does not require precious metals or expensive ligands, and the subsequent cross-coupling can be performed in one pot; all of which lessens the environmental and economic impact of the process.

Alkylboronic acid derivatives, on the other hand, provide air-stable, easy to handle alternatives to alkylboranes. Whether synthesized by a metal-catalyzed hydroboration reaction or by the quenching of an alkyl Grignard reagent with a boron electrophile such as  $\text{B}(\text{OMe})_3$ , the synthesis of alkylboronic acids and esters can also be achieved with much greater regiocontrol than alkylboranes. However, the lessened nucleophilicity of the carbon adjacent to the boronic acid derivative (as compared to an alkylborane) ensures that an already sluggish transmetalation is rendered even slower.

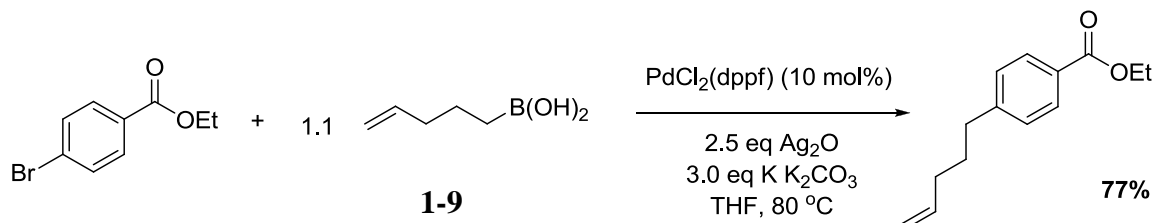
Indeed, Suzuki and co-workers noted that primary alkylboronic esters derived from the metal catalyzed hydroboration of alkenes did not cross-couple to aryl halides in the presence of standard bases like NaOMe or NaOH, conditions known to affect the cross-coupling of alkylboranes. Thallium(I) salts, which had been used previously to hasten slow transmetalation steps, were found to be effective additives for the Pd-catalyzed cross-coupling of alkylboronic esters, with  $\text{Tl}_2\text{CO}_3$  and  $\text{TlOH}$  performing well for catechol and pinacol esters, respectively (Scheme 1-11).<sup>44</sup> Interestingly, though known to be more nucleophilic than the analogous esters, alkylboronic *acids* were not successfully coupled under these conditions.



**Scheme 1-11:** Successful cross-coupling of alkyl boronic ester with Thallium salts.

Naturally, there was an impetus to find alternatives to the highly toxic thallium(I) salts. In 2001, Falck and co-workers demonstrated that a superstoichiometric amount of  $\text{Ag}_2\text{O}$  could mediate the Pd-catalyzed cross-coupling of a wide-variety of primary alkylboronic acids with aryl halides.<sup>45</sup> This marked a significant advance, as the air and moisture stable primary alkylboronic acids could now be cross-coupled without the use of thallium salts. Also of note was the complete selectivity for the cross-coupling reaction

over the Mizoroki-Heck reaction in alkylboronic acids that bore peripheral unsaturated groups (**1-9**, Scheme 1-12), an interesting foreshadowing of results we would obtain for the cross-coupling of secondary boronic esters.

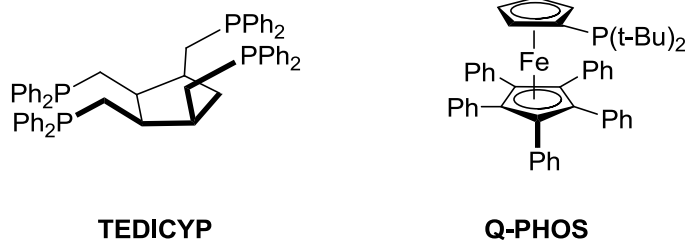


**Scheme 1-12:** The cross-coupling of primary boronic acids, as reported by Falck in 2001.

Though  $\text{Ag}_2\text{O}$  is inexpensive and not known for its toxicity, attempts were made to further simplify the protocol for cross-coupling primary boronic acid derivatives. In 2002, Molander and co-worker reported that primary alkylboronic acids could be cross-coupled to aryl halides and triflates in up to 80% yield when high loadings of  $\text{PdCl}_2(\text{dppf}) \bullet \text{CH}_2\text{Cl}_2$  were used. In this case, only potassium carbonate was needed to turn over the reaction.<sup>46</sup> Primary potassium trifluoroborate salts could also be cross-coupled effectively under similar conditions; unfortunately secondary trifluoroborates could not be employed, as they underwent a  $\beta$ -hydride elimination to the resulting alkene, although in undocumented amounts.<sup>47</sup>

Pd loadings that approach 10 mol% hinder the large-scale viability of Molander's protocol for both alkylboronic acids and trifluoroborate salts. Doucet and co-workers addressed this problem by employing the tetraphosphine ligand *Tedicyc* (Scheme 1-13) in conjunction with  $[\text{Pd}(\text{C}_3\text{H}_5)\text{Cl}]_2$ . This catalyst-ligand combination was so efficient at

turning over the reaction of aryl halides with primary alkyl boronic acids that catalyst loadings as low as 0.01 mol% could be used. However, in lowering the required Pd concentration one thousand-fold, Doucet in turn introduced a dependence on an exotic and expensive ligand.



**Scheme 1-13:** The *Tedicyp* and *Q-Phos* ligands developed by the Doucet and Hartwig groups, respectively.

In 2002, the Hartwig group released a comprehensive study on the synthesis and application of their newly-developed ferrocenyl ligand, *Q-Phos* (Scheme 1-13).<sup>30</sup> Impressively, Pd complexes of this bulky, monophosphine ligand were shown to have excellent reactivity for a variety of cross-coupling reactions, with the amination of aryl halides and the alkyl variant of the Suzuki-Miyaura reaction being chief among them. Primary boronic acids were made to be competent coupling partners under this catalytic system, but what's more, the bulky, electron-rich nature of the *Q-Phos* ligand also facilitated oxidative addition to such an extent that even sterically hindered, unactivated aryl chlorides were able to react with the primary boronic acid coupling partners. Unfortunately, the cross-coupling of *secondary* boronic acids remained difficult, even in the presence of this highly competent catalyst system. As such, when *sec*-butylboronic acid was coupled to *p*-<sup>t</sup>butyl bromobenzene, a moderate yield was obtained for the

secondary coupling product and the unwanted, linear isomer was observed (though not quantified). It would serve as a reminder that the efficient cross-coupling of *secondary* boronic acid derivatives, plagued by an even slower transmetalation and prone to isomerization through  $\beta$ -hydride elimination, was still out of reach.

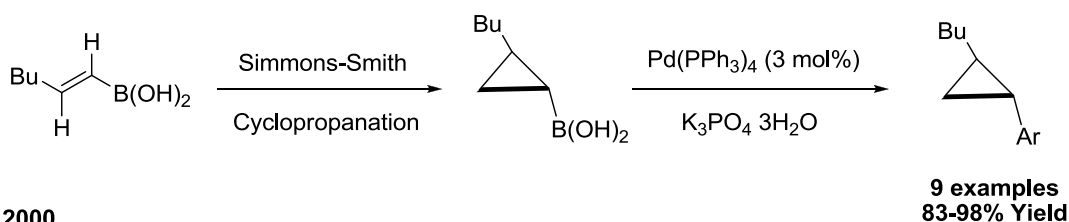
#### 1.4.2 Cross-Coupling of Secondary Boronic Acids

Initially, derivatives of cyclopropylboronic acid constituted the vast majority of successful cross-couplings of secondary boronic acids.<sup>3</sup> Ring strain on the cyclopropyl moiety withdraws p-character from the exocyclic C-B bond, effectively imparting an  $sp^2$ -hybridization on the bond. Furthermore, the  $\beta$ -hydride elimination that plagues other secondary boronic acids is precluded by the disfavored formation of a highly strained cyclopropenyl moiety. In fact, this fortuitous combination would allow cyclopropylboronic acids to maintain a monopoly in the field of secondary organoboron cross-couplings for the better part of a decade.<sup>48, 49</sup>

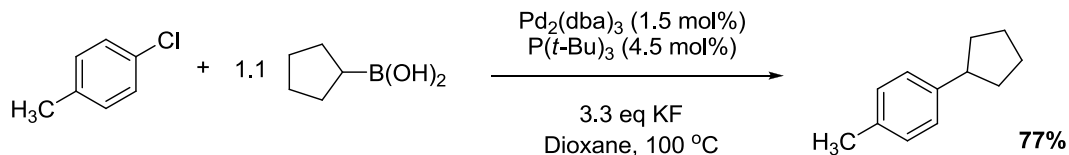
Deng and co-workers were the first to report the synthesis and subsequent Suzuki-type cross-coupling of substituted cyclopropylboronic acids.<sup>48</sup> Stereodefined alkenylboronic acids were transformed into the requisite cyclopropylboronic acids by Simmons-Smith cyclopropanation and then, using fairly mild coupling conditions, these secondary boronic acids were cross-coupled with aryl bromides to form arylated cyclopropanes (Scheme 1-14). Gratifyingly, the configuration of the cyclopropylboronic

acid was fully transmitted to the arylated coupling product.<sup>48</sup> The Chen group subsequently showed that cyclopropylboronic acids could be synthesized easily from the commercially available cyclopropylmagnesium bromide and, under nearly the identical conditions reported by Deng, these cyclopropylboronic acids were cross-coupled to arylbromides in high yield.<sup>50</sup>

**Deng 1996**



**Fu 2000**



**Scheme 1-14:** Successful protocols for the cross-coupling of both cyclopropyl (top) and cyclopentyl (bottom) boronic acids.

In 2000, Fu reported the first successful cross-coupling of a cyclopentylboronic acid as part of his full study on the use of Pd complexes of alkylphosphines for the Suzuki-Miyaura reaction (Scheme 1-14).<sup>51</sup> Using a 3:1 ratio of P(<sup>t</sup>Bu)<sub>3</sub> to Pd<sub>2</sub>(dba)<sub>3</sub> in the presence of KF, a 77% isolated yield was obtained for the cross-coupling of 4-chlorotoluene and cyclopentylboronic acid.<sup>51</sup> This result is noteworthy as the lower ring strain associated with the cyclopentyl structure renders the exocyclic C-B bond much more sp<sup>3</sup>-like than the cyclopropyl analogue. What's more, any safeguard against β-

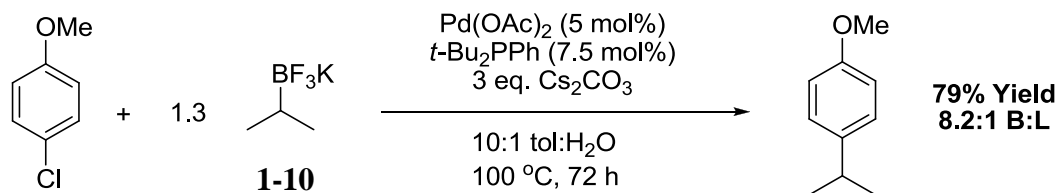
hydride elimination to cyclopentene is mostly lost. However, the symmetric nature of cyclopentylboronic acid renders any  $\beta$ -hydride elimination / Pd-reinsertion event invisible, as the arylated products resulting from this type of ring walking would be indistinguishable from the “desired” product.

#### 1.4.3 Cross-Coupling of Secondary Trifluoroboronate salts

As noted previously, air- and moisture-stable primary alkyl trifluoroboronate salts were found by Molander to be viable alternatives to the impossibly unstable alkylboranes.<sup>47</sup> Nevertheless, the introduction of *secondary* trifluoroboronates to the repertoire of usable cross-coupling partners has been hindered by the same factors that affect the other derivatives of organoboronic acids, namely protodeboronation and  $\beta$ -hydride elimination.

As with the secondary boronic acids, the first successful cross-coupling of secondary trifluoroboronates was in the form of a cyclopropyl derivative. In 2004, Deng showed that cyclopropyl trifluoroborates could be coupled to aryl bromides in high yield under modified Suzuki-Miyaura conditions.<sup>52</sup> Again, the cross-coupling was stereoretentive between the configurations of the substituted cyclopropyl trifluoroborate and the resulting arylated cyclopropane.<sup>52</sup> In 2008, the van Hoogenband group reported the first instance where cyclopentyl potassium trifluoroboronate was used in a cross-coupling reaction.<sup>53</sup> Later that same year, Molander disclosed successful conditions for

the cross-coupling of both cyclopropyl and cyclobutyl potassium trifluoroborates with aryl chlorides.<sup>54</sup>



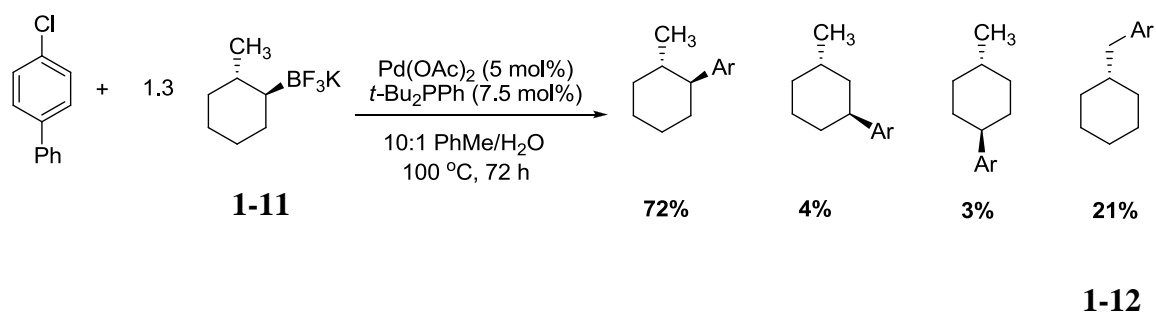
**Scheme 1-15:** Optimized conditions for branched selectivity in secondary alkyl trifluoroborate salt cross-coupling.

Despite the breakthroughs, successful cross-coupling was still limited to a choice few secondary trifluoroborates, mostly all symmetrical, cyclic structures. To address this issue, Molander turned to Parallel Microscale Experimentation, an automated technique which allows for the rapid screening of a variety of ligands, solvents and conditions for a given reaction.<sup>55</sup> A few pertinent results emerged from this study. First, the cross-coupling of both cyclopentyl- and cyclohexyl potassium trifluoroborate salts were optimized for ligand and conditions. The cyclopentyl trifluoroborate derivatives cleanly reacted in the presence of a bulky, electron donating phosphine ligand (*n*-BuPAd<sub>2</sub>) in 10:1 toluene:water. The cyclohexyl systems reacted well under similar conditions, with *t*-Bu<sub>2</sub>PPh acting as the optimal ligand. Secondly, and much more interestingly, the acyclic *sec*-propyl potassium trifluoroborate **1-10** was coupled to aryl chlorides under these optimized conditions, with selectivities for the desired branched to linear alkylation reaching as high as 8.2:1 (Scheme 1-15). This provided a major advance in the field, though the selectivities were very dependent on substrate,  $\beta$ -hydride



elimination was still occurring based on the presence of the linear isomer, and the conditions were by no means general.

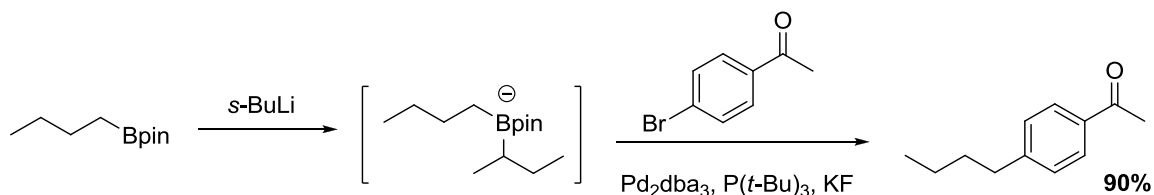
Finally, by the use of non-symmetrical substrates, the occurrence of  $\beta$ -hydride elimination and reinsertion was probed. Suzuki postulated early on that the very slow transmetalation step likely had more adverse effect on the cross-coupling of secondary organoboron species than the increased propensity for  $\beta$ -hydride elimination.<sup>42</sup> Though optimization is usually needed for each individual substrate, potassium trifluoroborates are thought to undergo a more facile transmetalation to Pd and can even prevent unwanted side-reactions.<sup>56</sup> That said, they are still prone to the deleterious  $\beta$ -hydride elimination and metal-reinsertion which can lead to chain walking. Using diastereomerically enriched unsymmetrical cyclohexyl potassium trifluoroborate **1-11**, Molander was able to confirm that this Pd ring-walking was occurring, since the aryl group was deposited throughout the ring, and even on the exocyclic methyl group (Scheme 1-16). Since this process occurs by Pd walking around the entire ring, in an enantiomerically enriched substrate this would lead to loss of stereochemistry. Bulky phosphine ligands favour reductive elimination relative to  $\beta$ -hydride elimination, and as such, this type of ligand offered the best selectivity for the desired product, though large amounts of isomerization were still observed (Scheme 1-16).<sup>55</sup> It is interesting to note that of the undesired products resulting from chain-walking, exocyclic arylation product **1-12** is the most prominent, further confirming the more facile reductive elimination at primary centres.



**Scheme 1-16:** Evidence of ring-walking, even under optimized conditions for secondary Molanderates.

#### 1.4.4 Cross-Coupling of Secondary Boronic Esters

In 2001, Zou and Falck demonstrated that primary alkyl boronic esters could be activated towards transmetalation by the *in situ* reaction of the boronic ester with *s*-BuLi. The resultant ‘ate’ complex easily transferred the primary alkyl group to Pd, thereby providing an alternative to Tl or Ag activation (Scheme 1-17).<sup>57</sup> Interestingly, the transmetalation of the secondary alkyl group, emanating from the *sec*-butyllithium base, was never observed. Thus, Zou and Falck demonstrated clearly *via* an intramolecular competition experiment, just how much more difficult the cross-coupling of secondary boronic esters is compared to the already difficult primary examples.



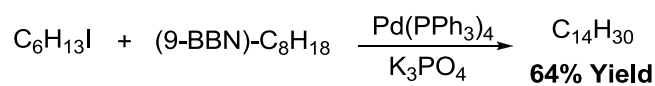
**Scheme 1-17:** The activation of alkyl boronic esters by *s*-BuLi and the demonstration of exclusive transmetalation of the primary alkyl chain.

It is not surprising, then, that no effective protocols for this important class of substrates exist, with all examples prior to our work<sup>12</sup> stemming from derivatives of cyclopropylboronic esters. Work by both Gevorgyan<sup>58</sup> and Charette<sup>49</sup> showed that, like with the boronic acids and trifluoroborates, the cross-coupling of cyclopropylboronic acid pinacolate esters is highly stereoretentive, meaning that the stereochemical information imparted to the secondary boronic ester is maintained throughout the C-C forming event. These results, coupled with the large variety of methods known to synthesize enantiomerically enriched secondary boronic esters, implied that the development of a general protocol for the cross-coupling of secondary boronic esters would have an indisputable impact on the field of asymmetric synthesis.

## 1.5 Suzuki-Miyaura Coupling of Primary $sp^3$ -hybridized Electrophiles

### 1.5.1 Primary Alkyl Electrophiles

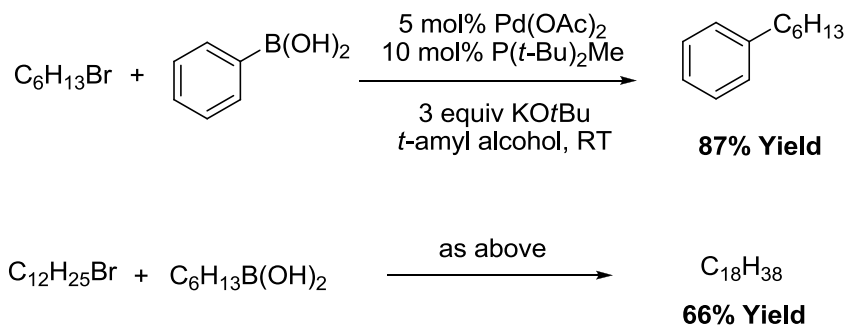
The development of cross-coupling protocols for alkyl electrophiles has been substantially more successful than that of their nucleophilic counterparts. Suzuki reported the Pd-catalyzed cross-coupling of an alkyl iodide to a *B*-alkyl-(9-BBN) derivative in 1992<sup>59</sup> (Scheme 1-18) and by the end of the decade, Knochel had developed a synthetically useful Ni-catalyzed Negishi-type coupling of alkyl iodides to organozinc reagents.<sup>40, 60</sup> The systematic development of a general protocol for both primary and secondary alkyl electrophiles however, would come through work done by the Fu group throughout the 2000s.



**Scheme 1-18:** Alkyl-Alkyl cross-coupling between alkyl iodides and primary organoboranes.<sup>59</sup>

In terms of cross-coupling viability, the limitations associated with alkyl electrophiles are akin to those of alkyl boronic ester derivatives; a slow oxidative addition replaces the sluggish transmetalation but both processes are vulnerable to  $\beta$ -hydride elimination.<sup>6</sup> The Fu group was well-armed to confront the issue of slow oxidative additions, given their previous experience in the field of electron-rich ligand development for the activation of aryl chlorides (*vide supra*). In 2001, Fu reported a general protocol for the Negishi cross-coupling of previously inert aryl and vinyl chlorides with organozinc species, using the electron rich  $\text{PCy}_3$  or  $\text{P}(\text{tBu})_3$  phosphine ligands. Though elevated temperatures were needed, it was shown that the  $\text{sp}^2$  C-Cl bond could, in fact, be

activated, leading to the syntheses of sterically congested biaryls and synthetically useful styrene motifs.<sup>61</sup> With a Pd-catalyst system capable of activating previously inert carbon-halide bonds, the Fu group turned its attention to another such example: alkyl bromides. Perhaps not surprisingly, when a very similar catalyst system was used (with the addition of  $K_3PO_4 \cdot H_2O$  base), primary alkyl bromides were coupled to *B*-alkyl-(9-BBN) organoboranes in moderate to good yields.<sup>62</sup> Fu's success with primary alkyl bromides was not limited to the difficult-to-handle organoboranes; with a modified ligand system and judicious choice of solvent following an extensive optimization, both alkyl and vinyl boronic acids could be reacted with alkyl bromides (Scheme 1-19).<sup>63</sup>



**Scheme 1-19:** Cross-coupling of both aryl- and alkyl boronic acids to primary alkyl bromides.

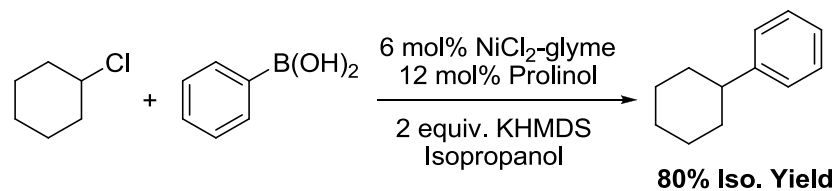
Unfortunately, activation of the notoriously inert alkyl *chloride* bond, known to be over 10 kcal/mol stronger than an alkyl bromide bond,<sup>64</sup> proved to be elusive under these conditions. Undeterred, the Fu group reported in 2002 that a  $Pd_2(dba)_3/PCy_3$  catalyst system could, with a super-stoichiometric amount of  $CsOH \cdot H_2O$ , activate primary alkyl chloride bonds towards oxidative addition.<sup>65</sup> Mechanistic work indicated

that a strongly negative entropy of activation existed for the cross-coupling of alkyl halides and, together with data on the effect of solvent polarity on activation energy, Fu determined that the oxidative addition of alkyl halides by Pd proceeded *via* an S<sub>N</sub>2 pathway.<sup>66</sup> The S<sub>N</sub>2-type mechanism of oxidative addition is well-established for Pd and Ir metal centres, and is favored by the low steric encumbrance of the primary alkyl halide.<sup>67</sup>

### 1.5.2 Suzuki-Miyaura Coupling of Secondary *sp*<sup>3</sup>-hybridized Electrophiles

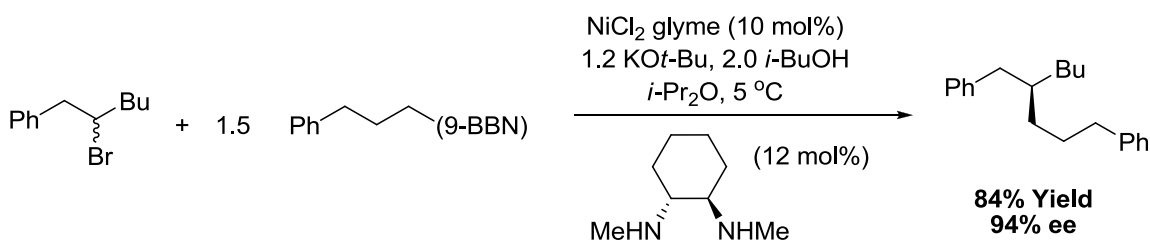
Given that the Suzuki-Miyaura reaction of *primary* alkyl electrophiles is tempered by a slow, S<sub>N</sub>2-type oxidative addition to Pd, the successful cross-coupling of the more hindered *secondary* alkyl halides should be expected to be even harder to achieve. Once again, inspiration for this new type of Suzuki-Miyaura protocol was found in work done on the analogous Negishi type reaction. Though pioneered by Knochel through the late 1990s, all examples reported were of primary alkyl bromides and iodides. It was not until 2003 that Fu reported the first examples of the successful Ni-catalyzed cross-coupling of *secondary* alkyl bromides and iodides with alkylzinc reagents.<sup>68</sup> One year later, a similar nickel-based catalyst system was used to affect the first Suzuki-Miyaura type reaction between secondary alkyl halides and phenylboronic acid.<sup>69</sup> In this case, replacing Ni with Pd led to a complete shut down of the reaction, indicating that a one-electron radical process, typical of Ni, was likely at play during the successful oxidative

addition step. In time, even the once unimaginable cross-coupling of secondary alkyl chlorides was achieved through Ni-catalyzed processes (Scheme 1-20).<sup>70</sup>



**Scheme 1-20:** Ni-catalyzed cross-coupling of *sec*-alkyl chloride with phenylboronic acid.

Like with the alkyl boronic esters, the true inspiration behind developing cross-coupling protocols for secondary alkyl electrophiles was to open the door to asymmetric C-C bond forming events. In 2008, Saito and Fu finally realized that goal, whereby a racemic secondary alkyl bromide was cross-coupled to a primary organoborane in the presence of a chiral diamine ligand (Scheme 1-21).<sup>71</sup> This stereoconvergent process led to alkyl-alkyl coupling products in high yields and enantiomeric excesses. Most recently, this asymmetric process has been extended to arylboranes<sup>72</sup> and aryl Grignards.<sup>73</sup>



**Scheme 1-21:** Stereoconvergent cross-coupling of a racemic homobenzylic secondary bromide and a primary organoborane.

Simply by optimizing catalytic systems, often by only varying the ligand, the Fu group has systematically, and almost single-handedly, created the field of asymmetric cross-coupling of alkyl electrophiles. It must be noted that, over a decade later, secondary boronic ester derivatives have *still* not been successfully coupled to secondary alkyl electrophiles, further outlining the difficulties that exist when working with secondary coupling partners.

## 1.6 General Summary and Outlook

With advances arriving in the form of trifluoroborate salts, transmetalation-facilitating additives for primary alkyl boron coupling and bulky, electron rich ligands to enable the oxidative addition of both primary and secondary alkyl electrophiles, the applicability of the Suzuki-Miyaura reaction had been almost completely flushed out in less than a generation after the seminal publication in 1979. That said, by the later stages of the 2000s, the cross-coupling of secondary boronic esters had remained virtually unknown, and would stand as one of the last challenges remaining to those pushing Suzuki-Miyaura methodologies.

It was against this backdrop that we undertook our studies into developing a general protocol for the cross-coupling of chiral secondary boronic esters with the retention of stereochemistry. That previous examples were rare and limited to very privileged systems (cyclopropyl boronic esters and larger, symmetric rings) was certainly



not from lack of interest or lack of trying. Indeed, most groups whose work is outlined above had pursued the topic with varying degrees of success. In the case of Fu, Hartwig and Molander, this preliminary work is published; for others, admission of their failed efforts would only happen after the fact.

Of course, those members of the Crudden group who would develop the silver-mediated protocol would benefit from the fortuitous link between the branched regioselectivity of the hydroboration reaction of styrene derivatives and the initial requirement, under our conditions, of the secondary boronic ester to be benzylic. The next two chapters will discuss the optimization and understanding of this new protocol and finally, its application to the cross-coupling of novel asymmetric secondary boronic esters to produce, in some case, previously inaccessible organic frameworks.

## 1.7 References

- (1) Carey, J. S.; Laffan, D.; Thomson, C.; Williams, M. T. Analysis of the reactions used for the preparation of drug candidate molecules. *Org. Biomol. Chem.* **2006**, 4, 2337-2347.
- (2) Suzuki, A. Cross-Coupling Reactions of Organoboranes: An Easy Way To Construct C-C Bonds (Nobel Lecture). *Angew. Chem. Int. Ed.* **2011**, 50, 6722-6737.
- (3) Doucet, H. Suzuki–Miyaura Cross-Coupling Reactions of Alkylboronic Acid Derivatives or Alkyltrifluoroborates with Aryl, Alkenyl or Alkyl Halides and Triflates. *Eur. J. Org. Chem.* **2008**, 2008, 2013-2030.
- (4) Rudolph, A.; Lautens, M. Secondary Alkyl Halides in Transition-Metal-Catalyzed Cross-Coupling Reactions. *Angew. Chem. Int. Ed.* **2009**, 48, 2656-2670.

- (5) Jana, R.; Pathak, T. P.; Sigman, M. S. Advances in Transition Metal (Pd,Ni,Fe)-Catalyzed Cross-Coupling Reactions Using Alkyl-organometallics as Reaction Partners. *Chem. Rev.* **2011**, 111, 1417-1492.
- (6) Miyaura, N.; Suzuki, A. Palladium-Catalyzed Cross-Coupling Reactions of Organoboron Compounds. *Chem. Rev.* **1995**, 95, 2457-2483.
- (7) Molander, G. A.; Canturk, B. Organotrifluoroborates and Monocoordinated Palladium Complexes as Catalysts—A Perfect Combination for Suzuki–Miyaura Coupling. *Ang. Chem. Int. Ed.* **2009**, 48, 2-24.
- (8) Matteson, D. S.; Man, H.; Ho, O. C. Asymmetric Synthesis of Stegobinone via Boronic Ester Chemistry. *J. Am. Chem. Soc.* **1996**, 118, 4560-4566.
- (9) Stymiest, J. L.; Dutheuil, G.; Mahmood, A.; Aggarwal, V. K. Lithiated Carbamates: Chiral Carbenoids for Iterative Homologation of Boranes and Boronic Esters. *Angew. Chem. Int. Ed.* **2007**, 46, 7491-7494.
- (10) Crudden, C. M.; Hleba, Y. B.; Chen, A. C. Regio- and Enantiocontrol in the Room-Temperature Hydroboration of Vinyl Arenes with Pinacol Borane. *J. Am. Chem. Soc.* **2004**, 126, 9200-9201.
- (11) Garrett, C. E.; Prasad, K. The Art of Meeting Palladium Specifications in Active Pharmaceutical Ingredients Produced by Pd-Catalyzed Reactions. *Adv. Synth. Catal.* **2004**, 346, 889-900.
- (12) Imao, D.; Glasspoole, B. W.; Laberge, V. S.; Crudden, C. M. Cross Coupling Reactions of Chiral Secondary Organoboronic Esters With Retention of Configuration. *J. Am. Chem. Soc.* **2009**, 131, 5024-5025.
- (13) Glasspoole, B. W.; Webb, J. D.; Crudden, C. M. Catalysis with chemically modified mesoporous silicas: Stability of the mesostructure under Suzuki–Miyaura reaction conditions. *J. Catal.* **2009**, 265, 148-154.

- (14) Grignard, V. Sur quelques nouvelles combinaisons organometallique du magnesium et leur application a des syntheses d'alcools et hydrocarbures. *C.R. Acad. Sci., Ser. Ilc: Chim.* **1900**, 130, 1322-1324.
- (15) Smith, M. B.; March, J. *March's Advanced Organic Chemistry*; John Wiley and Sons: New York, 2001; pp 2083.
- (16) Corriu, R. J. P.; Masse, J. P. Activation of Grignard reagents by transition-metal complexes. A new and simple synthesis of trans-stilbenes and polyphenyls. *J. Chem. Soc., Chem. Commun.* **1972**, 144a-144a.
- (17) Tamao, K.; Sumitani, K.; Kumada, M. Selective carbon-carbon bond formation by cross-coupling of Grignard reagents with organic halides. Catalysis by nickel-phosphine complexes. *J. Am. Chem. Soc.* **1972**, 94, 4374-4376.
- (18) Negishi, E. Palladium- or nickel-catalyzed cross coupling. A new selective method for carbon-carbon bond formation. *Acc. Chem. Res.* **1982**, 15, 340-348.
- (19) Baba, S.; Negishi, E. A novel stereospecific alkenyl-alkenyl cross-coupling by a palladium- or nickel-catalyzed reaction of alkenylalanes with alkenyl halides. *J. Am. Chem. Soc.* **1976**, 98, 6729-6731.
- (20) Miyaura, N.; Yamada, K.; Suzuki, A. A new stereospecific cross-coupling by the palladium-catalyzed reaction of 1-alkenylboranes with 1-alkenyl or 1-alkynyl halides. *Tetrahedron Lett.* **1979**, 20, 3437-3440.
- (21) Negishi, E.; King, A. O.; Okukado, N. Selective carbon-carbon bond formation via transition metal catalysis. 3. A highly selective synthesis of unsymmetrical biaryls and diarylmethanes by the nickel- or palladium-catalyzed reaction of aryl- and benzylzinc derivatives with aryl halides. *J. Org. Chem.* **1977**, 42, 1821-1823.
- (22) Brown, H. C.; Veeraraghavan Ramachandran, P. Versatile  $\alpha$ -pinene-based borane reagents for asymmetric syntheses. *J. Organomet. Chem.* **1995**, 500, 1-19.

- (23) Miyaura, N.; Yamada, K.; Suginome, H.; Suzuki, A. Novel and convenient method for the stereo- and regiospecific synthesis of conjugated alkadienes and alkenynes via the palladium-catalyzed cross-coupling reaction of 1-alkenylboranes with bromoalkenes and bromoalkynes. *J. Am. Chem. Soc.* **1985**, 107, 972-980.
- (24) Hull, K. L.; Lanni, E. L.; Sanford, M. S. Highly Regioselective Catalytic Oxidative Coupling Reactions: Synthetic and Mechanistic Investigations. *J. Am. Chem. Soc.* **2006**, 128, 14047-14049.
- (25) Ball, N. D.; Gary, J. B.; Ye, Y.; Sanford, M. S. Mechanistic and Computational Studies of Oxidatively-Induced Aryl-CF<sub>3</sub> Bond-Formation at Pd: Rational Design of Room Temperature Aryl Trifluoromethylation. *J. Am. Chem. Soc.* **2011**, 133, 7577-7584.
- (26) Grushin, V. V.; Alper, H. Alkali-induced disproportionation of palladium(II) tertiary phosphine complexes, [L<sub>2</sub>PdCl<sub>2</sub>], to LO and palladium(0). Key intermediates in the biphasic carbonylation of ArX catalyzed by [L<sub>2</sub>PdCl<sub>2</sub>]. *Organometallics* **1993**, 12, 1890-1901.
- (27) Amatore, C.; Carre, E.; Jutand, A.; M'Barki, M. A. Rates and Mechanism of the Formation of Zerovalent Palladium Complexes from Mixtures of Pd(OAc)<sub>2</sub> and Tertiary Phosphines and Their Reactivity in Oxidative Additions. *Organometallics* **1995**, 14, 1818-1826.
- (28) Martin, R.; Buchwald, S. L. Palladium-Catalyzed Suzuki-Miyaura Cross-Coupling Reactions Employing Dialkylbiaryl Phosphine Ligands. *Acc. Chem. Res.* **2008**, 41, 1461-1473.
- (29) Fu, G. C. The Development of Versatile Methods for Palladium-Catalyzed Coupling Reactions of Aryl Electrophiles through the Use of P(t-Bu)<sub>3</sub> and PCy<sub>3</sub> as Ligands. *Acc. Chem. Res.* **2008**, 41, 1555-1564.

- (30) Kataoka, N.; Shelby, Q.; Stambuli, J. P.; Hartwig, J. F. Air Stable, Sterically Hindered Ferrocenyl Dialkylphosphines for Palladium-Catalyzed C-C, C-N, and C-O Bond-Forming Cross-Couplings. *J. Org. Chem.* **2002**, *67*, 5553-5566.
- (31) Hartwig, J. F.; Paul, F. Oxidative Addition of Aryl Bromide after Dissociation of Phosphine from a Two-Coordinate Palladium(0) Complex, Bis(tri-*o*-tolylphosphine)Palladium(0). *J. Am. Chem. Soc.* **1995**, *117*, 5373-5374.
- (32) Barrios-Landeros, F.; Hartwig, J. F. Distinct Mechanisms for the Oxidative Addition of Chloro-, Bromo-, and Iodoarenes to a Bisphosphine Palladium(0) Complex with Hindered Ligands. *J. Am. Chem. Soc.* **2005**, *127*, 6944-6945.
- (33) Lam, K. C.; Marder, T. B.; Lin, Z. DFT Studies on the Effect of the Nature of the Aryl Halide Y-C<sub>6</sub>H<sub>4</sub>-X on the Mechanism of Its Oxidative Addition to Pd<sup>0</sup>L versus Pd<sup>0</sup>L<sub>2</sub>. *Organometallics* **2007**, *26*, 758-760.
- (34) Itami, K.; Tonogaki, K.; Ohashi, Y.; Yoshida, J. Rapid Construction of Multisubstituted Olefin Structures Using Vinylboronate Ester Platform Leading to Highly Fluorescent Materials. *Org. Lett.* **2004**, *6*, 4093-4096.
- (35) Braga, A. A. C.; Morgon, N. H.; Ujaque, G.; Maseras, F. Computational Characterization of the Role of the Base in the Suzuki-Miyaura Cross-Coupling Reaction. *J. Am. Chem. Soc.* **2005**, *127*, 9298-9307.
- (36) Amatore, C.; Jutand, A.; Le Duc, G. Kinetic Data for the Transmetalation/Reductive Elimination in Palladium Catalyzed Suzuki-Miyaura Reactions: Unexpected Triple Role of Hydroxide Ions Used as Base. *Chem. Eur. J.* **2011**, *17*, 2492-2503.
- (37) Moravskiy, A.; Stille, J. K. Mechanisms of 1,1-reductive elimination from palladium: elimination of ethane from dimethylpalladium(II) and trimethylpalladium(IV). *J. Am. Chem. Soc.* **1981**, *103*, 4182-4186.

- (38) Fujita, K.; Yamashita, M.; Puschmann, F.; Alvarez-Falcon, M.; Incarvito, C. D.; Hartwig, J. F. Organometallic Chemistry of Amidate Complexes. Accelerating Effect of Bidentate Ligands on the Reductive Elimination of N-Aryl Amidates from Palladium(II). *J. Am. Chem. Soc.* **2006**, 128, 9044-9045.
- (39) Grushin, V. V.; Marshall, W. J. Facile Ar-CF<sub>3</sub> Bond Formation at Pd. Strikingly Different Outcomes of Reductive Elimination from [(Ph<sub>3</sub>P)<sub>2</sub>Pd(CF<sub>3</sub>)Ph] and [(Xantphos)Pd(CF<sub>3</sub>)Ph]. *J. Am. Chem. Soc.* **2006**, 128, 12644-12645.
- (40) Devasagayaram, A.; Studemann, T.; Knochel, P. A New Nickel-Catalyzed Cross-Coupling Reaction Between sp<sup>3</sup> Carbon Centers. *Angew. Chem. Int. Ed. Engl.* **1995**, 34, 2723-2725.
- (41) Fairlamb, I. J. S.  $\pi$ -Acidic alkene ligand effects in Pd-catalysed cross-coupling processes: exploiting the interaction of dibenzylidene acetone (dba) and related ligands with Pd(0) and Pd(II). *Org. Biomol. Chem.* **2008**, 6, 3645-3656.
- (42) Miyaura, N.; Ishiyama, T.; Sasaki, H.; Ishikawa, M.; Sato, M.; Suzuki, A. Palladium-catalyzed inter- and intramolecular cross-coupling reactions of B-alkyl-9-borabicyclo[3.3.1]nonane derivatives with 1-halo-1-alkenes or haloarenes. Syntheses of functionalized alkenes, arenes, and cycloalkenes via a hydroboration-coupling sequence. *J. Am. Chem. Soc.* **1989**, 111, 314-321.
- (43) Uenishi, J.; Beau, J. M.; Armstrong, R. W.; Kishi, Y. Dramatic rate enhancement of Suzuki diene synthesis. Its application to palytoxin synthesis. *J. Am. Chem. Soc.* **1987**, 109, 4756-4758.
- (44) Sato, M.; Miyaura, N.; Suzuki, A. Cross-Coupling Reaction of Alkyl- or Arylboronic Acid Esters with Organic Halides Induced by Thallium(I) Salts and Palladium-Catalyst. *Chem. Lett.* **1989**, 18, 1405-1408.
- (45) Zou, G.; Reddy, Y. K.; Falck, J. R. Ag(I)-promoted Suzuki-Miyaura cross-couplings of n-alkylboronic acids. *Tetrahedron Lett.* **2001**, 42, 7213-7215.

- (46) Molander, G. A.; Yun, C. Cross-coupling reactions of primary alkylboronic acids with aryl triflates and aryl halides. *Tetrahedron* **2002**, 58, 1465-1470.
- (47) Molander, G. A.; Ito, T. Cross-Coupling Reactions of Potassium Alkyltrifluoroborates with Aryl and 1-Alkenyl Trifluoromethanesulfonates. *Org. Lett.* **2001**, 3, 393-396.
- (48) Wang, X.; Deng, M. Cross-coupling reaction of cyclopropylboronic acid with bromoarenes. *J. Chem. Soc., Perkin Trans. 1* **1996**, 2663-2664.
- (49) Charette, A.; De Freitas-Gil, R. P. Synthesis of contiguous cyclopropanes by palladium-catalyzed suzuki-type cross-coupling reactions. *Tetrahedron Lett.* **1997**, 38, 2809-2812.
- (50) Wallace, D. J.; Chen, C. Cyclopropylboronic acid: synthesis and Suzuki cross-coupling reactions. *Tetrahedron Lett.* **2002**, 43, 6987-6990.
- (51) Littke, A. F.; Dai, C.; Fu, G. C. Versatile Catalysts for the Suzuki Cross-Coupling of Arylboronic Acids with Aryl and Vinyl Halides and Triflates under Mild Conditions. *J. Am. Chem. Soc.* **2000**, 122, 4020-4028.
- (52) Fang, G.; Yan, Z.; Deng, M. Palladium-Catalyzed Cross-Coupling of Stereospecific Potassium Cyclopropyl Trifluoroborates with Aryl Bromides. *Org. Lett.* **2004**, 6, 357-360.
- (53) van den Hoogenband, A.; Lange, J. H. M.; Terpstra, J. W.; Koch, M.; Visser, G. M.; Visser, M.; Korstanje, T. J.; Jastrzebski, J. T. B. H. Ruphos-mediated Suzuki cross-coupling of secondary alkyl trifluoroborates. *Tetrahedron Lett.* **2008**, 49, 4122-4124.
- (54) Molander, G. A.; Gormisky, P. E. Cross-Coupling of Cyclopropyl- and Cyclobutyltrifluoroborates with Aryl and Heteroaryl Chlorides. *J. Org. Chem.* **2008**, 73, 7481-7485.

- (55) Dreher, S. D.; Dormer, P. G.; Sandrock, D. L.; Molander, G. A. Efficient Cross-Coupling of Secondary Alkyltrifluoroborates with Aryl Chlorides— Reaction Discovery Using Parallel Microscale Experimentation. *J. Am. Chem. Soc.* **2008**, 130, 9257-9259.
- (56) Butters, M.; Harvey, J. N.; Jover, J.; Lennox, A. J. J.; Lloyd-Jones, G. C.; Murray, P. M. Aryl Trifluoroborates in Suzuki–Miyaura Coupling: The Roles of Endogenous Aryl Boronic Acid and Fluoride. *Angew. Chem. Int. Ed.* **2010**, 49, 5156-5160.
- (57) Zou, G.; Falck, J. R. Suzuki-Miyaura cross-coupling of lithium n-alkylborates. *Tetrahedron Lett.* **2001**, 42, 5817-5819.
- (58) Rubina, M.; Rubin, M.; Gevorgyan, V. Catalytic Enantioselective Hydroboration of Cyclopropenes. *J. Am. Chem. Soc.* **2003**, 125, 7198-7199.
- (59) Ishiyama, T.; Abe, S.; Miyaura, N.; Suzuki, A. Palladium-Catalyzed Alkyl-Alkyl Cross-Coupling Reaction of 9-Alkyl-9-BBN Derivatives with Iodoalkanes Possessing  $\beta$ -Hydrogens. *Chem. Lett.* **1992**, 21, 691-694.
- (60) Giovannini, R.; Studemann, T.; Dussin, G.; Knochel, P. An Efficient Ni-Catalyzed Cross-Coupling Between  $sp^3$  Carbon Centres. *Angew. Chem. Int. Ed.* **1998**, 37, 2387-2390.
- (61) Dai, C.; Fu, G. C. The First General Method for Palladium-Catalyzed Negishi Cross-Coupling of Aryl and Vinyl Chlorides: Use of Commercially Available  $Pd(P(t-Bu)_3)_2$  as a Catalyst. *J. Am. Chem. Soc.* **2001**, 123, 2719-2724.
- (62) Netherton, M. R.; Dai, C.; Neuschz, K.; Fu, G. C. Room-Temperature Alkyl-Alkyl Suzuki Cross-Coupling of Alkyl Bromides that Possess  $\beta$ -Hydrogens. *J. Am. Chem. Soc.* **2001**, 123, 10099-10100.
- (63) Kirchhoff, J. H.; Netherton, M. R.; Hills, I. D.; Fu, G. C. Boronic Acids: New Coupling Partners in Room-Temperature Suzuki Reactions of Alkyl Bromides.



Crystallographic Characterization of an Oxidative-Addition Adduct Generated under Remarkably Mild Conditions. *J. Am. Chem. Soc.* **2002**, 124, 13662-13663.

(64) Kirchoff, J. H.; Dai, C.; Fu, G., C. A method for Palladium-Catalyzed Cross-Couplings of Simple Alkyl Chlorides: Suzuki Reactions Catalyzed by  $[\text{Pd}_2(\text{dba}_3)]/\text{PCy}_3$ . *Angew. Chem. Int. Ed.* **2002**, 41, 1945-1947.

(65) Kirchoff, J. H.; Dai, C.; Fu, G. C. A Method for Pd-Catalyzed Cross-Couplings of Simple Alkyl Chlorides: Suzuki Reactions Catalyzed by  $[\text{Pd}_2(\text{dba}_3)]/\text{PCy}_3$ . *Angew. Chem. Int. Ed.* **2002**, 41, 1945-1947.

(66) Hills, I. D.; Netherton, M. R.; Fu, G. C. Toward an Improved Understanding of the Unusual Reactivity of  $\text{Pd}^0$ /Trialkylphosphane Catalysts in Cross-Couplings of Alkyl Electrophiles: Quantifying the Factors That Determine the Rate of Oxidative Addition. *Angew. Chem. Int. Ed.* **2003**, 42, 5749-5752.

(67) Furuya, T.; Strom, A. E.; Ritter, T. Silver-Mediated Fluorination of Functionalized Aryl Stannanes. *J. Am. Chem. Soc.* **2009**, 131, 1662-1663.

(68) Zhou, J.; Fu, G. C. Cross-Couplings of Unactivated Secondary Alkyl Halides: Room-Temperature Nickel-Catalyzed Negishi Reactions of Alkyl Bromides and Iodides. *J. Am. Chem. Soc.* **2003**, 125, 14726-14727.

(69) Zhou, J.; Fu, G. C. Suzuki Cross-Couplings of Unactivated Secondary Alkyl Bromides and Iodides. *J. Am. Chem. Soc.* **2004**, 126, 1340-1341.

(70) Gonzalez-Bobes, F.; Fu, G. C. Amino Alcohols as Ligands for Nickel-Catalyzed Suzuki Reactions of Unactivated Alkyl Halides, Including Secondary Alkyl Chlorides, with Arylboronic Acids. *J. Am. Chem. Soc.* **2006**, 128, 5360-5361.

(71) Saito, B.; Fu, G. C. Enantioselective Alkyl-Alkyl Suzuki Cross-Couplings of Unactivated Homobenzylic Halides. *J. Am. Chem. Soc.* **2008**, 130, 6694-6695.

(72) Lundin, P. M.; Fu, G. C. Asymmetric Suzuki Cross-Couplings of Activated Secondary Alkyl Electrophiles: Arylations of Racemic  $\beta$ -Chloroamides. *J. Am. Chem. Soc.* **2010**, 132, 11027-11029.

(73) Lou, S.; Fu, G. C. Nickel/Bis(oxazoline)-Catalyzed Asymmetric Kumada Reactions of Alkyl Electrophiles: Cross-Couplings of Racemic  $\beta$ -Bromoketones. *J. Am. Chem. Soc.* **2010**, 132, 1264-1266.

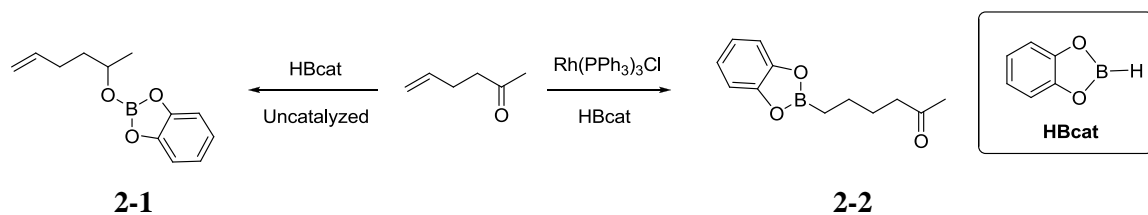
## Chapter 2

# The Cross-Coupling of Secondary Boronic Esters with Retention of Stereochemistry

### 2.1 Introduction

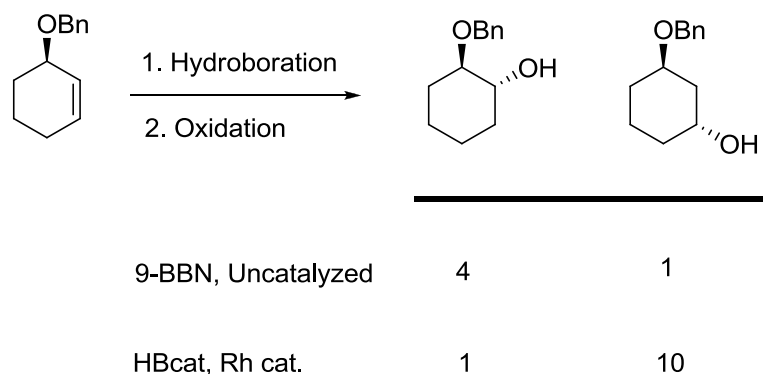
#### 2.1.1 Hydroboration of Styrene Derivatives

Our interest in the field of secondary boronic ester cross-coupling was borne out of previous work done in our group on the asymmetric hydroboration of styrene derivatives.<sup>1</sup> First disclosed in 1985 by Manning and Noth,<sup>2</sup> the metal-catalyzed hydroboration reaction was more selective and required milder conditions than its uncatalyzed counterpart. Indeed, in the presence of a catalytic amount of Wilkinson's catalyst, catecholborane (HBCat) is able to hydroborate alkenes at room temperature, foregoing the elevated temperatures needed for the uncatalyzed process. Most impressive, though, was the noted chemoselectivity of the catalyzed hydroboration of a ketone-containing olefin. In the uncatalyzed reaction, the oxophilicity of boron dominates, leading to a selective hydroboration of the ketone (**2-1**); conversely, in the Rh-catalyzed variant, the selectivity is reversed with complete selectivity for the olefin-hydroboration being observed (**2-2**, Scheme 2-1).



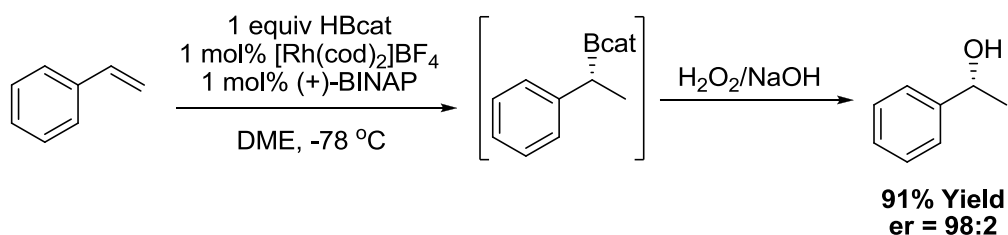
**Scheme 2-1:** Chemoselectivity of the Rh-catalyzed hydroboration reaction.<sup>2</sup>

Though remarkable *chemoselectivity* for olefins was observed, controlling the *regioselectivity* of the hydroboration across an unsymmetric olefin had not been pursued. The Evans group began to address this issue in 1988 with the first paper dedicated to the regioselectivity of the hydroboration in cyclic alkenes with pendant allylic alcohols and ethers serving as directing groups.<sup>3</sup> Interestingly, *anti* facial selectivity was observed for both the uncatalyzed hydroboration by HBcat and the reaction catalyzed by a phosphine–ligated cationic Rh complex. Where the processes diverge is in their respective regioselectivities, with the uncatalyzed reaction leading to the 2-substituted alcohol and the catalyzed reaction installing the boronic ester at the distal 3-position (Scheme 2-2).



**Scheme 2-2:** Regioselectivity of the Rh-catalyzed hydroboration reaction as demonstrated by Evans.<sup>3</sup>

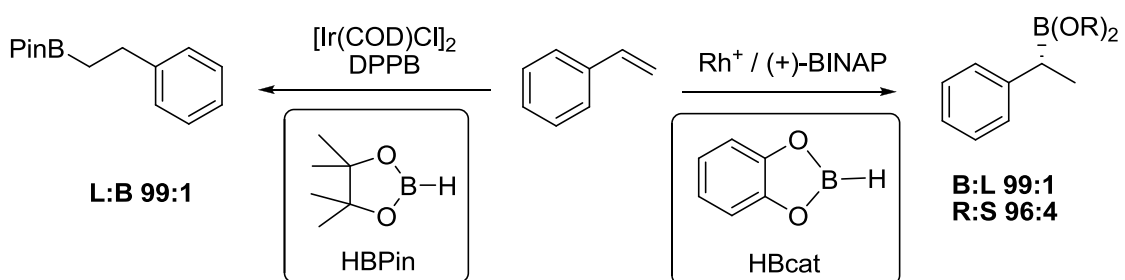
The question of *regio*- and *enantio*selectivity was more fully brought to light by the work of Hayashi and Ito in 1989.<sup>4</sup> They noted that the regioselectivity of the reaction could be changed to favor the Markovnikov product by using cationic Rh catalysts and phosphine ligands during the hydroboration of styrene using HBCat. For example, 1 mol% of  $[\text{Rh}(\text{COD})_2]\text{BF}_4$ , combined with 1,4-bis(diphenylphosphine)butane (dppb) to form an active catalyst capable of imposing a branched:linear ratio of >99:1 on the product boronic ester. That the phosphine ligand was in some way affecting the nature of the transition state during the regioselectivity-determining step made it conceivable that the same could be true of the *enantio*selectivity-determining step. Thus a non-racemic diphosphine ligand, (+)-BINAP, was used and after subsequent oxidation of the boronic ester, gave rise to the benzylic alcohol (Scheme 2-3) in high *regio*- (99:1) and *enantio*selectivity (85-95% ee).



**Scheme 2-3:** Branched selectivity achieved with the bidentate phosphine-ligated Rh-catalyzed hydroboration reaction.

Up to this point, the majority of metal-catalyzed hydroborations were performed with HBcat, as the tempering of its Lewis acidity by oxygen lone-pair donation to the empty boron p-orbital was needed to limit the uncatalyzed background reaction with olefins. Pinacolborane, (HBPin, Scheme 2-4) is considerably easier to handle and the boronic acid pinacolate esters that would result from its use in the hydroboration reaction are typically stable to air and chromatographic purification, unlike their catechol analogues. The steric bulk provided by the pinacol functionality could, however, decrease any selectivity for the more sterically congested branched site. Work in our laboratory showed that the hydroboration of styrenes could be achieved directly with HBPin at room temperature using a cationic rhodium catalyst, and that with judicious choice of bidentate phosphine ligand (dppb once again showed the most favorable results) very high B:L ratios could be obtained.<sup>5</sup> As in the preceding work by Hayashi and Ito, the high *regioselectivities* obtained with the bidentate phosphine ligand (dppb) allowed for the smooth transition to non-racemic bidentate ligands to interrogate *enantioselectivity*. Though BINAP-modified catalysts provided mixtures of branched and linear products when using HBpin, non-racemic Josiphos ligands gave moderate B:L ratios of about 3:1.

Amazingly, catalysts modified by this ligand gave *opposite enantiomers of the product, depending on whether HBPIn or HBcat was used as the hydroborating reagent*. A similar phenomenon was observed for hydroborations with Quinap-modified catalysts.<sup>6</sup> Furthermore, the Cruden group discovered that irrespective of ligand or styrene derivative, the use of iridium as a substitute for rhodium led to complete selectivity for the linear isomer (Scheme 2-4), illustrating the sensitive nature of this reaction.<sup>5</sup>



**Scheme 2-4:** Illustration of the regio- and enantioselectivity of the metal catalyzed hydroboration of styrene.

### 2.1.2 Elaboration of Hydroboration Products

In the twenty years after Manning and Noth's seminal paper on the metal-catalyzed hydroboration reaction,<sup>2</sup> the process had been advanced to include regioselectivities complementary to the uncatalyzed reaction and had been rendered enantioselective.<sup>6</sup> In terms of applicability, however, the process was falling short of its potential, as the resultant boronic esters were virtually exclusively being oxidized to

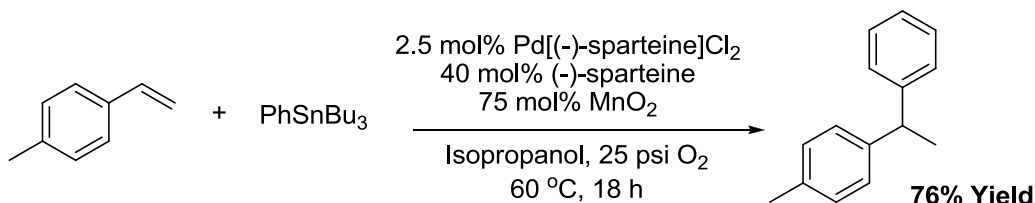
alcohols.<sup>4</sup> Considering the numerous routes to enantioenriched *sec*-phenethanol, this transformation is not hugely value added.<sup>7</sup>

Alternatives to boronic ester oxidation do exist, but are limited. Indeed, our group has developed an asymmetric hydroboration-homologation protocol to access 2-aryl propionic acids<sup>8</sup> and the amination protocol developed by the Brown group has led to chiral benzyl amines in high er from non-racemic benzyl boronic esters.<sup>9</sup> That said, an enantiospecific cross-coupling protocol, so important to the pharmaceutical industry,<sup>10</sup> was still lacking.

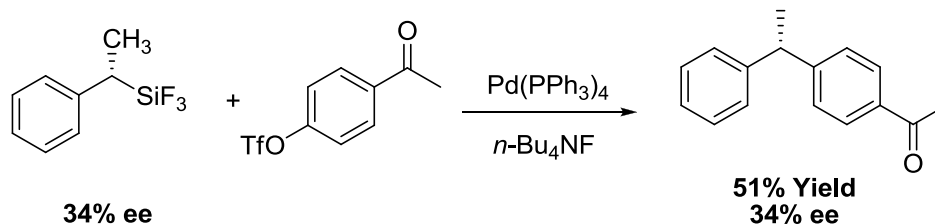
It was under this umbrella of thought that our group set forth to truly capitalize on the advances of the catalyzed hydroboration reaction by utilizing the resultant alkyl boronic ester moieties, not as alcohol precursors, but as Suzuki-type cross-coupling partners. Should this prove successful, it would stand to benefit both reactions, for at this time, no Suzuki-Miyaura protocol had yet been performed on chiral secondary boronic esters with the exception of cyclopropyl derivatives. Furthermore, the transformation of the hydroboration product to 1,1-diaryl alkanes provides an extremely valuable route to these difficult compounds. Indeed, prior to our Suzuki-Miyaura cross-coupling strategy, very few synthetic routes to 1,1-diarylethanes were known, amongst which stereospecific syntheses were even more rare (Scheme 2-5). Sigman and co-workers have put forth very elegant work on the hydroarylation of styrenes, though, despite using a near stoichiometric amount of a chiral ligand, observe no enantioselection in the product.<sup>11</sup> Hiyama's cross-coupling of benzyl silanes, though found to be almost completely stereospecific, is limited by the poor enantiomeric excesses of the starting materials.<sup>12</sup>



**Sigman 2007**



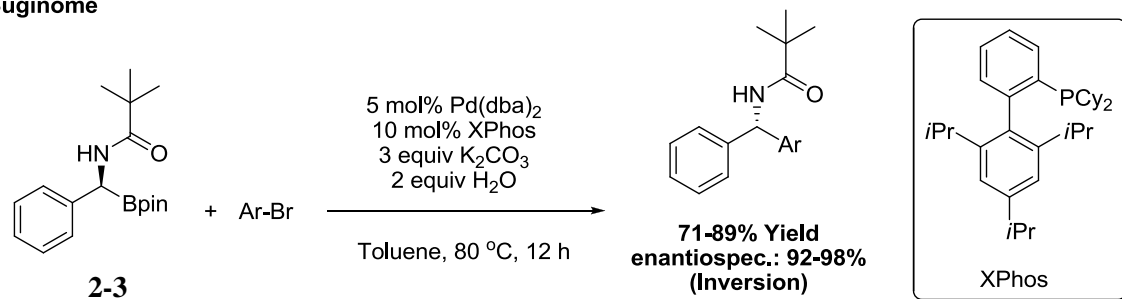
**Hiyama 1990**



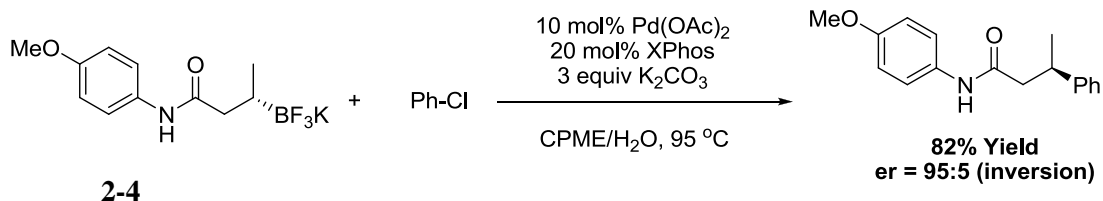
**Scheme 2-5:** Reductive hydroarylation coupling (top)<sup>11</sup> and fluoride-mediated silicon coupling (bottom) to 1,1-diarylethanes.<sup>12</sup>

Since our initial report on the stereoretentive cross-coupling of benzylic boronic esters,<sup>13</sup> chiral secondary boronic esters **2-3** and trifluoroboronate salts **2-4** have also been found to undergo successful, Pd-catalyzed cross-couplings with aryl halide electrophiles (Scheme 2-6). Indeed, Suginome,<sup>14</sup> and subsequently Molander,<sup>15</sup> took advantage of a putative intramolecular activation of the secondary boronic ester by an adjacent amide carbonyl moiety to facilitate the difficult transmetalation to Pd. Interestingly, a nearly complete *inversion* of stereochemistry is observed in both cases. This phenomenon is attributed to the aforementioned carbonyl's interaction with the vacant p-orbital of boron which effectively blocks Pd from reacting from the same face. Instead, a backside attack by Pd, leading to the observed inversion of stereochemistry, takes place.

### Suginome



### Molander



**Scheme 2-6:** Recent work from the groups of Suginome<sup>14</sup> (top) and Molander<sup>15</sup> (bottom) on the enantiospecific cross-coupling of secondary boronic ester derivatives.

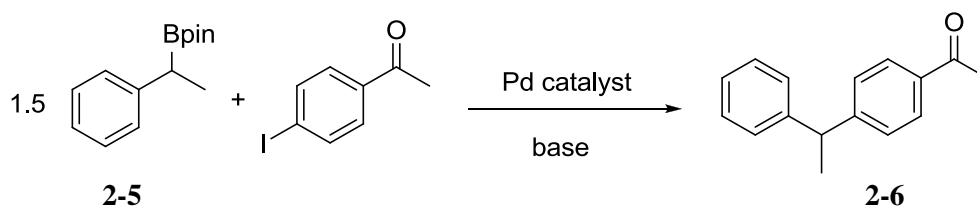
## 2.2 Cross-Coupling of Hydroborated Styrene Derivatives with Aryl Halides

### 2.2.1 Initial Reaction Development: From Zero to Sixty

The Hayashi hydroboration of styrene with catechol borane catalyzed by [Rh(COD)(BINAP)]BF<sub>4</sub> affords 1-phenylethylboronic acid pinacolate ester in high yield (65%), regioselectivity (98.5:1.5, branched:linear) and high enantioselectivity (94:6, R:S).<sup>4</sup> With both racemic and non-racemic starting materials in hand, we set out to develop successful coupling conditions of this secondary boronic ester with aryl halides.

The first successful cross-couplings were performed by postdoctoral fellow Daisuke Imao and will be summarized briefly here.<sup>13</sup> Initial attempts to affect the cross-coupling by standard routes failed (Table 2-1, entries 1,2), reasserting the difficulties associated with coupling secondary boronic esters outlined in Chapter 1. It was then decided that, of the pitfalls generally associated with secondary boronic esters as coupling partners, the sluggish transmetalation would need to be addressed first, followed then by the mitigation of any potential  $\beta$ -hydride elimination events. Inspiration was taken from the cross-coupling of primary boronic esters. Though primary *boranes* are readily transmetalated with strong inorganic bases (NaOMe, NaOH),<sup>16</sup> the inherently less reactive primary boronic acids and esters require more help, often in the form of thallium or silver salts.<sup>17</sup> In fact, for the difficult cross-coupling of bulky vinyl boronic acids, Kishi was able to demonstrate rate enhancements of two- and four orders of magnitude for Ag and Tl salts respectively, over hydroxide bases.<sup>18</sup> Shying away from toxic thallium salts,<sup>19</sup> we turned instead to silver as a transmetalation promoter. Gratifyingly, the addition of a superstoichiometric amount of Ag<sub>2</sub>O, in conjunction with a catalytic amount of the commercially available Pd(PPh<sub>3</sub>)<sub>4</sub> enabled the cross-coupling of 4-iodoacetophenone with boronic ester **2-5** in 30% GC yield (Table 2-1, entry 4). A larger excess of PPh<sub>3</sub> (with respect to Pd) was added to counter potential  $\beta$ -hydride elimination and this, together with a higher loading of Pd (8 mol%) led to cross-coupled product **2-6** in 65% GC yield (Table 2-1, entry 5).

**Table 2-1:** Development of Successful Cross Coupling Conditions.



entry	catalyst (%)	ligand (equiv.)	Base	yield (%)
1	Pd <sub>2</sub> (dba) <sub>3</sub> (2)	PPh <sub>3</sub> (8)	K <sub>3</sub> PO <sub>4</sub>	0
2	Pd <sub>2</sub> (dba) <sub>3</sub> (2)	PPh <sub>3</sub> (8)	Cs <sub>2</sub> CO <sub>3</sub>	0
3	Pd <sub>2</sub> (dba) <sub>3</sub> (2)	PPh <sub>3</sub> (4)	Ag <sub>2</sub> O	25
4	Pd(PPh <sub>3</sub> ) <sub>4</sub> (4)	none	Ag <sub>2</sub> O	30
5	Pd <sub>2</sub> (dba) <sub>3</sub> (4)	PPh <sub>3</sub> (8)	Ag <sub>2</sub> O	65
6	Pd <sub>2</sub> (dba) <sub>3</sub> (4)	PPh <sub>3</sub> (12)	Ag <sub>2</sub> O	64

Reaction Conditions: THF, 0.05 M, 70 °C, 24 h. Note: loadings given for *catalyst*, not necessarily Pd and that phosphine ligand equivalents are given with respect to the catalytic amount of Pd

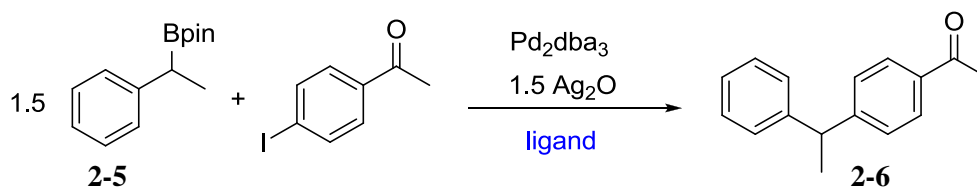
### 2.2.2 Ligand Effects on the Reaction

We next sought to improve upon this result, and by analyzing the effect of each component, we gained a better understanding of what allows this new, yet wholly uncomplicated, system to work where others failed.

The obvious place to seek improvement in yield was by examining the ligand used in the reaction. The large excess of PPh<sub>3</sub> was presumed to increase yield (compare Table 2-1, entries 3-5) by favoring a co-ordinatively saturated Pd centre during the catalytic cycle, thereby reducing the likelihood of yield-reducing β-hydride elimination reactions. Although an 8-fold excess of ligand to Pd is higher than desirable, PPh<sub>3</sub> is cheap (0.51 CAD/gram, Sigma-Aldrich) and abundantly available, therefore it would

require a significant jump in yield to justify using a different, more exotic ligand system for the reaction. With this in mind, we screened a wide variety of ligands and compared them to our standard conditions.

**Table 2-2:** Ligand screen for the cross coupling of an aryl iodide with a benzylic boronic esters.



entry	Pd loading (%)	ligand (mol%)	yield (%)
1	4	$\text{PCy}_3$ (16)	5
2	4	dppf (6.8)	2
3	4	BINAP (6)	trace
4	4	$^t\text{BuPBiPh}$ (6.4)	2
5	4	$\text{P}(p\text{-FPh})_3$ (32)	8
6	4	$\text{P}(\text{furyl})_3$ (32)	0
7	4	$\text{AsPh}_3$ (32)	0
8	4	$\text{P}(p\text{-MePh})_3$ (32)	41
9	4	$\text{PMePh}_2$	42
10	4	$\text{P}(p\text{-MeOPh})_3$ (16)	31
11	4	$\text{P}(p\text{-MeOPh})_3$ (32)	44
12	8	$\text{P}(p\text{-MeOPh})_3$ (64)	48
13	4	$\text{PPh}_3$ (16)	25
14	4	$\text{PPh}_3$ (32)	40
15	8	$\text{PPh}_3$ (64)	65

Reaction conditions: THF, 0.05 M, 70°C, 24 h.

Surprisingly, the cheapest, most readily available ligand (PPh<sub>3</sub>) outperformed all other ligands tested. The bidentate ligands tested (Table 2-2, entries 2,3) completely shut down the reaction, presumably by locking the Pd metal centre in a catalytically incompetent PdL<sub>4</sub> form. In terms of ligand electronics, electron releasing phosphines outperformed electron withdrawing ligands, though, again, neither could outmatch the bellwether triphenylphosphine (compare Table 2-2, entries 5,11 and 15).

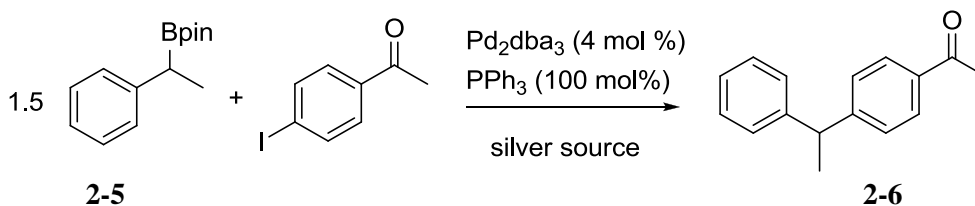
Though disappointed that the yield of the test reaction could not be augmented simply by switching ligands, we were encouraged that the ubiquitous PPh<sub>3</sub> gave the best results. Parallel studies in our group provided insight into *why* such a standard ligand was performing as well, if not better, than any other ligand tested. In measuring the kinetics of the reaction, it was determined that the reaction was first order in the secondary boronic ester and, somewhat unexpectedly, *zero order in aryl iodide*. Exotic (and expensive) phosphine<sup>20, 21</sup> and N-heterocyclic carbene (NHC) ligands<sup>22</sup> are frequently used in difficult cross-couplings, however both the electron-rich phosphines and NHCs rely on strong  $\sigma$ -donation to Pd to increase the rate of oxidative addition to an electrophile. As noted earlier, the oxidative addition to aryl halides can be, but is not always, the rate determining step (RDS) for the Suzuki-Miyaura reaction and rates depend on the halide used (I>Br>>Cl).<sup>23</sup> In our reaction, the use of an aryl iodide keen to undergo oxidative addition followed by a difficult transmetalation step renders the oxidative addition step kinetically silent and preempts any potential rate increase from electron-rich ligands. Also, electron-rich ligands are more easily oxidized which may affect their utility in this reaction (*vide infra*).

Interestingly, the very slow transmetalation seems to render the kinetics of active-catalyst formation insignificant as well. Elegant work done by the Baird group has shown that the choice of Pd pre-catalyst can have an effect on reaction rates and outcomes.<sup>24</sup> With this in mind, a highly active PdCp( $\eta^3$ -butene) catalyst was developed and has been shown to have excellent reactivity in a variety of Pd-catalyzed processes. When we employed this pre-catalyst in the silver-mediated cross-coupling of benzylic boronic esters, no improvement in yield was observed, suggesting that the formation of an active Pd-catalyst is not limiting.

### 2.2.3 Effect and Role of Silver Salts on the Reaction

Like PPh<sub>3</sub>, Ag<sub>2</sub>O is a common, relatively inexpensive reagent, and yet its addition to the reaction is critical to achieve turnover. The effect of other silver salts screened for the reaction is given in Table 2-3.

**Table 2-3:** Development of Successful Cross Coupling Conditions.



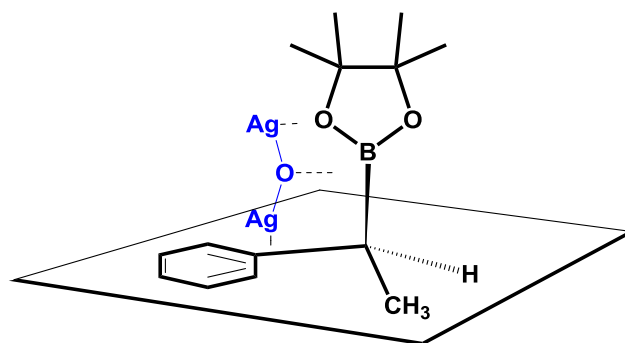
entry	silver source	equivalents	yield (%)
1	AgOAc	3	0
2	AgOTf	3	0

3	AgBF <sub>4</sub>	3	1
4	Ag <sub>2</sub> CO <sub>3</sub>	1.5	38
5	Ag <sub>2</sub> CO <sub>3</sub>	3	33
6	Ag <sub>2</sub> O	1.5	65
7	Ag <sub>2</sub> O	3	65

Reaction conditions: THF, 0.05 M, 70 °C, 24 h. Equivalents of silver source are given with respect to 4-iodoacetophenone, the stoichiometrically limiting reagent.

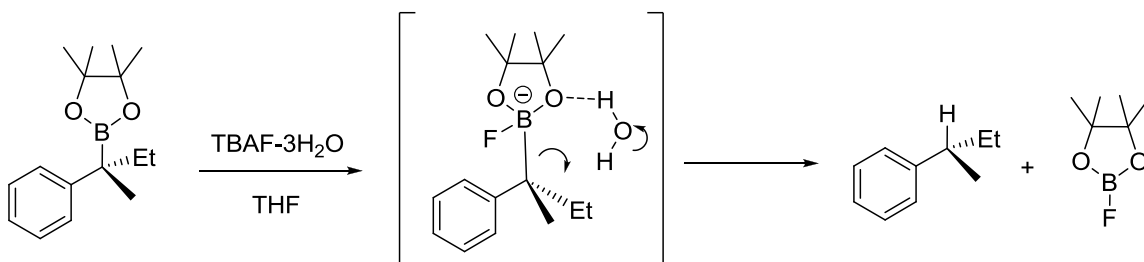
Several very interesting mechanistic insights can be gleaned from these data. It is apparent from comparing entries 1-3 and 4-7 of Table 2-3 that conversion is obtained only when the additive contains two silver atoms per molecule. This effect does not result from the total *amount* of silver added, as this has been accounted for by adding double the molar amount of additive for monomeric silver salts. This is also confirmed by entries 6 and 7 of Table 3, which show no increase in yield at 3 equivalents of silver (I) oxide as compared to 1.5 equivalents. Since maximum efficiency is observed at a 1:1 stoichiometric ratio of Ag<sub>2</sub>O to boronic ester, this is strongly suggestive that there is a favorable interaction between the two, with Ag(I) binding at two sites of the boronic ester. From this information, a plausible explanation for the role of Ag<sub>2</sub>O can be proposed: the boronic ester is activated to a putative boronate by way of the oxygen atom of Ag<sub>2</sub>O, secured in the proper location by the favorable interaction between the two bridged Ag atoms with the pinacolate ester oxygen and the  $\pi$ -system of the phenyl group, respectively (Figure 2-1). This is also in agreement with the observation that a site of unsaturation adjacent to the secondary boronic ester is required to achieve transmetalation (*vide infra*) as this provides the second coordination site for silver.





**Figure 2-1:** Proposed method of activation of benzylic boronic esters by  $\text{Ag}_2\text{O}$ .

Precedence for this type of activation exists for silver-mediated cross-couplings<sup>25</sup> and for the protodeboronation of secondary boronic esters.<sup>26</sup> In the latter case, fluoride ion can be used to activate a tertiary benzylic boronic ester which can then undergo a facile protodeboronation in the presence of  $\text{H}_2\text{O}$ . Interestingly, the protodeboronation occurs with retention of stereochemistry, indicating that protonation does not occur from either face, but rather from an  $\text{H}_2\text{O}$  molecule already bound to the boronic ester moiety (Scheme 2-7). Naturally, these findings have mechanistic implications with regard to the  $\text{Ag}_2\text{O}$  activation of secondary benzylic boronic esters, though it is unclear at this time whether the presumed coordination of  $\text{Ag}_2\text{O}$  leads to a transmetalation to silver<sup>27</sup> or merely activates the boronate towards transmetalation to Pd.



**Scheme 2-7:** Mechanism proposed by Aggarwal to account for stereospecific protodeboronation of boronic esters.<sup>26</sup>

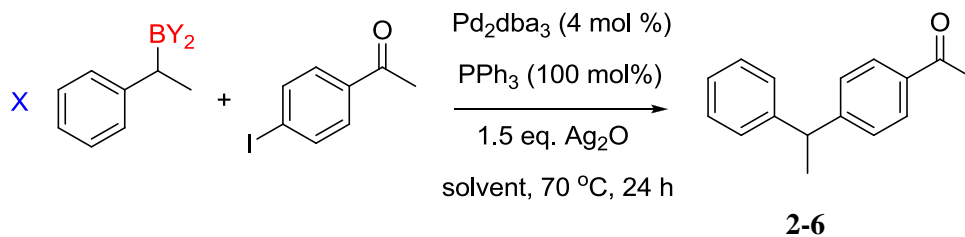
The mode of action being proposed for  $\text{Ag}_2\text{O}$  is both mild and tailored to a particular set of boronic esters. As such, this protocol can activate previously inert types of boronic esters all the while leaving other, classically more reactive, sites untouched. Surprisingly, primary alkyl boronic esters survive the silver-mediated reaction conditions almost completely untouched, although this impressive chemoselectivity begins to erode upon introduction of other bases which are known to activate primary boronic esters. The chemoselectivity of the reaction will be examined in detail in Section 2.4.

Lastly, concurrent work done in our group has shown that the role of  $\text{Ag}_2\text{O}$  may not be exclusively activation of the boronic ester. In fact, the catalytic cycle was shut down upon introduction of excess iodide ion as  $\text{Bu}_4\text{NI}$ , which likely indicates that silver is acting, at least in part, to remove iodide from the coordination sphere of Pd after the oxidative addition step. Corroborative evidence for this hypothesis was also obtained by  $^{31}\text{P}$  NMR (*vide infra*).

## 2.2.4 Attempted Cross-Coupling with a Potassium Trifluoroborate Analogue

Much of the early work on coupling  $sp^3$ -based boron nucleophiles was centered on the air stable and easy to handle potassium trifluoroborate analogues of boronic acids and esters.<sup>28</sup> Not only are these easily synthesized from a given boronic acid and aqueous  $KHF_2$ , but these salts typically couple efficiently at only a slight excess relative to aryl halide, limiting the wastage of large amounts of precious (often non-racemic) boronate ester.<sup>29</sup> Earlier work by Molander showed that *primary* alkyl trifluoroborate salts were competent coupling partners under modified Suzuki-Miyaura reaction conditions, but that the *secondary* boronate yielded only trace amounts of product.<sup>30</sup> We set out to determine if the conditions we had developed to couple secondary boronic esters would translate favorably to their trifluoroborate analogues, and if so, if they would lead to an improvement in yield.

**Table 2-4:** Effect of stoichiometry and the nature of the boronic acid derivative for a standard coupling.



entry	equivs	boron species	solvent	yield (%)
1	1.2	Bpin	THF	50
2	1.5	Bpin	THF	65

3	2.5	Bpin	THF	63
4	5	Bpin	THF	66
5	1.2	BF <sub>3</sub> K	THF	0
6	1.2	BF <sub>3</sub> K	20:1 THF:H <sub>2</sub> O	0

From the data compiled in Table 4, two important aspects of the reaction can be gleaned. The first is that ratcheting up the equivalents of the boronic acid pinacolate ester (BPin), does not result in a higher yield (Table 2-4, entries 2-4), despite the significant drop observed when lowering from 1.5 equivalents to 1.2 (Table 2-4, entries 1-2). The necessity of a relatively large (1.5x) excess of the precious boronic ester to obtain high conversion is certainly sub-optimal so we were hopeful that the potassium trifluoroborate analogue would be reactive under our optimized conditions. The initial coupling (Table 2-4, entry 5) was not promising, but then it is known that the active transmetalation species is not actually the fully fluorinated boronate, but actually a partially hydrolyzed form.<sup>31</sup> Indeed, almost all successful couplings using R-BF<sub>3</sub>K salts require the addition of macroscopic amounts of water<sup>32, 33</sup> or alcoholic solvent,<sup>34</sup> though even under an adjusted protocol, none of the cross-coupled product was observed (Table 2-4, entry 6).

This, of course, is very interesting because it demonstrates that the ability of Ag<sub>2</sub>O to mediate the reaction is not universal, but is dependent on the nature of the boronic acid derivative. Indeed, we have shown in the previous section that to properly activate boron to transmetalation, the silver additive must contain an oxygen atom flanked by not one, but two Lewis acidic silvers; it is now also clear that for its part, the

cross-coupling partner *must* provide the two corresponding Lewis basic sites, namely an oxaborole and an adjacent  $\pi$ -system.

### 2.2.5 Effect of Solvent and Adventitious Water on the Reaction

Table 2-5 illustrates the sensitive nature of the reaction with respect to temperature, water and solvent. The effect of water is curious; the reaction is tolerant to, but does not benefit from, a small amount of water (Table 2-5, entry 5), though as the concentration of water is increased from additive to co-solvent, yields suffer. Addition of molecular sieves meant to expunge trace amounts of adventitious water from THF actually decreases the yield significantly, indicating that trace amounts of water are likely needed for the reaction to proceed. As will be discussed later, small amounts of water in the reaction can also have a deleterious effect on the enantioselectivity of the cross-coupling reaction.

**Table 2-5:** Effect of solvent, temperature and additives on the standard reaction (as in Table 2-4).

entry	solvent	additive	temp.	yield (%)
1	THF		50	27
2	THF		70	65
3	THF		85	52
4	THF	4 A MS	70	35
5	20:1 THF:H <sub>2</sub> O		70	67
6	4:1 THF:H <sub>2</sub> O		70	9

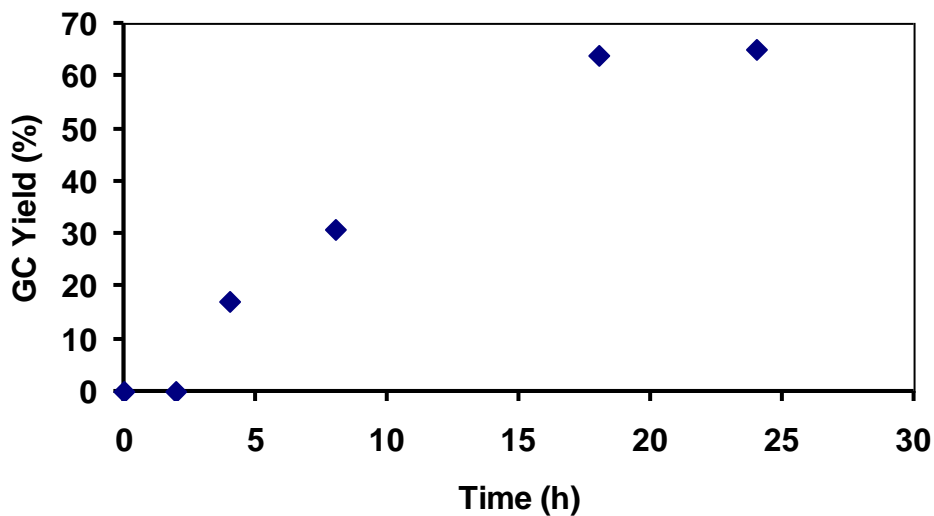
7	DMF		70	22
8	Toluene		70	29
9	<i>i</i> -PrOH		70	0
10	THF	Zn(BF <sub>4</sub> ) <sub>2</sub>	70	40
11	THF	Zn(BF <sub>4</sub> ) <sub>2</sub> (PdCl <sub>2</sub> )	70	46
12	THF	[( <sup>t</sup> Bu) <sub>4</sub> N][BF <sub>4</sub> ]	70	65
13	THF	BEt <sub>3</sub>	70	0

Zinc tetrafluoroborate and tetrabutylammonium tetrafluoroborate were added in an attempt to increase the rate of oxidative addition<sup>35</sup> and ionic strength of the reaction mixture, respectively, with little effect. This, of course, should not be seen as surprising after the oxidative addition of aryl iodides was found to be kinetically silent. BEt<sub>3</sub>, a strong reducing agent, was added to counter any possible detrimental effects arising from the oxidation of PPh<sub>3</sub> to OPPh<sub>3</sub>, though, in practice, it was found to completely shut the reaction down. In this case, a competitive transmetalation between our secondary boronic ester and the trialkylborane may be at play, though the absence of a strong base to activate the borane may preclude this pathway; in the event no ethylated product was observed.

### 2.2.6 Reaction Profile

The reaction was monitored over time to ascertain how long was needed to ensure maximum conversion and to determine whether a catalyst induction period was in play.

This was suggested by the low solubility of  $\text{Ag}_2\text{O}$  in THF and the qualitative observation of sudden metal deposits in the early stages of the reaction.



**Figure 2-2:** Time course for the silver-mediated cross-coupling of a secondary boronic ester and an aryl iodide. Standard reaction conditions (as in Table 2-4) were used.

As seen in Figure 2-2, an induction period was indeed observed. No turnover is observed for the first two hours, followed by slow conversion to product over an extended (18 h) time period. It should be noted that at the maximum conversion, the stoichiometrically limiting aryl iodide is completely consumed, suggesting that quantitative yields are prevented not by catalyst death, but by consumption of aryl iodide by deleterious side reactions. For example, side products stemming from homocoupling and arene dehalogenation are often detected in trace amounts, though typically in under 10% yield.

## 2.3 Scope of the Stereoretentive Cross-Coupling of Secondary Boronic Esters

### 2.3.1 Stereoretentive Cross-Coupling of a Secondary Boronic Ester

With a Suzuki-Miyaura protocol capable of cross-coupling benzylic boronic esters finally in hand, the highly regioselective metal-catalyzed hydroboration of styrenes can now be more fully exploited. The next logical step was to take advantage of the other important aspect of the hydroboration reaction, namely, its strong *enantioselectivity*. Thus, the asymmetric hydroboration of styrene was performed by a catalyst formed *in situ* by  $[\text{Rh}(\text{COD})]^+\text{BF}_4^-$  and the non-racemic (R)-BINAP. When care is taken to keep the reaction solution at  $-78\text{ }^\circ\text{C}$  during HBCat addition and pinacol quench, enantiomeric ratios approaching 94:6 (R:S) can be obtained.<sup>5</sup> In practice, enantiomeric ratios of 92:8 (R:S) are more common, and a batch with this, somewhat lowered enantiomeric ratio, was used for the initial studies on stereoretention.

Gratifyingly, when enantioenriched boronic ester (**R**)-**2-5** was cross-coupled to 4-iodoacetophenone under our newly developed conditions, a non-racemic coupling product was formed; in fact over 90% of the stereochemical information is translated from the boronic ester to the product (see Table 2-6, entry 1). This is reassuring, as significant erosion of stereochemical information during the cross-coupling would severely limit the applicability of this transformation to asymmetric synthesis.

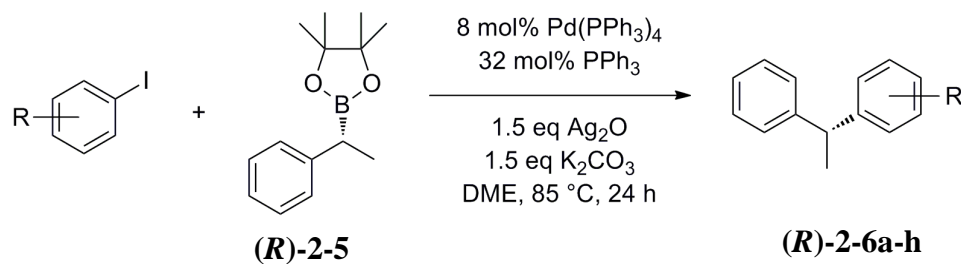


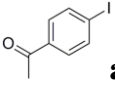
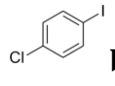
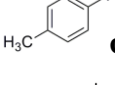
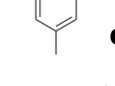
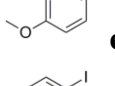
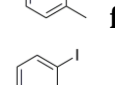

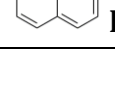
By comparing the optical rotations of (*R*)-1-phenyl-1-(4-acetylphenyl)ethane ((*R*)-2-6) prepared by our cross-coupling methodology to the enantioenriched samples reported by Hiyama,<sup>12</sup> the cross-coupling reaction was determined to proceed with *retention* of stereochemistry. It would appear, then, that the process is more consistent with the protodeboronation reported by Aggarwal<sup>26</sup> than the recent examples of stereoinvertive cross-couplings described by Suginome<sup>14</sup> and Molander.<sup>15</sup>

### 2.3.2 Scope of the reaction and Effect of Exogenous Base

The scope of the reaction with aryl iodides is presented in Table 2-6. The reaction is tolerant of various functionalities on the aryl iodide, although it seems to be hindered by steric bulk at the *ortho* position (Table 2-6, entries 3 and 6). In the case of 2-iodoacetophenone, the effect of *ortho* bulk is compounded by a potential sequestering of the Pd catalyst by means of coordination to the carbonyl moiety after oxidative addition, which leads to a complete shut down of turnover (compare entries 1 and 7). As expected, oxidative addition into an aryl chloride bond is extremely disfavored relative to an aryl iodide bond (especially in a PPh<sub>3</sub>-ligated system) and as such, cross-coupling of *para*-chloriodobenzene takes place selectively at the aryl iodide bond (entry 2).

**Table 2-6:** The scope of the stereoretentive cross-coupling of asymmetric secondary boronic esters and aryl iodides.



entry	substrate	Yield (iso.)	retention (Ag <sub>2</sub> O)	retention (Ag <sub>2</sub> O/K <sub>2</sub> CO <sub>3</sub> )
1	 <b>a</b>	65 (63)	92	98
2	 <b>b</b>	81 (62)	91	98
3	 <b>c</b>	86 (60)	92	98
4	 <b>d</b>	86 (64)	93	97
5	 <b>e</b>	48	93	98
6	 <b>f</b>	48	93	96
7	 <b>g</b>	0	---	---
8	 <b>h</b>	81 (65)	—	93

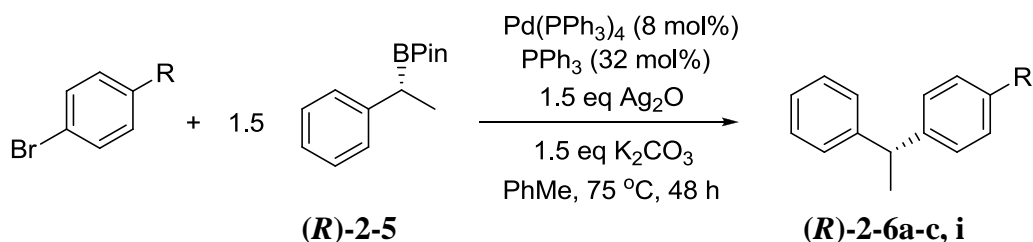
It was subsequently discovered by another member of the group, Martins Oderinde, that the addition of 1.5 equivalents of K<sub>2</sub>CO<sub>3</sub> with respect to aryl iodide in addition to the necessary Ag<sub>2</sub>O had little effect on yield, but produced a significant

augmentation in the stereoretention from boronic ester to coupled product. This dramatic effect will be discussed in detail in Section 2.5.

### 2.3.3 Aryl Bromides as Competent Coupling Partners

The positive effect of adding  $K_2CO_3$  to the reaction turned out to not be limited to matters of stereoretention. Aryl bromides, which previously had been inconsistent and very low yielding electrophiles for the reaction, suddenly became synthetically viable upon inclusion of  $K_2CO_3$ .

**Table 2-7:** Substrate scope for aryl bromides. Yields reported are based on NMR with internal standard, isolated yield in parentheses.



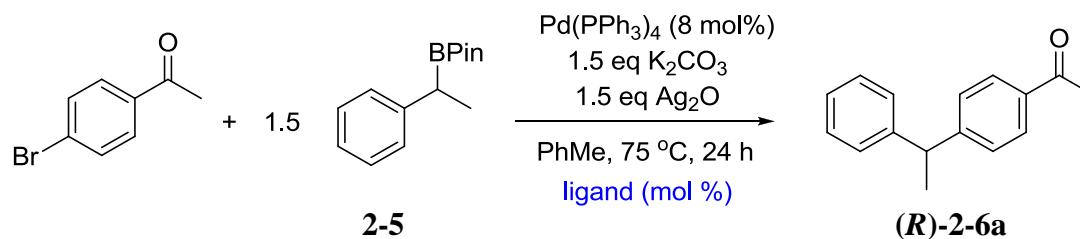
entry	R	yield (%)	stereoretention (%)
1	Ac	56 (49)	96
2	Cl	56 (42)	95
3	CH <sub>3</sub>	43 (31)	95
4	CHO	(42)	93

Prior to addition of  $K_2CO_3$ , yields for aryl bromides varied, but were consistently lower than 20%. The results shown in Table 2-7 indicate a decent substrate tolerance for

aryl bromides and that yields are now within reach of those obtained with aryl iodides. Encouragingly, the stereoretentions are also excellent.

Experiments performed concurrently with this work by our group showed that, where the reaction is zero order in aryl *iodide*, it is actually *first* order in aryl bromide. In spite of this, PPh<sub>3</sub> remained the best ligand of all those tested, including electron releasing (Table 2-8, entries 3-11), electron withdrawing (Table 2-8, entry 14), Buchwald (Table 2-8, entries 7-10) and Fu-type (Table 2-8, entries 5 and 6) ligands. The reasoning behind this is still unclear, though may have to do with the ability of PPh<sub>3</sub> to withstand the harsh reaction conditions without being oxidized (*vide infra*).

**Table 2-8:** Effect of various ligands on the cross-coupling of 4-bromoacetophenone to benzylic boronic ester **2-5**.



entry	ligand (mol %)	yield (%)
1	PPh <sub>3</sub> (64)	46
2	PPh <sub>3</sub> (3 eq Ag <sub>2</sub> O)	40
3	P( <i>p</i> -MeOPh) <sub>3</sub> (64)	36
4	P( <i>p</i> -MeOPh) <sub>3</sub> (32)	18
5	PCy <sub>3</sub> (64)	1
6	PCy <sub>3</sub> (32)	7
7	<sup>t</sup> Bu <sub>2</sub> P(BiPh) (64)	7
8	<sup>t</sup> Bu <sub>2</sub> P(BiPh) (32)	Trace

9	Xphos (64)	N.R.
10	Xphos (32)	N.R.
11	P( <i>p</i> -MePh) <sub>3</sub> (64)	44
12	AsPh <sub>3</sub> (64)	1
13	MePPh <sub>2</sub> (64)	11
14	P( <i>p</i> -fluorophenyl) <sub>3</sub> (64)	15
15	P(furyl) <sub>3</sub> (64)	1

Overall, the lower cost and higher availability of aryl bromides compared to aryl iodides may in fact make these substrates worthy of consideration despite the lower yields. What should not be overlooked either is that, should this Suzuki-Miyaura protocol be extended to *vinyl* electrophiles, accessing bromide substrates may become paramount considering the almost complete lack of commercially available vinyl iodides.

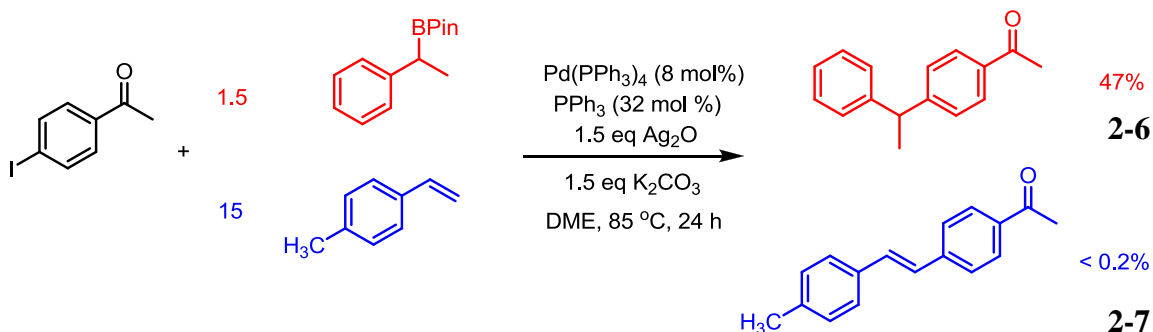
## 2.4 The Remarkable Chemoselectivity of the Reaction

### 2.4.1 Suzuki-Miyaura vs. Mizoroki-Heck Protocols

One of the major synthetic advances brought forth by transition-metal catalyzed cross-coupling reactions was the remarkable selectivity for reaction at certain sites even in the presence of others that may have been more reactive under previous protocols.<sup>36</sup> For instance, Tables 2-6 and 2-7 show that activation of an aryl halide bond occurs even in the presence of ketones and notoriously reactive aldehydes. The utility of this chemoselectivity is even more impressive when one transition metal catalyzed process

can be made to occur selectively in preference to another potential metal-catalyzed reaction.<sup>37</sup>

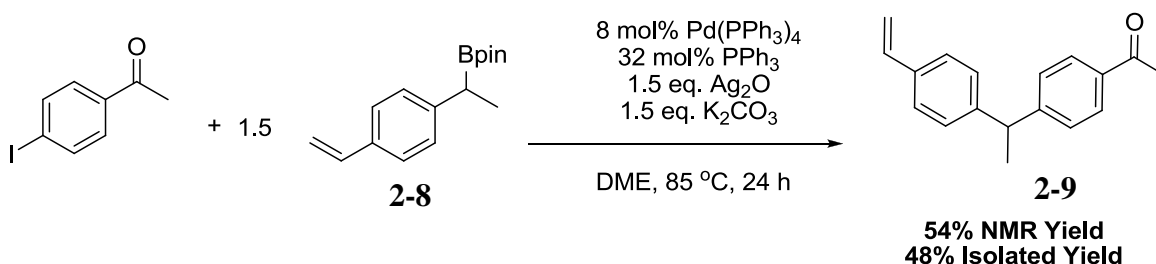
We were pleased to note, then, that under our optimized conditions, the stereoretentive cross-coupling of secondary boronic esters occurred exclusively, even in the presence of a *para*-substituted styrene (Scheme 2-8). The Pd-catalyzed Mizoroki-Heck reaction between the aryl iodide and the olefin was expected to at least be competitive with cross-coupling to the secondary boronic ester, but to our surprise, the would-be stilbene product **2-7** was present in less than 1% yield (as determined by High Resolution Mass Spectrometry) *even when the styrene was present in a ten-fold excess relative to the secondary boronic ester*.



**Scheme 2-8:** Chemoselectivity of the cross-coupling reaction even in presence of large excess of styrene derivative.

Interestingly, this remarkable preference for Suzuki-Miyaura type coupling over possible Mizoroki-Heck reactions also holds true even in an intramolecular case. Indeed, the cross-coupling of secondary boronic ester **2-8** proceeds flawlessly, leaving the pendant olefin group completely untouched during the reaction (Scheme 2-9) and cross-

coupled product **2-9** is the only product observed. Although the standard protocol for a successful Heck reaction typically requires higher temperatures (100-140 °C) than those employed here, it is still remarkable that less than 0.5% of the aryl iodide undergoes coupling with the Heck substrate.<sup>38</sup> This staggering chemoselectivity will increase the synthetic utility of the newly developed Suzuki-Miyaura cross-coupling protocol, permitting the use of olefin-containing secondary boronic esters.

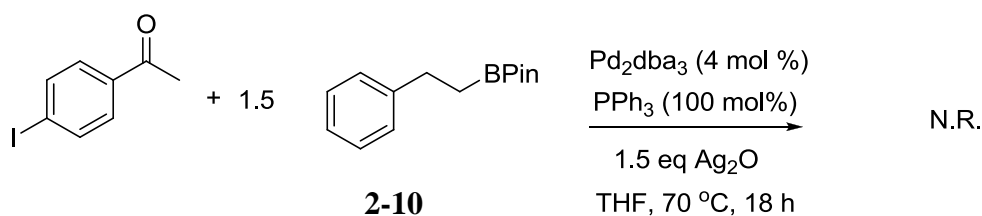


**Scheme 2-9:** The intramolecular chemoselectivity of the Suzuki-Miyaura process over a potential Mizoroki-Heck reaction.

#### 2.4.2 Branched vs. Linear Cross-Coupling

At the outset of this work, the cross-coupling of secondary boronic esters with aryl halides was one of the last hurdles facing the Suzuki-Miyaura reaction, as the cross-coupling of primary alkyl boranes, boronic esters and boronate salts had all been mastered. With this in mind, we were pleasantly surprised to find another example of extremely high chemoselectivity when a mixture of branched and linear boronic esters was subjected to our Ag-mediated reaction conditions and yielded the branched cross-

coupling product exclusively. Even in a non-competitive scenario, a pure sample of linear boronic ester **2-10** remains untouched by our conditions after 18 h (Scheme 2-10). The significance of this result is easily grasped: not only is our protocol able to cross-couple the previously elusive secondary boronic ester, but it also leaves the seemingly more reactive *primary* boronic esters untouched, allowing for a subsequent reaction at the primary site. In this way, our cross-coupling protocol is completely complementary to those previously published for linear boronic ester derivatives.<sup>30</sup>



**Scheme 2-10:** Chemical inertness of linear boronic esters to reaction conditions.

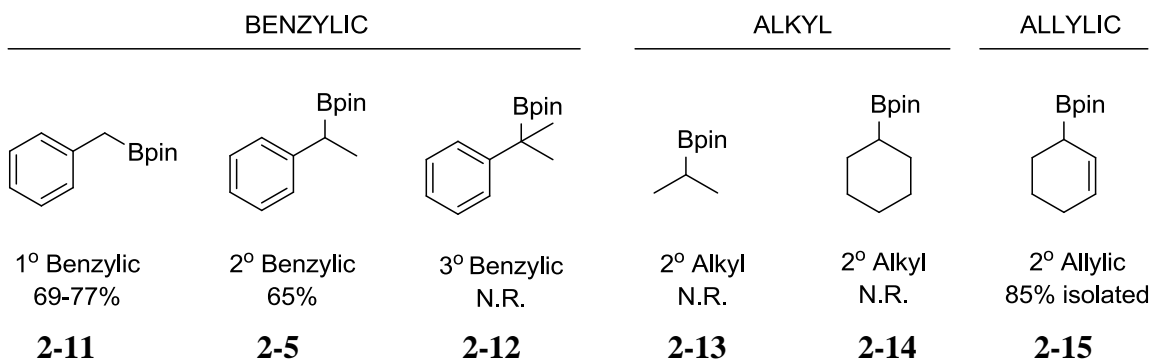
The chemoselective reactivity of a benzylic boronic ester over its primary analogue is worthy of note. Typically, boron centres are activated by bases much stronger than  $\text{Ag}_2\text{O}$ , a fact which may be responsible for the observed chemoselectivity. To verify this claim,  $\text{K}_2\text{CO}_3$  was added to a  $\text{Ag}_2\text{O}$ -mediated cross-coupling of a branched and linear boronic ester. Arylation still occurred preferentially at the secondary site, but in this case, the chemoselectivity was eroded slightly and arylation was observed at the linear site for the first time. Interestingly, that which improves the *enantioselectivity* of the reaction results in a decrease in the *chemoselectivity* of the reaction.



## 2.5 Towards a Mechanistic Understanding of the Reaction

### 2.5.1 The Nature of the Secondary Boronic Ester

Results obtained during both the optimization (Section 2.2) and selectivity (Section 2.4) studies suggested that a strong link exists between the silver source and the nature of the boronic ester. The chemoselectivity for the branched (benzylic) boronic ester over the linear (non-benzylic) boronic ester was also telling. A variety of secondary boronic esters was then examined in the coupling reaction to better understand what allowed the benzylic system to be so successful. Hopefully, this knowledge could then be used to expand the scope of competent coupling partners away from just benzylic boronic esters.



**Scheme 2-11:** Illustration of the importance of an adjacent olefin to ensure successful cross-coupling. Conditions = 1.0 eq. 4-iodoacetophenone, Pd(PPh<sub>3</sub>)<sub>4</sub> 8 mol %, 1.5 eq Ag<sub>2</sub>O, 1.5 eq K<sub>2</sub>CO<sub>3</sub>, DME, 85 °C, 24 h. NMR yields, unless otherwise indicated.

Initially, primary benzylic boronic ester **2-11** was tested and found to have similar activity as its secondary counterpart **2-5**, indicating that the reactivity of the secondary boronic ester was not due entirely to the branch point. Tertiary benzylic boronic ester **2-12** was also synthesized (by way of a lithiation-borylation strategy), but was found to be inert to our cross-coupling conditions, an occurrence that is ascribed to the even slower transmetalation processes for tertiary boronic esters.

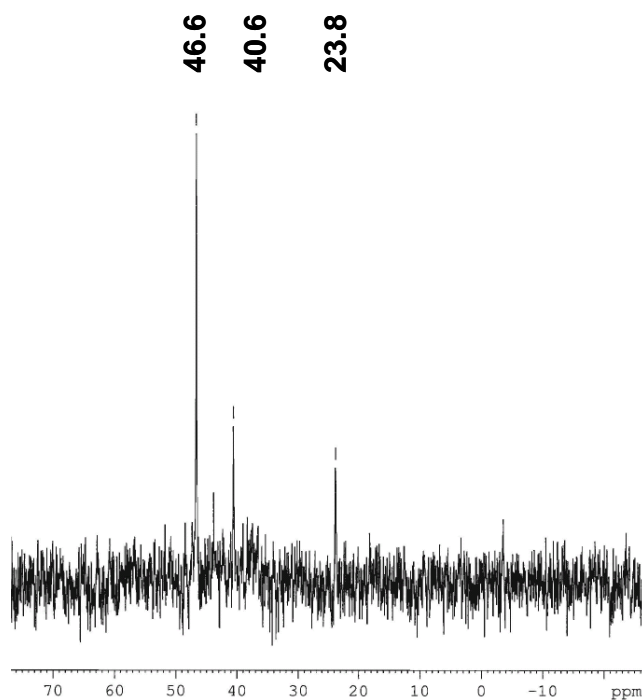
The benzylic requirement was next interrogated by subjecting the purely aliphatic *sec*-propylboronic acid pinacolate ester **2-13** to the reaction conditions (Scheme 2-11, Alkyl). Consistent with the conclusion from substrate **2-11** that the branch point is not the determining factor, neither this boronic ester, nor the less volatile cyclohexylboronic acid pinacolate ester **2-14** were found to undergo cross-coupling with 4-iodoacetophenone. In fact, both survived prolonged exposure to the reaction conditions completely intact. As fully saturated secondary boronic esters were shown to be completely inert to reaction conditions, it becomes clear that the benzylic moiety was intimately linked to successful cross-coupling under our protocol. Mindful of this, we synthesized *rac*-2-cyclohexenylboronic acid pinacolate ester **2-15** which differed from boronic ester **2-14** in being allylic rather than aliphatic. Gratifyingly, this allylic boronic ester was successfully cross-coupled to 4-iodoacetophenone in high isolated yield to definitively illustrate the importance of having an unsaturated group adjacent (be it benzylic or allylic) to the boronic for successful cross-coupling. Given that Ag<sub>2</sub>O is also needed to enable turnover, and that yields are optimized at a 1:1 stoichiometry between the two, it seems permissible

to assume that there must be an interaction between the silver and the obligatory  $\pi$ -system.

### 2.5.2 $^{31}\text{P}$ NMR Studies of the Reaction

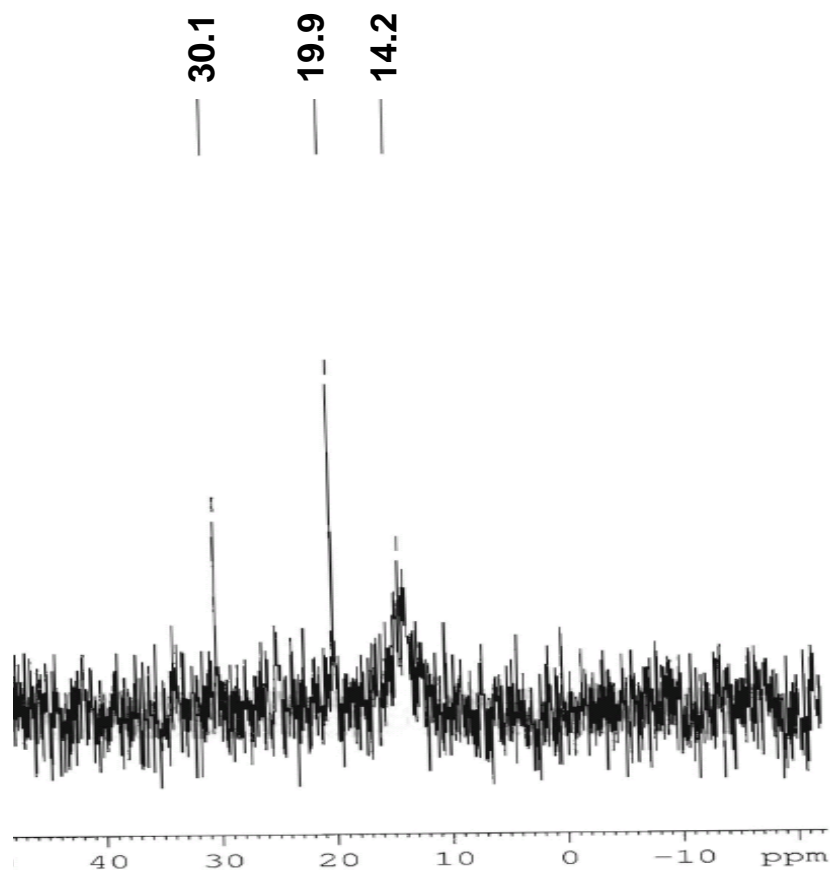
A  $^{31}\text{P}$  NMR study was undertaken to determine the nature of the Pd (and potential Ag) complexes present throughout the course of the reaction. It was hoped the study would also shed light on why  $\text{PPh}_3$  was so well suited as a ligand for the reaction. Given that the oxidative addition step appears to be kinetically silent, the two main roles of the ligand are to provide electron density to the metal centre and to occupy coordination sites to block a potential  $\beta$ -hydride event. Should the ligand become oxidized over the course of the reaction, its ability to bind to the metal would then be compromised; as electron-rich phosphines are more prone to oxidation, it could be the ability of  $\text{PPh}_3$  to withstand oxidation which enables it to form a stable, catalytically active Pd-complex.

When 8 equivalents of the electron-rich  $\text{PCy}_3$  ligand are used in place of  $\text{PPh}_3$ , the yield of the reaction remains under 20% after 24 h. Analysis of this crude reaction mixture by  $^{31}\text{P}$  NMR indicates that, though phosphorous exists in a few different electronic environments, the most prevalent species by far is the unwanted tricyclohexylphosphine oxide (46.6 ppm, Figure 2-3).



**Figure 2-3:**  $^{31}\text{P}$  NMR of a crude cross-coupling reaction mixture using  $\text{PCy}_3$ . The main peak at 46.6 ppm has been assigned to  $\text{OPCy}_3$ .

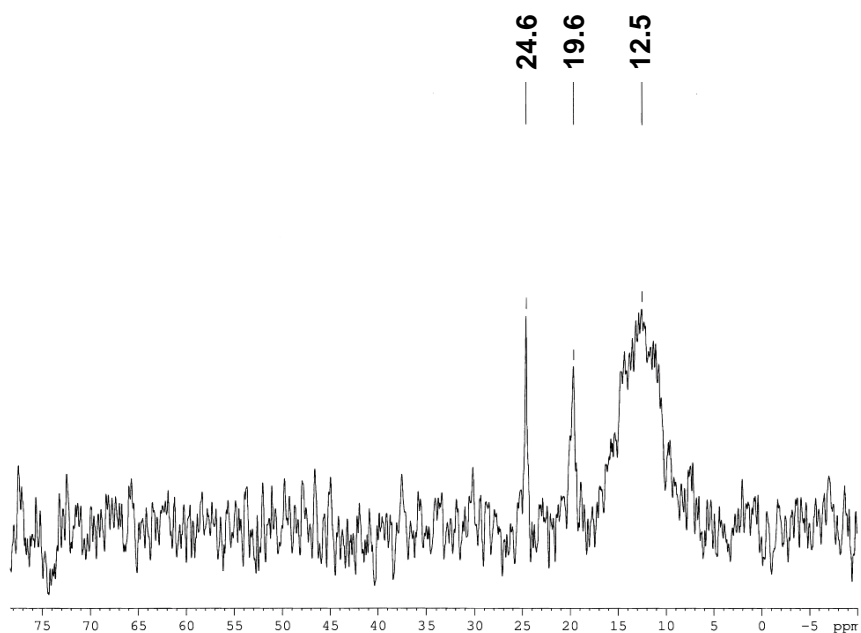
$\text{PPh}_3$  is not immune to oxidation either, though after 16 h of reaction time, it is  $\text{Pd}(\text{PPh}_3)_4$  (19.9 ppm), and not  $\text{OPPh}_3$  (typically attributed at 24 ppm,<sup>39</sup> though presumably either at 30.1 ppm in this case or absent altogether), that appears to be the main species of phosphorous observed in solution (Figure 2-4). The broad peak around 14 ppm, barely noticeable after 16 h of reaction time, would also become important to our understanding of the reaction.



**Figure 2-4:**  $^{31}\text{P}$  NMR after 16 h of cross-coupling with  $\text{PPh}_3$ .

It was unclear, however, what was causing the small amount of  $\text{PPh}_3$  oxidation, and whether or not it was occurring during the catalytic cycle or after the reaction had stopped turning over. It should be noted that matters were further convoluted by the similar resonances reported for triphenylphosphine oxide ( $\text{OPPh}_3$ , 24.4 ppm<sup>39</sup>) and the phosphine-ligated  $\text{Pd}^{2+}$ -complex resulting from oxidative addition to an aryl iodide ( $\text{PhPdI}(\text{PPh}_3)_2$ , 24.5 ppm<sup>24, 39</sup>)

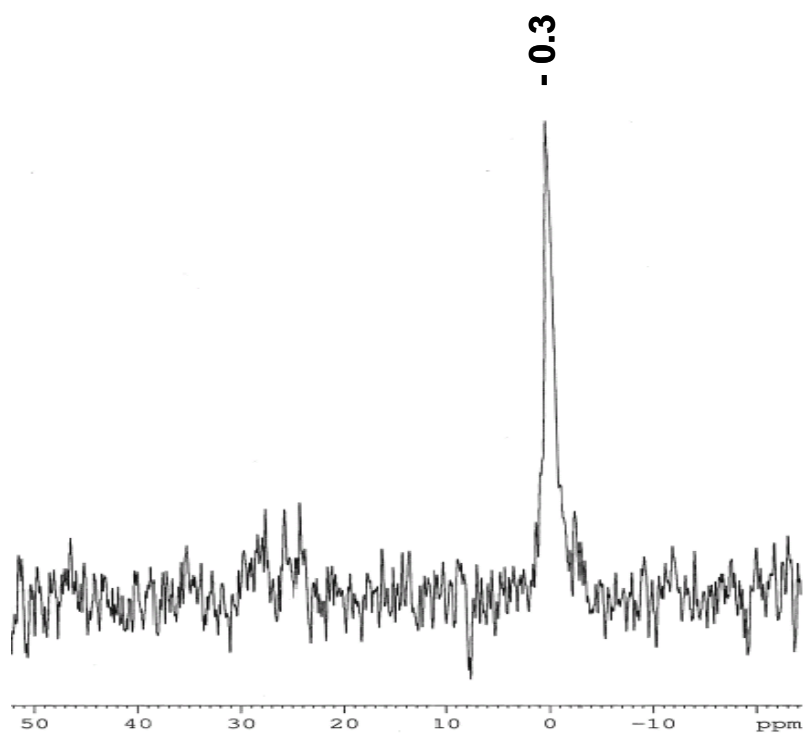
In order to see what phosphine species were most prevalent while turnover was still occurring, a cross-coupling reaction was quenched after only 8 h at 70 °C and examined by  $^{31}\text{P}$  NMR (Figure 2-5). As expected, both  $\text{Pd}(\text{PPh}_3)_4$  (19 ppm)<sup>40</sup> and the oxidative addition product,  $\text{PhPdI}(\text{PPh}_3)_n$  (25 ppm)<sup>24</sup>, were observed though the broad peak at 12 ppm had not been assigned as of yet. Because this broad peak at 12 ppm diminishes to near-baseline levels over the next 8 h (Figure 2-4) as catalytic turnover slows and eventually stops, it is likely that this resonance belongs to a species in the catalytic cycle which is consumed over time.



**Figure 2-5:**  $^{31}\text{P}$  NMR for cross-coupling reaction run under standard conditions, stopped after 8 h at 70 °C.

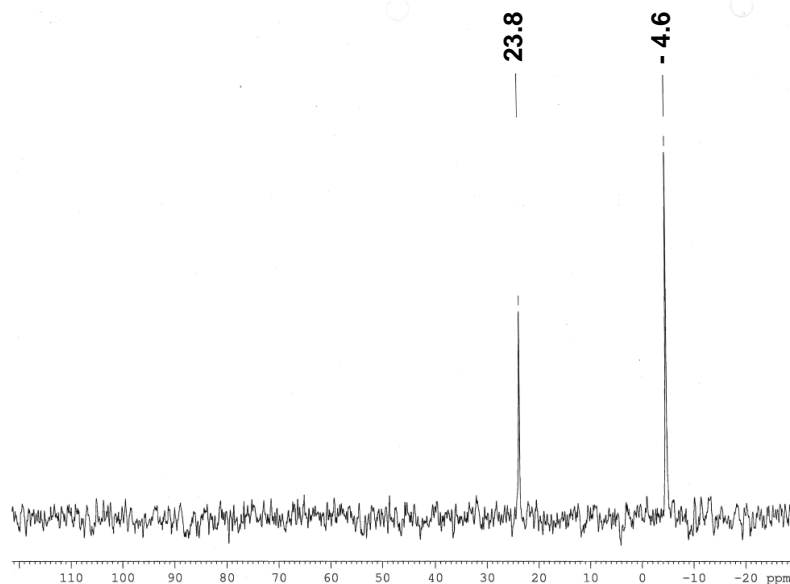
In an attempt to assign the signal at 12 ppm,  $^{31}\text{P}$  NMR spectra were obtained for a series of reactions with sequentially added reaction components. First,  $\text{PPh}_3$  itself was

observed at -4.2 ppm (calibrated to  $\text{H}_3\text{PO}_4$ ). Heating  $\text{PPh}_3$  in the presence of  $\text{Pd}_2\text{dba}_3$  (8:1  $\text{PPh}_3:\text{Pd}$ ) for 30 min did not result in discrete resonances for the expected phosphine-ligated  $\text{Pd}^0$  complexes, such as  $\text{Pd}(\text{PPh}_3)_4$  (19 ppm)<sup>40</sup> or  $\text{Pd}(\text{PPh}_3)_3$  (23 ppm)<sup>24</sup>. Instead, only a peak at -1 ppm was observed, consistent with Jutand's findings<sup>39</sup> that in large excesses of  $\text{PPh}_3$ , the phosphine-ligated  $\text{Pd}^0$ -species are in rapid equilibrium with each other and free phosphine, causing an upfield shift in the resonance (Figure 2-6).



**Figure 2-6:**  $^{31}\text{P}$  NMR of  $\text{Pd}_2\text{dba}_3$  and 8 equivalents of  $\text{PPh}_3$  (with respect to Pd), heated to 80 °C in THF for 8 h.

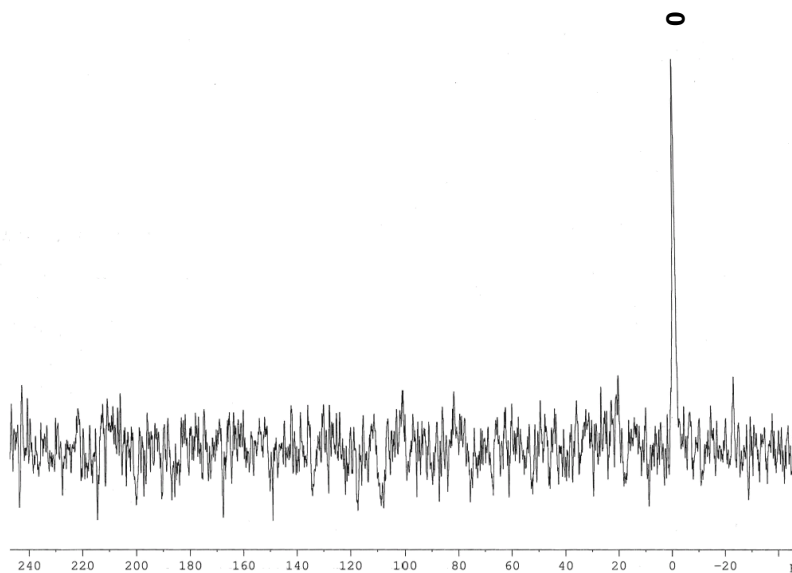
When aryl iodide is included and is heated to 70 °C with both the Pd source and PPh<sub>3</sub>, crisp resonances for the oxidative addition product (24 ppm) and free PPh<sub>3</sub> (-4 ppm) reemerge (Figure 2-7).



**Figure 2-7:** <sup>31</sup>P NMR of Pd<sub>2</sub>dba<sub>3</sub>, 8 equivalents of PPh<sub>3</sub> (with respect to Pd) and 4-iodoacetophenone after heating at 80 °C for 8 h in THF.

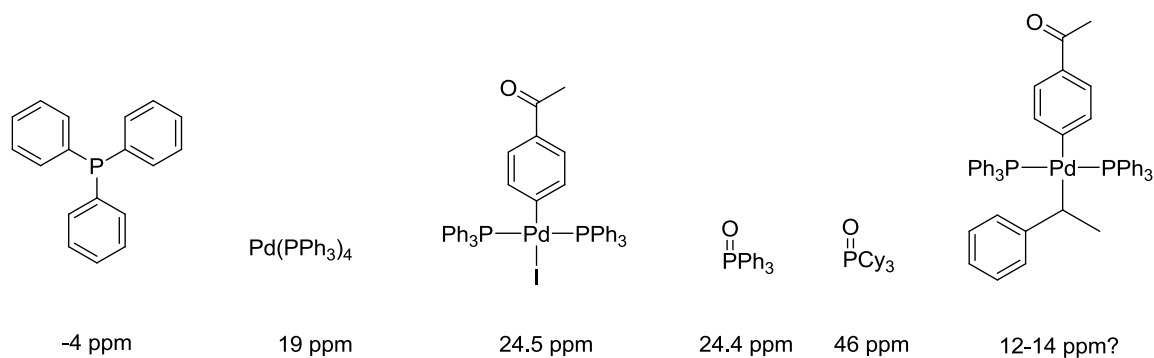
Interestingly, the inclusion of Ag<sub>2</sub>O to the reaction mixture causes the oxidative addition product to completely disappear, being replaced instead by the resonance at 0 ppm attributed to the rapid equilibration of Pd(PPh<sub>3</sub>)<sub>3</sub>, Pd(PPh<sub>3</sub>)<sub>2</sub> and free phosphine.<sup>39</sup> This provides further evidence for the secondary role of silver as iodide extractor (Figure 2-8).





**Figure 2-8:**  $^{31}\text{P}$  NMR of  $\text{Pd}_2\text{dba}_3$ ,  $\text{PPh}_3$ , aryl iodide and  $\text{Ag}_2\text{O}$  after 8 h heating at  $70\text{ }^\circ\text{C}$ .

Finally, inclusion of the secondary boronic ester completes the requirements for the Suzuki-Miyaura reaction, and it is only then that the peak at 12 ppm is observed (see Figures 2-4 and 2-5). Given that inclusion of the boronic ester is necessary to observe this peak, this resonance has been attributed to the species resulting from the transmetalation of the benzyl group to  $\text{L}_n\text{Pd}(\text{Ar})(\text{I})$  (Scheme 2-12). This hypothesis is corroborated by Hartwig's assignment of  $^{31}\text{P}$  NMR resonances in the range of 15-16 ppm to bis-arylated diphosphine Pt complexes.<sup>41</sup>



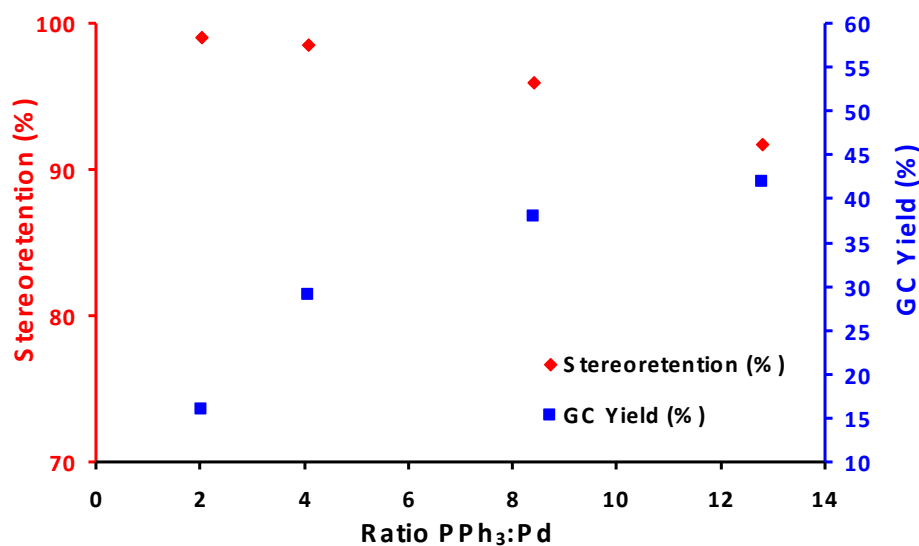
**Scheme 2-12:** Assigned  $^{31}\text{P}$  NMR chemical shifts for components of cross-coupling reaction mixture.

### 2.5.3 The Unexpected Effect of $[\text{PPh}_3]$ on Stereoretention

It was understood early on in the optimization studies that a large excess of  $\text{PPh}_3$  relative to Pd was needed to ensure high yields. Though yields were known to level off after around an eight-fold excess of ligand, larger excesses did give slightly better yields and were therefore often used. Interestingly, when the amount of triphenylphosphine was increased to a 12:1 ratio to Pd, the gains in stereofidelity observed with the addition of  $\text{K}_2\text{CO}_3$  appeared to be erased. This prompted us to further examine the effect of triphenylphosphine on both yield *and* the stereofidelity of cross-coupling.

The effects were first studied with our second-generation conditions, namely those mediated by both  $\text{Ag}_2\text{O}$  and  $\text{K}_2\text{CO}_3$ , in rigorously dried DME. The results were staggering.

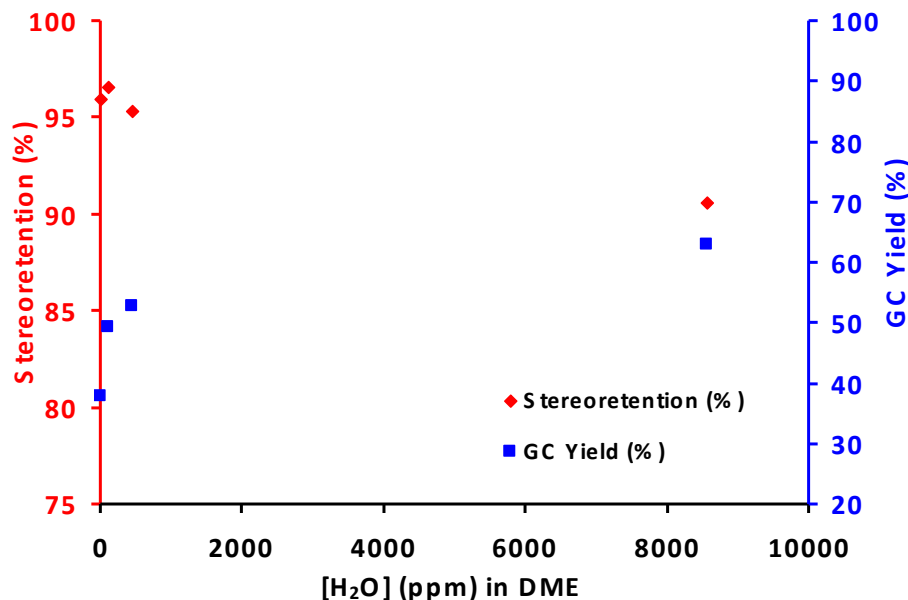
As expected, the yield of the reaction was maximized at high  $\text{PPh}_3$ :Pd ratios, presumably by disfavoring  $\beta$ -hydride elimination to styrene. What had not been anticipated, however, was the marked drop in stereoretention that accompanied the use of excess phosphine ligand (Figure 2-9). The relatively low maximum yield in anhydrous DME is also worthy of note, though this may have been predicted based on prior results which demonstrated the reaction's tolerance to low levels of water and the significant decrease in yield upon the inclusion of 4 Å MS. (Table 2-5, entry 4). In other words, the reaction requires some water to give maximum yields.



**Figure 2-9:** Effect of  $\text{PPh}_3$ :Pd ratio on reaction yield (blue) and stereoretention (red) in anhydrous DME.

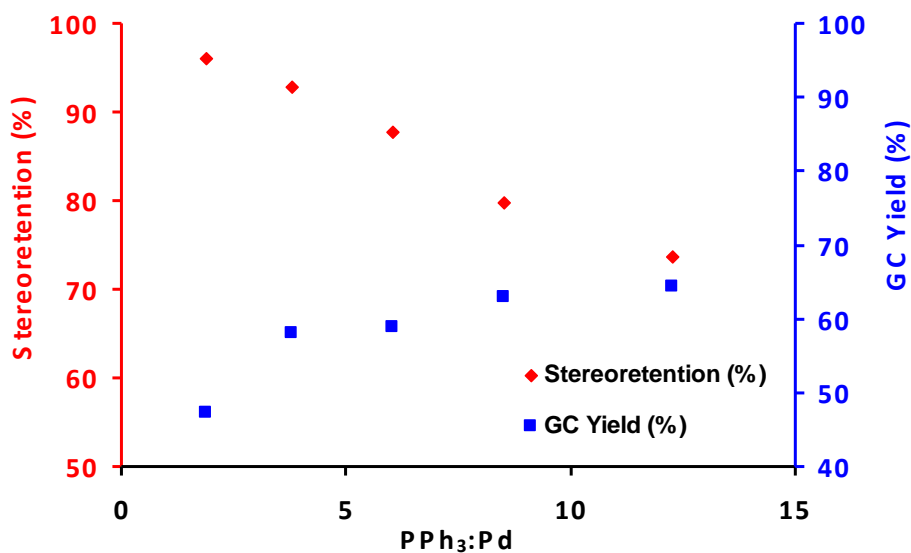
In order to quantify this, the effect of known amounts of water on the reaction yield and stereoretention were examined. As seen in Figure 2-10, increasing water concentrations (on the ppm scale) had a positive effect on yield, finally reproducing the

yields reported previously. Unfortunately, the concentration of water also had a deleterious effect on stereoretention. Interestingly, both elements of the reaction that have been shown to inflate yield (high PPh<sub>3</sub> loading, trace amounts of H<sub>2</sub>O) also lead to a lowered stereoretention.



**Figure 2-10:** Dramatic effect of H<sub>2</sub>O on reaction yield (red) and stereoretention (blue).

At H<sub>2</sub>O concentrations on the order of 6500-8500 ppm, the relationship between PPh<sub>3</sub>:Pd ratio, product yield and stereoretention was re-examined (Figure 2-11). Once again, a higher yield is obtained at the expense of stereofidelity in the presence of water. Also interesting are the high rate at which stereofidelity drops with increasing ligand loadings and the maintenance of respectable yields at low PPh<sub>3</sub>:Pd ratios. These data suggest that the ideal outcome might then be achieved simply by lowering the PPh<sub>3</sub>:Pd ratio used when adding a controlled amount of water.

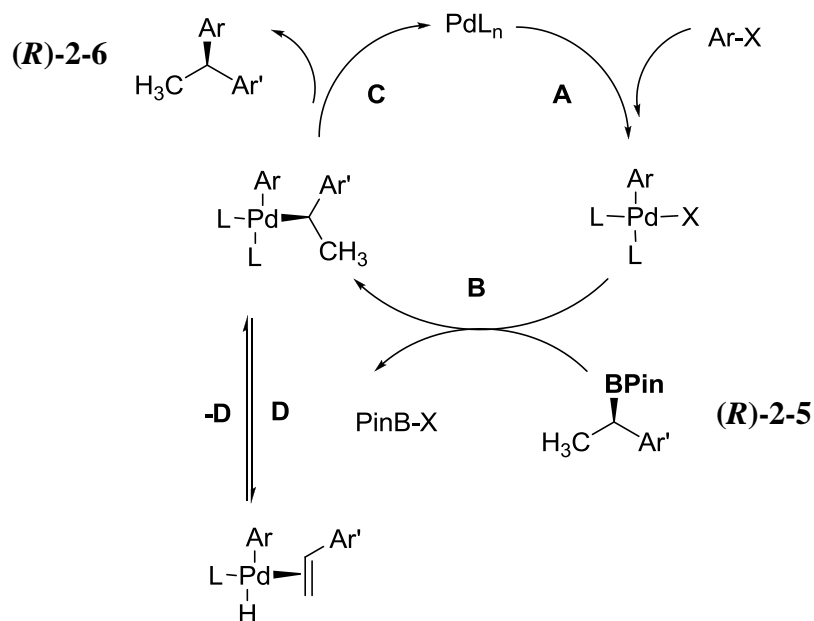


**Figure 2-11:** Effect of PPh<sub>3</sub> loading on yield (red) and stereoretention (blue) in the range of 6500-8500 ppm of H<sub>2</sub>O.

#### 2.5.4 Role of Ligand Excess and Proposed Mechanistic Cycle

In order to probe the reason for the loss of stereoretention with added PPh<sub>3</sub>, we first explored potential racemization events. The chiral boronic ester and cross-coupling product are benzylic and dibenzylic, respectively, which could make them susceptible to racemization through deprotonation. In the event, cross-coupling product (**R**)-**2-6** of er 97.5:2.5 was re-exposed to the harshest reaction conditions (12 eq. PPh<sub>3</sub>, DME/H<sub>2</sub>O (6000 ppm), 85 °C, 24 h, Pd(PPh<sub>3</sub>)<sub>4</sub>, Ag<sub>2</sub>O, ArI, K<sub>2</sub>CO<sub>3</sub>) and completely retained all of its stereochemical information. Therefore scrambling of the stereochemistry in the coupling product through the action of phosphine, base or Pd can be ruled out. The same experiment was performed with enantioenriched boronic acid (**R**)-**2-5**, which, when

added to the reaction mixture (without aryl iodide) under the most extreme conditions (as above), underwent less than 2% racemization. As both the chiral starting material and product are resistant to racemization, any erosion of stereochemistry must necessarily be occurring during the catalytic cycle itself.

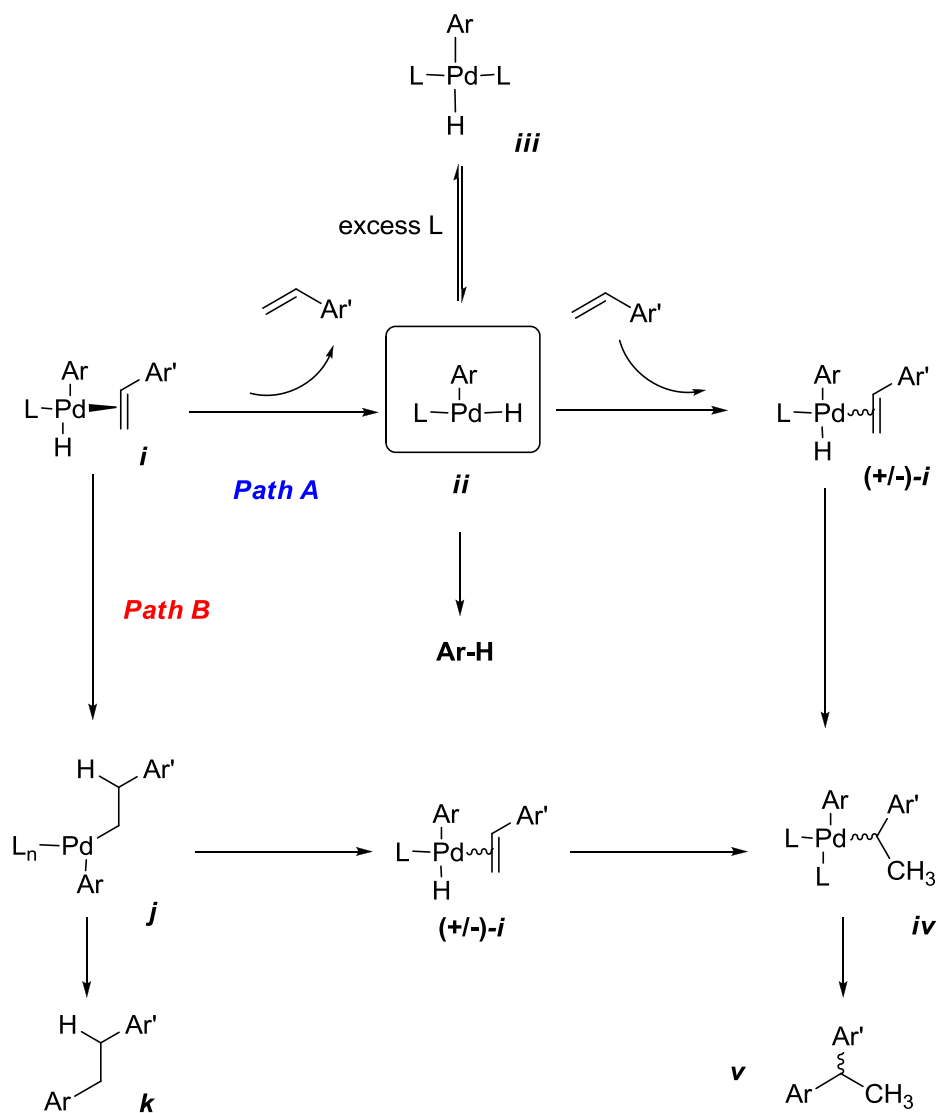


**Scheme 2-13:** Proposed basic catalytic cycle for the cross-coupling of secondary boronic esters. Note that the effects of base and  $\text{Ag}_2\text{O}$  have been omitted for clarity.

The proposed catalytic cycle for the cross-coupling of secondary boronic esters with aryl halides is outlined in Scheme 2-13. Oxidative addition to the aryl halide (**A**) is followed by transmetalation (**B**) to the secondary boronic ester with retention of configuration. At this point, successful reductive elimination (**C**) leads to the formation of the dibenzylic coupling product. The  $\beta$ -hydride elimination process (**D**) yielding the  $\eta$ -2

bound olefin is disfavored by high ligand concentration, and illustrates one positive effect of  $[\text{PPh}_3]$  on product yield.

The basic catalytic cycle proposed in Scheme 2-13, however, does not provide insight into how the  $[\text{PPh}_3]$  and  $\text{K}_2\text{CO}_3$  affect stereoretention. In attempting to understand these effects, the fate of the  $\eta$ -2 bound olefin resulting from  $\beta$ -hydride elimination was considered. After  $\beta$ -hydride elimination, as long as the olefin remains complexed to Pd on the same face of the olefin, no loss of stereochemical information (or yield) should be expected after reinsertion into the branched position (Scheme 2-13, process **-D**).



**Scheme 2-14:** Possible fates of the  $\beta$ -hydride elimination product *i* and their effects on stereoretention.

Unfortunately, the other possible reaction manifolds have different outcomes in terms of retention of configuration. Olefin decomplexation (Scheme 2-14, **Path A**) results in the loss of any stereochemical information brought up to this point and yields the potentially critical Pd-hydride intermediate, *ii*. The olefin now has the chance to re-

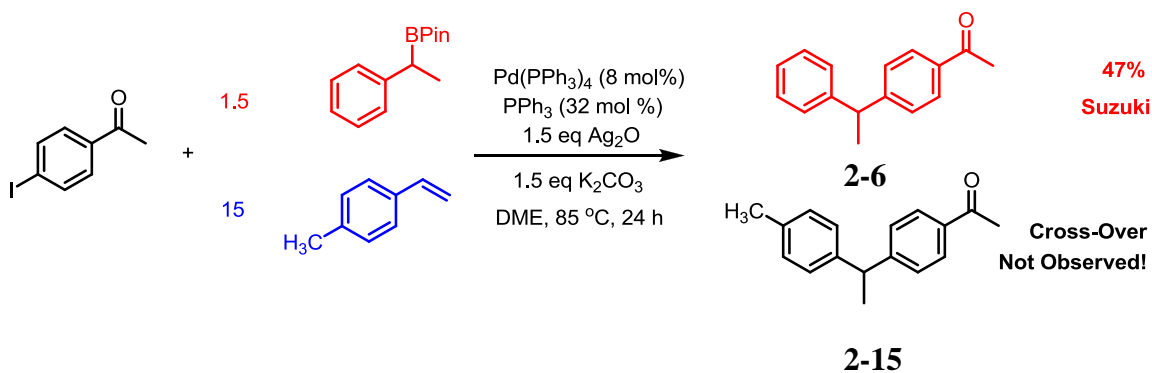


complex to the Pd-H complex, this time from *either face*, giving rise to racemic intermediate ( $\pm$ )-*i* and, after reinsertion and reductive elimination, ultimately leading to the formation of racemic product, *v*.

Mercifully in terms of the retention of configuration, the Pd-hydride *ii* can also undergo reductive elimination to form the reduced arene, Ar-H, precluding the formation of racemic ( $\pm$ )-*i*. The observation of small amounts of Ar-H during cross-couplings serves as evidence for the existence of this manifold. This process is favored at lowered loadings of PPh<sub>3</sub> and would lead to an increased stereoretention of the final product. Notably, this occurs at the expense of yield, as it irreversibly converts the limiting reagent (aryl halide) into unreactive arene. At higher concentrations of phosphine ligand, the Pd-H complex may exist in equilibrium with the fully ligated form *iii* which, given the steric demands of the bulky PPh<sub>3</sub> ligands, will exist in the *trans* conformation. The *trans* conformation prevents facile reductive elimination and increases the lifetime of Pd-H complex *ii*, ultimately allowing it to re-complex to an olefin in a stereo-eroding step. Although the effect of [PPh<sub>3</sub>] is likely to be complex given its involvement in so many pathways, insofar as the Pd-H complex is concerned, an increased ligand loading disfavors arene formation *via* reductive elimination and allows for olefin re-complexation, leading to an increased product yield with lowered enantiopurity. These hypotheses are consistent with the data obtained in Section 2.5.3.

An olefin cross-over study (Scheme 2-15) was undertaken to test the hypothesis of styrene decomplexation (Scheme 2-14, **Path A**). However, even in the presence of a ten-fold excess of *para*-substituted styrene relative to benzylic boronic ester, no cross-

over product **2-15** was observed. This result indicates that if olefin decomplexation is in fact operating in this system, the free styrene must then be adding back to the metal *before* breaking free of the solvent cage and accessing the bulk solution. Otherwise, there should not be any discrimination between this newly-formed styrene and the exogenously added substituted styrene.



**Scheme 2-15:** Attempted cross-over experiment to verify occurrence of olefin decomplexation from Pd.

Another possible reaction of intermediate *i* is insertion of the Pd-hydride into the complexed olefin with opposite regiochemistry, leading to primary alkyl Pd species *j* (Scheme 2-14, **Path B**). A second  $\beta$ -hydride elimination to form complex ( $\pm$ )-*i*, followed by insertion and reductive elimination to final product *v* would scramble stereochemistry. However, complex *j* would be expected to undergo facile reductive elimination yielding the linear cross-coupled product *k*, which is not detected in the reaction mixture. The absence of linear product *k* indicates that this process is not likely occurring under these

reaction conditions, however deuterium labeling studies are being undertaken to completely rule out this pathway.

The intermediacy of Pd-H complex *ii* would also serve to explain the increased stereoretention observed upon inclusion of  $K_2CO_3$ . Indeed, anything that removes the Pd-H complex from solution should cause an increase in stereoretention by preventing the non-selective re-addition of the olefin to Pd. In this case, the deprotonation of Pd-H by exogenous base leads to a bolstering of stereoretentions, from 90-93% to in excess of 98% retention. To investigate this hypothesis more fully, we substituted the sparingly soluble  $K_2CO_3$  for Hünig's base,  $EtN(iPr)_2$ . Fu has shown that amine bases can have favorable effects when used in the asymmetric Mizoroki-Heck reaction through more facile deprotonation of Pd-H complexes.<sup>42</sup> True to form, the reaction performed with Hünig's base yielded the cross-coupled product with higher enantiopurity (92% stereoretention) than that using  $K_2CO_3$  (88% stereoretention) under conditions meant to promote loss of stereochemistry, namely at high concentrations of  $PPh_3$ .

In the end, the lack of both cross-over and linear arylation products may well be the proof that neither racemization pathway **A** or **B** are actually at play. It is also conceivable that the slight erosion of *er*, confined to the catalytic cycle, stems from imperfect facial-selectivity of the transmetalation step, though without a solid understanding of that step, this has to remain speculative. That said, the near complete levels of stereoretention observed, even at high ligand loadings and in the absence of  $K_2CO_3$ , remind us that these racemization events, though not well understood, are in fact very minor processes.

## 2.6 Conclusions

The first general protocol for the cross-coupling of secondary boronic esters with retention of configuration has been described. Addition of the transmetalation-enabling base Ag<sub>2</sub>O proved to be critical along with a relatively large phosphine ligand to Pd ratio. Surprisingly, PPh<sub>3</sub> proved to be the best ligand for the cross-coupling of both aryl iodides *and* aryl bromides, despite the reaction being first order in ArBr.

The reaction also exhibits a remarkable chemoselectivity, with only the branched boronic esters resulting from the *regio*- and *enantio*-selective hydroboration of styrene undergoing coupling, even in the presence of the supposedly more reactive linear isomer. Interestingly, the cross-coupling of secondary boronic esters also occurs preferentially over the Mizoroki-Heck reaction in both intermolecular and intramolecular competition studies.

The translation of stereochemical information from boronic ester to coupled product is probably the most impressive attribute of the reaction, with stereoretentions ranging from 93-98%. Surprisingly, the small amount of stereochemical erosion was attributed not to racemization events in the product or starting material, but to processes inherent to the catalytic cycle. Indeed, it was postulated that a Pd-H intermediate was critical to the scrambling of configuration but that its effect could be mitigated by the use of exogenous base, though a lack of cross-over product warrants further investigation.

## 2.7 References

- (1) Crudden, C. M.; Edwards, D. R. Catalytic Asymmetric Hydroboration: Recent Advances and Applications in Carbon-Carbon Bond-Forming Reactions. *Eur. J. Org. Chem.* **2003**, 2003, 4695-4712.
- (2) Manning, D.; Noth, H. Catalytic Hydroboration with Rhodium Catalysts. *Angew. Chem. Int. Ed.* **1985**, 24, 878-879.
- (3) Evans, D. A.; Fu, G. C.; Hoveyda, A. H. Rhodium(I)-catalyzed hydroboration of olefins. The documentation of regio- and stereochemical control in cyclic and acyclic systems. *J. Am. Chem. Soc.* **1988**, 110, 6917-6918.
- (4) Hayashi, T.; Matsumoto, Y.; Ito, Y. Catalytic asymmetric hydroboration of styrenes. *J. Am. Chem. Soc.* **1989**, 111, 3426-3428.
- (5) Crudden, C. M.; Hleba, Y. B.; Chen, A. C. Regio- and Enantiocontrol in the Room-Temperature Hydroboration of Vinyl Arenes with Pinacol Borane. *J. Am. Chem. Soc.* **2004**, 126, 9200-9201.
- (6) Crudden, C. M.; Glasspoole, B. W.; Lata, C. J. Expanding the scope of transformations of organoboron species: carbon-carbon bond formation with retention of configuration. *Chem. Commun.* **2009**, 6704-6716.
- (7) Noyori, R.; Hashiguchi, S. Asymmetric Transfer Hydrogenation Catalyzed by Chiral Ruthenium Complexes. *Acc. Chem. Res.* **1997**, 30, 97-102.
- (8) Chen, A.C.; Ren, L.; Crudden, C.M. Catalytic asymmetric carbon-carbon bond forming reactions: preparation of optically enriched 2-aryl propionic acids by a catalytic asymmetric hydroboration-homologation sequence. *Chem. Commun.* **1999**, 611-612.

- (9) Fernandez, E.; Hooper, M. W.; Knight, F., I.; Brown, J. M. Catalytic asymmetric hydroboration-amination. *Chem. Commun.* **1997**, 173-174.
- (10) Carey, J. S.; Laffan, D.; Thomson, C.; Williams, M. T. Analysis of the reactions used for the preparation of drug candidate molecules. *Org. Biomol. Chem.* **2006**, 4, 2337-2347.
- (11) Gligorich, K. M.; Cummings, S. A.; Sigman, M. S. Palladium-Catalyzed Reductive Coupling of Styrenes and Organostannanes under Aerobic Conditions. *J. Am. Chem. Soc.* **2007**, 129, 14193-14195.
- (12) Hatanaka, Y.; Hiyama, T. Stereochemistry of the cross-coupling reaction of chiral alkylsilanes with aryl triflates: a novel approach to optically active compounds. *J. Am. Chem. Soc.* **1990**, 112, 7793-7794.
- (13) Imao, D.; Glasspoole, B. W.; Laberge, V. S.; Crudden, C. M. Cross Coupling Reactions of Chiral Secondary Organoboronic Esters With Retention of Configuration. *J. Am. Chem. Soc.* **2009**, 131, 5024-5025.
- (14) Ohmura, T.; Awano, T.; Suginome, M. Stereospecific Suzuki-Miyaura Coupling of Chiral  $\alpha$ -(Acylamino)benzylboronic Esters with Inversion of Configuration. *J. Am. Chem. Soc.* **2010**, 132, 13191-13193.
- (15) Sandrock, D. L.; Jean-Gerard, L.; Chen, C.; Dreher, S. D.; Molander, G. A. Stereospecific Cross-Coupling of Secondary Alkyl  $\beta$ -Trifluoroboratoamides. *J. Am. Chem. Soc.* **2010**, 132, 17108-17110.
- (16) Miyaura, N.; Ishiyama, T.; Ishikawa, M.; Suzuki, A. Palladium-catalyzed cross-coupling reactions of B-alkyl-9-BBN or trialkylboranes with aryl and 1-alkenyl halides. *Tetrahedron Lett.* **1986**, 27, 6369-6372.

- (17) Sato, M.; Miyaura, N.; Suzuki, A. Cross-Coupling Reaction of Alkyl- or Arylboronic Acid Esters with Organic Halides Induced by Thallium(I) Salts and Palladium-Catalyst. *Chem. Lett.* **1989**, 18, 1405-1408.
- (18) Uenishi, J.; Beau, J. M.; Armstrong, R. W.; Kishi, Y. Dramatic rate enhancement of Suzuki diene synthesis. Its application to palytoxin synthesis. *J. Am. Chem. Soc.* **1987**, 109, 4756-4758.
- (19) Schlesinger, A. M. *Robert Kennedy and His Times*; Houghton Mifflin: Boston, 1978; pp 1066.
- (20) Fu, G. C. The Development of Versatile Methods for Palladium-Catalyzed Coupling Reactions of Aryl Electrophiles through the Use of P(t-Bu)<sub>3</sub> and PCy<sub>3</sub> as Ligands. *Acc. Chem. Res.* **2008**, 41, 1555-1564.
- (21) Martin, R.; Buchwald, S. L. Palladium-Catalyzed Suzuki-Miyaura Cross-Coupling Reactions Employing Dialkylbiaryl Phosphine Ligands. *Acc. Chem. Res.* **2008**, 41, 1461-1473.
- (22) Marion, N.; Nolan, S. P. Well-Defined N-Heterocyclic Carbenes: Palladium(II) Precatalysts for Cross-Coupling Reactions. *Acc. Chem. Res.* **2008**, 41, 1440-1449.
- (23) Littke, A. F.; Dai, C.; Fu, G. C. Versatile Catalysts for the Suzuki Cross-Coupling of Arylboronic Acids with Aryl and Vinyl Halides and Triflates under Mild Conditions. *J. Am. Chem. Soc.* **2000**, 122, 4020-4028.
- (24) Norton, D. M.; Mitchell, E. A.; Botros, N. R.; Jessop, P. G.; Baird, M. C. A Superior Precursor for Palladium(0)-Based Cross-Coupling and Other Catalytic Reactions. *J. Org. Chem.* **2009**, 74, 6674-6680.
- (25) Nokami, T.; Tomida, Y.; Kamei, T.; Itami, K.; Yoshida, J. Palladium-Catalyzed Cross-Coupling Reactions of (2-Pyridyl)allyldimethylsilanes with Aryl Iodides. *Org. Lett.* **2006**, 8, 729-731.

- (26) Nave, S.; Sonawane, R. P.; Elford, T. G.; Aggarwal, V. K. Protodeboronation of Tertiary Boronic Esters: Asymmetric Synthesis of Tertiary Alkyl Stereogenic Centers. *J. Am. Chem. Soc.* **2010**, 132, 17096-17098.
- (27) Furuya, T.; Strom, A. E.; Ritter, T. Silver-Mediated Fluorination of Functionalized Aryl Stannanes. *J. Am. Chem. Soc.* **2009**, 131, 1662-1663.
- (28) Doucet, H. Suzuki–Miyaura Cross-Coupling Reactions of Alkylboronic Acid Derivatives or Alkyltrifluoroborates with Aryl, Alkenyl or Alkyl Halides and Triflates. *Eur. J. Org. Chem.* **2008**, 2008, 2013-2030.
- (29) Molander, G. A.; Canturk, B. Organotrifluoroborates and Monocoordinated Palladium Complexes as Catalysts—A Perfect Combination for Suzuki–Miyaura Coupling. *Angew. Chem. Int. Ed.* **2009**, 48, 2-24.
- (30) Molander, G. A.; Ito, T. Cross-Coupling Reactions of Potassium Alkyltrifluoroborates with Aryl and 1-Alkenyl Trifluoromethanesulfonates. *Org. Lett.* **2001**, 3, 393-396.
- (31) Butters, M.; Harvey, J. N.; Jover, J.; Lennox, A. J. J.; Lloyd-Jones, G. C.; Murray, P. M. Aryl Trifluoroborates in Suzuki–Miyaura Coupling: The Roles of Endogenous Aryl Boronic Acid and Fluoride. *Angew. Chem. Int. Ed.* **2010**, 49, 5156-5160.
- (32) Molander, G. A.; Fleury-Bregeot, N.; Hiebel, M. Synthesis and Cross-Coupling of Sulfonamidomethyltrifluoroborates. *Org. Lett.* **2011**, 13, 1694-1697.
- (33) Molander, G. A.; Beaumard, F. Cross-Coupling of Mesylated Phenol Derivatives with Potassium Ammonio- and Amidomethyltrifluoroborates. *Org. Lett.* **2011**, 13, 1242-1245.
- (34) Molander, G. A.; Biolatto, B. Efficient Ligandless Palladium-Catalyzed Suzuki Reactions of Potassium Aryltrifluoroborates. *Org. Lett.* **2002**, 4, 1867-1870.



- (35) Amatore, C.; Jutand, A. Anionic Pd(0) and Pd(II) Intermediates in Palladium-Catalyzed Heck and Cross-Coupling Reactions. *Acc. Chem. Res.* **2000**, 33, 314-321.
- (36) Jana, R.; Pathak, T. P.; Sigman, M. S. Advances in Transition Metal (Pd,Ni,Fe)-Catalyzed Cross-Coupling Reactions Using Alkyl-organometallics as Reaction Partners. *Chem. Rev.* **2011**, 111, 1417-1492.
- (37) Shenvi, R. A.; O'Malley, D. P.; Baran, P. S. Chemoselectivity: The Mother of Invention in Total Synthesis. *Acc. Chem. Res.* **2009**, 42, 530-541.
- (38) Heck, R. F. Palladium-catalyzed reactions of organic halides with olefins. *Acc. Chem. Res.* **1979**, 12, 146-151.
- (39) Amatore, C.; Jutand, A.; M'Barki, M. A. Evidence of the formation of zerovalent palladium from Pd(OAc)<sub>2</sub> and triphenylphosphine. *Organometallics* **1992**, 11, 3009-3013.
- (40) Mann, B. E.; Musco, A. Phosphorus-31 nuclear magnetic resonance spectroscopic characterisation of tertiary phosphine palladium(0) complexes: evidence for 14-electron complexes in solution. *J. Chem. Soc., Dalton Trans.* **1975**, 1673-1677.
- (41) Shekhar, S.; Hartwig, J. F. Distinct Electronic Effects on Reductive Eliminations of Symmetrical and Unsymmetrical Bis-Aryl Platinum Complexes. *J. Am. Chem. Soc.* **2004**, 126, 13016-13027.
- (42) Hills, I. D.; Netherton, M. R.; Fu, G. C. Toward an Improved Understanding of the Unusual Reactivity of Pd<sup>0</sup>/Trialkylphosphane Catalysts in Cross-Couplings of Alkyl Electrophiles: Quantifying the Factors That Determine the Rate of Oxidative Addition. *Angew. Chem. Int. Ed.* **2003**, 42, 5749-5752.

## **Chapter 3**

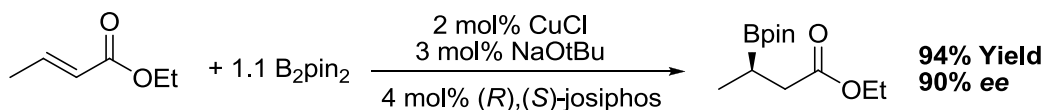
### **Lithiation-Borylation to Synthesize Novel Asymmetric Boronic Ester Cross-Coupling Partners**

#### **3.1 Introduction**

Our forays into the field of cross-coupling methodology were intended to both propagate the utility of the asymmetric hydroboration reaction and to address one of the last remaining challenges facing the Suzuki-Miyaura reaction, namely the cross-coupling of boronic esters with stereochemistry. By successfully cross-coupling benzylic boronic esters, we accomplished both of these goals, but a reliance on a particular substrate class limits the applicability of the method. The next logical step was to more fully investigate the cross-coupling of allylic boronic esters after the solitary example provided in the previous chapter was shown to be so readily cross-coupled. Indeed, to fully understand the scope and limitations of our new silver-mediated protocol, we would have to challenge it with a wider variety of secondary boronic esters. To do this, we would have to forgo our reliance on the hydroboration of styrenes to synthesize coupling partners, and instead turn to other known synthetic methods or investigate new routes of our own. In the end, this body of work became as much about the enantioselective synthesis of new boronic esters as the subsequent stereoretentive cross-coupling reaction we wished to promote.

### 3.1.1 Known Methods: Asymmetric Syntheses of Organoborons

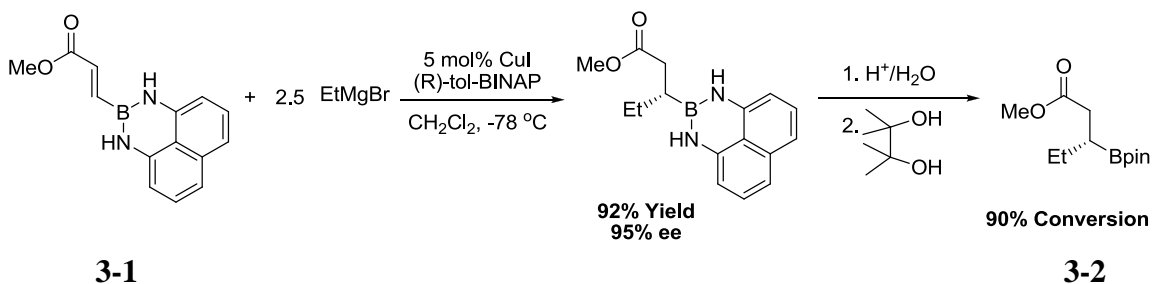
In the past decade, several asymmetric borylation reactions have been reported, all of which can be used to synthesize chiral secondary boronic esters.<sup>1-4</sup> For example, Yun has demonstrated that the Cu(I)-catalyzed asymmetric borylation of alkenes with bis(pinacolato)diboron, B<sub>2</sub>pin<sub>2</sub>, in the presence of chiral ligands can affect what is ultimately a hydroboration of the alkene with high *regio*- and *enantioselectivity* (Scheme 3-1).<sup>1,4</sup> The groups of Fernandez<sup>3</sup> and Hoveyda<sup>2</sup> also employed copper, along with chiral NHC ligands to borylate  $\alpha,\beta$ -unsaturated ketones and styrenyl-moieties, respectively. In the latter case, regioselectivities complementary to the Rh<sup>+</sup>-catalyzed hydroboration were observed. That said, the narrow substrate scope (often limited to Michael-acceptors) for these Cu(I)-catalyzed reactions belies their utility for the development of subsequent cross-coupling protocols.



**Scheme 3-1:** The asymmetric borylation of  $\alpha,\beta$ -unsaturated esters as reported by Yun and co-workers.<sup>4</sup>

Recently, Hall<sup>5</sup> has explored the possibility of asymmetrically adding alkyl Grignard reagents to  $\beta$ -borylated  $\alpha,\beta$ -unsaturated esters (**3-1**) to form chiral secondary boronic esters (Scheme 3-2). Using the boronic ester derived from 1,8-diaminonaphthalene (Bdan), Hall was able to temper the reactivity of the electrophilic

boron centre and successfully affect the addition of alkyl groups into borylated Michael-acceptors in high yield and enantioselectivity.<sup>5</sup> The resultant motif ( $\beta$ -borylated ester, **3-2**) along with the analogous amides, have recently been shown to undergo successful Suzuki-Miyaura type cross-coupling by Suginome<sup>6</sup> and Molander.<sup>7</sup>

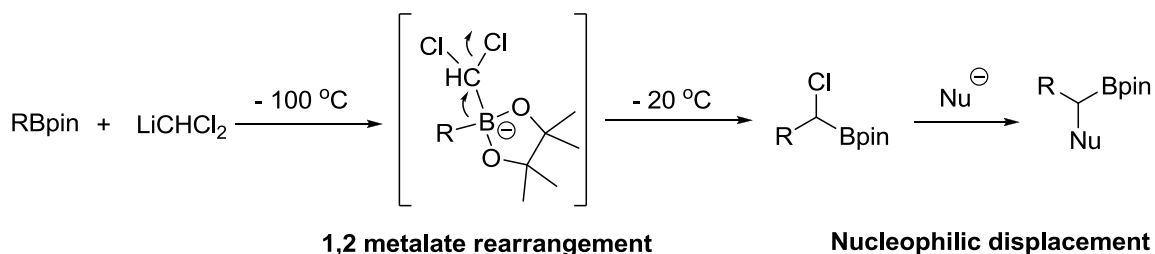


**Scheme 3-2:** Asymmetric alkylation of vinyl boronic esters as an alternative to hydroboration.

### 3.1.2 Matteson Chemistry

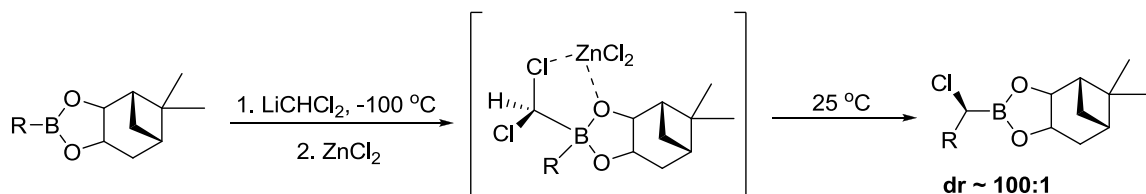
Naturally, the ability to create chiral boronic esters is not limited to additions across double bonds. Throughout the 1960s, Matteson and co-workers studied the reactivity of  $\alpha$ -haloalkane boronic esters with nucleophiles and ultimately proposed a boron-assisted  $S_N2$ -type mechanism for halide replacement.<sup>8</sup> However, the limited number of routes to  $\alpha$ -haloalkane boronic esters hindered the synthetic viability of the process. To address this, Matteson developed the one-carbon homologation of boronic esters by lithiated dichloromethane ( $LiCHCl_2$ ).<sup>9</sup> In essence, the electrophilic boron centre forms an adduct with the organolithium species which is followed by a 1,2-migration of

the organic group from boron to carbon, expelling a chloride and producing the desired  $\alpha$ -chloro boronic ester (Scheme 3-3).



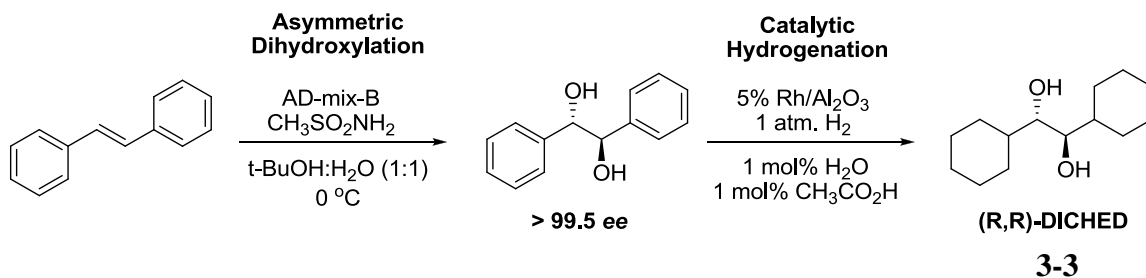
**Scheme 3-3:** Homologation of boronic esters by lithiated dichloromethane followed by nucleophilic displacement of a chloride.

Furthermore, when the boronic ester is derived from a chiral diol (such as pinanediol), one of the diastereotopic chlorides of the borate adduct leaves preferentially upon 1,2-migration, leading to moderate enantioselectivities in the product. In his *coup de grâce*, Matteson then realized that the addition of ZnCl<sub>2</sub> after borylation not only hastened the migration step, but also led to a remarkable improvement in enantioselectivity; indeed, the synthesis of asymmetric  $\alpha$ -chloro boronic esters by this method often proceeds at *dr*'s approaching or exceeding 100:1 (Scheme 3-4).<sup>10</sup>



**Scheme 3-4:** Diastereoselective variant of Matteson-type homologation using chiral auxiliary on boron (in this case, pinanediol).

The substrate-induced enantioselectivity is not limited to boronic esters derived from pinanediol. In 1996, Matteson reported the highly enantioselective synthesis of both (*S,S*)- and (*R,R*)-dicyclohexylethanediol ((*R,R*)-DICHD, **3-3**) in two steps from *trans*-stilbene (Scheme 3-5).

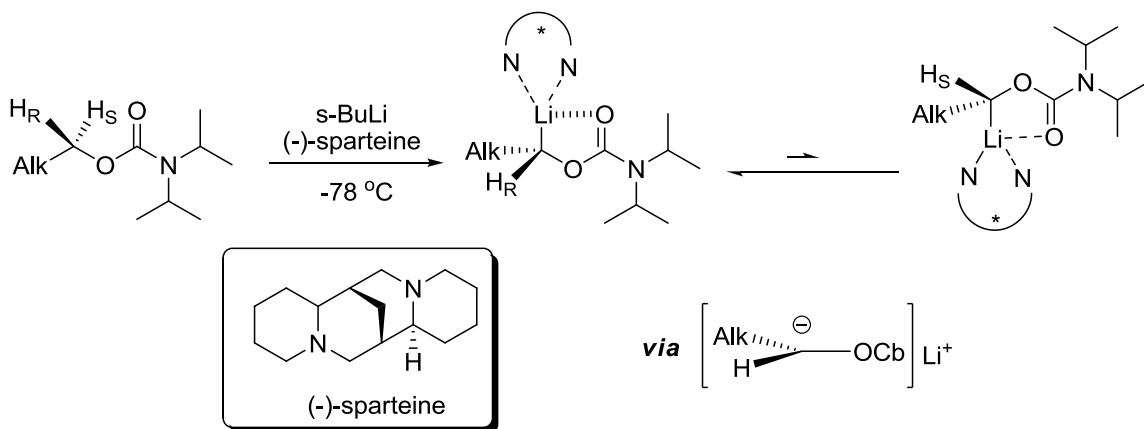


**Scheme 3-5:** Synthesis of (*R,R*)-DICHD for use as chiral auxiliary on boron for Matteson Homologation. Sharpless Asymmetric Dihydroxylation<sup>11</sup> is used to create the critical 1,2-diol motif.

Boronic esters derived from this chiral diol also yield  $\alpha$ -chloro boronic esters with very high *dr*.<sup>12</sup> Simply changing the antipode of the chiral diol gives the other enantiomer of the product. These asymmetric  $\alpha$ -chloro boronic esters can be isolated, but are more often subjected to attack by nucleophiles to undergo the stereochemistry-inverting replacement of the remaining halide (as in Scheme 3-3). As will be discussed, it would be the quenching of these  $\alpha$ -chloro alkylboronic esters with vinyl Grignard reagents that would lead us to a general and variable synthesis of chiral secondary allylic boronic ester cross-coupling partners.

### 3.1.3 Lithiated Carbamates

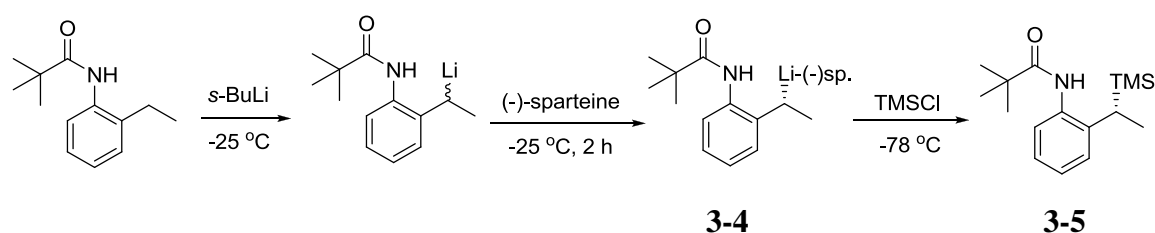
A similar, but complementary approach to synthesize chiral secondary boronic esters relies on the asymmetric deprotonation of pro-chiral alkylcarbamates. In the presence of a chiral ligand, usually (-)-sparteine, lithiation of the pro-chiral substrate is followed by an electrophile quench, which can lead to highly enantiomerically enriched products.<sup>13</sup> The effect of the adjacent carbamate is noteworthy; despite the tendency of lithiated carbanions to adopt a tetrahedral configuration (and therefore retain the asymmetry imparted on them by the chiral ligand), these ion pairs can become separated, leading to a planar, achiral intermediate. Recapturing  $\text{Li}^+$  (or the electrophile) from either face leads to a racemic product (Scheme 3-6). Both Hoppe<sup>13</sup> and Beak<sup>14</sup> have found that groups like carbamates and amides can, with help from the chiral (-)-sparteine ligand, stabilize the tight ion pair and ensure configurational stability in certain substrates.



**Scheme 3-6:** The enantioselective deprotonation of alkyl carbamates with *s*-BuLi and the chiral ligand (-)-sparteine. The enantioselectivity of the lithiation is determined by

stereodifferentiation in the deprotonation *and* the configurational stability of the resulting lithium/carbanion pair. In the example given, the lithiated carbamate is configurationally stable and does not undergo a significant amount of inversion *via* the planar intermediate.

The asymmetric deprotonation described above is not the only route to non-racemic products. Indeed, both a dynamic *thermodynamic* resolution and dynamic *kinetic* resolution can be employed. In the former, a non-selective lithiation is followed by the formation of the thermodynamically favored diastereomeric complex (**3-4**) with (-)-sparteine at relatively warm (-25 °C) temperatures. Quenching by the electrophile then proceeds after re-cooling to low temperatures (Scheme 3-7).<sup>14</sup>

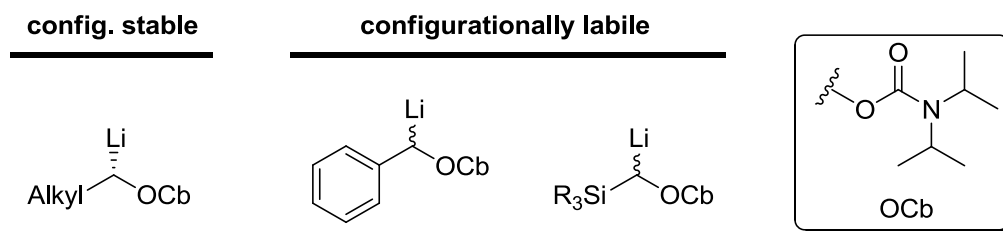


**Scheme 3-7:** Dynamic thermodynamic resolution to achieve enantioselective lithiation of benzyl group. TMS= trimethylsilyl.

In contrast, dynamic *kinetic* resolution occurs when the lithiated carbamate is configurationally labile, rapidly exchanging between diastereotopic forms of the ligated lithium complex. The enantiodetermining step then occurs as one diastereomer reacts preferentially with the electrophile.<sup>14</sup> An understanding of these factors will become necessary as we deviate from the configurationally stable lithiated *alkyl* carbamates, to both *silyl*- and *benzyl* carbamates in the course of our studies (Scheme 3-8). In the end, adjusting the activity of the electrophile enabled us to skirt the issue of configurational



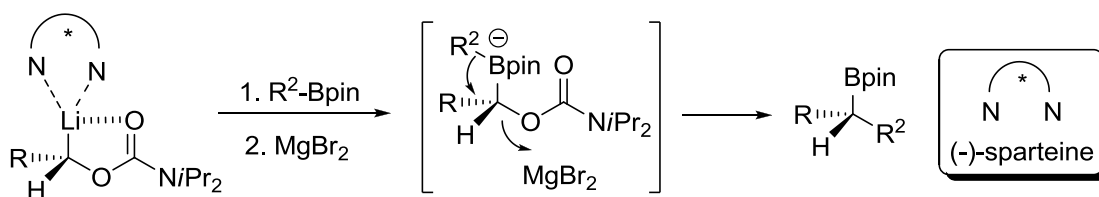
lability in the case of the benzyl substrates, though a completely new approach would be needed for the silyl case.



**Scheme 3-8:** Relative configurational stabilities of lithiated carbamates used throughout this work.

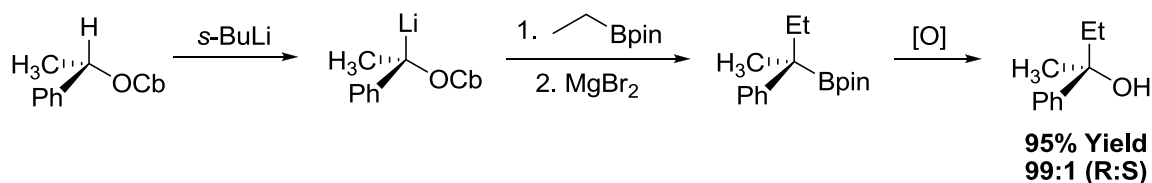
### 3.1.4 Lithiated Carbamates Used in Boronic Ester Homologation

Over the past five years, the Aggarwal group has applied the lithiation strategies of Beak and Hoppe to organoboron electrophiles.<sup>15, 16</sup> As in the case of Matteson chemistry, the organic functionality (be it alkyl, vinyl, aryl or, laterally, silyl) on boron can migrate to the adjacent carbon centre, expunging the carbamate group. Notably, unlike the Matteson homologation, the enantiodetermining step of this process occurs during lithiation step and not upon preferential removal of a diastereotopic chloride. The leaving group ability of the carbamate group, whose initial function was to stabilize the lithium-carbanion pair, is significantly less than that of a halide and so prolonged reflux and an excess of Lewis Acid are often required to affect the aforementioned 1,2-metalate rearrangement (Scheme 3-9)<sup>15</sup>.



**Scheme 3-9:** Enantioselective synthesis of secondary boronic esters by Aggarwal's method.

In the most synthetically relevant sequence of this lithiation-borylation strategy, Aggarwal was able to turn chiral secondary alcohols into non-racemic quaternary centres containing boron by way of a configurationally stable secondary carbamate.<sup>17</sup> The chiral boronic esters were subsequently oxidized in a stereoretentive manner to yield chiral tertiary alcohols (Scheme 3-10). The complete dearth of alternative routes to these structures demonstrated the power of this methodology, but, as was the case with the asymmetric hydroboration reaction in the previous decade, mere oxidation of non-racemic C-B bonds does not do justice to the elegance of the method by which they were created. Again, it would be our aim to apply a cross-coupling strategy to complement the lithiation-borylation methodology in order to access the ever-sought-after chiral C-C frameworks.



**Scheme 3-10:** Lithiation-borylation with enantioenriched secondary carbamates to yield non-racemic tertiary alcohols.

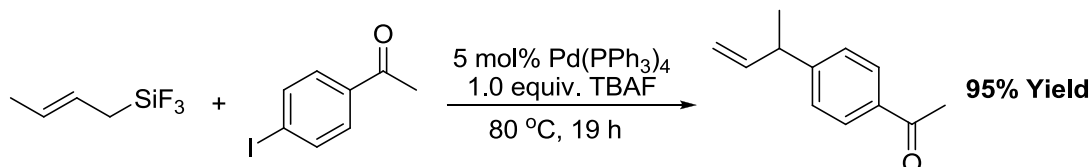
### 3.2 The Synthesis and Cross-Coupling of Secondary Allylic Boronic Esters

At first, the cross-coupling of a secondary allylic boronic ester was performed merely in an attempt to understand the chemoselectivity of the benzylic boronic esters. Unlike the saturated cyclohexyl-Bpin, 2-cyclohexenyl-Bpin was cross-coupled in high yield (Chapter 2, Scheme 2-11). The fact that the boronic ester needed to be either benzylic or allylic, and the implications of this on both the mechanism and the potential role of  $\text{Ag}_2\text{O}$ , were discussed in detail in the previous chapter. However, it was also recognized that our cross-coupling protocol should then be applicable to this entirely new, as yet untapped, type of substrate. With the lithiation-borylation strategies outlined above providing effective synthetic routes to secondary allylic boronic esters, we then turned our focus to the asymmetric synthesis, and stereoretentive cross-coupling, of this important class of molecule.

#### 3.2.1 Precedence for Allylic Cross-Coupling: Allyl Silanes

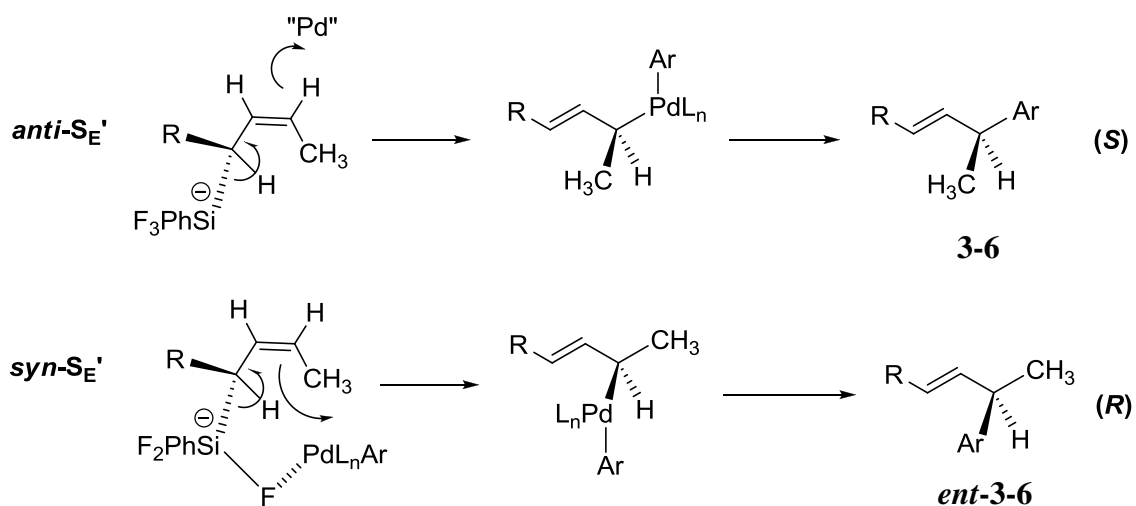
Though precedence does exist for the cross-coupling of allylic boronic acids and esters,<sup>18, 19</sup> the vast majority of work done on the topic of allylic coupling has focused on allyl silane derivatives. In 1991, Hiyama reported the fluoride-promoted, Pd-catalyzed

cross-coupling of allyl trifluorosilanes with aryl triflates (Scheme 3-11).<sup>20</sup> Interestingly, the increased nucleophilicity of the  $\gamma$ -carbon led to palladation at this (and not the  $\alpha$ -carbon) site and therefore high regioselectivities for the  $\gamma$ -arylated product were observed after the reductive elimination step.



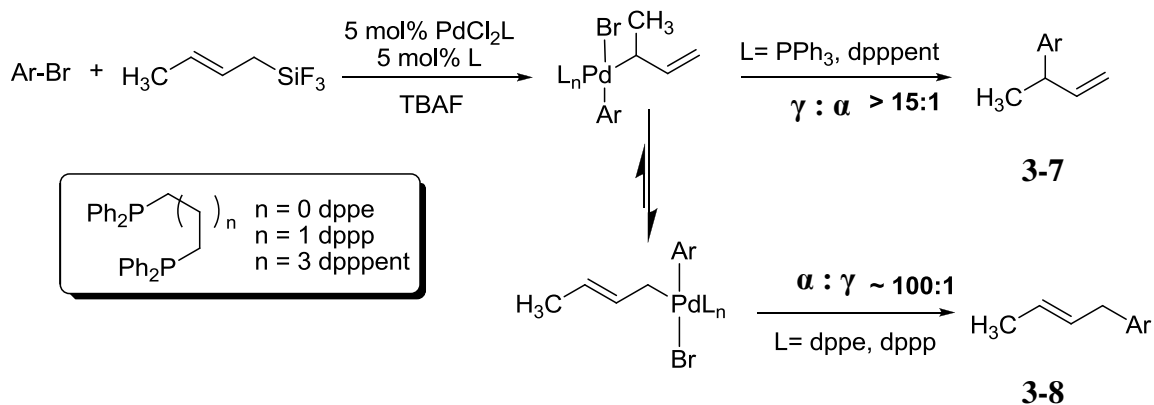
**Scheme 3-11:** Gamma-selectivity for the fluoride-promoted, Pd-catalyzed cross-coupling of allyl silanes.

Subsequently, Hiyama discovered that the stereochemistry of the cross-coupling reaction could be controlled by varying the fluoride source and solvent polarity.<sup>21</sup> Using enantioenriched allyl difluorophenylsilanes, the palladation still occurred exclusively at the  $\gamma$ -carbon site, but the enantioselective formation of the new C-C bond depended on the mechanism of the transmetalation. Polar solvents (such as DMF) resulted in open transition states, which in turn led to *anti*-S<sub>E</sub>' type transmetalation from silicon to Pd (Scheme 3-12, **3-6**). Conversely, when the reaction was performed in THF with CsF, it was proposed that a discrete Si-F-Pd interaction favored *syn*-facial attack to form the opposite enantiomer (Scheme 3-12, *ent*-**3-6**).



**Scheme 3-12:** Stereochemical consequences of a *anti-S<sub>E</sub>'* mechanism (top) favored by polar solvents and the *syn-S<sub>E</sub>'* mechanism (bottom) at play in THF.

Interestingly, the regioselectivity of the reaction can also be tailored by judicious choice of the phosphine ligand (Scheme 3-13). As noted above, transmetalation to allylic silanes occurs preferentially at the  $\gamma$ -site, though to ensure  $\gamma$ -selectivity in the arylated product, reductive elimination must take place before isomerization to the favored  $\alpha$ -isomer occurs. Steric crowding about the Pd complex generated by the bulky PPh<sub>3</sub> or bidentate phosphines with large bite angles (such as dppent) instigates a product-forming reductive elimination prior to isomerization, thus yielding the  $\gamma$ -product (**3-7**). In the case of sterically less-demanding phosphines (such as dppe and dppp), isomerization to the more substituted double bond takes place before reductive elimination can occur.<sup>22</sup>

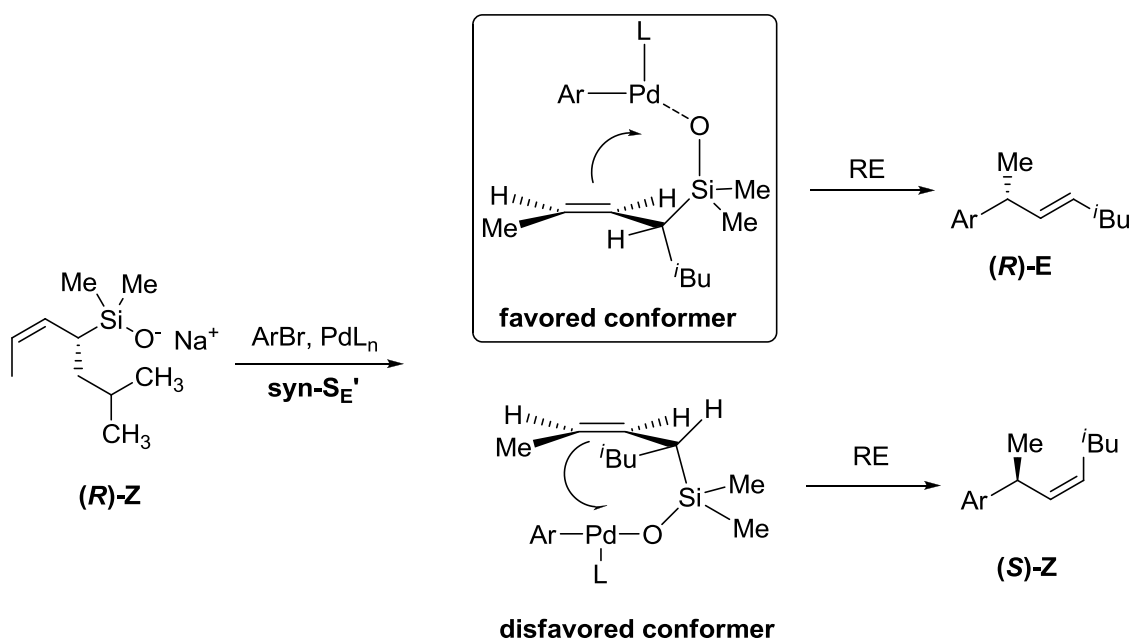


**Scheme 3-13:** Ligand-based regioselectivity for the cross-coupling of primary allyl silanes.

Laterally, Denmark has studied the cross-coupling of allylic silanoate salts with aryl bromides.<sup>23</sup> Much like the CsF-mediated cross-coupling of allyl trifluorosilanes investigated by Hiyama,<sup>21</sup> the transmetalation to allylic silanoate salts proceeds through a *syn*-S<sub>E</sub>' mechanism, owing in large part to a putative Si-O-Pd bridge (Scheme 3-14). Interestingly,  $\pi$ -acidic ligands, such as dibenzylidene acetone (dba), are also used to hasten the reductive elimination step (see Chapter 1, Scheme 1-9) and affect the overall regioselectivity of the reaction.

As part of the study, non-racemic,  $\alpha$ -substituted (secondary) allylic silanoates were prepared to investigate the role of olefin geometry on the stereochemical outcome of the cross-coupling reaction. The stereochemistry of the newly-formed C-C bond is determined by both the facial selectivity of the nucleophilic attack on Pd (*syn*-S<sub>E</sub>' or *anti*-S<sub>E</sub>', *vide supra*) and the reactive conformation of the allylic silanoate itself, which is

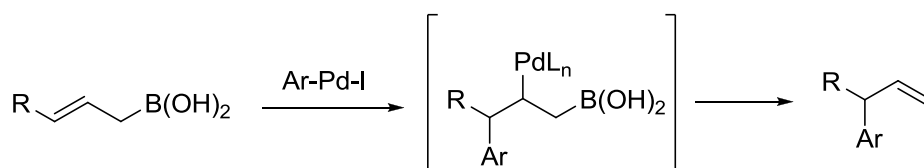
dictated by steric considerations such as  $A^{1,3}$  strain. The aforementioned Si-O-Pd linkage assures *syn*-facial selectivity for the transmetalation step, so enantioselectivity depends fully on the conformation of the allylic silanoate; in the event, it was found that, from a geometrically defined olefin, the only product enantiomer formed was that which arose from a conformer that placed the allylic proton synplanar to the olefin, and not the larger group. This conformation represents the minimization of  $A^{1,3}$  strain, as expected.



**Scheme 3-14:** The effect of olefin geometry on the stereochemical outcome of the cross-coupling of allyl silanoate salts with aryl bromides. The favored conformer (top) dominates as the allylic proton eclipses the double bond and not the bulky *iso*-butyl group (bottom).

### 3.2.2 Precedence for Allylic Cross-Coupling: Allyl Boronic Acids and Trifluoroboronates

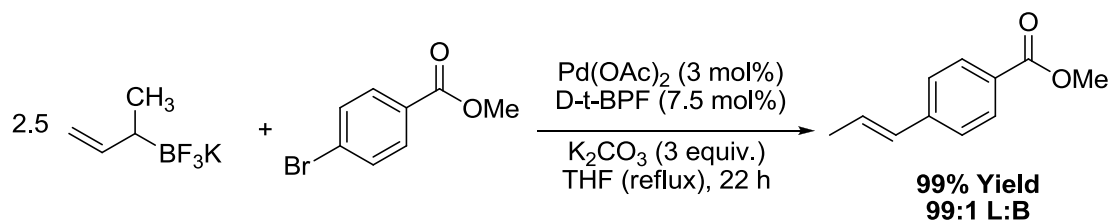
The  $\gamma$ -selective transmetalation event typical of allyl silanes is also observed in the limited examples of the cross-coupling of allyl boronic acid derivatives.<sup>18</sup> In the case of primary allyl boronic acids, Szábo has postulated that the arylated Pd-species (resulting from oxidative addition to an aryl iodide) does not directly transmetalate with the boronic acid, but instead adds across the allylic double bond. Subsequent  $\beta$ -boryl elimination by Pd regenerates the double bond, resulting in an overall  $\gamma$ -arylation (Scheme 3-15).



**Scheme 3-15:** Mechanism proposed by Szábo for the  $\gamma$ -regioselectivity for primary allylic boronic acids.

Miyaura has recently reported the successful cross-coupling of allylic trifluoroboronate salts, including a solitary example of a secondary system (Scheme 3-16).<sup>19</sup> As with allyl silanes, excellent  $\gamma$ : $\alpha$  ratios are observed when bidentate phosphines with large bite angles are used, though in this case, switching to ligands with smaller bite angles lead to only moderate selectivity for the  $\alpha$ -isomer. Interestingly,  $\text{PPh}_3$ , which when used in the cross-coupling of allyl trifluorosilanes led to *complete*  $\gamma$ -selectivity, only led to moderate  $\gamma$ : $\alpha$  ratios (78:22) for the cross-coupling of allyl trifluoroboronate salts.





**Scheme 3-16:** Solitary example of a racemic secondary allylic trifluoroboronate cross-coupling, as reported by Miyaura.<sup>19</sup> High  $\gamma$ -selectivity is observed.

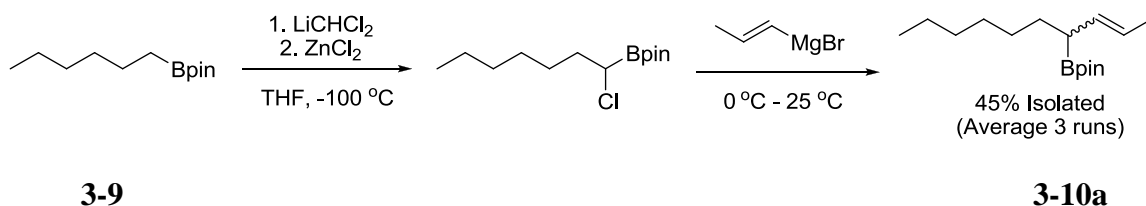
### 3.2.3 The Synthesis and Cross-Coupling of Secondary Allylic Boronic Esters

Given the complete dearth of successful cross-couplings of *secondary* allylic boronic esters (and only one reported example of a secondary allylic trifluoroboronate), we became very interested in extending our studies into the cross-coupling of secondary allylic boronic esters.

The original allylic boronic ester (*rac*-2-cyclohexenylboronic acid pinacolate ester) was synthesized via the Pd-catalyzed borylation of a racemic allylic alcohol. As it was unclear whether this borylation methodology could be applied to a wider variety of substrates, or even be performed asymmetrically, we turned our attention to lithiation-borylation strategies that would allow for the systematic variation of structure and for the creation of a chiral boronic ester.

Initially, a synthetic strategy involving the lithiated carbamates of Hoppe and Aggarwal was explored,<sup>15</sup> though conversion to the desired allylic boronic ester was found to be difficult and irreproducible. Greater success was found upon switching to a

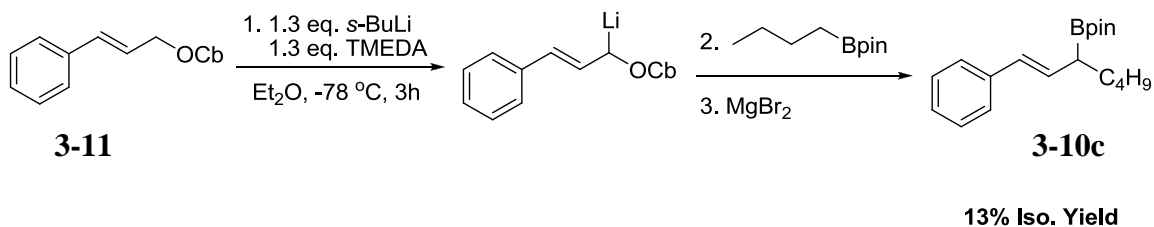
Matteson-type approach, whereby  $\alpha$ -chloroboronic esters were synthesized and eventually reacted with 1-propenylmagnesium bromide to yield the desired secondary boronic esters (Scheme 3-17, **3-10a**). This piece-wise method allows for significant structure variability, but even this approach was fraught with its own unique difficulties; indeed, incomplete consumption of the starting alkyl boronic ester often led to a difficult product isolation and, ultimately, a deflated yield. Though certainly sub-optimal, the sometimes low yielding process was tolerated as our interest lay in exploring the cross-coupling of these allylic boronic esters, not their synthesis.



**Scheme 3-17:** Synthesis of racemic secondary allylic boronic ester *via* Matteson chemistry.

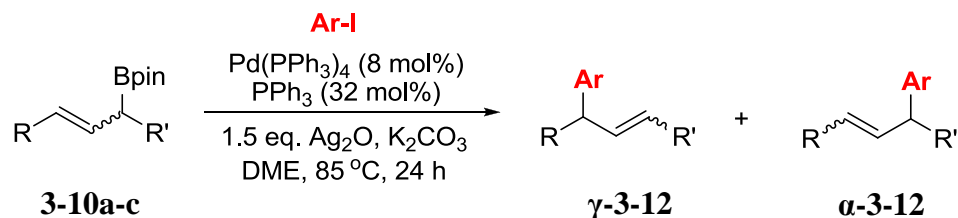
In the interest of preparing a wider variety of secondary allylic boronic esters, we next pursued the synthesis of boronic esters whereby the allylic group was in conjugation with an extended  $\pi$ -system. We turned first to a lithiation-borylation approach (Scheme 3-18). Though we were ultimately able to synthesize the desired secondary allylic boronic ester **3-10c** in sufficient quantities to allow for subsequent cross-coupling experiments, prohibitively low yields (possibly arising from a stabilized boronate complex) rendered the lithiation-borylation approach synthetically unviable. Fortunately,

an alternative Matteson-type approach ultimately led to the desired conjugated allylic boronic esters in yields approaching 50%.



**Scheme 3-18:** Poor-yielding synthesis of a conjugated allylic boronic ester by way of a lithiation-borylation approach. The multiple chromatography steps required to isolate the product from unconsumed alkyl boronic ester deflate the yield substantially.

With a suitable quantity of unconjugated secondary allylic boronic esters **3-10a-b**, and a sufficient amount of the conjugated boronic ester **3-10c** in hand, we then examined their reactivity under our silver-mediated cross-coupling protocol. As expected, several acyclic secondary allylic boronic esters coupled to a variety of aryl iodides in respectable yields (Table 3-1).

**Table 3-1:** Yields and selectivities for secondary allylic boronic ester couplings.

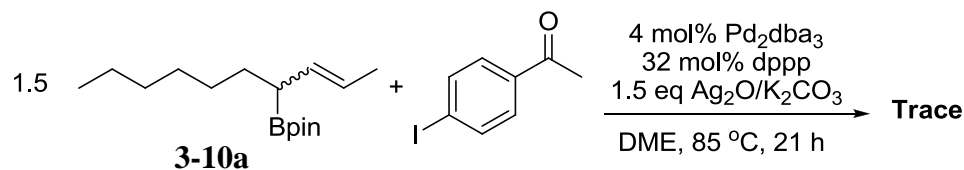
Entry	Boronic Ester	Aryl iodide	Yield <sup>a</sup>	$\gamma$ : $\alpha$ (crude) <sup>b</sup>	$\gamma$ : $\alpha$ (pure) <sup>b</sup>
1	 <b>3-10a</b>	 <b>a</b>	84	92:8	87:13
2	 <b>3-10a</b>	 <b>b</b>	83	83:17	79:21
3	 <b>3-10a</b>	 <b>c</b>	70	90:10	86:14
4	 <b>3-10a</b>	 <b>d</b>	72	91:9	90:10
5	 <b>3-10b</b>	 <b>a</b>	74	88:12 <sup>c</sup>	86:14
6	 <b>3-10c</b>	 <b>a</b>	58	12:88 <sup>c</sup>	8:92

(a) Isolated yields of isomer mixtures. (b) Ratio of isomers determined by NMR (c) Ratio of crude isomers determined by uncalibrated GC-MS integrations. The isomeric ratio of the crude reactions demonstrates that the ratio is not a result of preferential isolation of one isomer.

The Pd-catalyzed cross-coupling proceeded with good regioselectivity at the  $\gamma$ -site and was consistent (though variable in extent) for all aryl iodides tested (Table 3-1,

Entries 1-5). In the case of conjugated allylic boronic esters, however, the selectivity is reversed and the  $\alpha$ -regioisomer becomes preferred (Table 3-1, Entry 6).

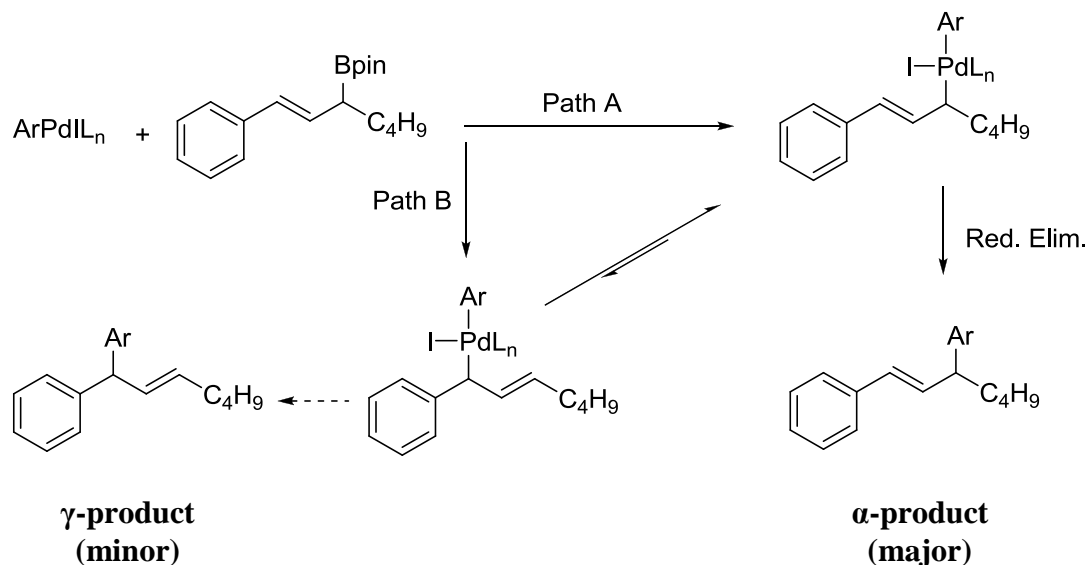
The  $\gamma$ : $\alpha$  ratios observed for the unconjugated systems (Table 3-1, Entries 1-5) are consistent with those observed by Miyaura for the cross-coupling of allyl trifluoroboronates when using  $\text{PPh}_3$  as a ligand.<sup>19</sup> Given that both Miyaura (trifluoroboronates)<sup>19</sup> and Hiyama (trifluorosilanes)<sup>22</sup> were able to fine tune, and in Hiyama's case, completely alter the regioselectivity of the cross-coupling by choice of ligand, we were optimistic that a ligand-based strategy would be applicable to secondary allylic boronic esters as well. Unfortunately, when dppp was substituted for  $\text{PPh}_3$  in a cross-coupling reaction, the allylic boronic ester **3-10a** remained untouched and only a trace amount of cross-coupled product was observed by GC-MS (Scheme 3-19). Naturally, the cross-coupling's dependence on  $\text{PPh}_3$  may have been predicted by the ligand screens performed for the analogous benzylic boronic ester in Chapter 2, which showed that all bidentate phosphines completely shut down the reaction.



**Scheme 3-19:** Attempted alteration of the regioselectivity for the cross-coupling of allylic boronic esters based on a ligand strategy.

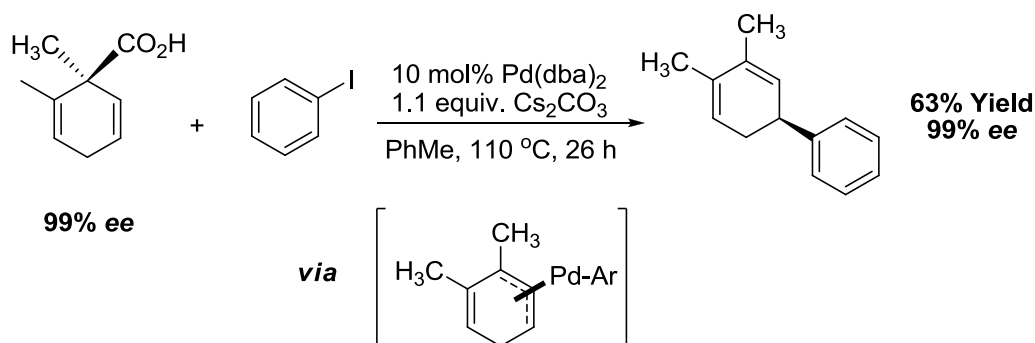
Our inability to alter the regioselectivity of the reaction by way of a ligand-based strategy places added importance on the *substrate*-based control of regioselectivity observed for the conjugated allylic boronic ester (Table 3-1, Entry 6). Presumably, the

conjugated allyl system either disfavors the typical  $S_E'$  transmetalation mechanism, or encourages isomerization to restore conjugation prior to reductive elimination (Scheme 3-20).



**Scheme 3-20:** Two possible pathways leading to  $\alpha$ -arylation in aryl systems. Path **A** proceeds through a direct transmetalation at the  $\alpha$ -site. In Path **B**, transmetalation occurs by way of the more typical  $S_E'$  mechanism, but rapid isomerization occurs to restore conjugation.

Despite being unprecedented in the cross-coupling of allyl silanes or boronic acid derivatives, regioselectivity based on conjugation has recently been reported in Pd-catalyzed decarboxylative coupling reactions (Scheme 3-21).<sup>24</sup>



**Scheme 3-21:** Pd-catalyzed decarbonylative coupling. The regioselectivity is dictated by the creation of conjugation in the non-aromatic ring.

The substrate-based regioselectivity observed for conjugated systems also indicates that Szábo's proposed mechanism<sup>18</sup> for the cross-coupling of primary allylic boronic acids with aryl iodides does not apply to the present study. Indeed, in his olefin-insertion mechanism, there is no allowance for changes in regioselectivity. Furthermore, no cross-coupling product is observed when the reaction of a secondary allylic boronic esters is attempted without  $\text{Ag}_2\text{O}$  or with lower loading of  $\text{PPh}_3$ , facts unaccounted for in the Szábo mechanism.

The regioselectivities (and changes thereof) observed for the cross-coupling of secondary allylic boronic esters (Table 3-1) are seemingly more congruous with the mechanism postulated by Miyaura,<sup>19</sup> and consistent with those reported for the analogous allyl trifluorosilanes, whereby  $\text{S}_{\text{E}}'$ -type transmetalation is followed by a potential isomerization. The role of  $\text{Ag}_2\text{O}$ , which is required for the successful cross-coupling of secondary allyl boronic esters, warrants further study. Clearly, the transmetalation event is still limiting, despite the allylic nature of the boronic ester. Though the cross-coupling

conditions reported by Miyaura for the primary (and single example of secondary) allylic trifluoroboronate salts did not require special additives,<sup>19</sup> this can be attributed to the special nature of the trifluoroboronates, whose reactivities are rarely comparable to the more traditional boronic esters. As suggested by the identical conditions required to ensure their successful cross-coupling, the secondary allylic boronic esters are seemingly most similar in reactivity to the benzylic boronic esters studied in detail in Chapter 2. In this case, the effect of Ag<sub>2</sub>O may again serve to activate boron while being positioned by the allylic olefin group (as in Chapter 2, Figure 2-1), though this time transmetalation occurs at the remote  $\gamma$ -site much like the analogous allyl silanes.

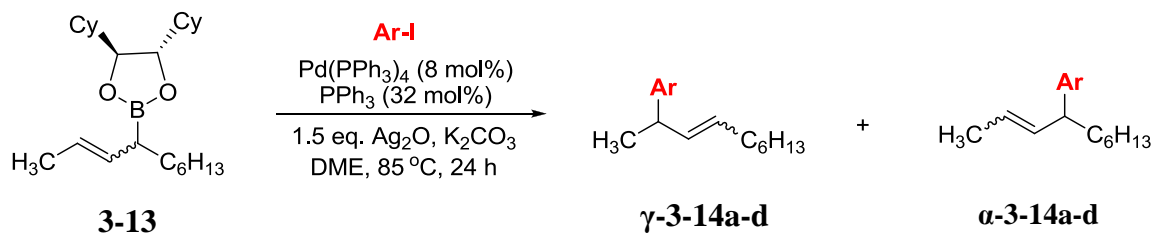
#### *3.2.4 Synthesis and Cross-Coupling of Non-Racemic Secondary Allylic Boronic Esters*

The results described above constitute the first, full look at the coupling of secondary allylic boronic esters. Despite the advance this provides to the synthetic methodology, the real importance of secondary cross-coupling partners has always been their inherent chirality. Therefore, in order to truly capitalize on this new type of cross-coupling, it would have to be extended to enantiomerically enriched substrates.

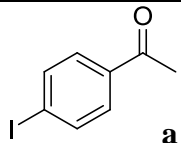
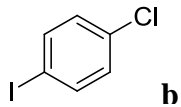
To accomplish this, the lithiation-borylation strategy was performed on an alkyl boronic ester, decorated with a dicyclohexane ethylene diol (Diched) chiral auxiliary. Though simply prepared by a condensation reaction between the enantiomerically pure diol and boronic acid, the process still requires a multi-step synthesis of the diol (Scheme 3-4), and, as with all auxiliaries, the chiral component is used in at least stoichiometric

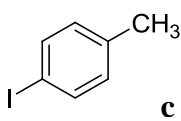
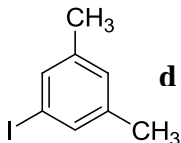


amounts. Nevertheless, the chiral allylic boronic ester was prepared in similar fashion to its racemic counterpart (Scheme 3-16), but in this case, the chiral dixed-auxilliary on boron allowed for a  $\text{ZnCl}_2$ -assisted diastereoselective alkyl-migration to take place, producing high diastereomeric ratios (98:2) in the desired allylic boronic ester (**3-13**). The non-racemic allylic boronic ester was then cross-coupled to a variety of aryl iodides. As shown in Table 3-2, both the yields and the  $\gamma:\alpha$  regioselectivities observed in the asymmetric products (**3-14a-d**) closely mirrored those of the corresponding racemic pinacolate ester, dismissing any potentially adverse effects stemming from the change in boronic ester. The high yields for the cross-coupling of the dixed-ester are especially important, as they preclude the need to transesterify to the pinacol ester prior to cross-coupling.



**Table 3-2:** Cross-Coupling of non-racemic allylic boronic esters

Entry	Aryl iodide	Yield <sup>a</sup>	$\gamma:\alpha$ (crude) <sup>b</sup>	$\gamma:\alpha$ (pure) <sup>b</sup>
1	 <b>a</b>	83	88:12	88:12
2	 <b>b</b>	72	82:18	80:20

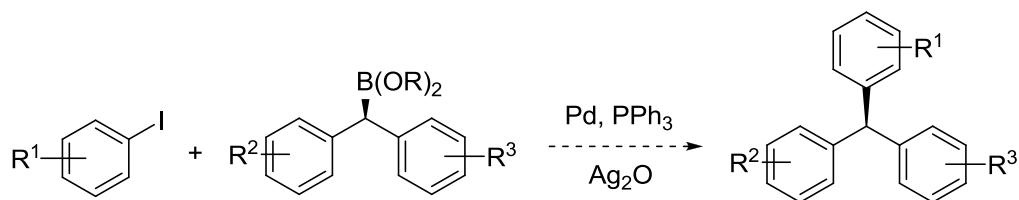
3		69	90:10	88:12
4		83	92:8	91:9

(a) Isolated yields of isomer mixtures. (b) Ratio of isomers determined by NMR.

The arylated products were then examined for their enantiomeric excess. Though preliminary results show that the products are almost certainly non-racemic, the isomeric mixture of both  $\gamma$ - and  $\alpha$ -products, combined with complications from an undefined olefin geometry, have conspired to prevent a quantitative assessment of the enantiomeric excess in the product. Indeed, the allylic boronic esters used in the cross-coupling reactions contained a mixture of *E* and *Z* olefins, owing to the configurational lability of the vinyl Grignard reagents used to make them. As Denmark has elegantly shown, *E* and *Z* isomers will lead to different reactive conformers, as the secondary allylic boronic ester adapts to avoid disfavored  $A^{1,3}$  interactions.<sup>23</sup> As such, the cross-coupling of an allylic boronic ester with poorly defined olefin geometry will necessarily give a mixture of enantiomers. To further complicate matters, the facial selectivity of transmetalation to allyl boronic esters is not known.

### 3.3 Triarylmethanes

The development of a successful protocol for the cross-coupling of secondary benzylic and allylic boronic esters constitutes a substantial advance in the field of Suzuki-Miyaura type methodology. Where much of the effort since our group's initial disclosure in 2009 has concentrated on expanding the scope and understanding the limitations of the reaction, we realized that for a novel methodology to truly be useful, it must facilitate the synthesis of important structural motifs or provide access to new, previously unattainable, molecules. With this in mind, we decided that the asymmetric synthesis of triarylmethanes provided a worthy challenge and one in which the power of our methodology could be suitably demonstrated (Scheme 3-22).



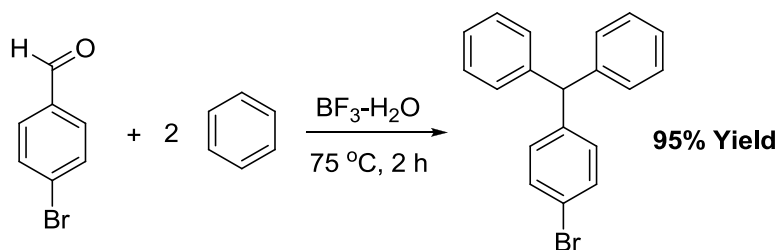
**Scheme 3-22:** Proposed route to asymmetric triarylmethanes by way of a Suzuki-Miyaura cross-coupling strategy.

### 3.3.1 Triarylmethanes: From Unsymmetrical to Enantiomerically Enriched

In addition to possessing an interesting, fan-like structure, the known applications of triarylmethanes are numerous and wide-ranging; in fact applications in photochromics, photochemistry,<sup>25</sup> medicinal<sup>26</sup> and analytical chemistry<sup>27</sup> have all been reported recently.

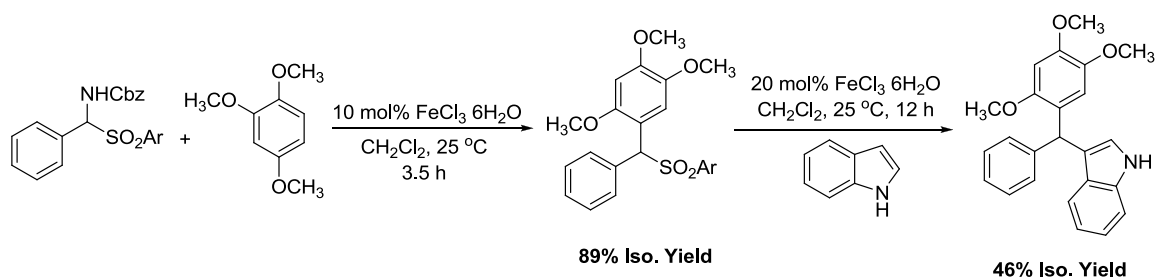
It comes as a surprise, then, to find that the methods to prepare this important class of compound are still underdeveloped.

Typically, triarylmethanes are prepared *via* a Friedel-Crafts type reaction of an aromatic aldehyde or aldimine with two equivalents of an electron rich arene.<sup>26</sup> This process is generally catalyzed by strong Lewis<sup>28</sup> or Brønsted acids<sup>29</sup> (Scheme 3-23), though the consecutive addition of arene groups, first to the aryl aldehyde and then to the resulting, more reactive dibenzyl alcohol, limits this strategy to the synthesis of symmetrical triarylmethanes.



**Scheme 3-23:** Brønsted Acid catalyzed synthesis of symmetrical triarylmethanes from arenes and aromatic aldehydes.<sup>29</sup>

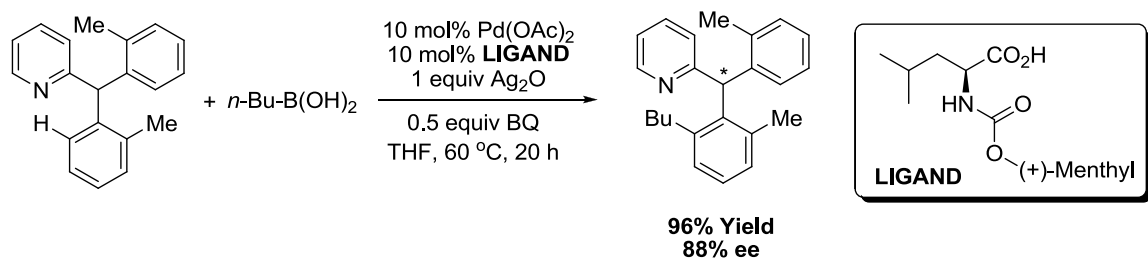
Recently, strategies permitting the synthesis of unsymmetrical triarylmethanes have been reported. In 2010, Kim and co-workers performed a two-step Friedel-Crafts reaction on an  $\alpha$ -amido sulfone to obtain an unsymmetrical triarylmethane in decent yields (8 examples, 53-91% yield).<sup>30</sup> In the presence of one equivalent of an electron rich arene, the iron-catalyzed electrophilic attack selectively expelled the protected amide to yield a diarylated sulfone. Subsequent isolation and reaction with a different electron rich arene gave rise to the desired unsymmetrical, yet racemic, triarylmethane (Scheme 3-24).



**Scheme 3-24:** Lewis Acid catalyzed synthesis of unsymmetrical triarylmethanes in two steps. Ar = *p*-tolyl, Cbz = carboxybenzyl.<sup>30</sup>

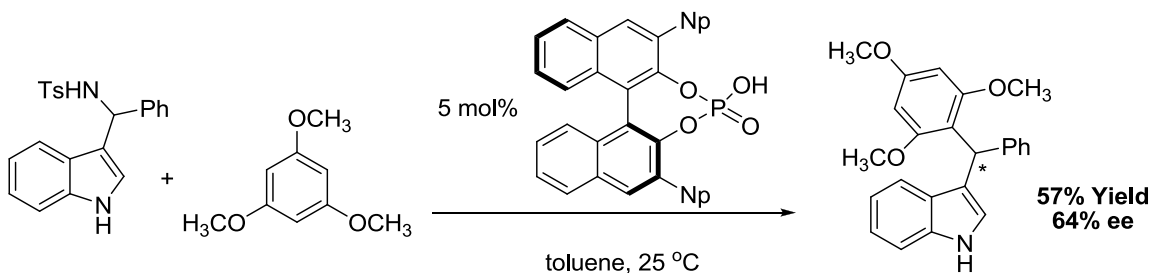
The ability to synthesize unsymmetrical triarylmethanes opened the door for an *asymmetric* synthesis as well. To do so, not only would three distinct aryl groups be required, but the stereochemistry of the central carbon would have to be controlled.

Prior to our work in the field, only one example of the enantioselective synthesis of triarylmethanes had been reported. In 2008, the Yu group reported an elegant study of the enantioselective activation of C-H bonds.<sup>31</sup> As part of the study, they were able to take a symmetrical, pyridyl-containing, triarylmethane and palladate the aryl group adjacent to the pyridyl-nitrogen at the *ortho*-position. Cross-coupling to a butyl boronic acid served to desymmetrize the triarylmethane. When performed in the presence of a chiral amino acid ligand, the desymmetrization was affected with a high level of enantiocontrol, though this methodology suffers from the severe limitation of requiring an *ortho*-pyridyl substrate (Scheme 3-25).



**Scheme 3-25:** The synthesis of asymmetric triarylmethanes by way of enantioselective C-H activation and cross-coupling.<sup>31</sup>

During our own investigations into the asymmetric synthesis of triarylmethanes, a report from the You group appeared in which triarylmethanes could be constructed enantioselectively by way of a bottom-up approach.<sup>32</sup> Similar to traditional Friedel-Crafts approaches to these structures, the approach begins with the reaction of indoles with aryl aldimines to give isolable protected secondary amines. Much like the dibenzyl alcohols produced upon reaction of the first equivalent of arene with aryl aldehydes, this secondary benzylic amine undergoes rapid reaction with a second, distinct indole or electron rich arene in the presence of a strong acid (Scheme 3-26). It is the use of a chiral Brønsted acid, however, that renders the second reaction enantioselective; in the end, a variety of triarylmethanes were synthesized with moderate enantioselectivity and in good yield, though substrate scope is still quite limited.



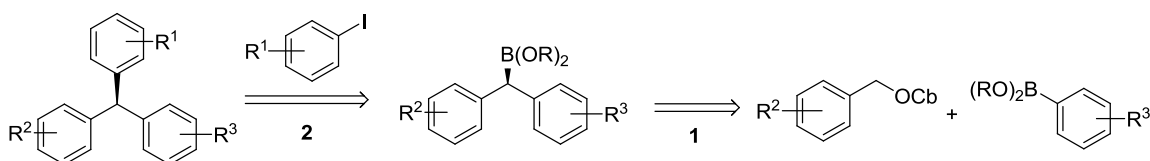
**Scheme 3-26:** The asymmetric synthesis of triarylmethanes *via* chiral Brønsted Acid catalysis. Np = 1-naphthyl, Ts = tosyl.<sup>32</sup>

Much progress has been made in the synthesis of triarylmethanes during the last two years, though at present, the two strategies outlined above are still the only known routes to the non-racemic target. A general protocol to asymmetric triarylmethanes, where each aromatic ring can be customized, is certainly still an important goal.

### 3.4 Asymmetric Triarylmethanes from Dibenzyl Boronic Esters

#### 3.4.1 Retrosynthetic Analysis

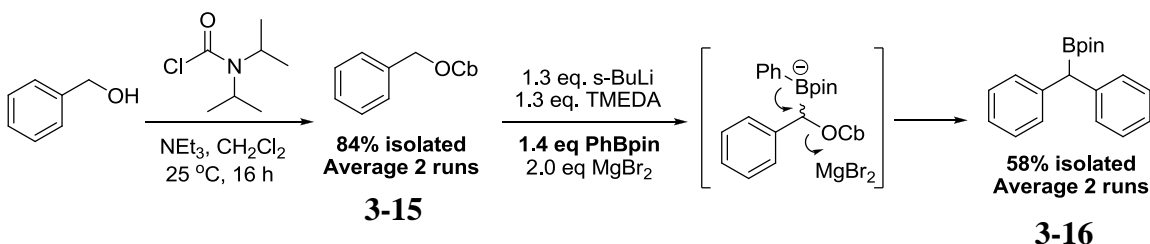
Our completely novel approach to the synthesis of asymmetric triarylmethanes would be to employ an enantiospecific cross-coupling of dibenzyl boronic esters with aryl halides. Though easily deconstructed in a retrosynthetic analysis (Scheme 3-27), there was no precedence for either the asymmetric synthesis of dibenzyl boronic esters *or* their enantiospecific cross-coupling at the outset of this work.



**Scheme 3-27:** Retrosynthetic analysis of an asymmetric triarylmethane through a lithiation-borylation (**1**) / Suzuki-Miyaura (**2**) strategy.

### 3.4.2 Racemic Synthesis of Symmetrical and Unsymmetrical Triarylmethanes

To determine if the critical cross-coupling step was in fact feasible, a simple, symmetric, dibenzylic boronic ester was synthesized through an Aggarwal-type lithiation-borylation strategy. The synthesis of the required benzyl carbamate (**3-15**) was performed in high isolated yield and underwent the requisite homologation reaction with phenyl boronic acid pinacolate ester without incident to yield dibenzylic boronic ester **3-16** (Scheme 3-28).

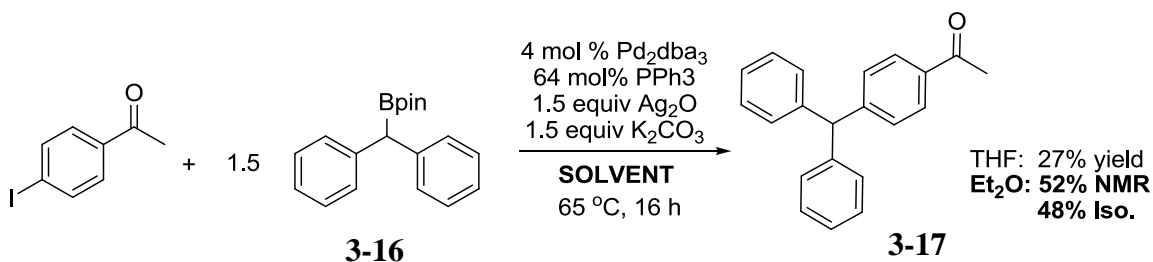


**Scheme 3-28:** The borylation of a lithiated carbamate to synthesize a dibenzylic boronic ester. TMEDA = tetramethylethylenediamine.

As one benzylic group had been shown to promote the cross-coupling of secondary boronic esters under our conditions, we were optimistic that the inclusion of a

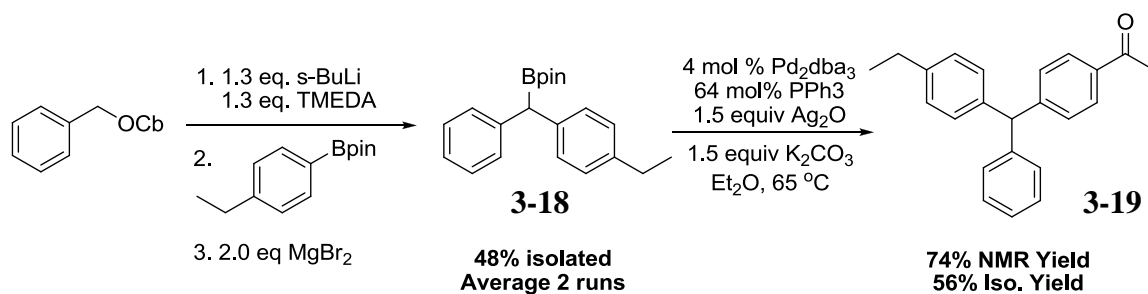


second benzyl system would not only permit cross-coupling, but perhaps even accelerate it. In the event, symmetric dibenzylic boronic ester **3-16** was cross-coupled to 4-iodoacetophenone in moderate isolated yield. Changing the solvent from THF to diethylether was found to dramatically increase yields (Scheme 3-29).



**Scheme 3-29:** The first synthesis of a symmetrical triarylmethane by Suzuki-Miyaura cross-coupling approach.

The synthesis of symmetrical triarylmethane **3-17** demonstrated that dibenzylic boronic esters were competent coupling partners under our Suzuki-Miyaura protocol. What's more, the method by which the boronic ester was synthesized made the nature of the aromatic rings easily interchangeable. Simply by choosing different aromatic groups on the benzyl carbamate and aryl boronic ester, an unsymmetrical dibenzylic boronic ester **3-18** was synthesized and isolated. Gratifyingly, this dibenzylic boronic ester was coupled in good yield under our cross-coupling protocol to give unsymmetrical triarylmethane **3-19** in good yield (Scheme 3-30).

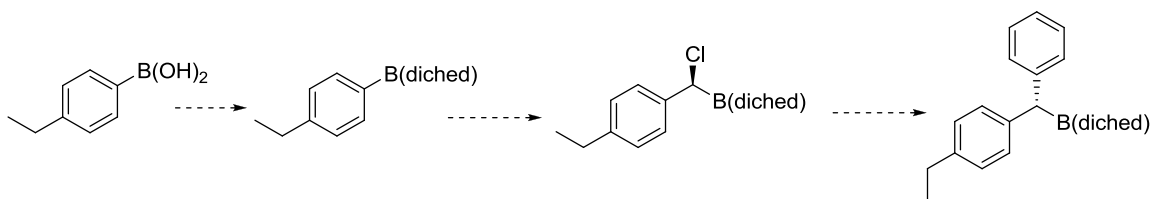


**Scheme 3-30:** The synthesis of an unsymmetrical dibenzylic boronic ester to synthesize the first unsymmetrical triarylmethane by a Suzuki-Miyaura cross-coupling approach. The reaction is performed in a vial with Teflon-coated cap to prevent loss of solvent at temperatures above its boiling point.

### 3.4.3 Synthesis of Non-Racemic Dibenzylic Boronic Esters by Matteson Chemistry

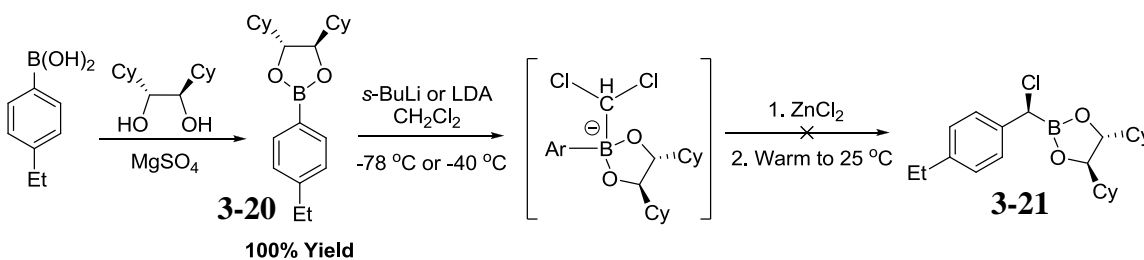
With a protocol to synthesize unsymmetrical triarylmethanes firmly in hand, it became imperative to devise an approach to non-racemic dibenzylic boronic esters which, we were optimistic, would lead to asymmetric triarylmethanes. Unfortunately, there were no known asymmetric examples of the starting materials, and so the development of this methodology would again fall to us.

Ostensibly, non-racemic dibenzylic boronic esters can be synthesized by one of the lithiation-borylation approaches outlined by Matteson<sup>9</sup> (Scheme 3-3) and Aggarwal<sup>15</sup> (Scheme 3-9). Though the *racemic* dibenzylic boronic esters had been synthesized by way of lithiated carbamates (Aggarwal), we had had greater success in the synthesis of the non-racemic allylic boronic esters with the Matteson approach, and decided to first apply this method for their dibenzylic counterparts (Scheme 3-31).



**Scheme 3-31:** Chosen approach to non-racemic dibenzylic boronic esters. diched = (*R,R*)-dicyclohexyl ethylenediol.

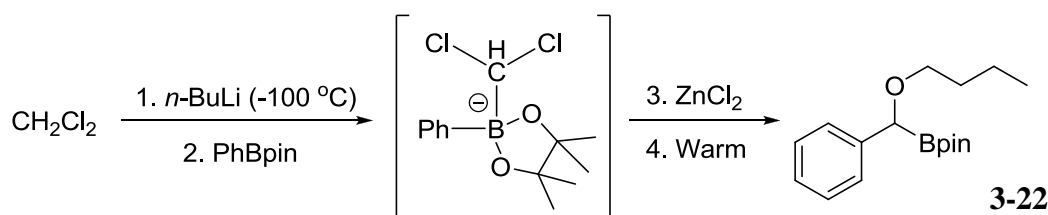
The (*R,R*)-diched ester of 4-ethylphenylboronic acid (**3-20**) was isolated in quantitative yield, though the preparation of the  $\alpha$ -chlorobenzyl boronic ester proved to be much more difficult than anticipated. Dichloromethane was lithiated in the presence of the boronic ester with both *n*-butyllithium at  $-78\text{ }^{\circ}\text{C}$  and freshly prepared LDA at  $-40\text{ }^{\circ}\text{C}$ . In both cases, no  $\alpha$ -chloroboronic ester (**3-21**) was observed by GC-MS after the cold addition of  $\text{ZnCl}_2$  and warming to room temperature (Scheme 3-32).



**Scheme 3-32:** Unsuccessful approach to non-racemic  $\alpha$ -chlorobenzyl boronic esters.

After the failure of this reaction, optimization reactions were performed on the analogous pinacolate ester. Also, to avoid any undesirable interactions between the strong base and Lewis acidic boronic ester, dichloromethane was lithiated at  $-100\text{ }^{\circ}\text{C}$  (to avoid formation of any carbenes) prior to the slow addition of a solution containing the boronic

ester. Interestingly, the starting boronic ester was consumed under these conditions, though the major product was proposed to be **3-22**, plausibly arising from the Zn-catalyzed removal of the benzylic chloride, attack by THF and subsequent ring opening (Scheme 3-33). Incomplete characterization precludes the unequivocal assignment of the  $\alpha$ -borylether as the unwanted side-product, nevertheless, the formation of this side-product, at the expense of the desired product is certain.

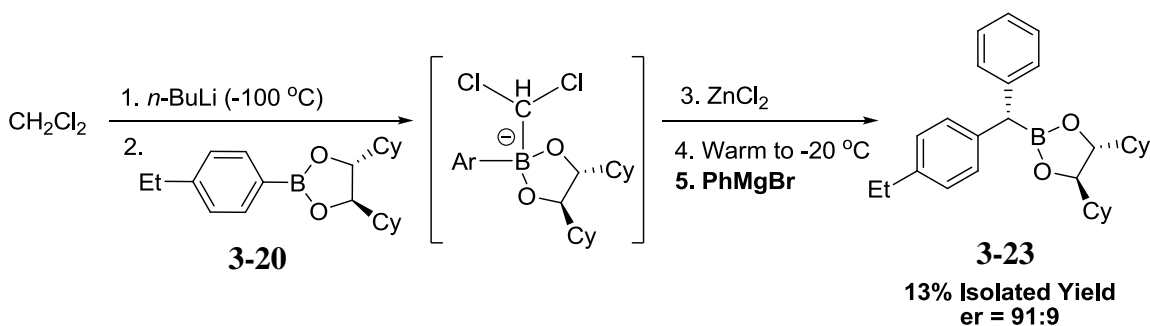


**Scheme 3-33:** Formation of an unexpected product during homologation of PhBpin with lithium dichloromethane.

In an attempt to avoid forming side-products arising from ring-opened THF, the reaction solvent was changed to diethyl ether, though in the event, starting material was completely recovered. The reaction was also performed in the absence of  $\text{ZnCl}_2$ ; happily, the homologation still occurred and, in this case, the desired  $\alpha$ -chloroboronic ester was found to be the major product. Though encouraging, the reaction would have to eventually be performed in the presence of  $\text{ZnCl}_2$  to ensure the diastereoselective removal of one chloride during the rearrangement step.<sup>9</sup> With this in mind, a reaction (including a stoichiometric amount of  $\text{ZnCl}_2$ ) was conducted and quenched at various temperatures during the warming process to ascertain at what point the desired product begins to be consumed by unwanted secondary reactions. It was determined that the desired  $\alpha$ -chloroboronic ester is formed between  $-40$  and  $-20\text{ }^\circ\text{C}$ , and by holding the temperature

constant at  $-20\text{ }^{\circ}\text{C}$ , the  $\alpha$ -chloroboronic ester becomes the major constituent of the reaction solution, with the undesired  $\alpha$ -borylether only present in trace amounts. Allowing this reaction to warm to  $0\text{ }^{\circ}\text{C}$ , however, leads to an equal mixture of the two products.

From these data, it was clear that the reaction mixture could not be allowed to warm past  $-20\text{ }^{\circ}\text{C}$ . It was decided that, after warming slowly to  $-20\text{ }^{\circ}\text{C}$ , the reaction would be quenched, not by the usual saturated  $\text{NH}_4\text{Cl}_{(\text{aq.})}$  solution, but by the Grignard reagent required to affect the boron-assisted invertive displacement of the chloride in the next step. In the event, a non-racemic dibenzylic boronic ester (**3-23**) was synthesized in high enantiopurity (91:9) but isolated in disappointingly low yields (Scheme 3-34). Worse, when this boronic ester was subjected to our cross-coupling protocol, the major product observed after 24 h at  $85\text{ }^{\circ}\text{C}$  was the proto-deboronated dibenzylalkane.

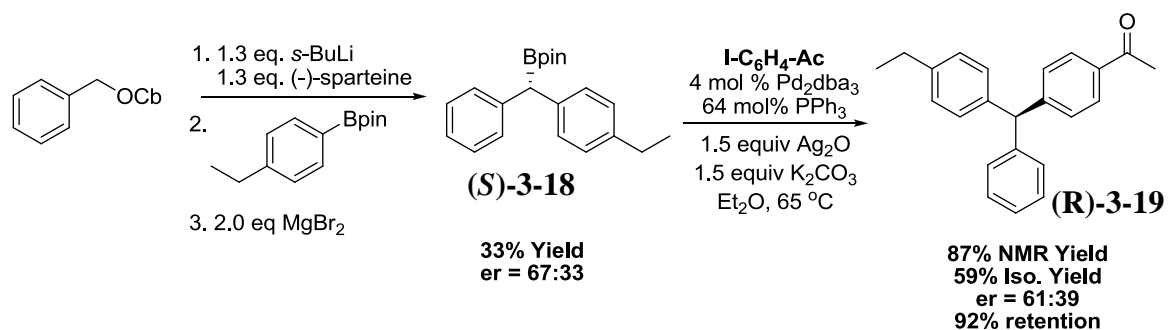


**Scheme 3-34:** One pot, enantioselective synthesis of dibenzylic boronic ester.

#### 3.4.4 Synthesis of Asymmetric Dibenzyl Boronic Esters via Lithiated Carbamates

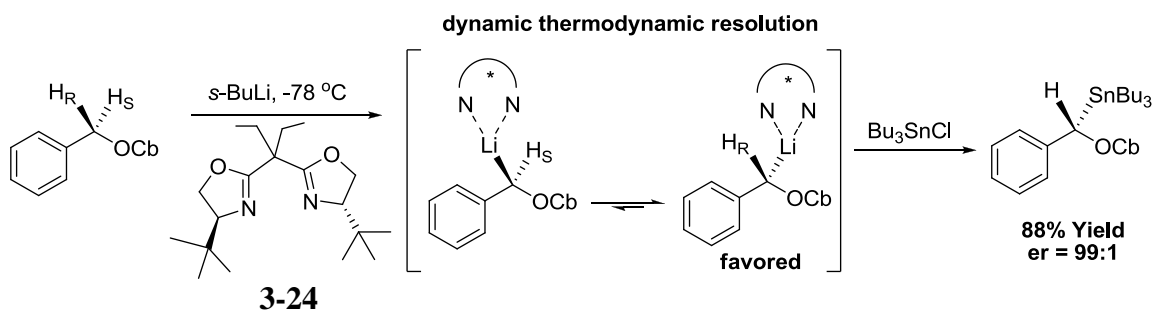
Despite making significant inroads into the asymmetric synthesis of dibenzyl boronic esters by way of Matteson-type chemistry, it was decided that the complementary approach provided by the borylation of lithiated carbamates might lead to a more consistent route to the desired product. In principle, the achiral ligand TMEDA need only be replaced by (-)-sparteine to achieve an enantioselective lithiation of the benzyl carbamate. As the subsequent borylation and 1,2-metalate rearrangement are known to be stereoretentive,<sup>15</sup> this should provide access to asymmetric dibenzyl boronic esters.

In practice, however, the configurational lability<sup>13</sup> of the lithiated primary benzylic carbamate (noted in Scheme 3-7) led to poor enantioselectivity in the dibenzyl boronic ester product ((*S*)-**3-18**). Compounding the problem, incomplete borylation was observed when using (-)-sparteine as a ligand, which led to a crude mixture of starting material and product. The dibenzyl boronic ester product is quite similar to the aryl boronic ester starting material, and therefore several purification steps were required to isolate it, which, ultimately, lowered the yield. Importantly, it should be noted that most all of the stereochemical information which *was* imparted to the dibenzyl boronic ester was transferred to the triarylmethane during cross-coupling (Scheme 3-35, (*R*)-**3-19**). Indeed, the cross-coupling was found to proceed in good yield and stereoloyalty, though the enantiopurity of the dibenzyl boronic ester coupling partner must be higher to truly assess the stereoretention of the reaction.



**Scheme 3-35:** Enantioselective synthesis of dibenzylic boronic ester with (-)-sparteine and subsequent, stereoselective cross-coupling to asymmetric triarylmethane.

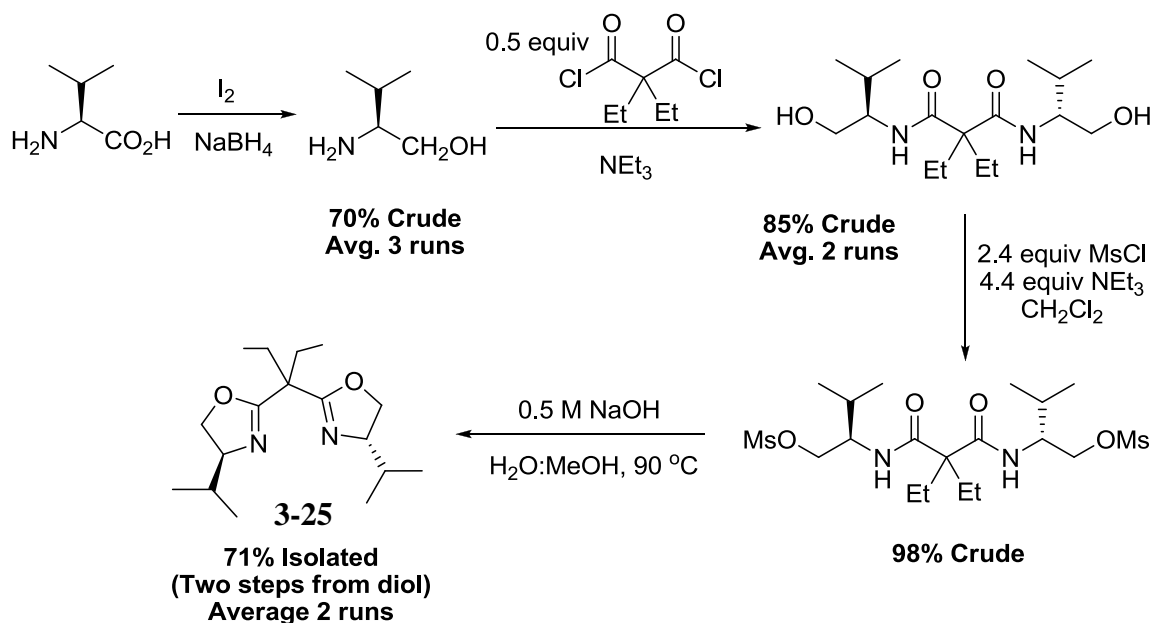
An examination of the literature revealed that chiral bisoxazoline ligands were also used for the enantioselective lithiation of benzyl carbamates<sup>33</sup> and thiocarbamates.<sup>34</sup> Indeed, Hoppe<sup>33, 34</sup> has shown that with chiral bisoxazoline ligands, the lithiation of benzyl carbamates still suffered from poor differentiation between the enantiotopic protons, but that upon prolonged lithiation times, equilibration to favor one diastereomeric complex had occurred. The lithiated carbamate, diastereomerically enriched through this dynamic thermodynamic resolution, was then quenched with a variety of small electrophiles to yield products in high enantiomeric excess (Scheme 3-36). Hoppe went on to argue that because the enantiomeric ratio of the products seems to be independent of the nature of the electrophile, enantioselectivity is not incurred through a dynamic kinetic resolution, whereby one lithiated carbamate epimer reacts preferentially with the electrophile.<sup>33</sup>



**Scheme 3-36:** Dynamic thermodynamic resolution of the lithiated benzyl carbamate with chiral bis(oxazoline) ligands.

Though the chiral bis(oxazoline) derived from L-tert-leucine **3-24** provided the greatest enantioselectivity for the stannylation of lithiated carbamates (Scheme 3-36), we had considerable difficulty preparing it. Fortunately, the L-valine analogue (**3-25**), which also offered high enantioselectivity for the aforementioned process, was easily synthesized in good overall yield (Scheme 3-37).

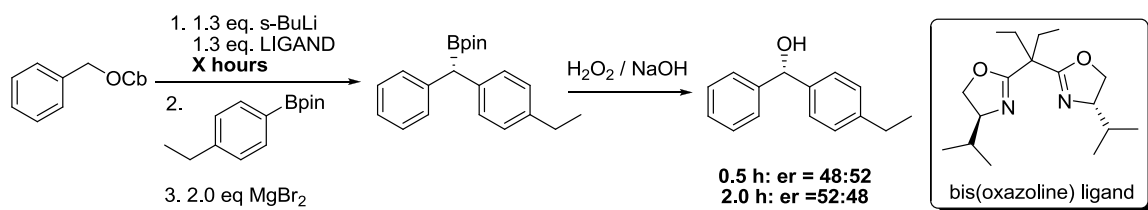




**Scheme 3-37:** The four step synthesis of a chiral bis(oxazoline) from the natural amino acid, L-leucine.<sup>35</sup>

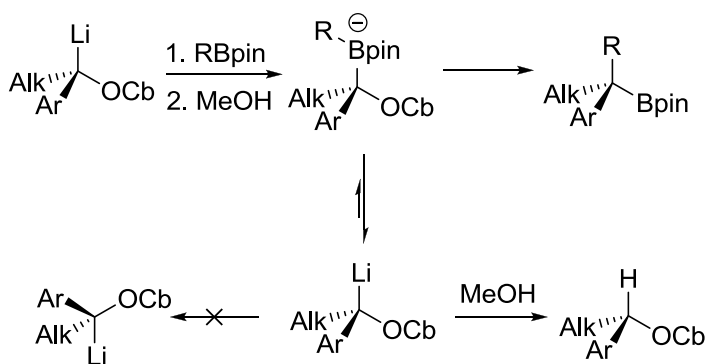
With the chiral (bis)oxazoline ligand in hand, we proceeded to interrogate its effectiveness in the enantioselective lithiation-borylation of benzyl carbamates. Mindful of the difficult purification step outlined above, the resultant dibenzylic boronic esters were oxidized *in situ* to their respective alcohols for analysis.

We were disappointed to note that the use of the chiral bis(oxazoline) ligand **3-25** in favor of (-)-sparteine actually gave *worse* enantioselection. In fact, the product was found to be virtually racemic. The lithiation time was lengthened from 0.5 h to 2 h in an attempt to encourage equilibration to one epimer, but, in the event, the product was still found to be racemic (Scheme 3-38).



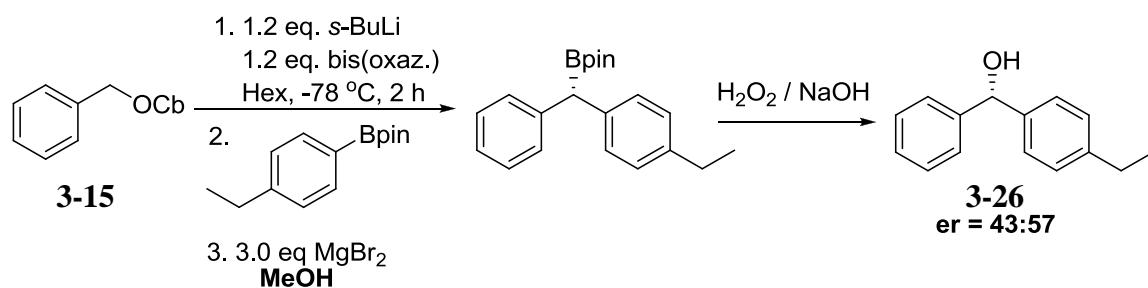
**Scheme 3-38:** Non-enantiospecific synthesis of dibenzylic boronic ester (and subsequent oxidation to secondary alcohol) with bis(oxazoline) ligand **3-25**

Bewildered, we considered possible racemization events. Aggarwal has recently shown that some of the stereochemical scrambling observed in the lithiation-borylation of *secondary* benzylic carbamates can be attributed to the reversible formation of the borate complex, prior to product-forming 1,2-metalate rearrangement.<sup>36</sup> Lithiated secondary benzylic carbamates are known to be configurationally stable up to -70 °C, but if they are reformed during the warming process, they are liable to invert configuration.<sup>13</sup> To address this issue, the Aggarwal group added MeOH to the reaction solution after borylation, such that any reversion to the lithiated carbamate during warming would be quenched by the proton source prior to racemization, decreasing the yield but preserving the enantiomeric purity (Scheme 3-39).



**Scheme 3-39:** Aggarwal's strategy of quenching lithiated carbamates resulting from decomplexation of the boronic ester prior to racemization.<sup>36</sup>

A similar methanol-quenching strategy applied to our system should not be expected to overcome the configurational lability of the *primary* benzyl carbamate (even at low temperatures), but could optimistically mitigate any erosion of the slight enantiomeric excess occurring during the warming process. In the event, a modest improvement in ee was observed for our system when methanol was added to the reaction mixture (Scheme 3-40), indicating that boronate decomplexation is, at least in small part, a factor in the racemization. However, as expected, the miniscule improvement was insufficient to render this process useful in our chemistry.

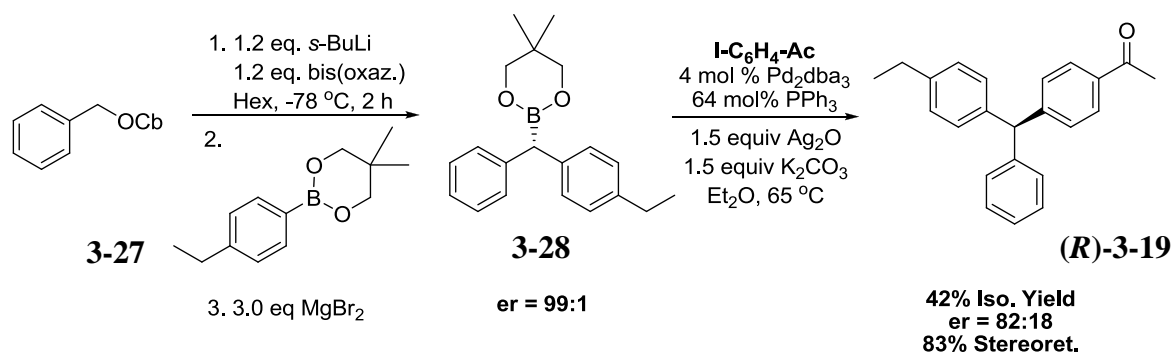


**Scheme 3-40:** Modest improvement in enantioselectivity in the synthesis of dibenzylic boronic esters by addition of MeOH after borylation.

More importantly, it was noted that the electrophiles used in Hoppe's study<sup>33</sup> (Bu<sub>3</sub>SnCl, Me<sub>3</sub>SiCl, CO<sub>2</sub>, MeI) were all relatively small and were therefore able to gain ready access to the lithiated nucleophile. By comparison, boronic acid pinacolate esters are bulky; in fact it is exactly this protective bulk around the electrophilic boron centre which renders them stable and easily handled. As proof of this effect, the analogous catecholate esters, lacking the bulk provided by the four methyl groups on the pinacol backbone, are unstable and often either transesterified to the pinacolate ester or used *in situ*.<sup>37</sup> It seemed plausible, then, that the steric bulk surrounding the electrophile could either alter the facial selectivity of the quench or disfavor the formation of the boronate complex, thereby facilitating the reverse reaction to the configurationally labile lithiated carbamate. Encouragingly, Aggarwal has also reported augmented diastereoselectivities for the addition of allylic boronic esters to aldehydes after tuning the steric properties of the boronic ester.<sup>38</sup>

To test this hypothesis, a less bulky aryl boronic ester **3-27** was synthesized and used in the lithiation-borylation reaction with the chiral bis(oxazoline) ligand. To our

delight, the change in electrophile sterics led the formation of the dibenzylic boronic ester **3-28** in over 98% ee. This near complete enantioselectivity is observed both with and without the addition of MeOH after borylation, indicating that with the less bulky boronic ester, boronate decomplexation is no longer a factor. This constitutes the first example of a fully enantioselective synthesis of a dibenzylic boronic ester (Scheme 3-41).



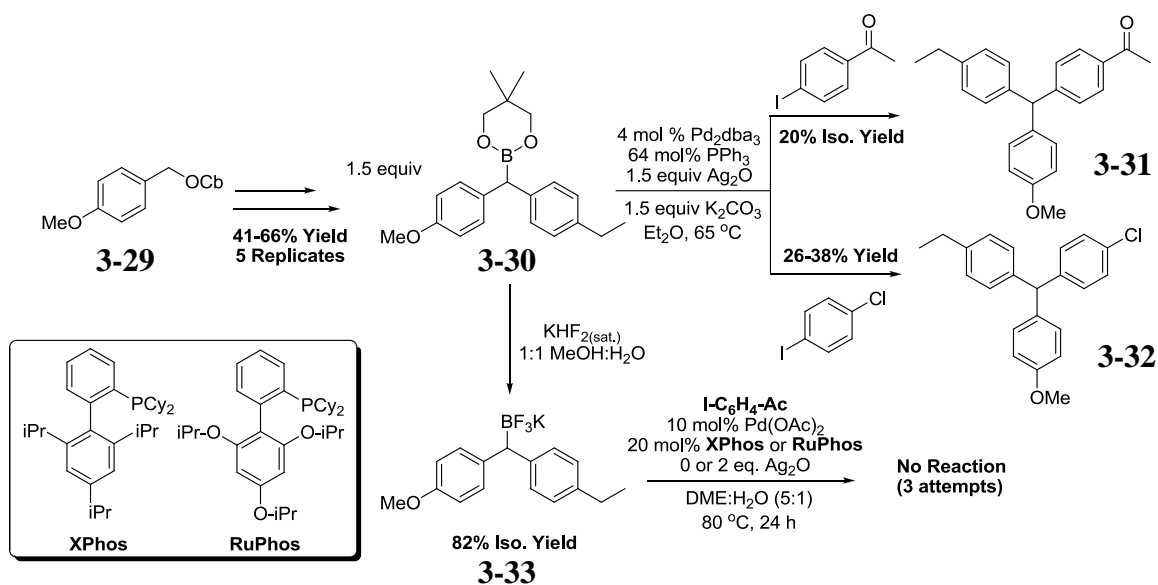
**Scheme 3-41:** Enantioselective synthesis of a dibenzylic boronic ester and subsequent cross-coupling to yield an asymmetric triarylmethane.

Once isolated, the neopentyl dibenzylic boronic ester was cross-coupled to 4-iodoacetophenone under our Suzuki-Miyaura conditions to yield the desired chiral triarylmethane (**(R)-3-19**) in moderate yield and good enantiomeric excess. Despite being an improvement over our initial asymmetric synthesis (Scheme 3-35, er = 61:39), the deflated yield and the atypically low stereoretention were cause for concern. In our mechanistic studies on the cross-coupling of non-racemic benzylic boronic esters (Chapter 2), it was found that the benzylic boronic ester underwent a small amount of racemization when subjected to the reaction conditions; the *di*benzylic boronic ester might be even more sensitive to the scrambling of stereochemical information. It is also

important to note that stereochemical information is being eroded in a system that does not possess  $\beta$ -hydrogens, lending further evidence that the small amount of racemization observed in the cross-coupling of secondary boronic esters is likely *not* coming from a  $\beta$ -hydride elimination process. For the time being, though, we focused on improving the yields of both the cross-coupling and especially the synthesis of the dibenzylic boronic ester.

#### *3.4.5 Higher Yielding Syntheses of Non-Racemic Dibenzylic Boronic Esters*

Despite the development of both the enantioselective synthesis of dibenzylic boronic esters and their unprecedented enantiospecific cross-coupling to asymmetric triarylmethanes, the applicability of this route was limited by low yields, especially for the synthesis of the boronic esters. These low yields were caused, in large part, by the similarity between the product boronic esters and their respective starting materials. In the interest of facilitating their isolation, the dibenzylic boronic esters would henceforth be designed to contain polar chromatographic handles, which would allow for facile separation from the non-polar aryl boronic ester.



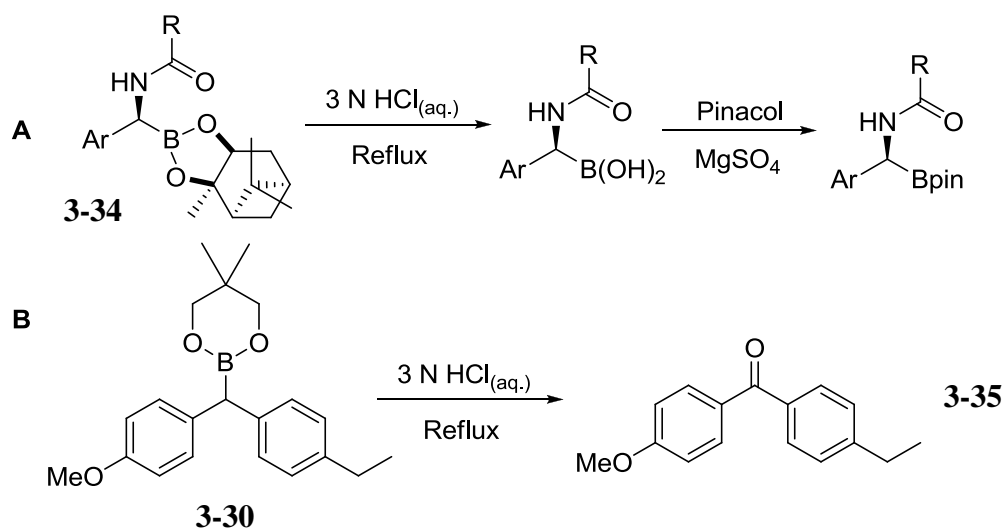
**Scheme 3-42:** Low yielding cross-coupling reactions of *p*-methoxy- neopentyl boronic ester (top) and transesterification to the analogous, and unreactive, potassium trifluoroboronate (bottom).

The inclusion of a *para*-methoxy functionality on the dibenzylic boronic ester did in fact lead to a drastic increase in isolated yields. Where the *p*-H substituted analogue was usually isolated in less than 30% yield, its more polar counter part was isolated in a respectable 41-66% yield over five replicates (Scheme 3-42, **3-30**). Importantly, the synthesis of boronic ester **3-30** was also highly enantioselective (er = 92:8) when the chiral bis(oxazoline) ligand was used (not shown).

Problems arose, however, during the cross-coupling of neopentyl boronic ester **3-30**. Despite a brief attempt at optimization, the isolated yields of triarylmethanes **3-31** and **3-32** never broached 40%, and were often much lower (Scheme 3-42). It was surmised that the neopentyl boronic ester was not stable to coupling conditions and was therefore transesterified to the analogous potassium trifluoroboronate (**3-33**) in good isolated

yields. The secondary trifluoroboronate salt was found to be unreactive under a variety of conditions, consistent with our previous findings (Chapter 2).

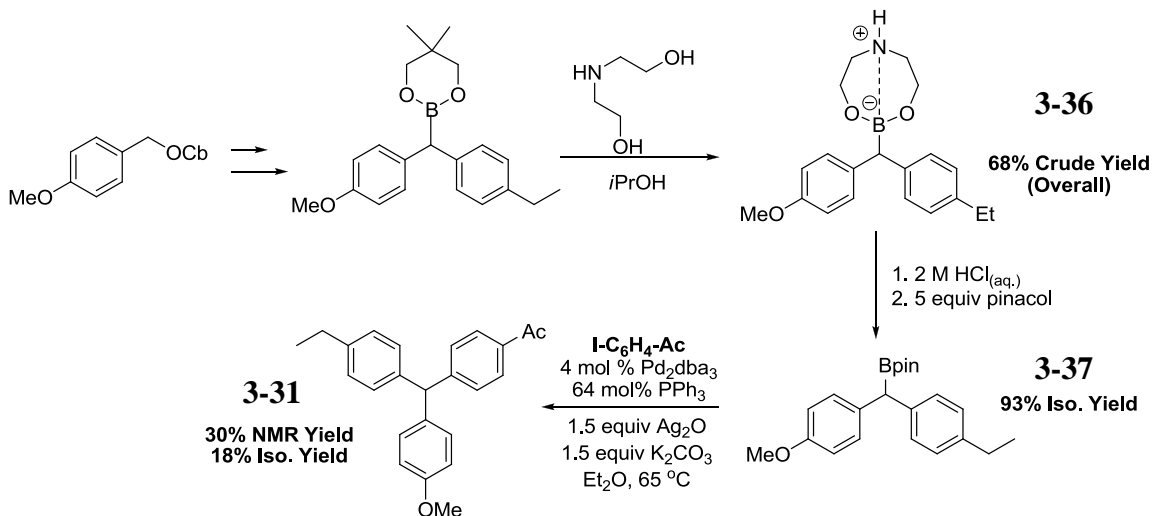
Transesterification to a known quantity, namely a pinacolate ester, proved difficult. Reacting the neopentyl boronic ester with a ten-fold excess of pinacol, as is typically employed in the transesterification from catechol to pinacol boronic esters,<sup>37</sup> failed. Addition of a Lewis acid was thought to improve the transesterification process, but both commercially available and freshly prepared  $\text{MgBr}_2$  were added (with a large excess of pinacol) to no avail. Suginome has recently shown that  $\alpha$ -amidobenzyl boronic esters (**3-34**) could be transesterified to pinacolate esters by first hydrolyzing to the boronic acid under acidic aqueous conditions.<sup>6</sup> In the case of a dibenzylic boronic ester, however, this led to oxidation all the way to the acetophenone derivative when performed under aerobic conditions (Scheme 3-43, **3-35**).



**Scheme 3-43:** Transesterification of boronic esters. **A:** Suginome's hydrolysis and pinacol quench of  $\alpha$ -amido benzylic boronic esters.<sup>6</sup> **B:** Similar approach with dibenzylic boronic esters leading to over oxidation.



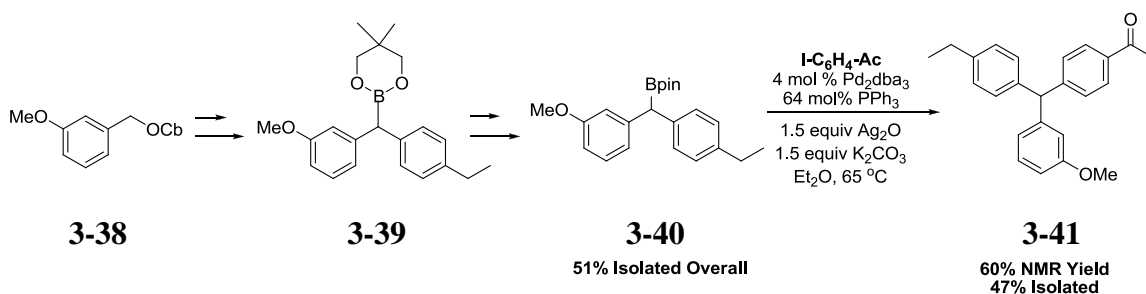
Ultimately, the successful conversion of a neopentyl dibenzylic boronic ester to the pinacolate analogue came by way of a Matteson protocol, whereby the ester was first converted to the zwitterionic salt **3-36** with diethanolamine prior to hydrolysis and pinacol quench. Not only does this approach affect the desired transesterification in good yield, but it can be applied directly to the crude solution following lithiation-borylation. Finally, the cross-coupling of the *p*-methoxy dibenzylic boronic acid pinacolate ester **3-37** proceeded in the almost identical low yields as the neopentyl analogue, indicating conclusively that the low yields in the coupling step were a function of the aryl substituents, and not necessarily the nature of the boronic ester (Scheme 3-44).



**Scheme 3-44:** One-pot synthesis of dibenzylic pinacolate ester from neopentyl analogue followed by cross-coupling with aryl iodide to yield trisubstituted triarylmethane.

To investigate the effect of the *para*-methoxy group on the cross-coupling step, a dibenzylic boronic ester with the methoxy group in the *meta*-position was synthesized (**3-**

**38**). Interestingly, our ability to do so simply by changing the starting benzyl alcohol, illustrates the generality of our method and its ability to change the component aromatic rings at will. In any case, the pinacolate ester **3-40** (by way of the neopentyl analogue **3-39** required to achieve good enantioselection) was isolated in the highest yield obtained to date (51%), but more importantly, the subsequent cross-coupling reaction led to triarylmethane **3-41** in good yield as well (60%, Scheme 3-45).



**Scheme 3-45:** Methodology to obtain both dibenzylic boronic ester and triarylmethane in high yield.

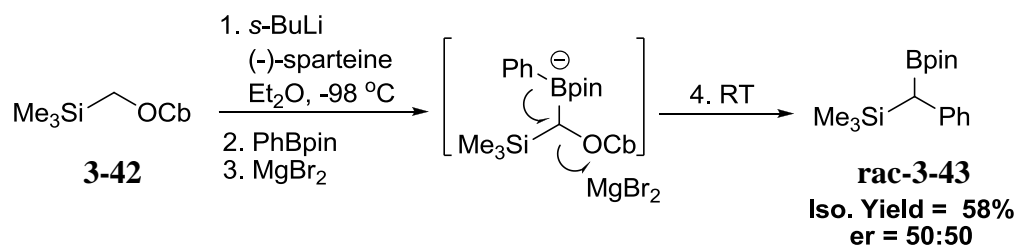
Through the strategy outlined above, the asymmetric synthesis of triarylmethanes has been shown to be possible through a Suzuki-Miyaura cross-coupling approach. This process also has a flexible substrate scope, with the nature of the each aryl ring being tunable, while still remaining enantioselective. With both the asymmetric synthesis of dibenzylic boronic esters and the high-yielding synthesis of unsymmetrical triarylmethanes developed independently in our group (and reported herein), we are currently working on combining the two developments to synthesize triarylmethanes in high yield and enantiopurity.

### 3.5 Lithiation-Borylation for the Synthesis of Asymmetric Allyl Silanes

The downstream application of the lithiation-borylation reaction is certainly not limited to the preparation of boronic esters destined for oxidation or cross-coupling. While serving as a visiting scholar in the laboratory of Varinder Aggarwal in early 2009, we sought to develop a simple route to asymmetric allyl silanes using a lithiation-borylation strategy.

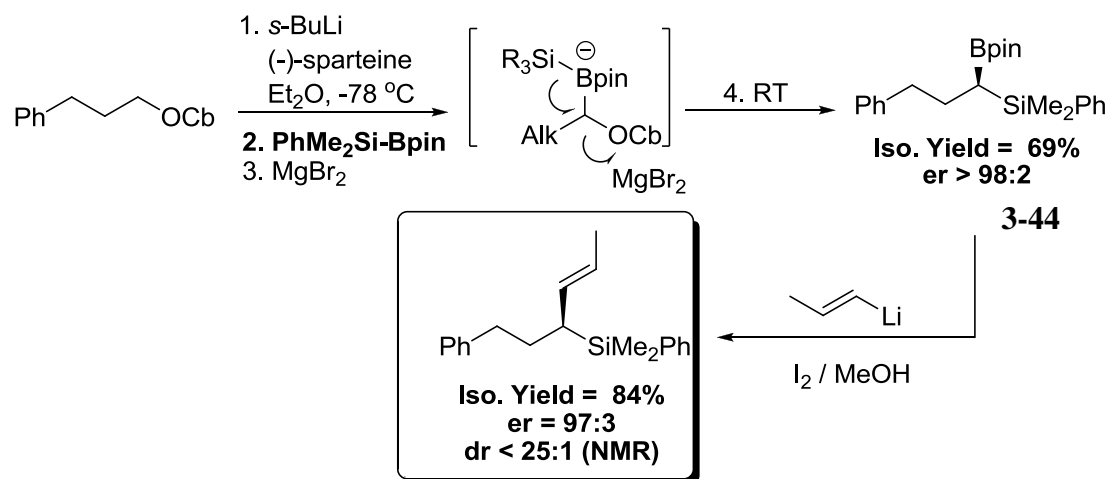
Tertiary and quaternary allyl silanes are synthetically useful intermediates<sup>39</sup> and, though there are several known avenues to their preparation,<sup>40, 41</sup> a definitive approach is still outstanding.

Our initial strategy was to perform a lithiation-borylation reaction on an  $\alpha$ -silyl carbamate **3-42**, which, after 1,2-metalate rearrangement, would give the  $\alpha$ -silyl boronate ester. Simply performing a Zweifel olefination of the boronate ester would lead to the desired allyl silane, hopefully in high enantiomeric and diastereomeric purity. Though this route was successfully employed to synthesize the critical  $\alpha$ -silyl boronate ester in decent yield, no enantioselection was observed in changing from the achiral TMEDA ligand to (-)-sparteine (Scheme 3-46). Indeed, racemic mixtures of the  $\alpha$ -silyl boronate ester **3-43** were obtained even when the supposed enantioselective lithiation event occurred at -100 °C. As noted earlier (*vide supra*) and by others,<sup>42</sup> lithiated  $\alpha$ -silyl methyl carbamates are configurationally unstable (owing to the stabilizing effect of the silyl group on  $\alpha$ -anions) and were destined to give racemic products from the outset.



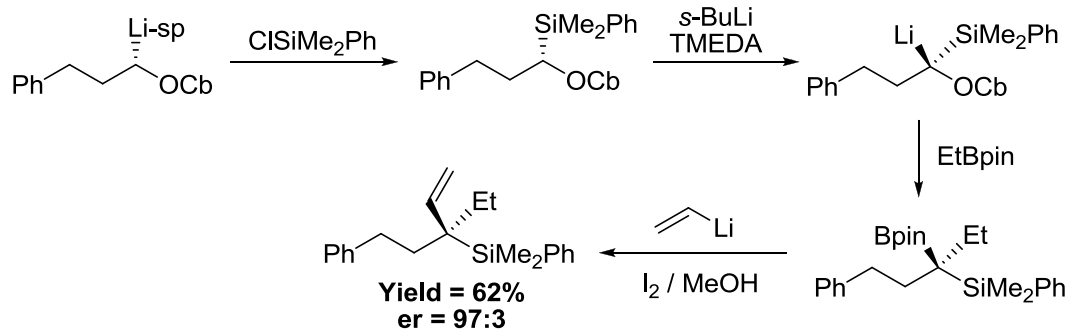
**Scheme 3-46:** Initial approach to the synthesis of asymmetric  $\alpha$ -silyl boronate esters. The configurational lability of the lithiated silyl methyl carbamate led to a racemic mixture in the product.

Once that was understood, we adopted a strategy that used lithiated carbamates of known configurational stability: alkyl carbamates. To do so, we would have to rely on a lesser-known *silyl*-migration after quenching the lithiated carbamate with a borylsilane. Silyl-migrations have been reported,<sup>43, 44</sup> though never in the case of lithiated carbamates. Gratifyingly, the reaction proceeded as planned, and, when the chiral (-)-sparteine ligand was used during the lithiation step, the  $\alpha$ -silyl boronate esters (**3-44**) were isolated in good yield and very high enantiomeric purity (Scheme 3-47).



**Scheme 3-47:** Successful route to tertiary allyl silanes in high yield and er and dr, by way of a non-racemic  $\alpha$ -silyl boronate ester.

Upon my return to Kingston, my co-workers in Bristol then applied a modified Zweifel olefination approach<sup>16</sup> to synthesize a variety of tertiary allyl silanes in high yield and enantiomeric purity (Scheme 3-47). It was subsequently discovered that lithiated tertiary  $\alpha$ -silyl carbamates, stemming from the reaction of a configurationally stable primary lithiated alkyl carbamate with a silyl electrophile, were configurationally stable themselves, and could be used towards the asymmetric synthesis of quaternary allyl silanes (Scheme 3-48).<sup>16</sup>



**Scheme 3-48:** Quaternary allyl silanes synthesized in high yield and er from lithiated alkyl carbamates.

### 3.6 Conclusions

Though initially limited to benzylic boronic esters, our Suzuki-Miyaura cross-coupling protocol has been extended to secondary allylic boronic esters. The regioselectivity of the reaction is noteworthy, with  $\gamma$ -selectivity dominating except in cases where  $\alpha$ -arylation preserves conjugation with an aromatic substituent. Preparing the secondary allylic boronic esters by way of Matteson-type homologation has allowed for systematic variance in the coupling partner's structure and, importantly a route to asymmetric synthesis. Finally, the enantiospecific cross-coupling of non-racemic secondary allylic boronic esters is also being pursued, and initial results are very promising.

As a means of showcasing our new methodology, the asymmetric synthesis of triarylmethanes was achieved *via* a cross-coupling strategy for the first time. The poor configurational stability of benzylic lithiated carbamates was overcome through the use

of a sterically unencumbered nucleophile, and the enantiospecific cross-coupling of non-racemic dibenzylic boronic esters led to asymmetric triarylmethanes in good yield and stereoretention.

Finally, a lithiation-borylation strategy was used to synthesize  $\alpha$ -silyl boronate esters in high yield and enantiomeric purity. These  $\alpha$ -silyl boronate esters are key intermediates in the synthesis of both tertiary and quaternary allyl silanes, important synthetic intermediates in their own right.

### 3.7 References

- (1) Mun, S.; Lee, J.; Yun, J. Copper-Catalyzed  $\beta$ -Boration of  $\alpha,\beta$ -Unsaturated Carbonyl Compounds: Rate Acceleration by Alcohol Additives. *Org. Lett.* **2006**, 8, 4887-4889.
- (2) Lee, Y.; Hoveyda, A. H. Efficient Boron-Copper Additions to Aryl-Substituted Alkenes Promoted by NHC-Based Catalysts. Enantioselective Cu-Catalyzed Hydroboration Reactions. *J. Am. Chem. Soc.* **2009**, 131, 3160-3161.
- (3) Lillo, V.; Prieto, A.; Bonet, A.; Diaz-Requejo, M. M.; Ramirez, J.; Perez, P. J.; Fernandez, E. Asymmetric  $\beta$ -Boration of  $\alpha,\beta$ -Unsaturated Esters with Chiral (NHC)Cu Catalysts. *Organometallics* **2009**, 28, 659-662.
- (4) Lee, J.; Yun, J. Catalytic Asymmetric Boration of Acyclic  $\alpha,\beta$ -Unsaturated Esters and Nitriles. *Angew. Chem. Int. Ed.* **2008**, 47, 145-147.
- (5) Lee, J. C. H.; Hall, D. G. Chiral Boronate Derivatives via Catalytic Enantioselective Conjugate Addition of Grignard Reagents on 3-Boronyl Unsaturated Esters and Thioesters. *J. Am. Chem. Soc.* **2010**, 132, 5544-5545.

- (6) Ohmura, T.; Awano, T.; Suginome, M. Stereospecific Suzuki-Miyaura Coupling of Chiral  $\alpha$ -(Acylamino)benzylboronic Esters with Inversion of Configuration. *J. Am. Chem. Soc.* **2010**, 132, 13191-13193.
- (7) Sandrock, D. L.; Jean-Gerard, L.; Chen, C.; Dreher, S. D.; Molander, G. A. Stereospecific Cross-Coupling of Secondary Alkyl  $\beta$ -Trifluoroboratoamides. *J. Am. Chem. Soc.* **2010**, 132, 17108-17110.
- (8) Matteson, D. S. Boronic ester neighboring groups. *Acc. Chem. Res.* **1970**, 3, 186-193.
- (9) Matteson, D. S.; Majumdar, D. Homologation of boronic esters to  $\alpha$ -chloro boronic esters. *Organometallics* **1983**, 2, 1529-1535.
- (10) Matteson, D. S.; Sadhu, K. M. Boronic ester homologation with 99% chiral selectivity and its use in syntheses of the insect pheromones (3S,4S)-4-methyl-3-heptanol and exo-brevicommin. *J. Am. Chem. Soc.* **1983**, 105, 2077-2078.
- (11) Sharpless, K. B.; Amberg, W.; Bennani, Y. L.; Crispino, G. A.; Hartung, J.; Jeong, K. S.; Kwong, H. L.; Morikawa, K.; Wang, Z. M. The osmium-catalyzed asymmetric dihydroxylation: a new ligand class and a process improvement. *J. Org. Chem.* **1992**, 57, 2768-2771.
- (12) Matteson, D. S.; Man, H.; Ho, O. C. Asymmetric Synthesis of Stegobinone via Boronic Ester Chemistry. *J. Am. Chem. Soc.* **1996**, 118, 4560-4566.
- (13) Hoppe, D.; Hense, T. Enantioselective Synthesis with Lithium/(-)-Sparteine Carbanion Pairs. *Angew. Chem. Int. Ed.* **1997**, 36, 2282-2316.
- (14) Beak, P.; Basu, A.; Gallagher, D. J.; Park, Y. S.; Thayumanavan, S. Regioselective, Diastereoselective, and Enantioselective Lithiation-Substitution Sequences: Reaction Pathways and Synthetic Applications. *Acc. Chem. Res.* **1996**, 29, 552-560.



- (15) Stymiest, J. L.; Dutheil, G.; Mahmood, A.; Aggarwal, V. K. Lithiated Carbamates: Chiral Carbenoids for Iterative Homologation of Boranes and Boronic Esters. *Angew. Chem. Int. Ed.* **2007**, 46, 7491-7494.
- (16) Aggarwal, V. K.; Binanzer, M.; de Ceglie, M. C.; Gallanti, M.; Glasspoole, B. W.; Kendrick, S. J. F.; Sonawane, R. P.; Vazquez-Romero, A.; Webster, M. P. Asymmetric Synthesis of Tertiary and Quaternary Allyl- and Crotylsilanes via the Borylation of Lithiated Carbamates. *Org. Lett.* **2011**, 13, 1490-1493.
- (17) Stymiest, J. L.; Bagutski, V.; French, R., M.; Aggarwal, V. K. Enantiodivergent conversion of chiral secondary alcohols into tertiary alcohols. *Nature* **2008**, 456, 778-783.
- (18) Sebelius, S.; Olsson, V. J.; Wallner, O. A.; Szabo, K. J. Palladium-Catalyzed Coupling of Allylboronic Acids with Iodobenzenes. Selective Formation of the Branched Allylic Product in the Absence of Directing Groups. *J. Am. Chem. Soc.* **2006**, 128, 8150-8151.
- (19) Yamamoto, Y.; Takada, S.; Miyaura, N.; Iyama, T.; Tachikawa, H.  $\gamma$ -Selective Cross-Coupling Reactions of Potassium Allyltrifluoroborates with Haloarenes Catalyzed by a Pd(0)/D-t-BPF or Pd(0)/Josiphos ((R,S)-CyPF-t-Bu) Complex: Mechanistic Studies on Transmetalation and Enantioselection. *Organometallics* **2009**, 28, 152-160.
- (20) Hatanaka, Y.; Ebina, Y.; Hiyama, T.  $\gamma$ -Selective cross-coupling reaction of allyltrifluorosilanes: a new approach to regiochemical control in allylic systems. *J. Am. Chem. Soc.* **1991**, 113, 7075-7076.
- (21) Hatanaka, Y.; Goda, K.; Hiyama, T. Regio- and stereoselective cross-coupling reaction of optically active allylsilanes: Stereocontrol of palladium-mediated SE' reactions. *Tetrahedron Lett.* **1994**, 35, 1279-1282.

- (22) Hatanaka, Y.; Goda, K.; Hiyama, T.  $\alpha$ -Selective cross-coupling reaction of allyltrifluorosilanes: Remarkable ligand effect on the regiochemistry. *Tetrahedron Lett.* **1994**, 35, 6511-6514.
- (23) Denmark, S. E.; Werner, N. S. On the Stereochemical Course of Palladium-Catalyzed Cross-Coupling of Allylic Silanolate Salts with Aromatic Bromides. *J. Am. Chem. Soc.* **2010**, 132, 3612-3620.
- (24) Chou, C.; Chatterjee, I.; Studer, A. Stereospecific Pd-Catalyzed Decarboxylative C(sp<sup>3</sup>)-(sp<sup>2</sup>) Coupling of 2,5-Cyclohexadiene-1-carboxylic Acid Derivatives with Aryl Iodides. *Angew. Chem. Int. Ed.* **2011**, 50, 1-5.
- (25) Irie, M. Light-induced reversible pH change. *J. Am. Chem. Soc.* **1983**, 105, 2078-2079.
- (26) Podder, S.; Choudhury, J.; Roy, U. K.; Roy, S. Dual-Reagent Catalysis within Ir-Sn Domain: Highly Selective Alkylation of Arenes and Heteroarenes with Aromatic Aldehydes. *J. Org. Chem.* **2007**, 72, 3100-3103.
- (27) Shchepinov, M. S.; Korshun, V. A. Recent applications of bifunctional trityl groups. *Chem. Soc. Rev.* **2003**, 32, 170-180.
- (28) Thirupathi, P.; Soo Kim, S. Friedel-Crafts Arylation Reactions of N-Sulfonyl Aldimines or Sulfonamidesulfones with Electron-Rich Arenes Catalyzed by FeCl<sub>3</sub>·6H<sub>2</sub>O: Synthesis of Triarylmethanes and Bis-heteroarylmethanes. *J. Org. Chem.* **2010**, 75, 5240-5249.
- (29) Prakash, G. K. S.; Panja, C.; Shakhmin, A.; Shah, E.; Mathew, T.; Olah, G. A. BF<sub>3</sub>-H<sub>2</sub>O Catalyzed Hydroxyalkylation of Aromatics with Aromatic Aldehydes and Dicarboxaldehydes: Efficient Synthesis of Triarylmethanes, Diarylmethylbenzaldehydes, and Anthracene Derivatives. *J. Org. Chem.* **2009**, 74, 8659-8668.

- (30) Thirupathi, P.; Kim, S. S. Regioselective Arylations of  $\alpha$ -Amido Sulfones with Electron-Rich Arenes through Friedel–Crafts Alkylations Catalyzed by Ferric Chloride Hexahydrate: Synthesis of Unsymmetrical and Bis-Symmetrical Triarylmethanes. *Eur. J. Org. Chem.* **2010**, 2010, 1798-1808.
- (31) Shi, B.; Mangel, N.; Zhang, Y.; Yu, J. Pd<sup>II</sup>-Catalyzed Enantioselective Activation of C(sp<sup>2</sup>)-H and C(sp<sup>3</sup>)-H Bonds Using Monoprotected Amino Acids as Chiral Ligands. *Angew. Chem. Int. Ed.* **2008**, 47, 4882-4886.
- (32) Sun, F.; Zheng, X.; Gu, Q.; He, Q.; You, S. Enantioselective Synthesis of nsymmetrical Triarylmethanes by Chiral Bronsted Acids. *Eur. J. Org. Chem.* **2010**, 2010, 47-50.
- (33) Lange, H.; Huenerbein, R.; Frolich, R.; Grimme, S.; Hoppe, D. Configurationally Labile Lithiated *O*-Benzyl Carbamates: Application in the Asymmetric Synthesis and Quantum Chemical Investigations on the Equilibrium of Diastereomers. *Chem. Asian J.* **2008**, 3, 78-87.
- (34) Lange, H.; Bergrander, K.; Frolich, R.; Kehr, S.; Nakamura, S.; Shibata, N.; Toru, T.; Hoppe, D. Highly Enantioselective Reactions of Configurationally Labile Epimeric Diamine Complexes of Lithiated *S*-Benzyl Thiocarbamates. *Chem. Asian J.* **2008**, 3, 101.
- (35) Evans, D. A.; Peterson, G. S.; Johnson, J. S.; Barnes, D. M.; Campos, K. R.; Woerpel, K. A. An Improved Procedure for the Preparation of 2,2-Bis[2-[4(S)- tert-butyl-1,3-oxazolanyl]]propane [(S,S)-tert-Butylbis(oxazoline)] and Derived Copper(II) Complexes. *J. Org. Chem.* **1998**, 63, 4541-4544.
- (36) Bagutski, V.; French, R. M.; Aggarwal, V. K. Full Chirality Transfer in the Conversion of Secondary Alcohols into Tertiary Boronic Esters and Alcohols Using Lithiation-Borylation Reactions. *Angew. Chem. Int. Ed.* **2010**, 49, 5142-5145.

- (37) Crudden, C. M.; Hleba, Y. B.; Chen, A. C. Regio- and Enantiocontrol in the Room-Temperature Hydroboration of Vinyl Arenes with Pinacol Borane. *J. Am. Chem. Soc.* **2004**, 126, 9200-9201.
- (38) Althaus, M.; Mahmood, A.; Suarez, J. R.; Thomas, S. P.; Aggarwal, V. K. Application of the Lithiation-Borylation Reaction to the Preparation of Enantioenriched Allylic Boron Reagents and Subsequent in Situ Conversion into 1,2,4-Trisubstituted Homoallylic Alcohols with Complete Control over All Elements of Stereochemistry. *J. Am. Chem. Soc.* **2010**, 132, 5922-5922.
- (39) Fleming, I.; Barbero, A.; Walter, D. Stereochemical Control in Organic Synthesis Using Silicon-Containing Compounds. *Chem. Rev.* **1997**, 97, 2063-2192.
- (40) Han, S. B.; Gao, X.; Krische, M. J. Iridium-Catalyzed anti-Diastereo- and Enantioselective Carbonyl (Trimethylsilyl)allylation from the Alcohol or Aldehyde Oxidation Level. *J. Am. Chem. Soc.* **2010**, 132, 9153-9156.
- (41) Kacprzynski, M. A.; May, T. L.; Kazane, S. A.; Hoveyda, A. H. Enantioselective Synthesis of Allyl Silanes Bearing Tertiary and Quaternary Si-Substituted Carbons through Cu-Catalyzed Allylic Alkylations with Alkylzinc and Arylzinc Reagents. *Angew. Chem. Int. Ed.* **2007**, 46, 4554-4558.
- (42) Simov, B. J.; Rohn, A.; Brecker, L.; Giester, G.; Hammerschmidt, F. Chiral Carbanions, Part 4: Borylation of (Trimethylsilyl)methyl *N,N*-Dialkylcarbamates-Diastereoselectivity and Structural Studies. *Synthesis* **2004**, 16, 2704-2710.
- (43) Hata, T.; Kitigawa, H.; Masai, H.; Kurahashi, T.; Shimizu, M.; Hiyama, T. Geminal Difunctionalization of Alkenylidene-Type Carbenoids by Using Interelement Compounds. *Angew. Chem. Int. Ed.* **2001**, 40, 790-792.
- (44) Shimizu, M.; Kurahashi, T.; Kitagawa, H.; Shimono, K.; Hiyama, T. gem-Silylborylation approach for tri- and tetrametalmethanes: the first synthesis of boryl(germyl)(silyl)(stannyl)methanes. *J. Organomet. Chem.* **2003**, 686, 286-293.

## Chapter 4

### Introduction to Mesoporous Silica Materials

#### 4.1 Introduction

Prior to the development of ordered mesoporous materials in the early 1990's, synthetic and naturally occurring zeolites were finding widespread application as adsorbents, molecular sieves and solid inorganic acid catalysts.<sup>1</sup> The Lewis acidity of metal cations adsorbed to the aluminosilicate framework, especially unstabilized multivalent cations, allow active zeolites to abstract hydride ions from alkane chains as the residual alkyl cation is deposited on the anionic framework.<sup>2</sup> The ability to adsorb and dissociate alkyl and alkenyl substrates makes zeolites catalytically active for hydrocarbon isomerization, alkylation and cracking, processes of considerable importance to the petrochemical industry. The steric constraints within the micropores bestow high selectivity on these reactions, both by limiting the substrate diffusivity towards the active sites and by rendering certain transition states more energetically favorable than others.<sup>3</sup> The small pore size, however, is limiting when larger substrates were used, instigating significant efforts to develop larger, mesoporous (20-500 Å) molecular sieves.

Researchers at the Mobil Corporation are credited with reporting the first ordered, large-pore silicate material, called MCM-41, in 1992,<sup>4</sup> though the Kuroda group had also synthesized an ordered, mesoporous silica two years prior.<sup>5</sup> When dispersed in basic

water, quaternary alkyl ammonium surfactants (eg. hexadecyltrimethylammonium bromide, C<sub>16</sub>TAB) aggregated first into spherical micelles and next into a hexagonal array of cylindrical rods. In the presence of a silica source, the surfactant array templates the condensation of the silica network around the micellar cylinders by electrostatic interaction between cationic headgroup and anionic silica species. Removal of the organic surfactant by calcination in air produces porous, hexagonally ordered silicates. The Mobil researchers found that by changing the chain length of the alkyl surfactant or by adding an organic swelling agent to the micelles such as trimethylbenzene (TMB) the pore size of the material could be varied between 20-100 Å, significantly larger than any zeolite.<sup>6</sup> The powder X-Ray diffraction patterns of MCM-41 were consistent with those of a hexagonally ordered material, though the lack of non-hk0 reflections indicated that, unlike zeolites, the walls of MCM-41 were amorphous.<sup>7</sup> Another striking difference between zeolites and MCM-41 was the comparative hydrothermal stability. Relative to its larger pore size, MCM-41 has thin silica walls (~10 Å), making the material susceptible to degradation under harsh conditions. The fact that the walls are amorphous adds to their instability relative to zeolites which have crystalline walls. This lack of hydrothermal stability was immediately recognized as problematic by the investigators at Mobil, who protected the vulnerable surface silanols of the material with trimethylsilane (TMS) groups. By rendering the surface more hydrophobic, a modest improvement in material stability was observed.<sup>6</sup>

Over the next five years, modifications to the MCM-41 synthesis yielded stronger, more robust materials, but the development of a non-ionic surfactant-templated silicate material (Santa-Barbara, material #15, SBA-15) by researchers at UC Santa Barbara proved to be the next real watershed moment.<sup>8</sup> Synthesized in acidic aqueous conditions with a triblock copolymer of polyethylene oxide and polypropylene oxide (P123 = (PEO)<sub>20</sub>(PPO)<sub>70</sub>(PEO)<sub>20</sub>) as a structure directing agent, SBA-15 has both larger pores (60-300 Å) and thicker walls (31-65 Å) than MCM-41.<sup>9</sup> At low pH, the triblock copolymer folds to present the hydrophilic ethylene oxide blocks to the aqueous surroundings.<sup>8</sup> Through electrostatic interactions with the protonated silica source, the ethylene oxide segments template the growth of the silica network about the surfactant mesophases, much in the same way that the cationic head group interacts with the anionic silica species in the standard basic preparation of MCM-41.<sup>4, 6</sup> The interface between the ethylene oxide blocks and the condensed silica network, however, is not completely distinct. Occlusion of polymeric chains of the surfactant into the silica framework of the as-prepared SBA-15 leads to microporous channels connecting the mesopores after surfactant removal.<sup>10</sup> Interestingly, the amount of micropores observed depends strongly on the temperature of synthesis. The microporosity of SBA-15 will play a role not only in the diffusion of molecules through the channel network, but also in the high surface area and the overall stability of the material.

With relatively facile syntheses of materials with improved stabilities, ordered mesoporous materials have become ubiquitous as solid supports for catalysis and separations.<sup>11</sup> As the utility of these materials has grown to include new applications, a

re-evaluation of the stability of these materials in new sets of conditions was required. Indeed, our studies into the stability of both MCM-41 and SBA-15 based catalyst supports used in the Suzuki-Miyaura reaction is the topic of following chapter.

## 4.2 Material Synthesis

### 4.2.1 Micelle Formation

The critical micelle concentration (CMC) and critical micelle temperature (CMT) are the minimum concentration of surfactant and temperature of solution needed for micelles to form. The CMC of a surfactant changes as a function of alkyl chain length, head group and its anionic counterion, as these factors affect the solvation of the surfactant in an aqueous phase. For surfactants typically used in MCM-41 syntheses, ( $C_nTAX$ , where  $n=12,16$  and  $X = Cl, Br, OH$ ) the CMC is about 0.03 wt % in aqueous solution. Small micellar spheres are initially formed, though as the concentration of the surfactant is increased past a second critical micelle concentration,  $CMC_2$ , elongated rods can be formed.<sup>7</sup>

Ultimately, the structure of the micelle formed in solution is determined by the surfactant ion pair packing parameter,  $g$  defined in Equation 4-1.<sup>12</sup>

$$g = V / [l a_0]$$



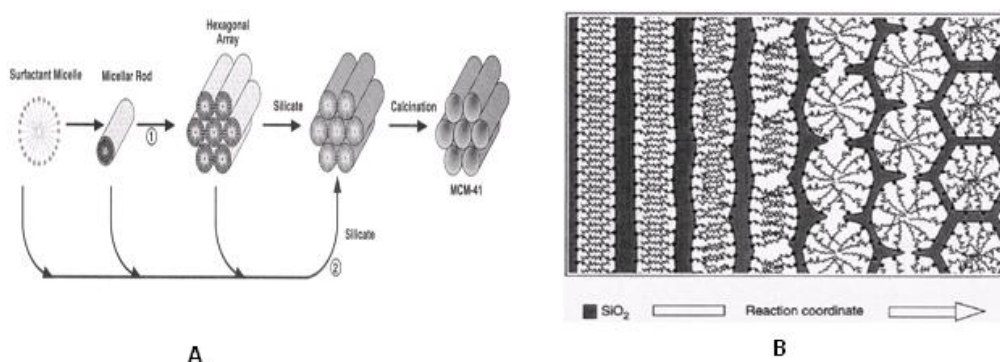
**Equation 4-1:** Surfactant Ion Pair Packing Parameter, where  $V$  = volume of surfactant chains,  $l$  = kinetic length of alkyl chain and  $a_o$  = the effective area of the surfactant head.

Higher values of  $g$  are representative of tightly packed micelles with small effective head group areas. With values of  $g$  increasing towards unity, flat, layered micelles are formed. Predictably, silicates made from this micelle regime would be of the lamellar mesophase. As the value of  $g$  drops, either through an increase in the charged head group area or a decrease in fatty chain volume, the micelles become more loosely packed, and as such, increasingly curved. In this way, the mesostructure of the material can be tailored (from lamellar, to hexagonal to the highly curved cubic) by judicious choice of surfactant.<sup>11</sup>

This model of micelle formation for mesoporous material synthesis makes the assumption that the surfactants behave the same way under reaction conditions as they would in strictly aqueous environments. This, in fact, is not completely accurate, as the charged (protonated or deprotonated, depending on synthesis pH) silicate monomers interact through Coulombic forces with the charged surfactant heads. A balancing of charge density at the organic-inorganic interface lowers repulsion between surfactant head groups leading to a more highly packed micelle than expected. This phenomenon can be interpreted as a decrease in the head group area ( $a_o$ ) causing an increase in the  $g$  value. The importance of this interaction becomes clear when trying to understand the mechanism of mesoporous material formation.

#### 4.2.2 Mechanism of Self Assembly of Ionic Surfactants

At the time of their discovery of MCM-41, Beck *et al.* proposed two possible mechanisms for the formation of ordered silicates through self-assembly, but were unable (or unwilling) to differentiate between the two.<sup>6</sup> The first route proposed involved a rod-like surfactant micelle aggregating into the stable hexagonal form followed by silica condensation about this preformed template. Conversely, a second route whereby the anionic silicate species is instrumental in the formation of first the surfactant rod micelles and then the hexagonal array was briefly mentioned (Figure 4-1, **A**). A better understanding of how the process took place would be critical for the development of materials with different mesostructures or even entirely new routes to obtaining ordered mesoporous materials.



**Figure 4-1:** Two early hypotheses of cationic surfactant self assembly. The routes initially proposed by Beck<sup>6</sup> (Route **A**) and the 'folded sheet' mechanism proposed by Stucky<sup>8</sup> (Route **B**) building off of Kuroda's work with kanemite.<sup>5</sup>

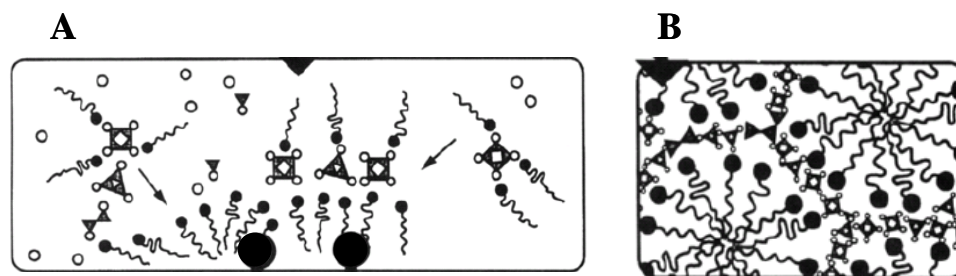
An early mechanistic hypothesis stemmed from the work of Kuroda *et al.* on the ion exchange between  $\text{Na}^+$  and  $\text{CTA}^+$  in the layered polysilicate, kanemite ( $\text{NaHSi}_2\text{O}_5 \cdot 3\text{H}_2\text{O}$ ).<sup>13, 14</sup> Exchanging  $\text{Na}^+$  for  $\text{CTA}^+$  changes the morphology of the silicate from layered to hexagonally mesoporous. Further condensation of the silica network about the structure directing  $\text{CTA}^+$  makes a material very similar to MCM-41. From this, it seemed plausible that a “folded sheet” mechanism was responsible for the development of hexagonally ordered materials. At this time, Stucky and co-workers postulated that the layered to hexagonal transition was governed by the surfactant ion pair packing parameter,  $g$ , decreasing as silicate oligomers condensed about the surfactant.<sup>13</sup> As the charge density of the silicates drops through oligomerization, they become less able to screen the repulsive forces between charged surfactant head groups, leading to a more curved surface and, ultimately, a hexagonal mesostructure (Figure 1, B). XRD evidence showed that the disappearance of the lamellar mesostructure was coincident with the formation hexagonal structure, though the folded sheet mechanism cannot account for systems in which the layered precursor is not formed.

An alternative mechanism was proposed by Davis *et al.* in which randomly oriented micellar surfactant rods are independently coated with silica before spontaneously aggregating into lower-energy hexagonal mesophases.<sup>7</sup> This was supported by *in situ*  $^{14}\text{N}$  NMR spectra that suggested that no liquid crystal arrays were formed at any point in the material synthesis. In fact, the  $^{14}\text{N}$  NMR data was consistent with the formation of micelles early in the synthesis, though this method does not distinguish between sphere and rod-like micelles.  $^{29}\text{Si}$  MAS NMR showed that the silica

network continued to condense long after the initial material precipitation, indicating that a meta-stable, as-synthesized material is formed initially and further strengthened upon hydrothermal treatment.

The  $^{14}\text{N}$  NMR evidence set forth by Davis was somewhat unconvincing, and to suggest that the surfactant aggregates into rod-like micelles was problematic for one important reason. That is, mesoporous materials can be synthesized from alkyl chain surfactants at concentrations *much lower* than the  $\text{CMC}_2$  (*vide supra*) and by shorter alkyl chain surfactants (such as  $\text{C}_{12}\text{TACl}$ ) that are not known to form rod-like micelles at *any* concentration.<sup>15</sup> Stucky *et al.* proposed that the surfactant assembly is initially directed by the ionic silicate species in solution, instead of vice versa (Figure 4-2).<sup>16</sup> Even above the CMC, surfactant molecules are in equilibrium with micelles and are free to interact with inorganic species in solution. The silicate can exist in monomeric, dimeric or oligomeric form in basic aqueous conditions. Because an oligomeric silanol has a lower pKa than the monomeric form, it interacts almost exclusively with the free surfactant groups. As was proposed previously,<sup>13</sup> it is the balancing of the charges between surfactant head group and anionic silicate that determines the packing parameter and ultimately the mesostructure of the material, except in this case, the stable form of the micelle is not pre-formed, but put together *with the assistance of the silicate oligomers*. Amongst other things, changes in solution pH, headgroup size and silica precursor affect how many surfactant molecules can interact with the oligomeric silicate, which influences the packing of the mesophase once fully formed. Because this model accurately predicted that mesoporous materials could be synthesized with other organic-inorganic regimes

( $S^+I^-$ ,  $S^-I^+$  where S= surfactant and I= inorganic) and because it was consistent with Davis' NMR data, Stucky's "cooperative formation" has been accepted as the most accurate mechanism for ionic surfactant self assembly of mesoporous materials.<sup>11</sup>



**Figure 4-2:** Stucky's Cooperative Micelle Formation Mechanism. Surfactant molecules congregate about silica polyanions (**A**), eventually forming the geometry favored by the Packing Parameter,  $g$  (**B**).<sup>17</sup> Image adapted from ref. 17.

#### 4.2.3 Molecular Self-Assembly with Block copolymer Surfactants

Zhao *et al.* proposed that under acidic conditions, P123 folds and aggregates into core-mantle type micelles, with a core of hydrophobic PPO blocks surrounded by the hydrophilic PEO blocks.<sup>8</sup> An anionic counterion mediates the interaction between the PEO block and the hydrated siloxane precursor, as both are expected to be positively charged at reaction pH ( $S^0H^+X^-I^+$  template).<sup>9</sup> Goldfarb and co-workers used EPR spectroscopy and cryogenic-TEM imaging to document the micelle and silica network formation on short time scales. The *in situ* EPR spectra of materials made with radically terminated block copolymers indicated that the PEO blocks experience two distinguishable environments as early as twenty minutes after silica addition: the free

moving blocks comprising the PEO mantle of the micelle and a second phase with drastically reduced mobility (Figure 4-3, A).<sup>18</sup> This second environment is assigned to the partial occlusion of the hydrophilic polymer block into the silica framework and is coincident with the development of the materials hexagonal order. A high proportion of the PEO block is initially immobilized in the silica network, though a substantial amount withdraws to the more mobile phase upon hydrothermal treatment. This is in agreement with previous studies that found that the overall volume of micropores in SBA-15 is lowered during hydrothermal treatment as the PEO blocks become more hydrophobic at increasing temperature.<sup>19</sup>

As a more tangible look at the operating mechanism, Goldfarb used cryo-TEM to observe the formation of micelles and mesophases in solution prior to the precipitation of the material.<sup>20</sup> Spheroidal micelles of P123 are formed in less than ten minutes and are slowly replaced by threadlike micelles as silica condensation changes the polarity about the mantle of the micelle. The threadlike micelles become more rigid and bundle into clusters, although the hexagonal mesostructure is not observed at the time of material precipitation. Freeze fracture images of the material taken 2 h after silica addition show a fully developed hexagonal mesophase. When similar experiments were carried out during MCM-41 synthesis, hexagonal order was observed in less than three minutes; the quicker organization of MCM-41 is attributed to the stronger coulombic forces between cationic headgroups and silicate anions.



**Figure 4-3:** P123 core-mantle surfactant assembly (Diagram **A**, adapted from ref. 18). PEO-block occlusion into silica network illustrated. Micropores form after surfactant removal, either by calcination or by extraction (Diagram **B**, adapted from ref. 19).

Occlusion of the PEO blocks into the silica network leads to microporous channels between the ordered mesopores which remain upon surfactant removal (Figure 4-3, **B**). Ryoo *et al.* reported that the surface area of SBA-15 was significantly larger than expected for a hexagonal array of cylindrical pores of a given size.<sup>19</sup> When the surface of the material was functionalized with octyldimethylsilane, however, the surface areas mirrored the expected values more closely. The alkyl group was bulky enough to block access to the micropore channels, but had only a negligible effect on the larger mesopores. Interestingly, when the material was treated with trimethylsilane, an intermediate surface area was obtained, as the smaller silane only sealed the smallest of the micropores. As a proof of concept, Ryoo<sup>19</sup> grew platinum wires within the pore structures of both SBA-15 and MCM-41. When the silica network of SBA-15 was dissolved, the platinum wires remained connected in agglomerates replicating the

hexagonal order of the original material. When the process was repeated for MCM-41, however, agglomeration of the wires was not observed, indicating the differences in the interconnectedness of the channels in the two materials.

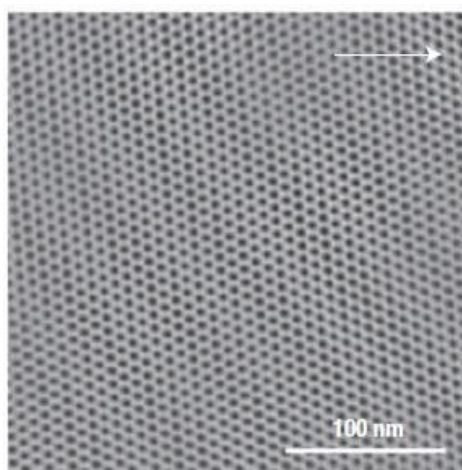
#### *4.2.2 Bulk Morphology of Materials*

Tailoring the macroscopic properties of materials is necessary to fully optimize the application of mesoporous materials to the fields of sensing, separation and catalysis. Where transparent monoliths of mesoporous silicas are desirable for their optical properties, thin films of material could find widespread use in membrane type separations. Thin films are obtained readily at solid / liquid and liquid / vapor interfaces, though these processes are slow and yield mesoporous channels parallel to the interface.<sup>21</sup> Brinker and co workers dip-coated a preformed solution of surfactant, acid and silica precursor onto a periodically ordered glass surface to rapidly obtain cubic ordered mesoporous thin films.<sup>22</sup> Solvent evaporation during the dip-coating process increases the rate of silica condensation and accelerates material formation in a process he termed “EISA” for evaporation induced self assembly. By altering the initial concentration of surfactant in the solution, thin films with various mesophases are selected for based on the packing parameter discussed above. In this case, the 3D cubic mesophase is desirable (and achievable) as it allows access to the pore network from the surface of the thin film.

Selectively aligning the mesostructure on a macroscopic scale prior to silica condensation is also possible. Kuroda and co workers employed a rubbed polyimide



surface to seed spherical, and eventually rod-like, surfactant micelles in the direction perpendicular to the rubbed surface.<sup>23</sup> This method provides structural periodicity on the centimeter scale, though pores running parallel to the material are inaccessible at the surface of the film (Figure 4-4). Stucky and co workers reported that liquid crystal mesophases can align parallel to the field of a strong magnet.<sup>24, 25</sup> Building on this discovery, Kuroda and co-workers synthesized thin films in the presence of a strong magnetic field (12 T) and observed that most pores aligned perpendicular to the surface of the film.<sup>26</sup> Interestingly, pores in small sections of the film were not completely aligned, with some tilted at 40-60° to the surface normal. This was attributed to premature silica network condensation, essentially locking the local mesophase in place before complete alignment could occur.



**Figure 4-4:** Reconstructed TEM image of single-crystalline mesoporous resulting from polyimide rubbing treatment of silica glass wafer. The rubbing direction is indicated by the inset arrow. Image taken from ref 23.

### 4.3 Hydrothermal Stability of Mesoporous Silica

The major drawback of ordered mesoporous silicates, even SBA-15, is that they are not as hydrothermally stable as their zeolite analogues.<sup>11</sup> The standard way of determining the stability of an ordered silicate is to monitor porosity and long range order after high temperature calcination or steaming. MCM-41 withstands humid air at 980 K for 2 h,<sup>27</sup> but its thin wall structure is vulnerable to boiling water, and degrades completely under these conditions in less than 12 hours.<sup>28</sup> SBA-15 is more stable, and can retain long range order after being steamed at 600 °C for 6 h, though a significant decrease in surface area is indicative of framework reorganization leading to the elimination of micropores.<sup>10</sup> In the presence of steam, framework siloxanes,  $\equiv\text{Si-O-Si}\equiv$ , are hydrolyzed to silanol groups  $\equiv\text{Si-OH}$ , but the rapid re-condensation of adjacent silanols prevents further degradation of the wall. In boiling water, however, the reorganization is not quick enough to counter siloxane hydrolysis and subsequent material degradation.

#### 4.3.1 Improved Material Stability

When prepared in typical fashion, MCM-41 and, to a lesser extent, SBA-15, are not stable enough to be effective replacements of zeolites. The materials are more susceptible to degradation in humid or aqueous conditions than in dry air, so considerable effort was put into making the material surfaces resistant to nucleophilic attack by water.

Tatsumi *et al.* protected the surfaces of MCM-41 and the cubic MCM-48 by functionalizing the surface silanols with trimethylsilane (TMS).<sup>29</sup> The functionalized (capped) material was rendered more hydrophobic and maintained long range order longer than the unfunctionalized materials when subjected to water vapor at room temperature for 30 days. These results indicate that surface modification can have positive effects on the bulk properties of the material, but the conditions used to monitor stability in this study were too mild to truly test the material.

The extent of silica condensation within the network can be measured by the number of Q-sites. Q<sub>x</sub>-sites are defined as Si(OSi)<sub>x</sub>(OH)<sub>4-x</sub>, and are distinguishable from each other by <sup>29</sup>Si MAS NMR. As the ratio of Q<sub>4</sub> to Q<sub>3</sub> sites is augmented, the material is more highly condensed and likely more stable to hydrothermal conditions. By adding NaCl to the reaction mixture during the synthesis of MCM-41, Cheng *et al.* reported<sup>30</sup> that MCM-41 retains its long range order after being subjected to 100 °C water for 4 days, increasing the lifetime of the material eight-fold. Cheng noticed that adding salt increased the ratio of Q<sub>4</sub> to Q<sub>3</sub> sites in the material and speculated that the cations in solution would affect the interaction between the cationic surfactant headgroup and the silicate species. This can be rationalized as an attenuation of the interaction between the charged surfactant and silicate by ionic screening.<sup>28</sup> With less attraction to the surfactant head groups, the silicate oligomers are free to polymerize more extensively.

The incorporation of heteroatoms, specifically Al and Ti, into the silica framework can also have a stabilizing effect on the material. When substituting Si<sup>4+</sup> in the framework of the wall, Al<sup>3+</sup> introduces a geometric defect into the structure of the

wall. The surrounding aluminosilicate network must also be charge balanced by a cation or proton to remain neutral. Shen and Kawi suggested that this distorted network has more entropy than a purely siliceous material thereby making it more thermodynamically stable.<sup>31</sup> Much in the same way, KIT-1, a material differing from MCM-41 only in the disordered nature of its mesopores, is more hydrothermally stable than the ordered MCM-41.<sup>32</sup> Impressively, MCM-41 synthesized with high Si/Al ratios (~25) maintained surface areas of about 1000 m<sup>2</sup>/g after soaking in boiling water for one week. On the other hand, standard MCM-41 was found to have lost almost all of its surface area when subjected to identical conditions; in fact, the surface areas recorded (slightly over 100 m<sup>2</sup>/g) are on par with amorphous silica.

Improvements to the stability of SBA-15 have also been made, but since this material is intrinsically more stable than the thin-walled MCM-41, the increases in stability have been less dramatic. Zhao and co-workers determined that increasing calcination temperature to 900 °C completely eliminates Q<sub>3</sub> sites from the material and increases the materials stability towards steaming.<sup>10</sup> The high-temperature calcinations restructure the silica network, by completely condensing remaining silanols. This process significantly reduces both the surface area and the pore size of the material. Carbon propping was also developed as a method to counter pore shrinkage during high temperature treatments.<sup>10</sup> Coating the pores with carbon from a glucose source prevents the thickening of the silica wall at the expense of pore size during calcination. The supporting carbon structure was then removed by calcination in air, yielding a material

that maintained order after steaming at 800 °C for 12 h and that saw slower decreases in pore size and surface area over time than non-propped materials.

Stabilizing SBA-15 by high calcination temperature and carbon propping is not efficient, and so methods to strengthen the material during the synthesis step were sought. Higher condensation of the silica wall structure is possible not only by increasing calcinations temperatures, but by employing a higher aging temperature as well.<sup>33</sup> Aging is typically done under static conditions at 80-100 °C for 48 h to allow for maximal silica condensation and for the most stable mesophase to form. Higher temperatures are generally not used to avoid distortion of the micelle and degradation of the block copolymer surfactant. A way to circumvent this problem was postulated by Li and co-workers. Li reported that materials could be aged at 160 °C and still show long range order when made using a mixed micelle of P123 and a semi-fluorinated surfactant FSO-100.<sup>33</sup> Adding salt further improved the long range order of the material, either by encouraging better ordering of the micelle or by increasing the interaction between the surfactant and the silicate species. Impressively, SBA-15 made with semi-fluorinated mixed micelles and aged between 140-160 °C retained long range order, mesoporosity and high surface area after a phenomenal 300 h of boiling water treatment. Incorporating Al (with a Si/Al ratio of 30) into the material rendered it even more stable, keeping a tighter pore size distribution during the stringent stability tests in boiling water.<sup>33</sup>

#### **4.4 Applications of Functionalized Mesoporous Silica**

In an initial review of the performance of Al-MCM-41 as a solid inorganic catalyst, Sayari reported that the aluminosilicate is a valuable alternative to zeolite based catalysts for a number of cracking, alkylation and dealkylation processes.<sup>34</sup> Indeed, the larger pore size and surface area provides facile access to the catalytically active sites of the material. The moderate acidity of these active sites, however, limits the unfunctionalized material's application as an inorganic catalyst. Thus there have been many attempts to prepare MCM-41 or SBA-15-type materials that are strongly acidic.

In 1997, Fryxell and co-workers functionalized a pore-expanded MCM-41 with thiol groups by condensing 3-mercaptopropyl trimethoxysilane (3-MPTMS) on the surface of the material.<sup>35</sup> Surface functionalization was instrumental in shifting focus from the catalytic activity of the ordered framework itself (mostly as a general acid catalyst) to being a solid support for a variety of possible applications. In a sense, this was an elaboration of surface protection by TMS in which the surface protecting alkyl chains are now teamed with a chemically active terminal functional group. The degree of functionalization could be controlled by varying both the population of surface silanols and the quantity of water molecules adsorbed to the material surface. Coupled with the aforementioned thiol functionality, the ordered material becomes an efficient and reusable scavenger of heavy metals from aqueous and organic solutions.<sup>36</sup>

Importantly, the thiol groups tethered to the surface of the material could also be oxidized to form strong sulphonic acids. Stein and co-workers performed near-quantitative protection of an alcohol by 2,3-dihydropyran with MCM-41-SO<sub>3</sub>H, a reaction that did not proceed at all in the presence of unfunctionalized MCM-41.<sup>37</sup> In

what would become one of the greatest advantages of using a mesoporous silicate catalyst discovered to date, the researchers were able to easily isolate the insoluble material from the product solution by filtration. Similar examples of acid catalysis using supported sulphones have since been reported by Van Rhijn<sup>38</sup> (synthesis of bisfuralalkanes) and also by Jones<sup>39</sup> (MAO-free ethylene polymerization).

#### **4.5 The Beginnings of Our Involvement**

The pendant thiol groups, grafted to the pore walls and outer surface of the mesoporous silica, need not be oxidized to the corresponding sulphonic acid to be useful. In fact, sulphur's strong affinity for heavy metals makes thiol-functionalized mesoporous materials ideal candidates for both metal sensing<sup>40</sup> and scavenging.<sup>41</sup> As product contamination by heavy metals (and subsequent remediation) continues to dampen the cost-effectiveness of transition metal catalysts used in the pharmaceutical industry,<sup>42</sup> new and improved methods for metal scavenging are constantly being sought out.

Common methods of Pd-removal involve multiple chromatographic or recrystallization steps to reduce the product contamination to acceptable levels of Pd.<sup>42</sup> Seeking to improve on this time-consuming and expensive process, the Crudden group was able to show that the addition of amine-functionalized SBA-15 to a high-yielding Grubb's Metathesis reaction was able to almost completely remove the offending Ru-metal from solution without chromatography after filtration of the insoluble silica.<sup>41</sup> Naturally, once a method to effectively remove the catalyst after completion of the

reaction had been developed, there was motivation to then be able to reuse the precious metal. Indeed, more than for metal scavenging, it would be in the area of reusable, ‘leach-proof’ catalysis that functionalized mesoporous materials would truly make their mark. Our contributions to the field, specifically investigations into the stability of mesoporous silica supports and heavy-metal leaching, are outlined in the next chapter.

#### 4.6 References

- (1) Hafner, J.; Benco, L.; Bucko, T. Acid-based catalysis in zeolites investigated by density-functional methods. *Top. Catal.* **2006**, 37, 41-54.
- (2) Benco, L.; Bucko, T.; Hafner, J.; Toulhoat, H. Periodic DFT Calculations of the Stability of Al/Si Substitutions and Extraframework  $Zn^{2+}$  Cations in Mordenite and Reaction Pathway for the Dissociation of  $H_2$  and  $CH_4$ . *J. Phys. Chem. B* **2005**, 109, 20361-20369.
- (3) Vos, A. M.; Rozanska, X.; Schoonheydt, R. A.; van Santen, R. A.; Hutschka, F.; Hafner, J. A Theoretical Study of the Alkylation Reaction of Toluene with Methanol Catalyzed by Acidic Mordenite. *J. Am. Chem. Soc.* **2001**, 123, 2799-2809.
- (4) Kresge, C. T.; Leonowicz, M. E.; Roth, W. J.; Vartuli, J. C.; Beck, J. S. Ordered mesoporous molecular sieves synthesized by a liquid-crystal template mechanism. *Nature* **1992**, 359, 710-712.
- (5) Yanagisawa, T.; Shimizu, T.; Kuroda, K.; Kato, C. The Preparation of Alkyltrimethylammonium-Kanemite Complexes and Their Conversion to Microporous Materials. *Bull. Chem. Soc. Jpn.* **1990**, 63, 988-990.



- (6) Beck, J. S.; Vartuli, J. C.; Roth, W. J.; Leonowicz, M. E.; Kresge, C. T.; Schmitt, K. D.; Chu, C. T. W.; Olson, D. H.; Sheppard, E. W. A new family of mesoporous molecular sieves prepared with liquid crystal templates. *J. Am. Chem. Soc.* **1992**, 114, 10834-10843.
- (7) Chen, C.; Burkett, S. L.; Li, H.; Davis, M. E. Studies on mesoporous materials II. Synthesis mechanism of MCM-41. *Microporous Materials* **1993**, 2, 27-34.
- (8) Zhao, D.; Feng, J.; Huo, Q.; Melosh, N.; Fredrickson, G. H.; Chmelka, B. F.; Stucky, G. D. Triblock Copolymer Syntheses of Mesoporous Silica with Periodic 50 to 300 Angstrom Pores. *Science* **1998**, 279, 548-552.
- (9) Zhao, D.; Huo, Q.; Feng, J.; Chmelka, B. F.; Stucky, G. D. Nonionic Triblock and Star Diblock Copolymer and Oligomeric Surfactant Syntheses of Highly Ordered, Hydrothermally Stable, Mesoporous Silica Structures. *J. Am. Chem. Soc.* **1998**, 120, 6024-6036.
- (10) Zhang, F.; Yan, H.; Yan Meng, Y.; Yu, C.; Tu, B.; Zhao, D. Understanding Effect of Wall Structure on the Hydrothermal Stability of Mesostructured Silica SBA-15. *J. Phys. Chem. B* **2005**, 109, 8723-8732.
- (11) Wan, Y.; Zhao On the Controllable Soft-Templating Approach to Mesoporous Silicates. *Chem. Rev.* **2007**, 107, 2821-2860.
- (12) Huo, Q.; Margolese, D. I.; Stucky, G. D. Surfactant Control of Phases in the Synthesis of Mesoporous Silica-Based Materials. *Chem. Mater.* **1996**, 8, 1147-1160.
- (13) Monnier, A.; Schüth, F.; Huo, Q.; Kumar, D.; Margolese, D.; Maxwell, R. S.; Stucky, G. D.; Krishnamurty, M.; Petroff, P.; Firouzi, A.; Janicke, M.; Chmelka, B. F. Cooperative Formation of Inorganic-Organic Interfaces in the Synthesis of Silicate Mesostructures. *Science* **1993**, 261, 1299-1303.

- (14) Inagaki, S.; Fukushima, Y.; Kuroda, K. Synthesis of highly ordered mesoporous materials from a layered polysilicate. *J. Chem. Soc., Chem. Commun.* **1993**, 680-682.
- (15) Ozeki, S.; Ikeda, S. The Stability of Spherical Micelles of Dodecyltrimethylammonium Chloride in Aqueous NaCl Solutions. *Bull. Chem. Soc. Jpn.* **1981**, 54, 552-555.
- (16) Huo, Q.; Margolese, D. I.; Ciesla, U.; Demuth, D. G.; Feng, P.; Gier, T. E.; Sieger, P.; Firouzi, A.; Chmelka, B. F. Organization of Organic Molecules with Inorganic Molecular Species into Nanocomposite Biphase Arrays. *Chem. Mater.* **1994**, 6, 1176-1191.
- (17) Huo, Q.; Margolese, D. I.; Ciesla, U.; Demuth, D. G.; Feng, P.; Gier, T. E.; Sieger, P.; Firouzi, A.; Chmelka, B. F. Organization of Organic Molecules with Inorganic Molecular Species into Nanocomposite Biphase Arrays. *Chem. Mater.* **1994**, 6, 1176-1191.
- (18) Ruthstein, S.; Frydman, V.; Kababya, S.; Landau, M.; Goldfarb, D. Study of the Formation of the Mesoporous Material SBA-15 by EPR Spectroscopy. *J. Phys. Chem. B* **2003**, 107, 1739-1748.
- (19) Ryoo, R.; Ko, C. H.; Kruk, M.; Antochshuk, V.; Jaroniec, M. Block-Copolymer-Templated Ordered Mesoporous Silica: Array of Uniform Mesopores or Mesopore-Micropore Network? *J. Phys. Chem. B* **2000**, 104, 11465-11471.
- (20) Ruthstein, S.; Schmidt, J.; Kesselman, E.; Talmon, Y.; Goldfarb, D. Resolving Intermediate Solution Structures during the Formation of Mesoporous SBA-15. *J. Am. Chem. Soc.* **2006**, 128, 3366-3374.
- (21) Manne, S.; Gaub, H. E. Molecular Organization of Surfactants at Solid-Liquid Interfaces. *Science* **1995**, 270, 1480-1482.

- (22) Lu, Y.; Ganguli, R.; Drewien, C. A.; Anderson, M. T.; Brinker, J. C.; Gong, W.; Guo, Y.; Soyez, H.; Dunn, B.; Huang, M. H.; Zink, J. I. Continuous formation of supported cubic and hexagonal mesoporous films by sol-gel dip-coating. *Nature* **1997**, 389, 364-368.
- (23) Miyata, H.; Suzuki, T.; Fukuoka, A.; Sawada, T.; Watanabe, M.; Noma, T.; Takada, K.; Mukaide, T.; Kuroda, K. Silica films with a single-crystalline mesoporous structure. *Nat. Mater.* **2004**, 3, 651-656.
- (24) Tolbert, S. H.; Firouzi, A.; Stucky, G. D.; Chmelka, B. F. Magnetic Field Alignment of Ordered Silicate-Surfactant Composites and Mesoporous Silica. *Science* **1997**, 278, 264-268.
- (25) Firouzi, A.; Schaefer, D. J.; Tolbert, S. H.; Stucky, G. D.; Chmelka, B. F. Magnetic-Field-Induced Orientational Ordering of Alkaline Lyotropic Silicate-Surfactant Liquid Crystals. *J. Am. Chem. Soc.* **1997**, 119, 9466-9477.
- (26) Yamauchi, Y.; Sawada, M.; Noma, T.; Ito, H.; Furumi, S.; Sakka, Y.; Kuroda, K. Orientation of mesochannels in continuous mesoporous silica films by a high magnetic field. *J. Mater. Chem.* **2005**, 15, 1137-1140.
- (27) Kim, J. M.; Kwak, J. H.; Jun, S.; Ryoo, R. Ion Exchange and Thermal Stability of MCM-41. *J. Phys. Chem.* **1995**, 99, 16742-16747.
- (28) Ryoo, R.; Jun, S. Improvement of Hydrothermal Stability of MCM-41 Using Salt Effects during the Crystallization Process. *J. Phys. Chem. B* **1997**, 101, 317-320.
- (29) Koyano, K. A.; Tatsumi, T.; Tanaka, Y.; Nakata, S. Stabilization of Mesoporous Molecular Sieves by Trimethylsilylation. *J. Phys. Chem. B* **1997**, 101, 9436-9440.
- (30) Das, D.; Tsai, C.; Cheng, S. Improvement of hydrothermal stability of MCM-41 mesoporous molecular sieve. *Chem. Commun.* **1999**, 473-474.

- (31) Shen, S.; Kawi, S. Understanding of the Effect of Al Substitution on the Hydrothermal Stability of MCM-41. *J. Phys. Chem. B* **1999**, 103, 8870-8876.
- (32) Ryoo, R.; Kim, J. M.; Ko, C. H.; Shin, C. H. Disordered Molecular Sieve with Branched Mesoporous Channel Network. *J. Phys. Chem.* **1996**, 100, 17718-17721.
- (33) Li, C.; Wang, Y.; Guo, Y.; Liu, X.; Guo, Y.; Zhang, Z.; Wang, Y.; Lu, G. Synthesis of Highly Ordered, Extremely Hydrothermal stable SBA-15/Al-SBA-15 under the Assistance of Sodium Chloride. *Chem. Mater.* **2007**, 19, 173-178.
- (34) Sayari, A. Catalysis by Crystalline Mesoporous Molecular Sieves. *Chem. Mater.* **1996**, 8, 1840-1852.
- (35) Feng, X.; Fryxell, G. E.; Wang, L. Q.; Kim, A. Y.; Liu, J.; Kemner, K. M. Functionalized Monolayers on Ordered Mesoporous Supports. *Science* **1997**, 276, 923-926.
- (36) Liu, J.; Feng, X.; Fryxell, G. E.; Wang, L.; Kim, A. Y.; Gong, M. Hybrid Mesoporous Materials with Functionalized Monolayers. *Adv. Mater.* **1998**, 10, 161-165.
- (37) Lim, M. H.; Blanford, C. F.; Stein, A. Synthesis of Ordered Microporous Silicates with Organosulfur Surface Groups and Their Applications as Solid Acid Catalysts. *Chem. Mater.* **1998**, 10, 467-470.
- (38) Van Rhijn, W.,M.; De Vos, D.,E.; Sels, B.,F.; Bossaert, W.,D. Sulfonic acid functionalised ordered mesoporous materials as catalysts for condensation and esterification reactions. *Chem. Commun.* **1998**, 317-318.
- (39) Hicks, J. C.; Mullis, B. A.; Jones, C. W. Sulfonic Acid Functionalized SBA-15 Silica as a Methylaluminoxane-Free Cocatalyst/Support for Ethylene Polymerization. *J. Am. Chem. Soc.* **2007**, 129, 8426-8427.

(40) Du, J.; Cipot-Wechsler, J.; Lobez, J. M.; Loock, H.; Crudden, C. M. Periodic Mesoporous Organosilica Films: Key Components of the Fibre-Optic-Based Heavy-Metal Sensors. *Small* **2010**, 6, 1168-1172.

(41) McEleney, K.; Allen, D. P.; Holliday, A. E.; Crudden, C. M. Functionalized Mesoporous Silicates for the Removal of Ruthenium from Reaction Mixtures. *Org. Lett.* **2006**, 8, 2663-2666.

(42) Garrett, C. E.; Prasad, K. The Art of Meeting Palladium Specifications in Active Pharmaceutical Ingredients Produced by Pd-Catalyzed Reactions. *Adv. Synth. Catal.* **2004**, 346, 889-900.

## Chapter 5

# Material Stability and the Protective Effect of the Suzuki-Miyaura Reaction

### 5.1 Introduction

#### *5.1.1 Supported Metal as Catalyst*

A large leap in mesoporous material supported catalysis was made when our laboratory<sup>1</sup> and others<sup>2</sup> recognized that thiol- and amino-functionalized materials could act not only as heavy metal scavengers, but once charged with a transition metal, they can be catalytically active for a variety of cross-coupling reactions. Thiol-functionalized SBA-15 loaded with Pd (SBA-15-SH•Pd) was shown to be catalytically active for the Suzuki-Miyaura, Mizoroki-Heck and Sonogashira cross-couplings and could easily be isolated and reused.<sup>1</sup> The advantage of immobilizing Pd on a scavenging material is that any Pd that would otherwise be leached into solution is quickly recaptured by adjacent thiol groups in the material. For low levels of metal leaching and for its recyclability, SBA-15-SH•Pd was a potentially promising alternative to both homogeneous and even other heterogeneous catalysts for Pd-catalyzed reactions known to undergo high-levels of leaching. To culminate our work in the area of supported catalysis, we felt that a true understanding of the system was both important and lacking, not only for pedagogic reasons, but also as a means to uncover and address the limitations of functionalized mesoporous silica in Pd-catalysis. Catalyst heterogeneity, the role of mesostructure and

the stability of various silica supports to actual reaction conditions were all investigated in detail, ultimately leading to the development of a sturdier, highly-recyclable aluminosilicate catalyst support.<sup>3</sup>

### *5.1.2 Heterogeneity of Pd-loaded SBA-15*

The true heterogeneity of supported catalysts was hotly contested in the late 2000s.<sup>4</sup> This was no different for SBA-15-SH•Pd-type catalysts. In 2007, Richardson and Jones<sup>5</sup> concurrently with our group,<sup>6</sup> examined the true nature and mobility of the active palladium species when loaded on thiol-functionalized mesoporous silica. Prior to the comprehensive study performed independently by both groups, common catalyst-heterogeneity tests had indicated that Pd loaded onto thiol-functionalized mesoporous silica was a leach-proof, fully-heterogeneous catalyst.<sup>1</sup> The Jones study focused on a series of poison studies to determine the heterogeneity of the supported catalyst. Interestingly, decreased activity or complete cessation of catalysis was observed upon introduction of large excesses of supported thiols or amines, indicating that the catalytically active Pd accesses the free solutions. Interaction of this Pd with the thiol-based scavenger effectively poisons the catalyst, through a mechanism of over coordination to the leached Pd metal. A variety of supported poisons including Quadrapure (thiol functionalized polystyrene), polyvinyl pyridine and even metal-free SBA-15-SH all hindered, and in some cases, completely stopped catalysis. Although the Jones study focused primarily on the Mizoroki-Heck reaction which has significantly harsher

conditions than the Suzuki-Miyaura, Crudden's study of the latter reaction with a similar catalyst also came to the same conclusion. One critical piece of information to emerge was the importance of the ratio of S: Pd, as too high of a ratio (which likely leads to Pd being too tightly bound to the surface) leads to a loss of catalytic activity. In addition, through the most detailed study of the three-phase-test reported to date, the Crudden group showed that this test is only effective in certain solvents.<sup>6</sup> Highly polar solvents such as water or water/DMF mixtures do not provide sufficient mobility for the Pd, which appears to remain relatively close to the surface, even though it is only active in solution. Thus for both of these important reactions, under the conditions tested, a 'release and catch' mechanism is most likely at play, though the consistently low levels of palladium leaching into the final solution indicate that the system is functionally heterogeneous.

## **5.2 Effect of Suzuki-Miyaura Reaction on Material Support**

### *5.2.1 A New Paradigm for Material Stability*

Though not as stable to hydrothermal conditions as the zeolites they were meant to replace, mesoporous silicas are able to withstand very harsh conditions for extended periods of time. This is especially true of the thicker walled variants, such as SBA-15.<sup>7</sup> But since mesoporous silicas were conceived as larger-pore analogues of the microporous



zeolites, then it follows that their worth (in the form of stability) would be judged by tests optimized for zeolites. As zeolites are used mostly as cracking catalysts at high temperatures, subjecting them to high temperatures or super-heated steam allows for proper assessment of stability under conditions typical of use. The evolution of mesoporous silica from zeolite analogue to metal scavenger and, ultimately, catalyst support has subjected these ordered silica materials to conditions far more destructive than super-heated steam. In fact, the prevalence of mesoporous silica in heterogeneous catalysis<sup>1,6,8</sup> has rendered the hydrothermal tests obsolete.

We first came to grasp this problem as we sought to assess the stability of a variety of mesoporous silicas used as supports in the Suzuki-Miyaura reaction. The potential utility of SBA-15 supported catalysts had been well-demonstrated by the high catalytic activity and low metal-leaching, though it became important to quantify the recyclability of each support in order to justify the time-consuming synthesis of the material. Naturally, a support that takes a week to make and only effectively catalyzes a reaction for a handful of hours would not be considered effective.

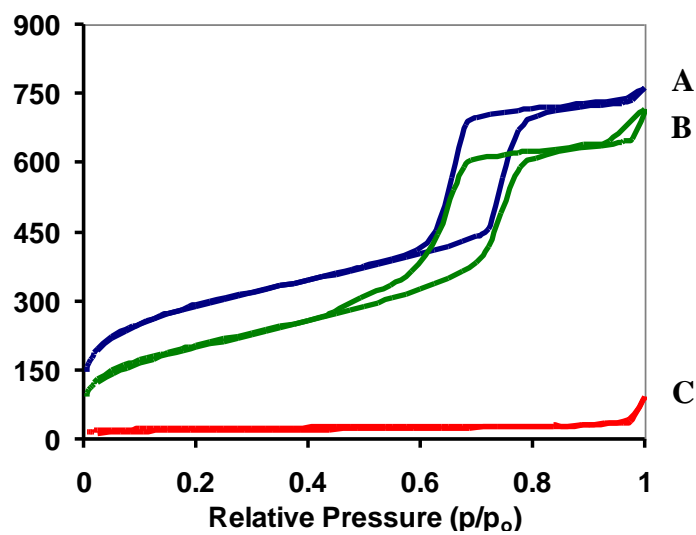
The stability of MCM-41, for example, is limited by its thin wall structure. Previous reports indicate that despite having walls of only 10 Å, it can withstand high temperature calcination, though seemingly not 12 h in boiling water.<sup>9</sup> Neither of these tests gives any real suggestion as to how MCM-41 would perform under Suzuki-Miyaura conditions. In a preliminary recycling study, we determined that Pd loaded onto thiol-functionalized MCM-41 was able to catalyze two consecutive small-scale Suzuki-Miyaura reactions, before becoming completely inactive during the third use. This

effective lifespan, totaling less than 5 h, was further proof that a new test of stability was needed. The factors leading to material degradation during catalysis, ones that are stronger and swifter than mere heat and steam would also have to be determined.

### *5.2.2 Effect of Aqueous Base on Material Structure*

The Suzuki-Miyaura reaction has a strict requirement for base to enable catalytic turnover, as discussed in detail in Chapter 1. Given that aqueous base is also known to attack silica,<sup>10</sup> we focused our attention first on the effect of aqueous base on material stability. In order to test the stability of various materials to the reaction conditions without sacrificing large quantities of the organic substrates or precious Pd metal, a set of conditions was developed that would emulate the Suzuki-Miyaura reaction media. These conditions consisted of stirring the insoluble silica material at 80 °C in 20:1 DMF:H<sub>2</sub>O under inert atmosphere in the presence of the slightly soluble K<sub>2</sub>CO<sub>3</sub> in the absence of reaction substrates. The insoluble materials were then filtered, washed and examined by nitrogen porosimetry. This is the most common method of evaluating mesoporosity, surface area and order of mesoporous materials and, in general, a hysteresis in the nitrogen isotherm is indicative of mesoporosity and order. Though lots of information about a material can be gleaned from this powerful technique, in the current study, the presence (or lack thereof) of this hysteresis is simply used to determine whether the material tested had maintained its mesoporosity or has completely degraded.

As Pd-catalyst supports for the Suzuki-Miyaura reaction, mesoporous silicas survive multiple recycles totaling over 12 h of total lifetime.<sup>3,6</sup> When tested against these *pseudo*-reaction conditions, however, both MCM-41 and SBA-15-type materials completely lost their mesoporosity in *under 8 h*, further illustrating the dichotomy between the hydrothermal conditions typically used to assess material stability and strongly basic conditions, meant to mirror those of the Suzuki-Miyaura cross-coupling reaction (Figure 5-1).<sup>11</sup>

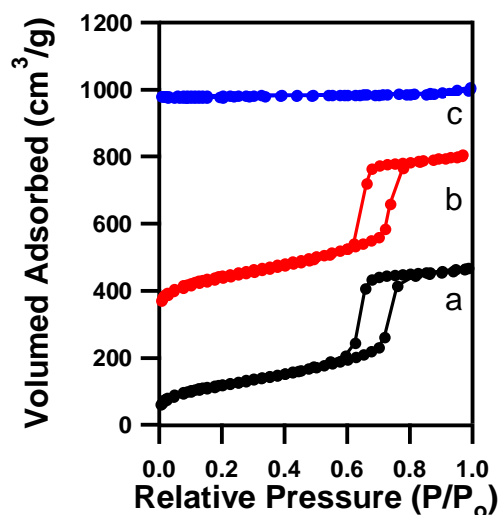


**Figure 5-1:** Isotherms of pristine SBA-15 (A), SBA-15 after 8 h of Suzuki-Miyaura recycles (B) and SBA-15 after 8 h of *pseudo*-reaction conditions (C).

For the systematic determination of which reaction elements were causing this marked negative effect on the material, we subjected a common batch of SBA-15 prepared in the presence of NaCl (so-called SBA-15-NaCl) to the *pseudo*-conditions. As noted in the previous chapter, when used in conjunction with special, fluorinated

surfactants, the use of NaCl during material preparation can lead to a dramatic increase in material stability,<sup>12</sup> however when used with the typical P123 surfactant, NaCl provides a material which is *more prone to degradation than SBA-15*. The less stable SBA-15-NaCl, falling somewhere between MCM-41 and authentic SBA-15, allows for the rapid screening of conditions but is still robust enough to survive innocuous testing conditions (perhaps unlike MCM-41). The results obtained in this study were eventually applied to SBA-15 prepared in the absence of NaCl.

As noted above, the hot aqueous base required for the Suzuki-Miyaura reaction is likely the main factor in the accelerated material degradation. Aqueous base attacks the electrophilic surface silanols affecting a reordering of the condensed network and ultimately having a deleterious effect on the order of the material.<sup>10</sup> The dramatic effect of aqueous base is clearly demonstrated in (Figure 5-2). After 8 h of treatment with DMF:H<sub>2</sub>O at 80 °C (the typical reaction temperature), there was no loss of order (compare Figures 5-2a and 5-2b). However, upon addition of base, the pore structure of SBA-15-NaCl completely collapsed (Figure 5-2c).



**Figure 5-2:** Effect of base on the structure of an ordered mesoporous silica. (a) SBA-15-NaCl (b) SBA-15-NaCl heated in 20:1 DMF: H<sub>2</sub>O, 8 h (c) SBA-15-NaCl heated with base. Note that plots (b) and (c) are offset vertically to facilitate viewing.

One caveat that had to be addressed in this study was that the silica material and the exogenous base were insoluble and slightly soluble, respectively, in the solvent system used. It could follow, then, that the addition of granular K<sub>2</sub>CO<sub>3</sub>, in conjunction with the rotating stir bar, could degrade the material by means of a grindstone effect. Mesoporous materials are not immune to macroscopic phenomena; in fact, work in our group has shown that grinding chiral mesoporous materials can lower the enantiopurity of a chiral material. With this in mind, SBA-15-NaCl was subjected to identical conditions as above, but without the addition of water. Gratifyingly, the material maintained its mesoporosity over the course of the 8 h treatment, indicating that not only was any effect of mechanical degradation minimal, but also that water, together with base, was responsible for structural collapse of the material. Indeed, the shortened life spans of the

mesoporous catalyst supports in Suzuki-Miyaura reactions have been assigned, unequivocally, to the use of hot aqueous base. Of course, this finding is in line with the strong evidence for aqueous base dissolving other types of silica.<sup>10</sup>

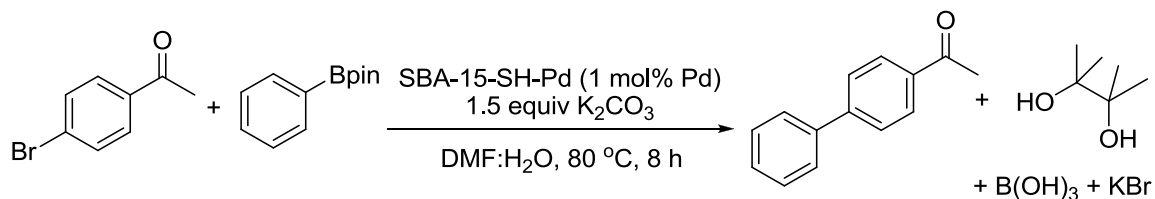
### 5.2.3 An Unforeseen Protective Effect of the Reaction

The *pseudo*-reaction studies showed very clearly that aqueous base, required for the Suzuki-Miyaura reaction to turnover, was leading to dramatic decreases in material stability. One other critical piece of information, however, was that although supported catalysts used in actual reactions were surviving significantly *longer* than would be predicted by the *pseudo*-studies themselves (Figure 5-1). Surprisingly, there seemed to be a protective effect of the reaction itself.

Further evidence for this empirical protective effect was obtained by subjecting SBA-15-NaCl to the destructive *pseudo*-reaction conditions (DMF:H<sub>2</sub>O, 80 °C, K<sub>2</sub>CO<sub>3</sub>, 8 h), except in this instance, a fresh solvent system was replaced by the filtrate of a Suzuki-Miyaura reaction that had proceeded to completion. Even with the addition of a full ration of new K<sub>2</sub>CO<sub>3</sub> to go along with the excess present in the filtrate from the previous reaction, the material maintained its mesoporosity after the 8 h test. Clearly, the *pseudo*-reactions had not fully reproduced the actual reaction conditions.

Again, elements of the Suzuki-Miyaura reaction itself were systematically tested for their effect on material stability, though this time for a potentially *stabilizing* influence. The initial stability studies did not take into account the starting materials,

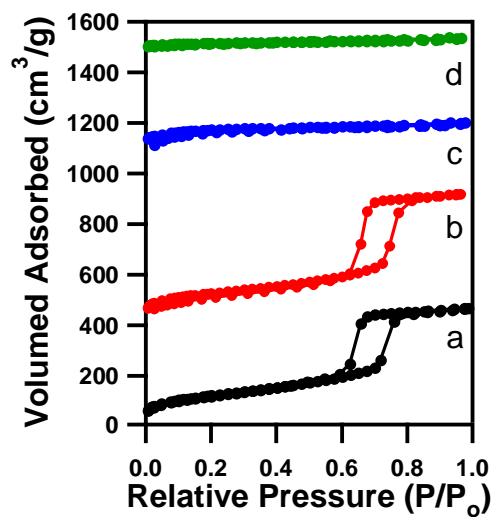
products or side-products of an actual reaction, nor did they make use of thiol-functionalized or Pd loaded material. The coupling partners (4-bromoacetophenone and phenyl boronic acid pinacolate ester) and final product were already known by previous work in the group to have a negligible effect on material structure. What had never been tested were the side-products of a successful Suzuki-Miyaura reaction, namely potassium bromide and boric acid (Scheme 5-1). KBr is produced after the bromide ion is expelled from the Pd-coordination sphere, presumably by hydroxide base. As previously discussed,  $B(OH)_3$  is produced as the otherwise inactive arylboronic acid transmetalates to Pd, driven in no small part by the formation of another boron-oxygen bond.



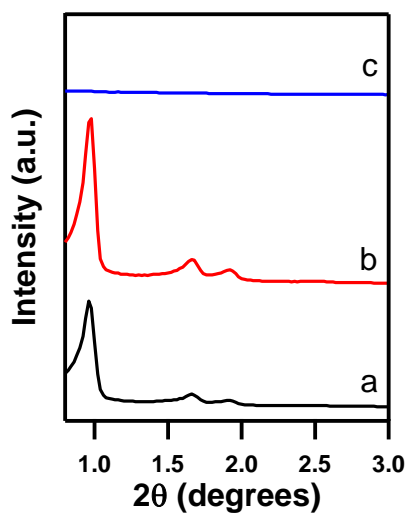
**Scheme 5-1:** Unsymmetrical biaryl synthesized *via* mesoporous silica supported, Pd-catalyzed Suzuki-Miyaura cross-coupling reaction. The side-products,  $B(OH)_3$ , KBr and pinacol are also noted.

Both of these side-products were added, along with SBA-15-NaCl, to two separate *pseudo*-condition experiments. Perhaps unsurprisingly, the material exposed to base in the presence KBr underwent the familiar, rapid degradation (compare Figures 5-3a and 5-3c), however the addition of the other major side-product, boric acid, resulted in

virtually complete retention of porosity (Figure 5-3b) and long range order (Figure 5-4b, X-Ray Diffraction).



**Figure 5-3:** Effect of Reaction side-products on mesoporous silica. (a) SBA-15-NaCl. Under *pseudo*-reaction conditions with (b)  $B(OH)_3$  (c) KBr and (d) No additive.



**Figure 5-4:** X-Ray Diffraction (XRD) to determine long range order. SBA-15-NaCl (a) and after *pseudo*-conditions in the presence of (b)  $B(OH)_3$  and (c) KBr.



#### 5.2.4 Elucidation of the Mechanism of Boric Acid Protection

Two possible explanations were considered for the stabilizing effect of boric acid on the material mesostructure. Firstly, the boron could be integrating itself into the condensed silica structure,<sup>13,14</sup> especially in areas of the network where attack by aqueous base would present surface silanols and previously internal siloxanes. Alternatively, the boric acid could simply be buffering the aqueous base in solution, tempering the destructive effect of hydroxide on the condensed silica network. The latter hypothesis was tested by recording pH measurements throughout the course of a new set of *pseudo*-reaction studies, with and without the addition of B(OH)<sub>3</sub>. As pH measurements in 20:1 DMF:H<sub>2</sub>O are not comparable to aqueous pH readings, reaction aliquots were taken and diluted ten-fold in distilled water before recording a calibrated pH measurement. The pH was then back-calculated to account for the dilution step.

Once again, SBA-15-NaCl was subjected to the harsh *pseudo*-reaction conditions and pH measurements of aliquots of known volume were taken hourly (Table 5-1). Not surprisingly, the reaction solution was found to be strongly basic, though, interestingly, the pH drops significantly towards the end of the 4 h study. As expected, the material was subsequently found to be completely degraded. Taken together, these results indicate that aqueous base destroys the ordered silica framework, but in so doing, hydroxide becomes incorporated in newly formed silanols and, eventually, the pH of the solution drops.

**Table 5-1:** pH of solution during *pseudo*-reaction (left) and in the presence of B(OH)<sub>3</sub> (centre). The material from the latter experiment was re-subjected to *pseudo*-conditions and the pH was recorded (right).

Time	Pseudo	First Pseudo + B(OH) <sub>3</sub>	Second Pseudo
0.5	9.5	7.5	7
1	9.5	7.4	7
2	9.4	7.2	7.7
3	8.5	-	7.6
4	8.1	7.3	7

When the same experiment is conducted in the presence of an equimolar equivalent of B(OH)<sub>3</sub> to K<sub>2</sub>CO<sub>3</sub>, the pH of the solution is reproducibly much lower than in the previous case and even after 8 h, no sudden drop in pH is observed. Consistent with previous work, the material from this experiment completely maintained its mesoporosity.

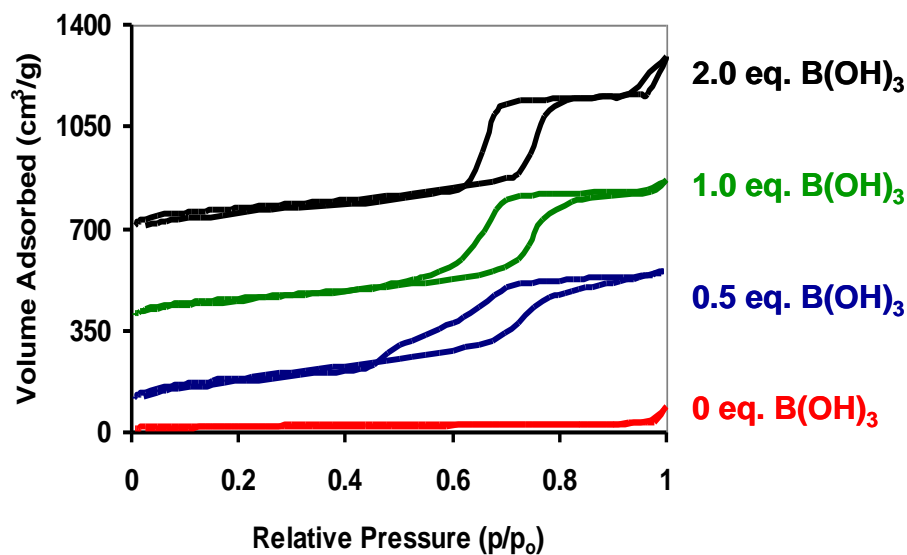
It is reasonable to say then that the boric acid produced in a Suzuki-Miyaura reaction effectively lowers the pH of the solution and mitigates the strong destructive effect of aqueous base on the material. However, at this point, boron incorporation into the silica network could still not be ruled out. To address this issue, we subjected the siliceous material SBA-15-NaCl to *pseudo*-reaction conditions for 4 h in the presence of B(OH)<sub>3</sub>. As expected, the pH of the solution was significantly lower than in the absence

of boric acid and the mesoporous material emerged completely intact. In the event that  $B(OH)_3$  is stabilizing the material (at least in part) through boron incorporation into the silica network, then a legacy stabilizing effect should exist when the same material is re-subjected to harsh conditions. In actual practice, this material performed no differently than a fresh batch of SBA-15-NaCl under *pseudo*-reaction conditions and completely lost its mesoporosity. In addition, we examined the solid-state  $^{11}B$  NMR of treated materials and found no evidence of boron incorporation above that seen in the background of the glass probe

### 5.3 Alumina-Doped Mesoporous Silicas

#### 5.3.1 Stabilizing Effect of Alumina

Since the effect of boric acid is concentration dependent, reactions that quickly attain high conversion of the organic substrates (producing boric acid as a side product) will result in greater material stability. This stabilizing effect is time-dependent and therefore material degradation can (and does) still occur in the early stages of a reaction before the substrate begins to react. To test this hypothesis, we subjected SBA-15-NaCl to *pseudo* reaction conditions (hot aqueous base but no substrate) and added varying amounts of boric acid. As can be seen in Figure 5-5, stability increases as the concentration of boric acid increases.



**Figure 5-5:**  $N_2$  isotherms of SBA-15-NaCl subjected to *pseudo*-reaction conditions and increasing amounts of  $B(OH)_3$ .

Rather than relying on the production of boric acid from the reaction, a more effective stabilizing strategy would be one where the protective effect would be intrinsic to the material itself, protecting the silica network from the outset. With this in mind, we investigated the stabilizing effect of alumina-doped mesoporous silicas. The hydrothermal stability of aluminum-containing materials has received significant attention due to the interest in preparing mesoporous materials with high-acidity for cracking applications.<sup>15, 16</sup> Al-doped mesoporous materials have been reported to have remarkable stability under hydrothermal conditions (300 h in boiling water and 6 h of steaming at 600 °C),<sup>12</sup> however stability to aqueous base had not been examined prior to our work. Though turning to alumina-doping as a stabilizing approach may seem to be counter-intuitive after the inconclusive results obtained from the *boron* incorporation

studies, two points are worthy of note. Firstly, we were unable to show that boron had ever incorporated into the silica network in the first place, foregoing any stabilizing effect and secondly, even if it had, it would have been limited to the outer layers of the network. In order to incorporate aluminum fully in the material, we planned to add Al salts during the preparation of the material to ensure its dispersion throughout the entire network.

Several rationales have been proposed for the stabilizing effect of aluminum.<sup>17</sup> When incorporated into the walls of mesoporous materials, so-called “structural Al” decreases the overall order of the material,<sup>18</sup> making it thermodynamically more stable. Additionally, since structural Al is tetra-coordinated, it imparts an anionic character to the aluminosilicate wall, protecting the surface from attack by hydroxide,<sup>19, 20</sup> which is the starting point for degradation by hydrolysis of Si-O-Si bonds.<sup>21</sup> Even extra-framework, octahedral Al is proposed to have a protective effect, by reacting with surface silanols, protecting them and the reactive siloxane bridges from attack by base. Shen and Kawi demonstrated this conclusively by coating the surface of pre-formed all-silica MCM-41 with Al<sub>2</sub>O<sub>3</sub>, which resulted in a material that retained high surface area after one week in boiling water.<sup>22</sup>

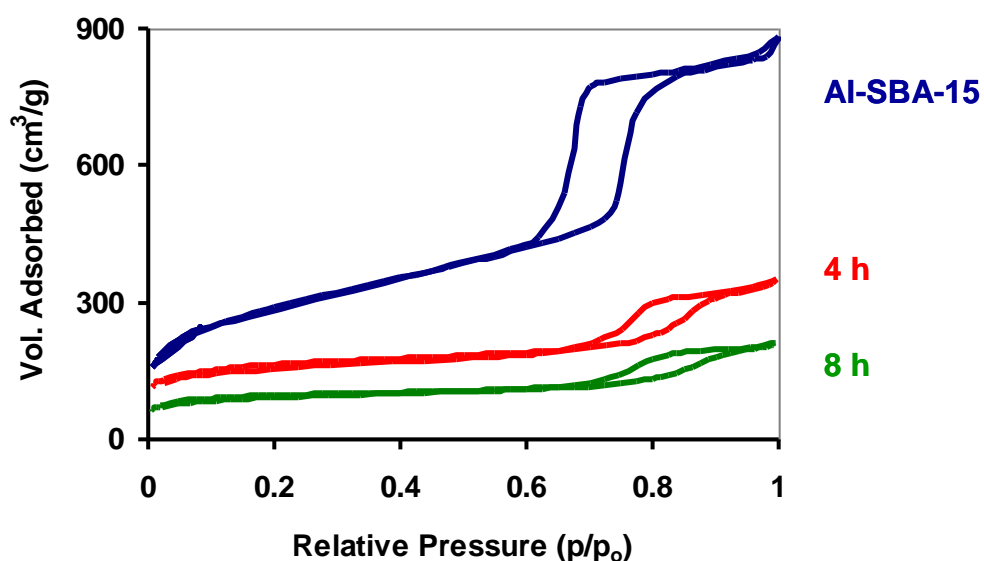
### 5.3.2 Stability of Alumina-Doped Silica to Reaction Conditions

Aluminum-doped SBA-15<sup>23</sup> was initially prepared following the method of Li *et al.*<sup>12</sup> in the hope that it would show resistance to aqueous base. Li had shown that the stability of the material prepared by incorporating Al during materials synthesis depended

strongly on both the temperature and the pH of the mother liquor during hydrothermal treatment, with the sturdiest materials being prepared at pH 5 and temperatures in excess of 100 °C. Using these conditions, we prepared aluminum-doped ordered materials, which will be designated Al-SBA-15. The presence of a large signal at 52 ppm in the <sup>27</sup>Al NMR of the doped materials indicates that aluminum was primarily incorporated into the network in a tetrahedral arrangement, bound to four silicon centers through siloxane bonds.<sup>24</sup> The broadness of this signal, however, makes it difficult to rule out the presence of small amounts of extra-framework octahedral aluminum. Interestingly, during exposure to the *pseudo*-reaction conditions, the tetrahedral form of aluminum becomes more prevalent, indicating that the extra-framework Al is either being removed from the material, or incorporated during the reorganization of the silicate wall structure (Appendix).

The stability of the first wave of Al-SBA-15 materials was assessed by way of the standard *pseudo*-reaction conditions, developed to emulate the Suzuki-Miyaura reaction. We were extremely pleased to note that some batches of Al-SBA-15 were completely resistant to structural collapse under these conditions for over 24 h, though the irreproducibility of this result required a more thorough examination of synthetic procedures. In the end, well over a dozen mesoporous materials were synthesized and tested for their stability, which allowed for the painstaking determination of which factors were critical to obtain sturdy materials. Chief among them were that the pH needed to be closely monitored, NaCl should not be added and aluminum ought to be added prior to the hydrothermal process and not during a post-synthetic process. Once fully appreciated,

these synthetic parameters were used to prepare materials that were reproducibly more stable to the *pseudo*-reaction conditions than purely siliceous SBA-15. Though the material is clearly undergoing restructuring and losing mesoporosity over time (Figure 5-6), the fact that *any* mesoporosity is maintained after 4 and even 8 h under these conditions contrasts it quite favorably to all other materials tested to this point. That Al-SBA-15 is able to protect *itself* at least partially from aqueous base augured well for its use as a support in an actual reaction where the stabilizing effect of the reaction would also come into play.



**Figure 5-6:** Al-SBA-15 (top) subjected to *pseudo*-reaction conditions for 4 h (middle) and 8 h (bottom).

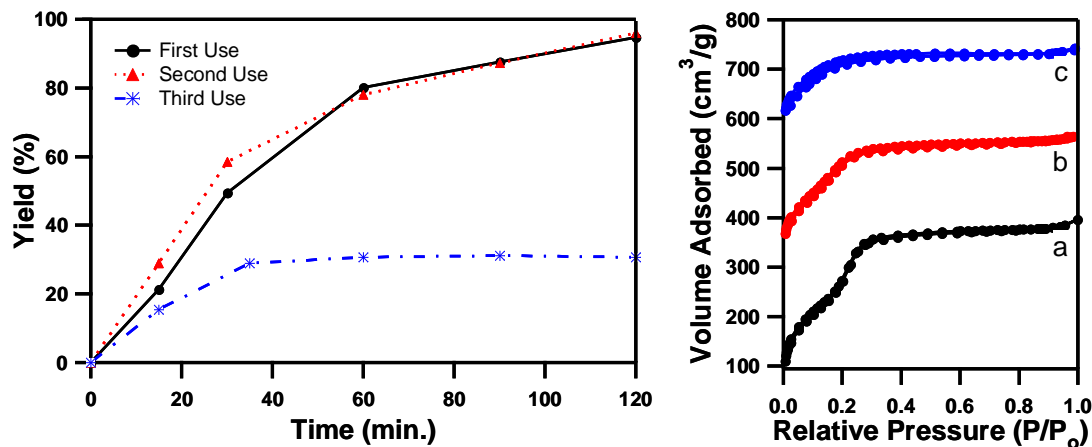
#### 5.4 Pd Catalysis on Mesoporous Supports

#### 5.4.1 MCM-41 Pd Catalysts

With wall thicknesses of only  $\sim 10$  Å, and short lifetimes demonstrated in the *pseudo*-reaction studies, thiol-functionalized MCM-41 Pd catalysts (henceforth MCM-41-SH•Pd) were not expected to be highly reusable catalysts. Near quantitative conversions for the first two cycles (Figure 5-7) indicated that catalysis is not limited by the smaller pore size of MCM-41 materials, though a sudden loss of activity is observed during the third run. Examination of the material's structural integrity over time (Figure 5-7) indicated that the MCM-41-SH Pd catalyst underwent almost complete degradation after less than 5 h of use in the Suzuki-Miyaura reaction. Thus in the case of MCM-41, the stabilizing effect of boric acid produced during the reaction is unable to overcome the fragility of the thin walls. The most interesting fact gleaned from this study was that in all cases, *the loss of activity occurred concurrently with the loss of order*. This demonstrates that maintaining the ordered nature of the support is critical for the activity of this family of catalysts. Interestingly, our group has previously shown that active catalysts can be made with amorphous silica<sup>6</sup> and therefore mesoporosity and long-range order are not necessary *per se* for catalysis in Pd-silicate materials. However, it appears that loss of order in a previously mesoporous support results in a complete loss of catalytic activity, likely by trapping active Pd species in the collapsed pore structure. Two possible explanations are consistent with these findings: either catalysis is occurring within the pores, or the reaction occurs outside the mesostructure but Pd has to mobilize into



solution. In any case, the pore structure, and specifically the Pd found within it, has to be accessible to the bulk solution for catalysis to occur.



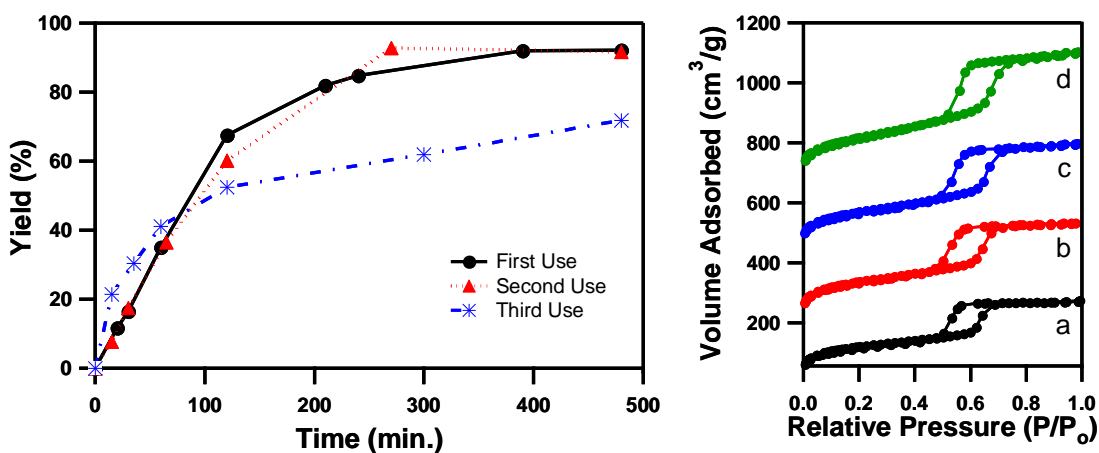
**Figure 5-7:** Yields (left) and corresponding N<sub>2</sub> isotherms (right) of pristine catalyst (a), and after one (b) and three (c) uses.

Various methods have been described to improve the hydrothermal stability of MCM-41, including hydrothermal restructuring,<sup>9</sup> the addition of inorganic salts during the synthesis,<sup>9, 25</sup> and doping alumina into the material (*vide supra*). The effect of hydrothermally treating MCM-41 after silica condensation (H<sub>x</sub> MCM-41-SH•Pd, 0.77 mmol S/g material) was examined initially. Although the catalyst showed similar activity in the Suzuki-Miyaura coupling, hydrothermal treatment did not afford an increase in stability over the course of multiple uses. Materials with higher thiol content were also prepared (MCM-41-xSH•Pd, 1.50 mmol S/g material) in the hope that the increased organic functionality would protect the surface by rendering it more hydrophobic.<sup>26</sup>

Again, only slight improvements of the material stability were observed. Although we were pleased that MCM-41 type catalysts were able to catalyze the Suzuki-Miyaura reaction and, to an extent, be recycled, we realized that they were not viable solutions for long-term use and so focused our attention on the thicker walled SBA-15 family of materials.

#### 5.4.2 SBA-15 Pd Catalysts

When coupled with the stabilizing effect of boric acid, the substantially thicker walls of SBA-15 were expected to better withstand the harsh reaction conditions than MCM-41 based materials. Granted, the *pseudo*-reaction studies indicated that Al-SBA-15-based materials should last even longer, though it was important to perform a recycle study on the purely siliceous SBA-15 support first as a means of comparison. In the event, SBA-15-SH•Pd (0.62 mmol S/g material) remained ordered and catalytically active for a considerably longer time than its MCM-41-based counterpart, as expected. As shown in Figure 5-8, the catalyst retains virtually all its order after three runs, corresponding to a total of 24 h, although a slight drop in catalytic activity is observed in the last run.

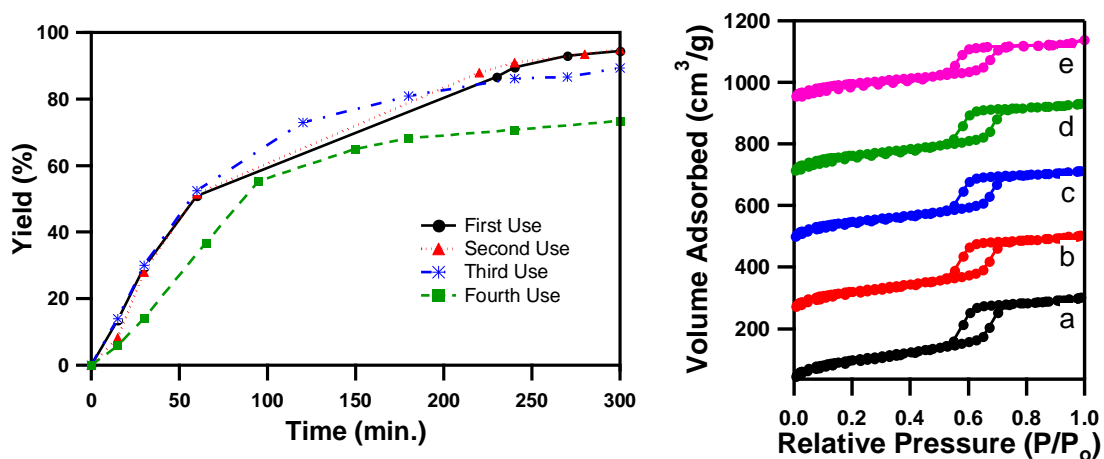


**Figure 5-8:** Yield and corresponding N<sub>2</sub> isotherms for (a) SBA-15-SH Pd and three consecutive uses (b-d) in the Suzuki-Miyaura reaction.

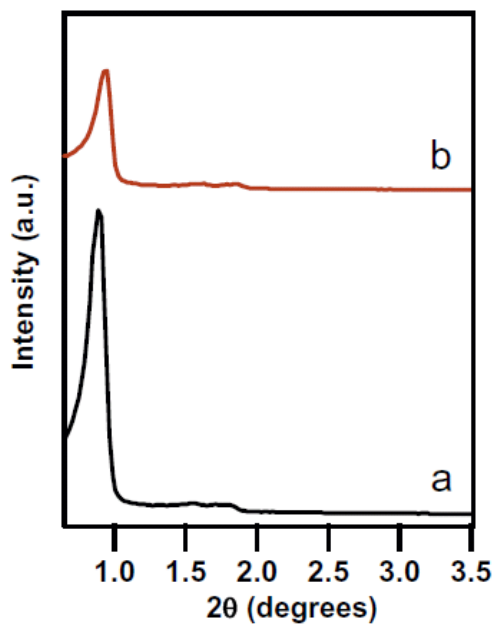
#### 5.4.3 Al-SBA-15 Pd Catalysts

As unfunctionalized Al-SBA-15 materials had shown very promising stabilities to aqueous base during the *pseudo*-reaction studies, we were optimistic that it would serve as a rugged support for Pd catalysis. Indeed, an Al-SBA-15-SH•Pd material prepared with 1.79 mmol S/g also remained well ordered over 20 h of Suzuki reaction time and, unlike the SBA-15-SH•Pd catalysts, retained full catalytic activity, within error, throughout the course of the entire recycle sequence (Figure 5-9). Examination of the material by TEM (Figures 5-11 and 5-12) showed that the Al-SBA-15-SH•Pd catalyst is still highly ordered after 20 h of use. XRD analysis of a second series of recycles confirms that the long range order of the material is maintained after three catalyst uses,

although the intensity of the 100 signal is decreased compared with pristine material (Figure 5-10).

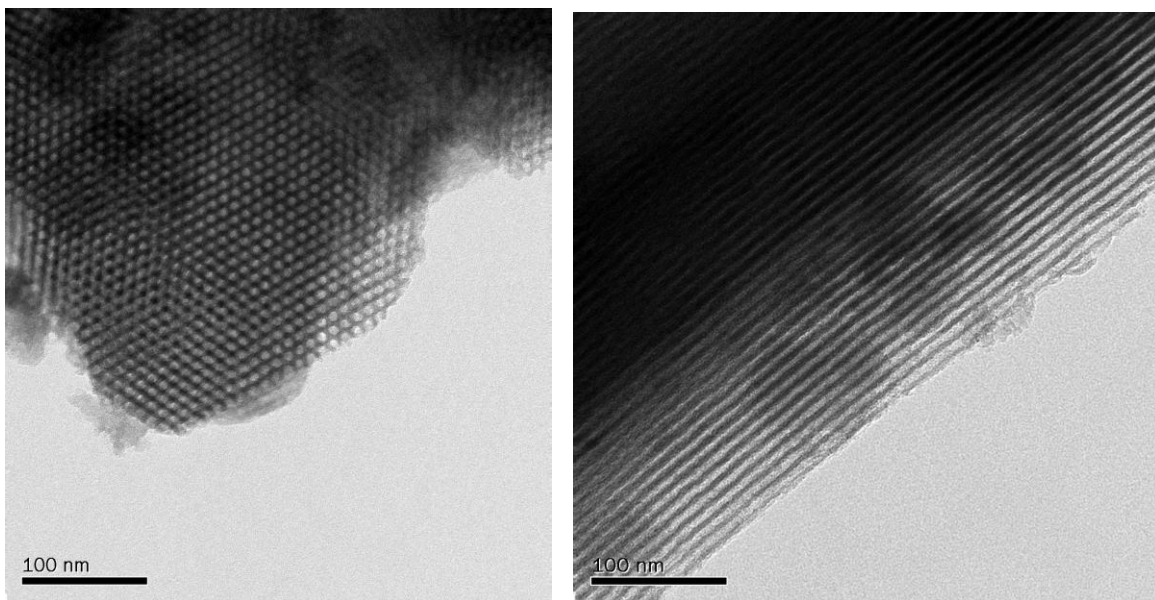


**Figure 5-9:** Yield (left) and N<sub>2</sub> isotherms (right) for pristine Al-SBA-15-SH Pd catalyst (a) and four consecutive uses (b-e).

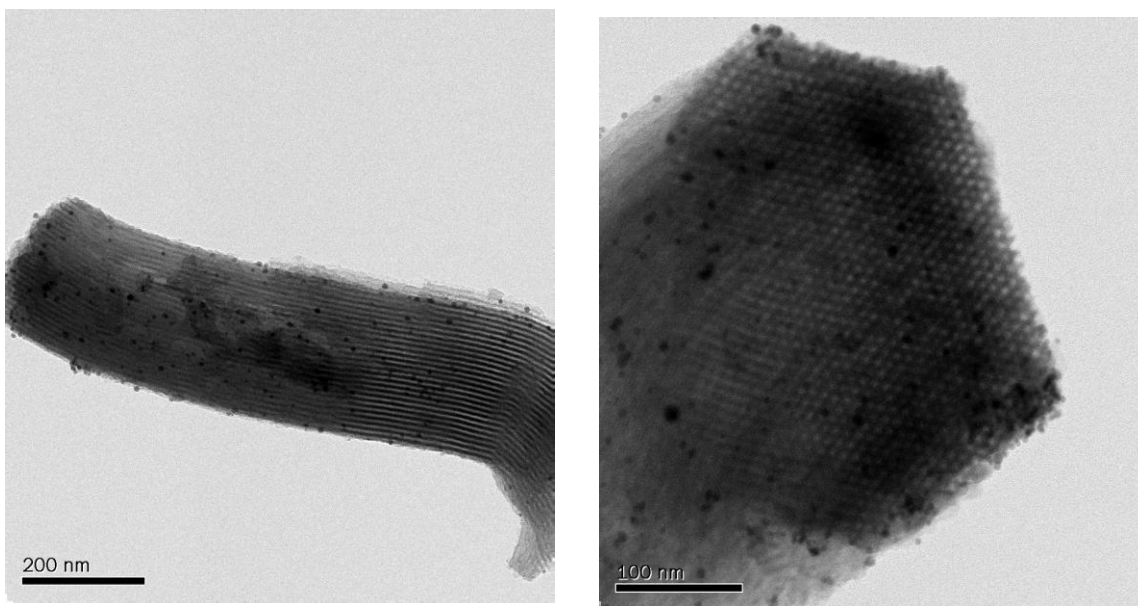


**Figure 5-10:** XRD pattern of pristine Al-SBA-15-SH-Pd and (b) after 3 uses totalling 15 h reaction time.

The observation of Pd nanoparticles by TEM, seen as dark spots primarily in the pores of the material and occasionally on the exterior, is consistent with our previous studies of SBA-15-SH•Pd. It is these nanoparticles, or rather their small size, which justify the use of mesoporous silica as a Pd support used in catalysis over the cheaper, more easily prepared, amorphous silica. Aggregation of Pd into large nanoparticles lowers reactivity by confining most of the catalytic amount of metal to the interior of the nanoparticle, and thus rendering it inaccessible to the bulk solution. TEM analysis indicates that not only is the vast majority of Pd being kept within the pores of these mesoporous materials, but that the relatively small pore size, and tight pore size distribution limit the size of the nanoparticles. These small nanoparticles with high surface areas may be the key to the prolonged activity of these catalysts.



**Figure 5-11:** TEM images of pristine Al-SBA-15-SH Pd catalyst prior to use.



**Figure 5-12:** TEM images of Al-SBA-15-SH Pd catalyst after four recycles totaling 20 h of use. Note the maintained ordered mesoposity and the Pd nanoparticles.

Another impressive facet of Al-SBA-15-SH•Pd is its ability to catalyze large scale reactions. In fact, this type of supported catalyst consistently brought gram-scale reactions to completion and in the course of one recycle study, one batch of catalyst cross-coupled nearly 4 g of bromoacetophenone with phenyl boronic acid pinacolate ester. The catalyst is also able to achieve high turnover numbers in a single reaction; 4.6 mg of Al-SBA-15-SH•Pd (0.1 mol% Pd) was able to convert a 4 mmol scale reaction to completion, translating to around 1000 turnovers.

#### *5.4.4 Pd Leaching with Al-SBA-15 Catalysts*

What makes these Pd loaded, thiol-functionalized mesoporous silicas unique is their ability to catalyze consecutive reactions without leaching their toxic<sup>27</sup> metal cargo into a product that may be destined for human consumption. Therefore, any improvement in the stability of these catalyst supports would be for naught should this new scaffold cause an unexpected rise in metal leaching. Gratifyingly, Al-SBA-15-SH•Pd catalyzed a simple Suzuki-Miyaura reaction to completion and, after filtration, retained 99.98% of its Pd. This staggeringly low level of leaching is, if anything, better than that reported with SBA-15 based catalysts.

## **5.5 Conclusions**

It has only been in the last decade that functionalized mesoporous silicas have been used as heterogeneous supports for catalysis, and only very recently that the true nature of this catalysis has been understood. The present study sought to shed light on the mechanism of material degradation under Suzuki-Miyaura reaction conditions. In addition to demonstrating how the materials were degrading, our study led to an understanding of the protective nature of the reaction itself, by way of the boric acid produced *in situ*. It appears likely that the boric acid serves to mitigate the destructive effect that aqueous base has on the condensed silica structure of the material primarily by acting as a buffer, though the occurrence, and effect of boron incorporation into the network needs further elaboration.

Seeking to make a robust material that did not rely on this protective effect for its survival we synthesized an alumina-doped SBA-15 analogue which fared better under the *pseudo*-reaction conditions than authentic SBA-15. When loaded with Pd, the thiol-functionalized Al-SBA-15 performed well, effectively catalyzing the Suzuki-Miyaura reaction over the course of multiple recycles while maintaining its mesoporosity and, importantly, keeping hold of almost *all* of the Pd entrusted to it.

## 5.6 References

(1) Crudden, C. M.; Sateesh, M.; Lewis, R. Mercaptopropyl-Modified Mesoporous Silica: A Remarkable Support for the Preparation of a Reusable, Heterogeneous Palladium Catalyst for Coupling Reactions. *J. Am. Chem. Soc.* **2005**, 127, 10045-10050.



- (2) Shimizu, K.; Maruyama, R.; Komai, S.; Kodama, T.; Kitayama, Y. Pd-sepiolite catalyst for Suzuki coupling reaction in water: Structural and catalytic investigations. *J. Catal.* **2004**, 227, 202-209.
- (3) Glasspoole, B. W.; Webb, J. D.; Crudden, C. M. Catalysis with chemically modified mesoporous silicas: Stability of the mesostructure under Suzuki-Miyaura reaction conditions. *J. Catal.* **2009**, 265, 148-154.
- (4) Phan, N. T. S.; van der Sluys, M.; Jones, C. J. On the Nature of the Active Species in Palladium-Catalyzed Mizoroki-Heck and Suzuki-Miyaura Couplings- Homogeneous or Heterogeneous Catalysts, A Critical Review. *Adv. Synth. Catal.* **2006**, 348, 679.
- (5) Richardson, J. M.; Jones, C. W. Strong evidence of solution-phase catalysis associated with palladium leaching from immobilized thiols during Heck and Suzuki coupling of aryl iodides, bromides, and chlorides. *J. Catal.* **2007**, 251, 80-93.
- (6) Webb, J. D.; MacQuarrie, S.; McEleney, K.; Crudden, C. M. Mesoporous silica-supported Pd catalysts: An investigation into structure, activity, leaching and heterogeneity. *J. Catal.* **2007**, 252, 97-109.
- (7) Zhao, D.; Huo, Q.; Feng, J.; Chmelka, B. F.; Stucky, G. D. Nonionic Triblock and Star Diblock Copolymer and Oligomeric Surfactant Syntheses of Highly Ordered, Hydrothermally Stable, Mesoporous Silica Structures. *J. Am. Chem. Soc.* **1998**, 120, 6024-6036.
- (8) Shimizu, K.; Koizumi, S.; Hatamachi, T.; Yoshida, H.; Komai, S.; Kodama, T.; Kitayama, Y. Structural investigations of functionalized mesoporous silica-supported palladium catalyst for Heck and Suzuki coupling reactions. *J. Catal.* **2004**, 228, 141-151.
- (9) Ryoo, R.; Jun, S. Improvement of Hydrothermal Stability of MCM-41 Using Salt Effects during the Crystallization Process. *J. Phys. Chem. B.* **1997**, 101, 317-320.

- (10) Brinker, C. J.; Scherer, G. W. *Sol-Gel Science: The Physics and Chemistry of Sol-Gel Processing*; Academic Press: 1989; pp 908.
- (11) Luo, Y.; Hou, Z.; Li, R.; Zheng, X. Synthesis of ultrastable ordered mesoporous aluminosilicates molecular sieves with “hard template”. *Microporous Mesopor. Mater.* **2008**, 110, 583-589.
- (12) Li, C.; Wang, Y.; Guo, Y.; Liu, X.; Guo, Y.; Zhang, Z.; Wang, Y.; Lu, G. Synthesis of Highly Ordered, Extremely Hydrothermal stable SBA-15/Al-SBA-15 under the Assistance of Sodium Chloride. *Chem. Mater.* **2007**, 19, 173-178.
- (13) Sayari, A.; Danumah, C.; Moudrakovski, I. L. Boron-Modified MCM-41 Mesoporous Molecular Sieves. *Chem. Mater.* **1995**, 7, 813-815.
- (14) Sayari, A.; Moudrakovski, I.; Danumah, C.; Ratcliffe, C. I.; Ripmeester, J. A.; Preston, K. F. Synthesis and Nuclear Magnetic Resonance Study of Boron-Modified MCM-41 Mesoporous Materials. *J. Phys. Chem.* **1995**, 99, 16373-16379.
- (15) Lourenço, J. P.; Fernandes, A.; Henriques, C.; Ribeiro, M. F. Al-containing MCM-41 type materials prepared by different synthesis methods: Hydrothermal stability and catalytic properties. *Microporous Mesopor. Mater.* **2006**, 94, 56-65.
- (16) Yue, Y.; Gedeon, A.; Bonardet, J.; D'Espinose, J.; Fraissard, J.; Melosh, N. Direct synthesis of Al-SBA mesoporous molecular sieves: characterization and catalytic activities. *Chem. Commun.* **1999**, 1967-1968.
- (17) Shen, S.; Kawi, S. Understanding of the Effect of Al Substitution on the Hydrothermal Stability of MCM-41. *J. Phys. Chem. B.* **1999**, 103, 8870-8876.
- (18) Luan, Z.; Cheng, C.; Zhou, W.; Klinowski, J. Mesopore Molecular Sieve MCM-41 Containing Framework Aluminum. *J. Phys. Chem.* **1995**, 99, 1018-1024.
- (19) Russo, P. A.; Ribeiro Carrott, M. M. L.; Padre-Eterno, A.; Carrott, P. J. M.; Ravikovitch, P. I.; Neimark, A. V. Interaction of water vapour at 298 K with Al-MCM-41

materials synthesised at room temperature. *Microporous Mesopor. Mater.* **2007**, 103, 82-93.

(20) Lutz, W.; Gessner, W.; Bertram, R.; Pitsch, I.; Fricke, R. Hydrothermally resistant high-silica Y zeolites stabilized by covering with non-framework aluminum species. *Microporous Mater.* **1997**, 12, 131-139.

(21) Kim, J. M.; Ryoo, R. Disintegration of Mesoporous Structures of MCM-41 and MCM-48 in Water. *Bull. Korean Chem. Soc.* **1996**, 17, 66-68.

(22) Shen, S.; Kawi, S. Understanding of the Effect of Al Substitution on the Hydrothermal Stability of MCM-41. *J. Phys. Chem. B.* **1999**, 103, 8870-8876.

(23) Luan, Z.; Hartmann, M.; Zhao, D.; Zhou, W.; Kevan, L. Alumination and Ion Exchange of Mesoporous SBA-15 Molecular Sieves. *Chem. Mater.* **1999**, 11, 1621-1627.

(24) Shen, S. C.; Kawi, S. MCM-41 with Improved Hydrothermal Stability: Formation and Prevention of Al Content Dependent Structural Defects. *Langmuir* **2002**, 18, 4720-4728.

(25) Das, D.; Tsai, C.; Cheng, S. Improvement of hydrothermal stability of MCM-41 mesoporous molecular sieve. *Chem. Commun.* **1999**, 473-474.

(26) Koyano, K. A.; Tatsumi, T.; Tanaka, Y.; Nakata, S. Stabilization of Mesoporous Molecular Sieves by Trimethylsilylation. *J. Phys. Chem. B.* **1997**, 101, 9436-9440.

(27) Ducoulombier-Crépineau, C.; Feidt, C.; Rychen, G. Platinum and Palladium transfer to milk, organs and tissues after a single oral administration to lactating goats. *Chemosphere* **2007**, 68, 712-715.

## Chapter 6

### Experimental Procedures

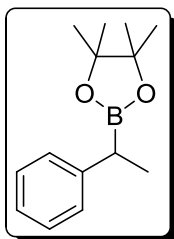
#### 6.1 Cross-Coupling of Benzylic Boronic Esters

##### 6.1.1 General Experimental Considerations

Unless otherwise noted, all reactions were performed under inert atmosphere using dried glassware. Solvents were dried by standard methods before being degassed by a minimum of three *freeze-pump-thaw* cycles and stored over 4 Å molecular sieves. Pinacol borane, catechol borane and styrene derivatives were distilled at reduced pressure and stored under inert atmosphere at -20 °C. Aryl halides were purified before use following accepted protocols,<sup>1</sup> Ag<sub>2</sub>O was purified by continuous hot water extraction in a Soxhlet condenser over three days and dried under vacuum in the presence of P<sub>2</sub>O<sub>5</sub>. Both Pd<sub>2</sub>(dba)<sub>3</sub> and Pd(PPh<sub>3</sub>)<sub>4</sub> were used as purchased from Aldrich and Strem, respectively. PPh<sub>3</sub> was purified by recrystallization from absolute ethanol. Cross-coupling reactions were assembled in the glovebox in 4-dram vials, sealed with air-tight Teflon caps and placed in an 85 °C oil bath for 24 h (aryl iodides) or 48 h (aryl bromides). Once cooled, the reactions were filtered through celite, washed with copious amounts of diethyl ether and hexanes and concentrated *in vacuo*. Crude yields were determined by gas chromatography (GC) with an internal standard (octadecane) and a calibration curve or

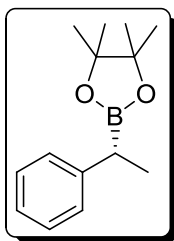
by NMR with hexamethylbenzene (HMB) or dimethoxybenzene (DMB) serving as internal standards. NMR spectra were recorded at 400 MHz ( $^1\text{H}$ ), and 100 MHz ( $^{13}\text{C}$ ) in  $\text{CDCl}_3$ . GC analyses were performed on an HP 6850 network FID-GC with automatic injector. The column used was an HP-5 of 30 m in length with an internal diameter of 0.32 mm. The inlet conditions were 250 °C, 25 psi and a flow rate of 28.9 ml/min using a splitless injector with helium as the carrier gas. The method used had an initial temperature of 70 °C with an immediate increase to 240 °C using a 6 °/min ramp. Thin Layer Chromatography was performed on aluminum backed silica plates with F-254 indicator. Visualization was accomplished with a UV source (254, 365 nm) and by treatment with phosphomolybdic acid. Column chromatography was performed with flash grade silica (Silicycle, 50  $\mu\text{m}$  particle size, 60 Å porosity) and reagent grade solvents. Determination of stereochemistry was performed by analysis on a supercritical fluid chromatograph. Analytical supercritical fluid chromatography (SFC) was performed on a Berger SFC HPLC using the specified chiracel Berger Silica column and specified conditions of co-eluent, flow rate and pressure.

### 6.1.2 Synthesis of benzylic boronic ester cross-coupling partners



**Synthesis of *rac*-pinacol(1-phenylethyl)boronate (2-5).** In a nitrogen-filled glovebox, styrene (746 mg, 7.16 mmol) and pinacol borane

(HBPIn, 1.12 g, 8.73 mmol) were added to a THF solution of preformed [Rh(COD)(dppb)] [BF<sub>4</sub>] (50.42 mg, 0.07 mmol, 1 mol %) in a dried vial. The reaction solution was sealed and stirred at box temperature for 3 d. The desired product was isolated in 92% yield by flash chromatography (40:1-20:1 hexanes:ethyl acetate). GC and NMR analyses indicated the branched to linear ratio of the hydroborated products to be 98.5:1.5. <sup>1</sup>H NMR: (400 MHz, CDCl<sub>3</sub>): δ 7.21-7.14 (m, 4 H), δ 7.07-7.04 (m, 1 H), 2.36 (q, *J* = 7.5, 1 H), 1.25 (d, *J* = 7.5, 3 H), 1.14 (s, 6 H), 1.13 (s, 6 H). <sup>11</sup>B NMR: (160 MHz, CDCl<sub>3</sub>): δ 33.4. <sup>13</sup>C NMR: (100 MHz, CDCl<sub>3</sub>): δ 145.0, 128.3, 127.8, 125.1, 88.3, 24.63, 24.59, 17.1



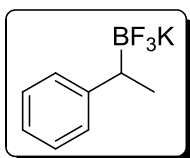
**Synthesis of (*R*)-pinacol(1-phenylethyl)boronate via asymmetric hydroboration ((*R*)-2-5).** In a nitrogen filled glovebox, [Rh(COD)-<sub>2</sub>][BF<sub>4</sub>] (23.1 mg, 0.057 mmol) and (*R*)-BINAP (42.3 mg, 0.068 mmol) were taken up in dimethoxyethane (DME, 4 mL) and stirred in a dried Schlenk tube. After 10 min, freshly distilled styrene (273 mg, 2.62 mmol) was added to yield a bright orange solution. In a dried 25 mL RBF, catechol borane (HBCat, 415 mg, 3.46 mmol) was taken up in 2 mL of DME. Both solutions were removed from the glovebox and cooled to -78 °C. The HBCat solution was transferred via cannula to the solution of styrene and Rh<sup>+</sup> catalyst. After 5 h of stirring at temperatures below -69 °C, solid pinacol (1.02 g, 8.63 mmol) was added and the tube was quickly purged with Ar<sub>(g)</sub>. Purification by column chromatography (20:1 hexanes: ethyl acetate) yielded the desired product in 65% yield with a branched to linear ratio of 99:1 by GC. The product had an

enantiomeric ratio of 92:8, as determined by SFC chromatography after oxidation of the boronic ester to the corresponding alcohol. This is accomplished by adding a deoxygenated, 2:1 v/v mixture of 1 M NaOH / H<sub>2</sub>O<sub>2</sub> (30% aq.) to a stirring, THF solution of the boronic ester at 0 °C for 1 h. (Column OD-H, 5% MeOH, 2 mL, 200 bar).

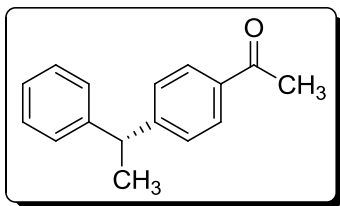
**Synthesis of enantioenriched benzylic boronic ester via asymmetric lithiation-borylation.** *N,N*-diisopropyl ethylcarbamate (1.229 g, 163.7 g/mol, 7.104 mmol) and (-)-sparteine (2.089 g, 8.912 mmol) were taken up in freshly distilled diethyl ether (25 mL) and the solution was cooled to -78 °C with a dry ice/acetone bath. While keeping the internal temperature below -73 °C, *s*-BuLi (7.2 mL, 1.3M) was added under vigorous stirring. After 4.5 h lithiation at low temperature, a solution of phenylboronic acid pinacolate ester (PhBPin, 1.579 g, 7.740 mmol in 5 mL diethyl ether) was added dropwise, keeping the internal temperature below -70 °C. After 0.5 h borylation, a three-fold excess of freshly prepared MgBr<sub>2</sub> diethyletherate was added and the reaction was allowed to warm to room temperature before being subjected to reflux conditions for 16 h. The crude reaction mixture was washed (2x50 mL NH<sub>4</sub>Cl<sub>(sat.)</sub>) and the combined aqueous layers were washed with 3x50 mL diethyl ether. The combined organic layers were then concentrated *in vacuo* and purified *via* column chromatography (25:1 hexanes:diethyl ether) to give a 47% isolated yield of the desired product. The enantiomeric ratio of the secondary boronic ester product was determined to be 98.7:1.3 after air-free stereoretentive oxidation to the corresponding alcohol. This is accomplished by adding a deoxygenated, 2:1 v/v mixture of 1 M NaOH / H<sub>2</sub>O<sub>2</sub> (30% aq.) to a stirring,

THF solution of the boronic ester at 0 °C for 1 h. (Column OD-H, 5% MeOH, 2 mL, 200 bar).

### 6.1.3 Synthesis of Enantioenriched 1,1-diarylethanes with Aryl Iodides



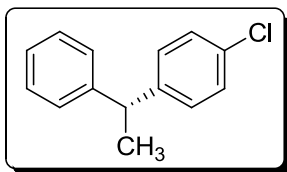
**Attempted Cross-Coupling of potassium (1-phenylethyl)trifluoroborate.** In a nitrogen-filled glovebox, 4-iodoacetophenone (12.93 mg, 245.9 g/mol, 0.053 mmol), potassium (1-phenylethyl)trifluoroborate salt (16.42 mg, 211.8 g/mol, 0.078 mmol), Ag<sub>2</sub>O (17.79 mg, 234 g/mol, 0.076 mmol), Pd<sub>2</sub>(dba)<sub>3</sub> (1.79 mg, 915 g/mol, 0.002 mmol, 7.4 mol% Pd), PPh<sub>3</sub> (8.79 mg, 262 g/mol, 0.034 mmol, 8.4:1 P:Pd) and 17.09 mg of *n*-octadecane (internal standard, 254 g/mol, 0.067 mmol) were added to a flame-dried Schlenk flask, to which 1.7 g of THF was added through a septum. Once removed from the glovebox, 0.1 mL of degassed H<sub>2</sub>O (Ar<sub>(g)</sub> bubbled through for 1 h.) was added through a septum and the flask was submerged in 75 °C oil for 24 h. The crude reaction was filtered through a celite plug and washed with copious amounts of diethyl ether and hexanes, though no cross-coupling product was observed by GC.



**Synthesis of (*R*)-1-phenyl-1-(4-acetylphenyl)ethane ((*R*)-2-6a).** In a nitrogen-filled glovebox, 4-iodoacetophenone (12.45 mg, 245.9 g/mol, 0.051 mmol), (*R*)-pinacol(1-phenylethyl)boronate (17.41 mg, 232 g/mol, 0.075 mmol, er = 93.3:6.7) Ag<sub>2</sub>O (17.68 mg,



232 g/mol, 0.076 mmol), Pd<sub>2</sub>(dba)<sub>3</sub> (1.186 mg, 915.7 g/mol, 0.0020 mmol, 8.1 mol% Pd), PPh<sub>3</sub> (8.54 mg, 262 g/mol, 0.033 mmol) were taken up in DME (1.0 mL). The reaction was sealed, and stirred at 85 °C for 24 h. The desired product was isolated by column chromatography (gradient 20:1 to 10:1 hexanes: ethyl acetate) in 63% yield. The enantiomeric ratio was determined by SFC analysis (AD-H Column, 5% MeOH, 2 mL, 200 bar) to be 91.5:8.5, a 98% retention of er. **<sup>1</sup>H NMR** (400 MHz, CDCl<sub>3</sub>) δ 7.90 (d, 2 H), 7.35-7.22 (m, 7 H) 4.23 (q, *J* = 7.2, 1 H), 2.59 (s, 3 H), 1.68 (d, *J* = 7.2, 3 H). **<sup>13</sup>C NMR**: (100 MHz, CDCl<sub>3</sub>): δ 197.8, 152.4, 146.0, 135.7, 128.9, 128.8, 128.1, 127.9, 126.7, 45.2, 26.8, 21.6. **HRMS (EI-TOF)**: calcd for [M]<sup>+</sup> (C<sub>16</sub>H<sub>16</sub>O) *m/z* 224.1201; found 224.1197.

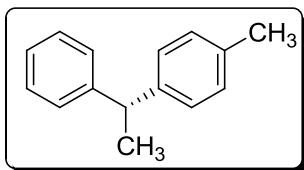


**Synthesis of (*R*)-1-phenyl-1-(4-chlorophenyl)ethane ((*R*)-2-**

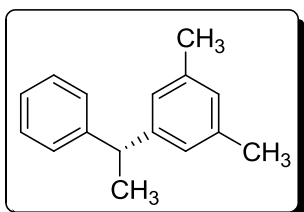
**6b)**. In a nitrogen-filled glove box, 4-chloriodobenzene (35.96 mg, 238.4 g/mol, 0.151 mmol), (*R*)-pinacol(1-

phenylethyl)boronate (51.20 mg, 232 g/mol, 0.221 mmol, er = 94:6), Ag<sub>2</sub>O (52.81 mg, 232 g/mol, 0.228 mmol), K<sub>2</sub>CO<sub>3</sub> (32.20 mg, 138 g/mol, 0.233 mmol), Pd(PPh<sub>3</sub>)<sub>4</sub> (13.82 mg, 1155.6, 0.0120 mmol) and PPh<sub>3</sub> (12.58 mg, 262 g/mol 0.0480 mmol) were weighed into a dried vial and taken up in 3 mL of DME. The reaction was sealed and stirred at 85 °C for 24 h. The reaction mixture was cooled and filtered through celite. The desired product was isolated by column chromatography (pentane) in a 75% yield. The enantiomeric ratio was determined by SFC (OD, 1% MeOH, 2 mL, 200 bar) to be 92.8:7.2, a 98.7% retention of er. **<sup>1</sup>H NMR** (400 MHz, CDCl<sub>3</sub>) δ 7.33-7.16 (m, 9 H), 4.15

(q,  $J = 7.2$  Hz, 1 H), 1.64 (d,  $J = 7.2$  Hz, 3 H).  $^{13}\text{C}$  NMR: (100 MHz,  $\text{CDCl}_3$ ):  $\delta$  145.94, 145.00, 131.87, 129.12, 128.60, 128.59, 127.66, 126.38, 44.32, 21.94. **HRMS (EI-TOF)**: calcd for  $[\text{M}]^+$  ( $\text{C}_{14}\text{H}_{13}\text{Cl}$ )  $m/z$  216.0706; found 216.0702.

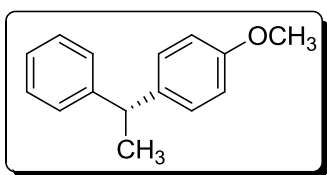


**Synthesis of (*R*)-1-phenyl-1-(4-methylphenyl)ethane ((*R*)-2-6c).** In a nitrogen filled glove box, *p*-iodotoluene (33.09 mg, 217.9 g/mol, 0.152 mmol), (*R*)-pinacol(1-phenylethyl)boronate (53.26 mg, 232 g/mol, 0.229 mmol, e.r 94:6),  $\text{Ag}_2\text{O}$  (52.66 mg, 232 g/mol, 0.227 mmol),  $\text{K}_2\text{CO}_3$  (32.68 mg, 138 g/mol, 0.237 mmol),  $\text{Pd}(\text{PPh}_3)_4$  (14.82 mg, 1155.6 g/mol, 0.0128 mmol) and  $\text{PPh}_3$  (12.56 mg, 262 g/mol, 0.0479 mmol) were weighed into a dried vial and taken up in 3 mL of DME. The reaction was sealed and stirred at 85 °C for 24 h. The reaction mixture was cooled and filtered through celite. The desired product was isolated by column chromatography (pentane) in a 60% isolated yield. The enantiomeric ratio was determined by SFC (OD, 1% MeOH, 2 mL, 200 bar) to be 93:7, a 99% retention of er.  $^1\text{H}$  NMR (400 MHz,  $\text{CDCl}_3$ )  $\delta$  7.29-7.07 (m, 9 H), 4.11 (q,  $J = 7.2$  Hz, 1 H), 2.30 (s, 3 H), 1.62 (d,  $J = 7.3$  Hz, 3 H)  $^{13}\text{C}$  NMR: (100 MHz,  $\text{CDCl}_3$ ):  $\delta$  148.57, 143.38, 135.46, 129.02, 128.31, 127.54, 127.46, 125.92, 44.35, 21.92, 20.99. **HRMS (EI-TOF)**: calcd for  $[\text{M}]^+$  ( $\text{C}_{15}\text{H}_{16}$ )  $m/z$  196.1252; found 196.1256.



**Synthesis of (*R*)-1-phenyl-1-(3,5-dimethylphenyl)ethane ((*R*)-2-6d).** In a nitrogen filled glove box, 3,5-

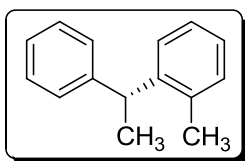
dimethyliodobenzene (32.58 mg, 234.9 g/mol, 0.140 mmol), (*R*)-pinacol(1-phenylethyl)boronate (53.47 mg, 232 g/mol, 0.230 mmol, e.r 94:6), Ag<sub>2</sub>O (52.01 mg, 234 g/mol, 0.224 mmol), K<sub>2</sub>CO<sub>3</sub> (31.11 mg, 138 g/mol, 0.225 mmol), Pd(PPh<sub>3</sub>)<sub>4</sub> (13.15 mg, 1155.6 g/mol, 0.0114 mmol) and PPh<sub>3</sub> (12.80 mg, 262 g/mol, 0.0488 mmol) were weighed into a dried vial and taken up in 3 mL of DME. The reaction was sealed and stirred at 85 °C for 24 h. The reaction mixture was cooled and filtered through celite. The desired product was isolated by column chromatography (50:1 Pentane:Et<sub>2</sub>O) in a 77% yield (containing ca. 10% homo-coupled). The isolated yield without potassium carbonate was 64% (<sup>1</sup>H NMR yield = 86%). The enantiomeric ratio was determined by SFC (OD, 1% <sup>i</sup>PrOH, 2 mL, 100 bar) to be 91.3:8.7, a 97% retention of er. **<sup>1</sup>H NMR** (400 MHz, CDCl<sub>3</sub>) δ 7.32-7.15 (m, 6 H), 6.83 (m, 3 H), 4.07 (q, *J* = 7.2 Hz, 1 H), 2.27 (s, 6 H), 1.61 (d, *J* = 7.2 Hz, 3 H). **<sup>13</sup>C NMR**: (100 MHz, CDCl<sub>3</sub>): δ 146.71, 146.42, 137.90, 128.45, 127.91, 127.86, 126.04, 125.59, 44.83, 22.05, 21.52. **HRMS (EI-TOF)**: calcd for [M]<sup>+</sup> (C<sub>16</sub>H<sub>18</sub>) *m/z* 210.1409; found 210.1402.



#### Synthesis of (*R*)-1-phenyl-1-(4-methoxyphenyl)ethane

**((*R*)-2-6e)**. In a nitrogen filled glove box, 4-iodoanisole (35.08 mg, 233.9 g/mol, 0.150 mmol), (*R*)-pinacol(1-phenylethyl)boronate (52.67 mg, 232 g/mol, 0.227 mmol, e.r 94:6), Ag<sub>2</sub>O (52.34 mg, 234 g/mol, 0.226 mmol), K<sub>2</sub>CO<sub>3</sub> (32.12 mg, 138 g/mol, 0.232 mmol), Pd(PPh<sub>3</sub>)<sub>4</sub> (13.55 mg, 1155.6 g/mol, 0.0117 mmol) and PPh<sub>3</sub> (12.33 mg, 262 g/mol, 0.0470 mmol) were weighed into a dried vial and taken up in 3 mL of DME. The reaction was sealed and

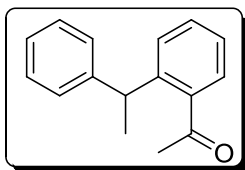
stirred at 85 °C for 24 h. The reaction mixture was cooled and filtered through celite. The desired product was isolated by column chromatography (50:1 Pentane:Et<sub>2</sub>O) in a 71% yield. The enantiomeric ratio was determined by SFC (OD, 1% MeOH, 2 mL, 200 bar) to be 93.1:6.9, a 99% retention of er. <sup>1</sup>H NMR (400 MHz, CDCl<sub>3</sub>) δ 7.34-7.17 (m, 7 H), 6.89-6.85 (m, 2 H), 4.15 (q, *J* = 7.2 Hz, 1 H), 3.82 (s, 3 H), 1.66 (d, *J* = 7.2 Hz, 3 H). <sup>13</sup>C NMR: (100 MHz, CDCl<sub>3</sub>): δ 157.94, 146.90, 138.68, 128.64, 128.47, 127.66, 126.06, 113.84, 55.37, 44.06, 22.20. HRMS (EI-TOF): calcd for [M]<sup>+</sup> (C<sub>15</sub>H<sub>16</sub>O) *m/z* 212.1201; found 212.1211.



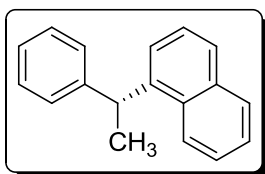
#### Synthesis of (*R*)-1-phenyl-1-(2-methylphenyl)ethane ((*R*)-2-6f).

In a nitrogen filled glove box, *o*-iodotoluene (31.20 mg, 217.9 g/mol, 0.143 mmol), (*R*)-pinacol(1-phenylethyl)boronate (50.15 mg, 232 g/mol, 0.216 mmol, e.r 94:6), Ag<sub>2</sub>O (51.21 mg, 234 g/mol, 0.221 mmol), K<sub>2</sub>CO<sub>3</sub> (30.40 mg, 138 g/mol, 0.220 mmol), Pd(PPh<sub>3</sub>)<sub>4</sub> (13.05 mg, 1155.6 g/mol, 0.0113 mmol) and PPh<sub>3</sub> (12.11 mg, 262 g/mol, 0.0462 mmol) were weighed into a dried vial and taken up in 3 mL of DME. The reaction was sealed and stirred at 85 °C for 24 h. The reaction mixture was cooled and filtered through celite. The desired product was isolated by column chromatography (50:1 Pentane:Et<sub>2</sub>O) in a 64% yield (containing ca. 8% homo-coupled product). The enantiomeric ratio was determined by SFC (OJ, 1.5% <sup>i</sup>PrOH, 2 mL, 200 bar) to be 89.9:10.1, a 96% retention of er. <sup>1</sup>H NMR (400 MHz, CDCl<sub>3</sub>) δ 7.31-7.15 (m, 9 H), 4.34 (q, *J* = 7.2 Hz, 1 H), 2.26 (s, 3 H), 1.63 (d, *J* = 7.2 Hz, 3 H). <sup>13</sup>C

**NMR:** (100 MHz, CDCl<sub>3</sub>):  $\delta$  146.35, 144.04, 136.23, 130.53, 128.43, 127.81, 126.80, 126.21, 126.15, 125.94, 41.13, 22.25, 19.90.



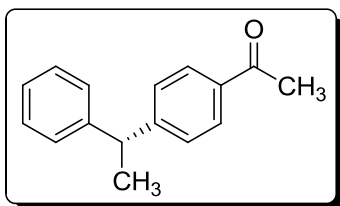
**Attempted synthesis of 1-phenyl-1-(2-acetylphenyl)ethane ((R)-2-6g).** In a nitrogen filled glove box, 2-iodoacetophenone (11.64 mg, 0.0473 mmol), *rac*-pinacol(1-phenylethyl)boronate (17.27 mg, 232 g/mol, 0.0744 mmol), Ag<sub>2</sub>O (17.30 mg, 234 g/mol, 0.0747 mmol), Pd<sub>2</sub>(dba)<sub>3</sub> (1.91 mg, 915 g/mol, 0.00209 mmol) and PPh<sub>3</sub> (9.24 mg, 262 g/mol, 0.0352 mmol) were weighed into a dried vial and taken up in 1 mL of THF. The reaction was sealed and stirred at 70 °C for 18 h. The reaction mixture was cooled and filtered through celite followed by washing two times with ether. The reaction mixture was concentrated and 4 mg of hexamethylbenzene (HMB) was added as an NMR standard. No product was observed by NMR.



**Synthesis of (R)-1-(1-phenylethyl)naphthalene ((R)-2-6h).** In a nitrogen filled glove box, 1-iodonaphthalene (40.67 mg, 254.1 g/mol, 0.160 mmol), (*R*)-pinacol(1-phenylethyl)boronate (55.52 mg, 232 g/mol, 0.239 mmol, e.r 93.6:6.4), Ag<sub>2</sub>O (53.78 mg, 234 g/mol, 0.232 mmol), K<sub>2</sub>CO<sub>3</sub> (31.71 mg, 138 g/mol, 0.229 mmol), Pd(PPh<sub>3</sub>)<sub>4</sub> (14.55 mg, 1155.6 g/mol, 0.0126 mmol) and PPh<sub>3</sub> (13.23 mg, 262 g/mol, 0.0504 mmol) were weighed into a dried vial and taken up in 3 mL of DME. The reaction was sealed and stirred at 85 °C for 24 h. The

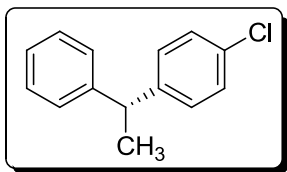
reaction mixture was cooled and filtered through celite. The desired product was isolated by column chromatography (20:1 Hex:EtOAc) in a 65% yield. The enantiomeric ratio was determined by SFC (OD, 2% MeOH, 2 mL, 200 bar) to be 87:13, a 93% retention of *er*. **<sup>1</sup>H NMR** (400 MHz, CDCl<sub>3</sub>) δ 7.86-7.78 (m, 1 H), 7.64-7.59 (m, 1 H), 7.54-7.50 (m, 1 H), 7.28-7.16 (m, 4 H), 7.06-6.90 (m, 4 H), 6.96-6.90 (m, 1 H), 4.70 (q, *J* = 7.1 Hz, 1 H), 1.54 (d, *J* = 7.2 Hz, 3 H). **<sup>13</sup>C NMR**: (100 MHz, CDCl<sub>3</sub>): δ 146.78, 141.68, 134.12, 131.84, 128.91, 128.56, 127.76, 127.12, 126.10, 125.99, 125.57, 125.45, 124.46, 124.11, 40.70, 22.70. **HRMS (EI-TOF)**: calcd for [M]<sup>+</sup> (C<sub>18</sub>H<sub>16</sub>) *m/z* 232.1252; found 232.1258.

#### 6.1.4 Synthesis of Enantioenriched 1,1-diarylethanes with Aryl Bromides

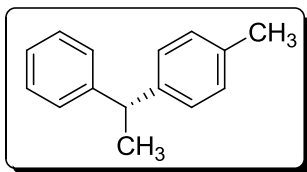


**Synthesis of (*R*)-1-phenyl-1-(4-acetylphenyl)ethane ((*R*)-2-6a).** In a nitrogen-filled glovebox, 4-bromoacetophenone (30.6 mg, 199 g/mol, 0.154 mmol), (*R*)-pinacol(1-phenylethyl)boronate (53.6 mg, 232 g/mol, 0.231 mmol, *er* = 94:6) Ag<sub>2</sub>O (52.7 mg, 234 g/mol, 0.225 mmol), Pd(PPh<sub>3</sub>)<sub>4</sub> (13.8 mg, 1155.6 g/mol, 0.012 mmol, 7.8 mol% Pd), PPh<sub>3</sub> (12.7 mg, 262 g/mol, 0.048 mmol, 8.0:1 P:Pd), K<sub>2</sub>CO<sub>3</sub> (63.8 mg, 138 g/mol, 0.462 mmol) and 21.9 mg of *n*-octadecane (internal standard, 254 g/mol, 0.086 mmol) were taken up in 2.1 g of toluene. The reaction was sealed, and stirred at 75 °C for 48 h. The crude reaction was filtered through a celite plug and washed with copious amounts of diethyl ether and hexanes. GC yield was determined to be 57%. The desired product was

then isolated by column chromatography (gradient 20:1 to 10:1 hexanes: ethyl acetate) in 49% yield. The enantiomeric ratio was determined by SFC analysis (AD-H Column, 5% MeOH, 2 mL, 200 bar) to be 90:10, a 96% retention of er.

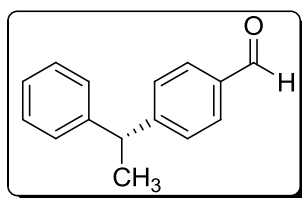


**Synthesis of (*R*)-1-phenyl-1-(4-chlorophenyl)ethane ((*R*)-2-6b).** In a nitrogen-filled glovebox, 4-bromochlorobenzene (29.25 mg, 191.4 g/mol, 0.153 mmol), (*R*)-pinacol(1-phenylethyl)boronate (53.3 mg, 232 g/mol, 0.229 mmol, er = 98.5:1.5) Ag<sub>2</sub>O (53.8 mg, 234 g/mol, 0.229 mmol), Pd(PPh<sub>3</sub>)<sub>4</sub> (13.75 mg, 1155.6 g/mol, 0.012 mmol, 7.8 mol% Pd), PPh<sub>3</sub> (13.0 mg, 262 g/mol, 0.050 mmol, 8.2:1 P:Pd) and K<sub>2</sub>CO<sub>3</sub> (62.6 mg, 138 g/mol, 0.454 mmol) were taken up in 2.2 g of toluene. The reaction was sealed, and stirred at 75 °C for 48 h. The crude reaction was filtered through a celite plug and washed with copious amounts of diethyl ether and hexanes. The solution was concentrated *in vacuo* after which an NMR internal standard (HMB, 4.29 mg) was added. The NMR yield of the reaction was determined to be 56%. The crude mixture was then purified by column chromatography (pentane) to give 13.9 mg, representing a 49% isolated yield. The enantiomeric ratio was determined by SFC analysis (OD Column, 0.1% MeOH, 2 mL, 200 bar) to be 93:7, a 94% retention of er.



**Synthesis of (*R*)-1-phenyl-1-(4-methylphenyl)ethane ((*R*)-2-6c).** In a nitrogen-filled glovebox, 4-bromotoluene (28.3 mg,

170.9 g/mol, 0.166 mmol), (*R*)-pinacol(1-phenylethyl)boronate (57.8 mg, 232 g/mol, 0.249 mmol, er = 94:6) Ag<sub>2</sub>O (59.8 mg, 234 g/mol, 0.0258 mmol), Pd(PPh<sub>3</sub>)<sub>4</sub> (15.6 mg, 1155.6 g/mol, 0.0135 mmol, 8.1 mol% Pd), PPh<sub>3</sub> (14.1 mg, 262 g/mol, 0.0538 mmol, 7.2:1 P:Pd) and K<sub>2</sub>CO<sub>3</sub> (70.7 mg, 138 g/mol, 0.512 mmol) were taken up in 2.3 g of toluene. The reaction was sealed, and stirred at 75 °C for 48 h. The crude reaction was filtered through a celite plug and washed with copious amounts of diethyl ether and hexanes. The solution was concentrated *in vacuo* after which an NMR internal standard (dimethoxybenzene, DMB, 5.92 mg) was added. The NMR yield of the reaction was determined to be 43%. The crude mixture was then purified by column chromatography (pentane) to give 11.3 mg, representing a 31% isolated yield. The enantiomeric ratio was determined by SFC analysis (OD Column, 1% MeOH, 2 mL, 200 bar) to be 89.5:10.5, a 95% retention of er.

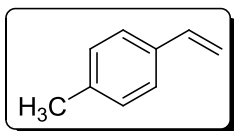


**Synthesis of (*R*)-1-phenyl-1-(4-benzaldehyde)ethane ((*R*)-2-6i).** In a nitrogen-filled glovebox, 4-bromobenzaldehyde (29.00 mg, 184.9 g/mol, 0.157 mmol), (*R*)-pinacol(1-phenylethyl)boronate (51.32 mg, 232 g/mol, 0.229 mmol, er = 94:6) Ag<sub>2</sub>O (53.8 mg, 234 g/mol, 0.221 mmol), Pd(PPh<sub>3</sub>)<sub>4</sub> (13.71 mg, 1155.6 g/mol, 0.012 mmol, 7.8 mol% Pd), PPh<sub>3</sub> (12.53 mg, 262 g/mol, 0.048 mmol, 7.9:1 P:Pd) and K<sub>2</sub>CO<sub>3</sub> (62.9 mg, 138 g/mol, 0.456 mmol) were taken up in 2.1 g of toluene. The reaction was sealed, and stirred at 75 °C for 48 h. The crude reaction was filtered through a celite plug and washed with copious amounts of diethyl ether and hexanes. The crude mixture was then purified by



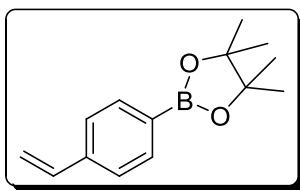
column chromatography (20:1 hexanes:ethyl acetate) to give 13.9 mg, representing a 42% isolated yield. The enantiomeric ratio was determined by SFC analysis (OD Column, 2% MeOH, 2 mL, 200 bar) to be 88:12, a 93% retention of er. **<sup>1</sup>H NMR** (400 MHz, CDCl<sub>3</sub>) δ 9.89 (s, 1 H), 7.73 (d, *J* = 8.0 Hz, 2 H), 7.31 (d, *J* = 8.0 Hz, 2 H), 7.24 (m, 2 H), 7.13 (m, 3 H), 4.15 (q, *J* = 7.2 Hz, 1 H), 1.60 (d, *J* = 7.2 Hz, 3 H). **<sup>13</sup>C NMR**: (100 MHz, CDCl<sub>3</sub>): δ 191.0, 152.6, 144.0, 133.6, 129.0, 127.6, 127.3, 126.6, 125.5, 44.0, 20.5. **HRMS (EI-TOF)**: calcd for [M]<sup>+</sup> (C<sub>18</sub>H<sub>16</sub>) *m/z* 210.1045; found 210.1053.

#### 6.1.5 The Remarkable Chemoselectivity of the Reaction



**Competitive Intermolecular Mizoroki-Heck Reaction and Potential Cross-Over Study.** In a nitrogen-filled glovebox, 4-iodoacetophenone (12.28 mg, 245.9 g/mol, 0.050 mmol), (*R*)-pinacol(1-phenylethyl)boronate (17.23 mg, 232 g/mol, 0.074 mmol, 148 equiv., er = 98:2), Ag<sub>2</sub>O (17.73 mg, 234 g/mol, 0.076 mmol), Pd(PPh<sub>3</sub>)<sub>4</sub> (4.65 mg, 1155.6 g/mol, 0.004 mmol, 8.0 mol% Pd), PPh<sub>3</sub> (4.15 mg, 262 g/mol, 0.016 mmol, 8.0:1 P:Pd), K<sub>2</sub>CO<sub>3</sub> (10.03 mg, 138 g/mol, 0.073 mmol), 18.26 mg of *n*-octadecane (internal standard, 254 g/mol, 0.071 mmol) and 83.28 mg of *p*-methylstyrene (118 g/mol, 0.70 mmol, 14.1 equiv.) were taken up in 1.0 g of DME. The reaction was sealed with a Teflon cap complete with rubber septum and removed from the glovebox. Outside of the glovebox, 7.40 mg of an H<sub>2</sub>O/DME mixture (7.33 mg H<sub>2</sub>O in 145.3 mg DME) were added *via* syringe, through the

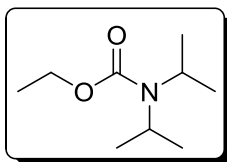
rubber septum, for a final water concentration of 354 ppm in the reaction solution. The septum was covered with Teflon tape and generously wrapped with parafilm before being subjected to an 85 °C oil bath for 22 h. The crude reaction was filtered through a celite plug and washed with copious amounts of diethyl ether and hexanes. GC yield (of the Suzuki-Miyaura cross-coupling product) was determined to be 47%. The crude reaction solution was analyzed by HPLC-HRMS for Mizoroki-Heck or cross-over products; the cross-over product was not observed, where the Mizoroki-Heck derived stilbene was observed in less than 0.2% yield. When the experiment was performed under conditions known to erode enantioselectivity in the cross-coupling reaction (namely 12 equiv. PPh<sub>3</sub> and no K<sub>2</sub>CO<sub>3</sub> added), appreciable levels of cross-over and Mizoroki-Heck products were still not detected at 6.5 equivalents of *p*-methylstyrene to 4-iodoacetophenone, which represents a larger than 4-fold excess to the benzylic boronic ester coupling partner.



**Synthesis of 4-(pinacolboronate)-styrene.** 0.9841 g of 4-(boronic acid)-styrene (114 g/mol, 8.632 mmol, 1.0 equiv.) and 1.0227 g of pinacol (118 g/mol, 8.632 mmol, 1.0 equiv.) were taken up in 25 mL of diethyl ether. 1.082 g of MgSO<sub>4</sub> (120 g/mol, 9.02 mmol, 1.04 equiv.) was added and the dispersion was stirred at room temperature for 17 h. The reaction was filtered and concentrated under vacuum to yield 1.802 g of a clear liquid, representing a 91% isolated yield. **<sup>1</sup>H NMR:** (400 MHz, CDCl<sub>3</sub>) δ 7.77 (d, *J* = 8 Hz, 2 H), 7.39 (d, *J* = 8 Hz, 2 H), 6.71 (dd, *J* = 17.2 Hz, 10.8 Hz, 1 H), 5.80 (d, *J* = 17.6, 1 H), 5.27 (d, *J* = 10.8 Hz, 1 H), 1.33 (s, 12 H). **<sup>11</sup>B NMR:** (160 MHz, CDCl<sub>3</sub>): δ 30.8. **<sup>13</sup>C**

**NMR:** (100 MHz, CDCl<sub>3</sub>)  $\delta$  140.3, 136.9, 135.1, 125.5, 114.8, 83.8, 75.0, 24.9. **HRMS**

**(EI-TOF):** calcd for [M]<sup>+</sup> (C<sub>14</sub>H<sub>19</sub>O<sub>2</sub>B)  $m/z$  230.1478; found 230.1473.



**Synthesis of *N,N*-Diisopropyl-carbamic acid ethyl ester.** *N,N*-

diisopropylcarbamoyl chloride (0.728 g, 163.65 g/mol, 4.45 mmol, 1.05 equiv.) and freshly distilled triethylamine (0.62 mL, 0.726 g/mL,

101.2 g/mol, 4.45 mmol, 1.5 equiv.) were taken up in 20 mL of CH<sub>2</sub>Cl<sub>2</sub>. Ethanol (0.25 mL, 0.789 g/mL, 46 g/mol, 4.25 mmol, 1.0 equiv.) was added and the solution was stirred under refluxing conditions for 16 h, with salts eventually precipitating out of solution.

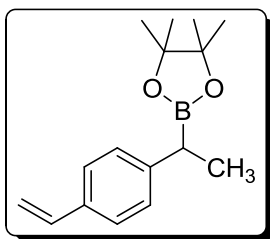
The solution was washed with sat. NH<sub>4</sub>Cl<sub>(aq.)</sub> and the aqueous layer was extracted with 3 x 25 mL CH<sub>2</sub>Cl<sub>2</sub>. The crude oil was purified by silica gel chromatography (20:1 hexanes:ethyl acetate, 1 inch by 5 inch column). The pure fractions were concentrated under light vacuum, but even this mild removal of solvent led to a product loss. In the

end 442.3 mg of carbamate were isolated, or a 60% yield. **<sup>1</sup>H NMR:** (400 MHz, CDCl<sub>3</sub>)

$\delta$  4.06 (q,  $J = 7.2$  Hz, 2 H), 4.0-3.5 (s, br, 2 H), 1.20 (t,  $J = 7.2$  Hz, 3 H), 1.13 (d,  $J = 6.8$

Hz, 12 H). **<sup>13</sup>C NMR:** (100 MHz, CDCl<sub>3</sub>)  $\delta$  155.8, 60.3, 45.6 (br), 20.6 (br), 14.6. **HRMS**

**(EI-TOF):** calcd for [M+H]<sup>+</sup> (C<sub>9</sub>H<sub>19</sub>O<sub>2</sub>N)  $m/z$  174.1494; found 174.1487.

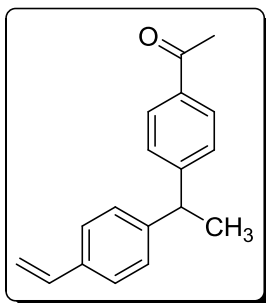


**Synthesis of 4-(ethyl-1-boronic acid pinacolate ester)-styrene**

**(2-8).** *N,N*-diisopropylethylcarbamate (156.4 mg, 173 g/mol,

0.904 mmol, 1.0 equiv.) and *N,N,N,N*-tetramethylethyldiamene

(TMEDA, 140.0 mg, 116 g/mol, 1.21 mmol, 1.34 equiv.) were taken up in 4.5 mL diethyl ether and cooled to  $-78\text{ }^{\circ}\text{C}$  in a dry ice/acetone bath. *s*-butyllithium (1.05 mL, 1.02 M, 1.09 mmol, 1.2 equiv.) was added dropwise to the cold solution, maintaining an internal temperature of under  $-70\text{ }^{\circ}\text{C}$ . After 5 h of lithiation, an ethereal solution of 4-(pinacolboronate)-styrene (227.3 mg, 230 g/mol, 0.987 mmol, 1.09 equiv., 1.5 mL Et<sub>2</sub>O) was added dropwise. After 1 h borylation, freshly prepared MgBr<sub>2</sub> diethyl etherate (3.0 equiv.) was added to the cold solution as an ethereal solution. MgBr<sub>2</sub> diethyl etherate is prepared by adding the necessary amount of 1,2-dibromoethane, in this case, 3 equivalents per boronic ester to an excess of Mg turnings in dry ether. The contents of the dense layer that dissociates from the ether are added to the reaction solution *via* syringe, causing the internal temperature of the reaction to temporarily spike to  $-55\text{ }^{\circ}\text{C}$ . After addition of the MgBr<sub>2</sub>, the solution is allowed to warm slowly before being heated to reflux overnight. An aliquot submitted for GC-MS analysis indicated that conversion to the desired product was much lower than expected. After aqueous workup, two silica gel chromatography steps (50:1 hexanes:ethyl acetate) were required to separate the product from the starting boronic ester, and therefore only 11.8 mg (5% yield) of white solid was isolated. **<sup>1</sup>H NMR:** (400 MHz, CDCl<sub>3</sub>)  $\delta$  7.24 (d,  $J = 8.4$ , 2 H), 7.11 (d,  $J = 8.4$  Hz, 2 H), 6.61 (dd,  $J = 17.6$  Hz, 10.8 Hz, 1 H), 5.61 (dd,  $J = 17.6$  Hz, 0.8 Hz, 1 H), 5.09 (dd,  $J = 10.8$  Hz, 0.8 Hz, 1H), 2.35 (q,  $J = 7.6$  Hz, 1 H), 1.25 (d,  $J = 7.2$  Hz, 3 H), 1.14 (s, 6 H), 1.13 (s, 6 H). **<sup>11</sup>B NMR:** (160 MHz, CDCl<sub>3</sub>):  $\delta$  33.5. **<sup>13</sup>C NMR:** (100 MHz, CDCl<sub>3</sub>)  $\delta$  144.9, 136.9, 134.5, 127.9, 126.2, 112.5, 83.3, 24.9, 24.6, 16.9.



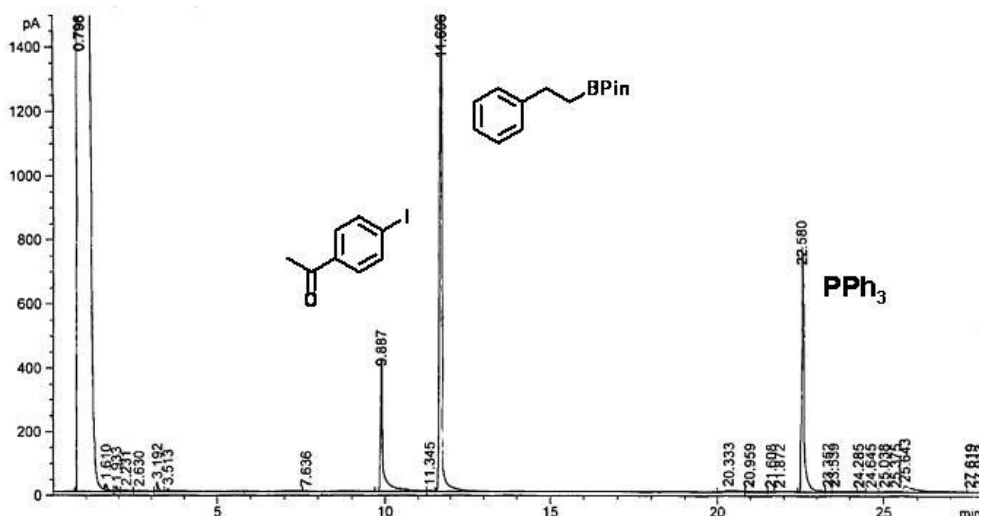
**Intramolecular Mizoroki-Heck / Suzuki-Miyaura**

**Competition: Synthesis of rac-1-(4-styrenyl),1-(4-**

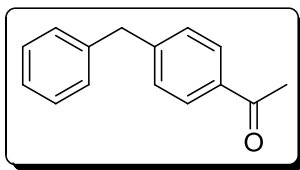
**acetylphenyl)ethane (2-9).** In a nitrogen-filled glovebox, 4-iodoacetophenone (6.91 mg, 245.9 g/mol, 0.0281 mmol), 4-(ethyl-1-boronic acid pinacolate ester)-styrene (11.0 mg, 0.043 mmol,

1.53 equiv.) Ag<sub>2</sub>O (10.20 mg, 234 g/mol, 0.0436 mmol), Pd(PPh<sub>3</sub>)<sub>4</sub> (2.85 mg, 1155.6 g/mol, 0.0025 mmol, 8.8 mol% Pd), PPh<sub>3</sub> (2.31 mg, 262 g/mol, 0.009 mmol, 7.5:1 P:Pd) were taken up in DME (0.7 mL). The reaction was sealed, and stirred at 85 °C for 23 h. Once cooled, the reaction was filtered through celite and washed with copious amounts of diethyl ether. The solvents were evaporated *in vacuo* and an internal NMR standard was added (hexamethylbenzene, HMB, 7.8 mg). The Suzuki-Miyaura cross-coupling product was obtained in 54% NMR yield. The diarylated product was purified by column chromatography (20:1 hexanes: ethyl acetate) to give 7.03 mg of a clear oil, representing a 48% isolated yield. The Mizoroki-Heck stilbene product was not detected in significant amounts by GC-MS or NMR. **<sup>1</sup>H NMR:** (400 MHz, CDCl<sub>3</sub>) δ 7.80 (d, *J* = 8 Hz, 2 H), 7.27 (d, *J* = 8 Hz, 2 H), 7.23 (d, *J* = 8 Hz, 2 H), 7.09 (d, *J* = 8.4 Hz, 2 H), 6.61 (dd, *J* = 17.6 Hz, 10.8 Hz, 1 H), 5.63 (dd, *J* = 17.6 Hz, 0.8 Hz, 1 H), 5.13 (dd, *J* = 10.8 Hz, 0.8 Hz, 1 H), 4.12 (q, *J* = 7.2 Hz, 1 H), 2.50 (s, 3 H), 1.58 (d, *J* = 7.2 Hz, 3 H). **<sup>13</sup>C NMR:** (100 MHz, CDCl<sub>3</sub>) δ 151.8, 145.0, 136.4, 135.8, 135.3, 128.6, 127.8, 127.8, 126.4, 113.5, 44.6, 26.6, 21.5, 15.3 (Carbonyl peak not observed). **HRMS (EI-TOF):** calcd for [M]<sup>+</sup> (C<sub>18</sub>H<sub>18</sub>O) *m/z* 250.1358; found 250.1351.

**Linear Boronate Subjected to Branched Coupling Conditions.** In a nitrogen-filled glovebox, iodoacetophenone (13.3 mg, 0.054 mmol), (2-phenylethyl)boronic acid pinacol ester **2-10** (17.7 mg, 0.076 mmol), Ag<sub>2</sub>O (17.7 mg, 0.076 mmol), Pd<sub>2</sub>(dba)<sub>3</sub> (1.76 mg, 0.0019 mmol, 7.1 mol% Pd), PPh<sub>3</sub> (9.28 mg, 0.035 mmol) were taken up in THF (1.2 g). The vial was sealed, and stirred at 70 °C for 18 h after which it was cooled to room temperature before being filtered through celite and washed with copious amounts of diethyl ether. Analysis by GC (aliquot taken up in dichloromethane) indicates no coupling product and the preservation of the linear boronate.



#### 6.1.6 Scope of Reactive Boronic Esters under Silver-Mediated Protocol



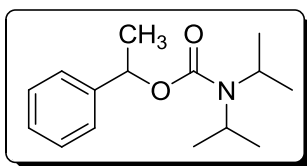
**Cross-Coupling of primary Benzylboronic acid pinacol ester (2-11).** In a nitrogen-filled glovebox, 4-iodoacetophenone (12.47 mg, 245.9 g/mol, 0.051 mmol), Ag<sub>2</sub>O (19.09 mg, 234

g/mol, 0.0816 mmol, 1.60 equiv.), Pd(PPh<sub>3</sub>)<sub>4</sub> (4.79 mg, 1155.6 g/mol, 0.0042 mmol, 8.1 mol% Pd), PPh<sub>3</sub> (4.75 mg, 262 g/mol, 0.018 mmol, 8.3:1 P:Pd) and K<sub>2</sub>CO<sub>3</sub> (10.89 mg, 138 g/mol, 0.079 mmol) were taken up in DME (1.0 g). The reaction was sealed with a teflon cap complete with a rubber septum and removed from the glovebox. Outside the glovebox, benzylboronic acid pinacolate ester **2-11** (15.5 mg, 218 g/mol, 0.071 mmol, 1.4 equiv.) was added *via* syringe through the septum. The solution was then stirred at 85 °C for 20 h. Once cooled, the reaction was filtered through celite and washed with copious amounts of diethyl ether. The solvents were evaporated *in vacuo* and an internal NMR standard was added (hexamethylbenzene, HMB, 7.80 mg). The NMR yield of the reaction was determined to be 69%. The cross-coupled product was then purified by silica gel chromatography (20:1 hexanes:ethyl acetate) to yield 6.3 mg of clear oil, representing a 59% isolated yield. **<sup>1</sup>H NMR:** (400 MHz, CDCl<sub>3</sub>) δ 7.81 (d, *J* = 8 Hz, 2 H), 7.20 (m, 5 H), 7.10 (d, *J* = 7.2 Hz, 2 H), 3.96 (s, 2 H), 2.50 (s, 3 H). **<sup>13</sup>C NMR:** (100 MHz, CDCl<sub>3</sub>) δ 197.8, 146.8, 140.1, 135.3, 129.1, 129.0, 128.7, 126.4, 41.9, 26.7. (One aromatic peak doubled). **HRMS (EI-TOF):** calcd for [M]<sup>+</sup> (C<sub>15</sub>H<sub>14</sub>O) *m/z* 210.1045; found 210.1049.

**Cross-Coupling of *primary* Benzylicboronic acid pinacol ester 2-11 (without K<sub>2</sub>CO<sub>3</sub>).**

In a nitrogen-filled glovebox, 4-iodoacetophenone (12.22 mg, 245.9 g/mol, 0.050 mmol), Ag<sub>2</sub>O (17.94 mg, 234 g/mol, 0.076 mmol), Pd(PPh<sub>3</sub>)<sub>4</sub> (4.71 mg, 1155.6 g/mol, 0.0041 mmol, 8.0 mol% Pd), and PPh<sub>3</sub> (4.48 mg, 262 g/mol, 0.017 mmol, 8.2:1 P:Pd) were taken up in DME (1.0 g). The reaction was sealed with a teflon cap complete with a rubber

septum and removed from the glovebox. Outside the glovebox, benzylboronic acid pinacolate ester **2-11** (17.7 mg, 218 g/mol, 0.081 mmol, 1.62 equiv.) was added *via* syringe through the septum. The solution was then stirred at 85 °C for 20 h. Once cooled, the reaction was filtered through celite and washed with copious amounts of diethyl ether. The solvents were evaporated *in vacuo* and an internal NMR standard was added (hexamethylbenzene, HMB, 5.23 mg). The NMR yield of the reaction was determined to be 77%. The small difference in yields between the experiments with and without K<sub>2</sub>CO<sub>3</sub> may be attributed to the larger excess of primary benzylic boronic ester in the latter case.

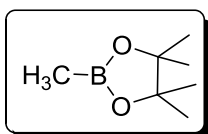


#### Synthesis of *N,N*-Diisopropyl carbamic acid (1-phenylethyl)

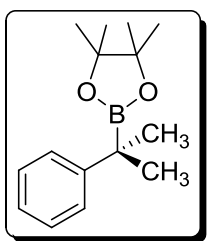
**ester.** *N,N*-diisopropylcarbamoyle chloride (1.011 g, 163.65 g/mol, 6.18 mmol, 1.0 equiv.) and freshly distilled triethylamine (0.9 mL, 0.726 g/mL, 101.2 g/mol, 6.45 mmol, 1.05 equiv.) were taken up in 20 mL of CH<sub>2</sub>Cl<sub>2</sub>. *sec*-Phenethanol (0.753 g, 122 g/mol, 6.1 mmol, 1.0 equiv.) was added and the solution was stirred under refluxing conditions for 24 h, with salts eventually precipitating out of solution. The solution was washed with H<sub>2</sub>O and the aqueous layer was extracted with 3 x 25 mL CH<sub>2</sub>Cl<sub>2</sub>. The crude oil was purified by silica gel chromatography (6:1 hexanes:ethyl acetate, 2 inch by 5 inch column). No yield was recorded, though an NMR of the crude mixture indicated that the ratio of product to starting secondary alcohol was ~ 1:1 after 24 h of reflux. **<sup>1</sup>H NMR:** (400 MHz, CDCl<sub>3</sub>) δ 7.38 (m, 4 H), 7.28 (m, 1 H), 5.87 (q, *J* = 6.4 Hz, 1 H), 4.3-3.6 (d, br, 2 H), 1.57 (d, *J* = 6.4 Hz, 3 H), 1.23 (d, *J* = 6.4 Hz, 12 H). **<sup>13</sup>C NMR:** (100 MHz, CDCl<sub>3</sub>) δ 155.1, 142.8,



128.4, 127.4, 126.0, 72.7, 45.9 (br), 22.9, 22.2 (br). **HRMS (EI-TOF):** calcd for  $[M]^+$  ( $C_{15}H_{23}O_2N$ )  $m/z$  249.1729; found 249.1719.

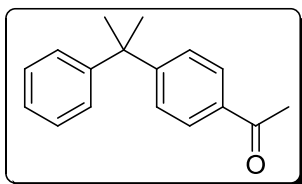


**Synthesis of methyl boronic acid pinacolate ester.** 1.5066 g of methylboronic acid (60 g/mol, 25.11 mmol, 1.0 equiv.) and 3.282 g of pinacol (118 g/mol, 27.8 mmol, 1.1 equiv.) were taken up in 70 mL of diethyl ether. Once dissolved, 3.03 g of  $MgSO_4$  (120 g/mol, 25.3 mmol, 1.0 equiv.) was dispersed in the solution, which was stirred at 25 °C for 48 h. The dispersion was filtered by vacuum and washed with copious amounts of diethyl ether. The homogeneous solution was then concentrated *in vacuo* to a volume of 10 mL and passed through a silica plug. The desired boronic acid was obtained in 87% yield. Contamination by pinacol caused future esterifications to be performed with equivalent stoichiometries of boronic acid and diols.  **$^1H$  NMR:** (400 MHz,  $CDCl_3$ )  $\delta$  1.26 (s, 12 H), 0.26 (s, 3 H).  **$^{11}B$  NMR:** (160 MHz,  $CDCl_3$ ):  $\delta$  33.  **$^{13}C$  NMR:** (100 MHz,  $CDCl_3$ )  $\delta$  83.0, 24.9 (Methyl peak, broadened by B, not assigned). **HRMS (EI-TOF):** calcd for  $[M]^+$  ( $C_7H_{15}O_2B$ )  $m/z$  142.1165; found 142.1169.



**Synthesis of (1-methyl, 1-phenyl)ethyl boronic acid pinacolate ester (2-12).** *N,N*-Diisopropyl carbamic acid (1-phenylethyl) ester (280 mg, 279 g/mol, 1.00 mmol, 1.0 equiv.) was taken up in diethyl ether and cooled to -78 °C in a dry ice/acetone bath. *s*-Butyllithium (1.4 mL, 1.16

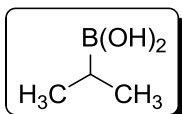
M, 1.62 mmol, 1.6 equiv.) was added dropwise to the cold solution. After 5 h of lithiation, an ethereal solution of methylboronic acid pinacolate ester (186.6 mg, 142 g/mol, 1.31 mmol, 1.3 equiv., 1.5 mL Et<sub>2</sub>O) was added dropwise to give a bright yellow solution, which faded to an orange colour over time. After 1 h borylation, commercially available MgBr<sub>2</sub> diethyl etherate (1.3 equiv.) was added to the cold solution in solid form by removing the septum and adding the solid at once. After addition of the MgBr<sub>2</sub>, the solution is allowed to warm slowly before being heated to reflux overnight. After aqueous workup, the tertiary benzylic boronic ester was purified by silica gel chromatography (loaded with 50:1 hexanes:ethyl acetate, eluted with 20:1 hexanes:ethyl acetate R<sub>f</sub> = 1/7) in 50% yield. **<sup>1</sup>H NMR:** (400 MHz, CDCl<sub>3</sub>) δ 7.36-7.28 (m, 4 H), 7.17 (m, 1 H), 1.37 (s, 6 H), 1.23 (s, 12 H). **<sup>11</sup>B NMR:** (160 MHz, CDCl<sub>3</sub>): δ 34. **<sup>13</sup>C NMR:** (100 MHz, CDCl<sub>3</sub>) δ 148.6, 128.1, 126.3, 125.0, 83.3, 25.6, 24.5 (One aromatic peak not assigned). **HRMS (EI-TOF):** calcd for [M]<sup>+</sup> (C<sub>15</sub>H<sub>24</sub>O<sub>2</sub>B) *m/z* 247.1869; found 247.1865.



**Attempted cross-coupling of (1-methyl, 1-phenyl)ethyl boronic acid pinacolate ester (2-12).** In a nitrogen-filled glovebox, 4-iodoacetophenone (26.07 mg, 245.9 g/mol, 0.104 mmol), (1-methyl, 1-phenyl)ethyl boronic acid pinacolate ester **2-12** (41.0 mg, 246 g/mol, 0.166 mmol, 1.6 equiv.), Ag<sub>2</sub>O (40.59 mg, 234 g/mol, 0.173 mmol, 1.7 equiv.), Pd<sub>2</sub>(dba)<sub>3</sub> (3.84 mg, 915 g/mol, 0.0042 mmol, 8.1 mol% Pd), and PPh<sub>3</sub> (21.44 mg, 262 g/mol, 0.081 mmol, 0.79 equiv., 9.6:1 P:Pd) were taken up in THF (2.2 g). The reaction was sealed in

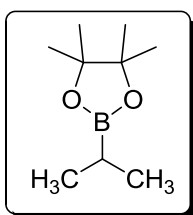
the glovebox with a teflon cap, removed, and placed in a 70 °C oil bath for 22 h. Once cooled, the reaction was filtered through celite and washed with copious amounts of diethyl ether. The crude reaction solution was analyzed by GC, which indicated that no product had been formed and that the tertiary benzylic boronic ester had survived the reaction conditions.

**Attempted cross-coupling of (1-methyl, 1-phenyl)ethyl boronic acid pinacolate ester **2-12** under modified conditions.** In a nitrogen-filled glovebox, 4-iodoacetophenone (9.15 mg, 245.9 g/mol, 0.036 mmol), (1-methyl, 1-phenyl)ethyl boronic acid pinacolate ester **2-12** (13.2 mg, 246 g/mol, 0.054 mmol, 1.5 equiv.), Ag<sub>2</sub>O (12.35 mg, 234 g/mol, 0.053 mmol, 1.5 equiv.), Pd<sub>2</sub>(dba)<sub>3</sub> (1.26 mg, 915 g/mol, 0.0014 mmol, 7.6 mol% Pd), and PPh<sub>3</sub> (6.89 mg, 262 g/mol, 0.026 mmol, 0.73 equiv., 9.3:1 P:Pd) were taken up in DME (0.75 g). The reaction was sealed in the glovebox with a teflon cap, removed, and placed in a 75 °C oil bath for 16 h. Once cooled, the reaction was filtered through celite and washed with copious amounts of diethyl ether and an internal NMR standard (hexamethylbenzene, HMB, 3.93 mg) was added. GC analysis of the filtered reaction indicated that no product had been formed and that the starting boronic ester was left unconsumed.

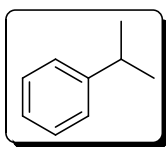


**Cross-Coupling of isopropylboronic acid.** In a nitrogen-filled glovebox, iodobenzene (20.47 mg, 203.9 g/mol, 0.100 mmol), isopropyl boronic acid (13.11 mg, 88 g/mol, 0.148 mmol, 1.5 equiv.), Ag<sub>2</sub>O (44.52 mg, 234 g/mol,

0.189 mmol, 1.9 equiv.), Pd<sub>2</sub>(dba)<sub>3</sub> (3.65 mg, 915 g/mol, 0.0040 mmol, 8.0 mol% Pd), and PPh<sub>3</sub> (19.77 mg, 262 g/mol, 0.07 mmol, 0.75 equiv., 8.8:1 P:Pd) were taken up in THF (0.75 g). The reaction was sealed in the glovebox with a teflon cap, removed, and placed in a 70 °C oil bath for 16 h. Once cooled, the reaction was filtered through celite and washed with copious amounts of diethyl ether. A GC comparison of the crude reaction mixture and an authentic sample of cumene indicated that the cross-coupling reaction did not occur to any appreciable degree.

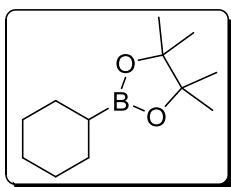


**Synthesis of isopropylboronic acid pinacolate ester (2-13).** 0.837 g of 1-isopropylboronic acid (87.9 g/mol, 9.52 mmol, 1.0 equiv.) and 1.124 g of pinacol (118 g/mol, 9.52 mmol, 1.0 equiv.) were taken up in 10 mL of diethyl ether. Once dissolved, 1.151 g of MgSO<sub>4</sub> (120 g/mol, 9.59 mmol, 1.0 equiv.) was dispersed in the solution, which was stirred at 25 °C for 22 h. The dispersion was filtered by vacuum and washed with copious amounts of diethyl ether. The homogeneous solution was then concentrated *in vacuo* to yield a crude oil which was purified by silica gel chromatography (20:1 hexanes:ethyl acetate). The high volatility of the product boronic ester led to reduced yields, especially after removal of trace amounts of solvent by high vacuum. Ultimately, 563 mg of pure product were obtained, representing a 35% isolated yield. **<sup>1</sup>H NMR:** (400 MHz, CDCl<sub>3</sub>) δ 1.26 (s, 12 H), 1.13-1.04 (m, br, 1 H), 1.00 (d, *J* = 7.2 Hz, 6 H). **<sup>11</sup>B NMR:** (160 MHz, CDCl<sub>3</sub>): δ 35. **<sup>13</sup>C NMR:** (100 MHz, CDCl<sub>3</sub>) δ 82.8, 24.7, 18.0.



#### **Attempted Cross-Coupling of isopropylboronic acid pinacolate ester.**

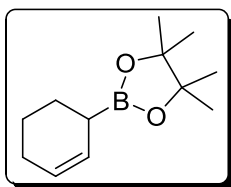
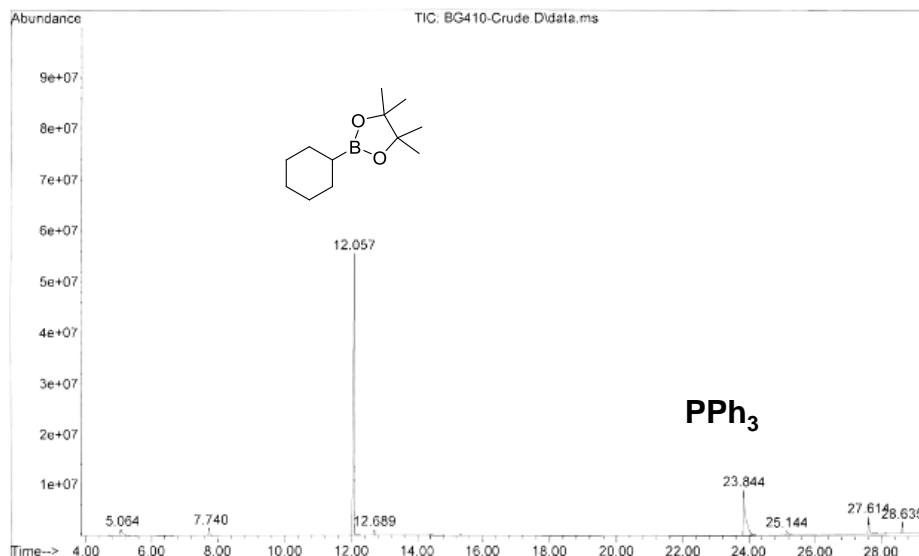
In a nitrogen-filled glovebox, iodobenzene (20.9 mg, 203.9 g/mol, 0.103 mmol), isopropylboronic acid pinacolate ester **2-13** (38.1 mg, 170 g/mol, 0.224 mmol, 2.2 equiv., excess used to offset high volatility of the short-chain boronic ester), Ag<sub>2</sub>O (38.0 mg, 234 g/mol, 0.162 mmol, 1.6 equiv.), Pd<sub>2</sub>(dba)<sub>3</sub> (3.60 mg, 915 g/mol, 0.0039 mmol, 7.6 mol% Pd), and PPh<sub>3</sub> (26.8 mg, 262 g/mol, 0.102 mmol, 1.0 equiv., 12.8:1 P:Pd) were taken up in diethyl ether (1.0 g). The reaction was sealed in the glovebox with a teflon cap, removed, and placed in a 65 °C oil bath for 14 h. Once cooled, the reaction was filtered through celite and washed with copious amounts of diethyl ether. A GC comparison of the crude reaction mixture and an authentic sample of cumene indicated that the cross-coupling reaction did not occur to any appreciable degree, but that the isopropylboronic acid pinacolate ester survived the reaction conditions.



#### **Attempted Cross-Coupling of cyclohexylboronic acid pinacolate**

**ester (2-14).** In a nitrogen-filled glovebox, 4-iodoacetophenone (12.23 mg, 245.9 g/mol, 0.050 mmol), cyclohexylboronic acid pinacolate ester **2-14** (Frontier Chemical, 15.44 mg, 210 g/mol, 0.074 mmol, 1.48 equiv), Ag<sub>2</sub>O (17.83 mg, 234 g/mol, 0.076 mmol, 1.5 equiv.), Pd(PPh<sub>3</sub>)<sub>4</sub> (4.65 mg, 1155.6 g/mol, 0.0040 mmol, 8.0 mol% Pd), and PPh<sub>3</sub> (9.40 mg, 262 g/mol, 0.036 mmol, 0.72 equiv., 13:1 P:Pd) were taken up in DME (1.1 g). The reaction was sealed in the glovebox with a

teflon cap, removed, and placed in a 85 °C oil bath for 18 h. Once cooled, the reaction was filtered through celite and washed with copious amounts of diethyl ether. GC analysis of the crude reaction solution indicates that no cross-coupling occurred and that the secondary boronic ester had survived intact.



**Synthesis of 1-(boronic acid pinacolate ester)-2-cyclohexene (2-**

**15).** *p*-Toluene sulfonic acid (0.0247g, 0.1 eq.),

bis(pinacolato)diboron ( $B_2pin_2$ , 1.397 g, 4 eq.) and Pd catalyst (di- $\mu$ -

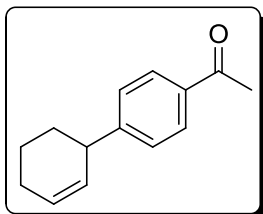
chlorobis[2-[(dimethylamino)methyl]phenyl-C-N]-dipalladium(II)) (0.0422 g, 0.05 eq)

were taken up in a flame dried Schlenk flask under a positive pressure of  $Ar_{(g)}$ . DMSO (3

mL) and MeOH (3 mL) were added *via* syringe and the reaction solution was stirred at 50

°C for 24 h. The reaction was then extracted with 3x10mL of diethyl ether and dried over

MgSO<sub>4</sub> before purification by column chromatography (40:1 Hexanes: ethyl acetate). The product was isolated in 42% yield and matched the published characterization data.<sup>2</sup>



**Cross-Coupling of 1-(boronic acid pinacolate ester)-2-cyclohexene (2-15).** In a nitrogen filled glove box, 4-iodoacetophenone (12.5 mg, 0.051 mmol), 1-(boronic acid pinacolate ester)-2-cyclohexene (16.5 mg, 0.079 mmol), Ag<sub>2</sub>O (19.34 mg, 0.083 mmol), K<sub>2</sub>CO<sub>3</sub> (11.16 mg, 0.081 mmol), Pd(PPh<sub>3</sub>)<sub>4</sub> (5.82 mg, 0.005 mmol) and PPh<sub>3</sub> (8.55 mg, 0.033 mmol) were weighed into a dried vial and taken up in 1 mL of DME. The reaction was sealed and stirred at 85 °C for 24 h. The reaction mixture was then cooled and filtered through a celite plug. The desired product was isolated by column chromatography (20:1-10:1 hexanes:ethyl acetate) in a 58% yield. <sup>1</sup>H NMR (400 MHz, CDCl<sub>3</sub>) δ 7.83 (d, *J* = 8 Hz, 2 H), 7.24 (d, *J* = 8 Hz, 2 H), 5.85 (m, *J* = inc. 2.4 Hz, 1 H), 5.62 (dd, *J* = 10 Hz, 2 Hz, 1 H), 3.98 (m, 1 H), 2.52 (s, 3 H), 2.04 (m, 2 H), 1.95 (m, 1 H), 1.72-1.62 (m, 1 H), 1.61-1.53 (m, 1 H), 1.50-1.42 (m, 1 H) <sup>13</sup>C NMR: (100 MHz, CDCl<sub>3</sub>): δ 197.9, 152.5, 135.2 (2C), 129.1, 128.5, 128.0, 41.9, 32.4, 26.6, 25.0, 21.1.

#### 6.1.7 <sup>31</sup>P NMR Studies of the Reaction

**Suzuki-Miyaura Cross-Coupling with PCy<sub>3</sub> Ligand.** In a nitrogen filled glove box, 4-iodoacetophenone (10.95 mg, 245.9 g/mol, 0.045 mmol), *rac*-pinacol(1-

phenylethyl)boronate **2-5** (15.62 mg, 232 g/mol, 0.067 mmol, 1.6 equiv.), Ag<sub>2</sub>O (15.48 mg, 234 g/mol, 0.066 mmol, 1.6 equiv.), Pd<sub>2</sub>(dba)<sub>3</sub> (1.51 mg, 915 g/mol, 0.0016 mmol, 8.1% Pd), PCy<sub>3</sub> (7.62 mg, 280 g/mol 0.027 mmol, 0.66 equivs., 8.4:1 P:Pd) and a GC calibration curve internal standard (octadecane, 10.13 mg, 254 g/mol, 0.039 mmol) were weighed into a dried vial and taken up in 1.1 mL of THF. The reaction was sealed and stirred at 70 °C for 23 h. The reaction mixture was cooled and filtered through celite, and the GC yield of the cross-coupled product was determined to be 18%. <sup>31</sup>P NMR was performed on the crude reaction solution after calibration to an H<sub>3</sub>PO<sub>4</sub> standard (0 ppm). The major peak (46.6 ppm) was assigned to tricyclohexylphosphine oxide.

**Suzuki-Miyaura Cross-Coupling with PPh<sub>3</sub> Ligand.** In a nitrogen filled glove box, 4-iodoacetophenone (12.74 mg, 245.9 g/mol, 0.052 mmol), *rac*-pinacol(1-phenylethyl)boronate **2-5** (19.15 mg, 232 g/mol, 0.082 mmol, 1.6 equiv.), Ag<sub>2</sub>O (17.38 mg, 234 g/mol, 0.074 mmol, 1.42 equiv.), Pd<sub>2</sub>(dba)<sub>3</sub> (2.00 mg, 915 g/mol, 0.0021 mmol, 8.4% Pd), PPh<sub>3</sub> (9.85 mg, 262 g/mol 0.038 mmol, 0.72 equivs., 9.0:1 P:Pd) and a GC calibration curve internal standard (octadecane, 19.46 mg, 254 g/mol, 0.076 mmol) were weighed into a dried vial and taken up in 1.1 mL of THF. The reaction was sealed and stirred at 70 °C for 18 h. The reaction mixture was cooled and filtered through celite, and the GC yield of the cross-coupled product was determined to be 60%. <sup>31</sup>P NMR was performed on the crude reaction solution after calibration to an H<sub>3</sub>PO<sub>4</sub> standard (0 ppm). A minor peak at 30.1 ppm was assigned to triphenylphosphine oxide, with the more pronominant peak at 19.9 ppm being assigned to Pd(PPh<sub>3</sub>)<sub>4</sub>.



**Suzuki-Miyaura Cross-Coupling with PPh<sub>3</sub>: Quenching the reaction while still turning over (8 h).** In a nitrogen filled glove box, 4-iodoacetophenone (12.99 mg, 245.9 g/mol, 0.053 mmol), *rac*-pinacol(1-phenylethyl)boronate **2-5** (17.23 mg, 232 g/mol, 0.074 mmol, 1.4 equiv.), Ag<sub>2</sub>O (17.70 mg, 234 g/mol, 0.076 mmol, 1.43 equiv.), Pd<sub>2</sub>(dba)<sub>3</sub> (1.81 mg, 915 g/mol, 0.0020 mmol, 7.5% Pd), PPh<sub>3</sub> (9.22 mg, 262 g/mol 0.035 mmol, 0.66 equivs., 8.8:1 P:Pd) and a GC calibration curve internal standard (octadecane, 18.21 mg, 254 g/mol, 0.072 mmol) were weighed into a dried vial and taken up in 1.1 mL of THF. The reaction was sealed and stirred at 70 °C for 8 h. The reaction mixture was cooled and filtered through celite, and the GC yield of the cross-coupled product was determined to be 32%. <sup>31</sup>P NMR was performed on the crude reaction solution after calibration to an H<sub>3</sub>PO<sub>4</sub> standard (0 ppm). Peaks at 24.6 ppm and 19.6 ppm were assigned to the oxidative addition product and Pd(PPh<sub>3</sub>)<sub>4</sub>, respectively, but the major signal was a very broad peak centred at 12.5 ppm. This peak has been assigned to alkylated/arylated Pd species resulting from transmetallation to the benzylic boronic ester. No evidence for triphenylphosphine oxide was found at this stage (8 h) of the reaction.

**Assigning the major species during turnover of the Suzuki-Miyaura Cross-coupling: PPh<sub>3</sub> and Pd<sub>2</sub>(dba)<sub>3</sub>.** In a nitrogen-filled glovebox, Pd<sub>2</sub>(dba)<sub>3</sub> (1.73 mg, 915 g/mol, 0.0019 mmol) and PPh<sub>3</sub> (9.34 mg, 262 g/mol, 0.036 mmol, 9.5:1 P:Pd) were taken up in 1 g of THF and heated to 70 °C for 8 h. <sup>31</sup>P NMR was performed on the crude reaction

solution after calibration to an  $\text{H}_3\text{PO}_4$  standard (0 ppm). The major peak observed in the  $^{31}\text{P}$  NMR was at 0 ppm

**Assigning the major species during turnover of the Suzuki-Miyaura Cross-coupling:**

**$\text{PPh}_3$ ,  $\text{Pd}_2(\text{dba})_3$  and  $\text{ArI}$ .** In a nitrogen-filled glovebox,  $\text{Pd}_2(\text{dba})_3$  (1.84 mg, 915 g/mol, 0.0020 mmol),  $\text{PPh}_3$  (9.95 mg, 262 g/mol, 0.038 mmol, 9.5:1 P:Pd) were taken up in 1 g of THF and heated to 70 °C for 8 h.  $^{31}\text{P}$  NMR was performed on the crude reaction solution after calibration to an  $\text{H}_3\text{PO}_4$  standard (0 ppm). Two major peaks were observed; the largest (at -4.6 ppm) was assigned to free  $\text{PPh}_3$  whereas the second peak at 23.8 ppm was assigned to the Pd species resulting from oxidative addition.

**Assigning the major species during turnover of the Suzuki-Miyaura Cross-coupling:**

**$\text{PPh}_3$ ,  $\text{Pd}_2(\text{dba})_3$ ,  $\text{ArI}$  and  $\text{Ag}_2\text{O}$ .** In a nitrogen-filled glovebox,  $\text{Pd}_2(\text{dba})_3$  (1.75 mg, 915 g/mol, 0.0019 mmol),  $\text{PPh}_3$  (9.77 mg, 262 g/mol, 0.037 mmol, 9.7:1 P:Pd) were taken up in 1 g of THF and heated to 70 °C for 8 h.  $^{31}\text{P}$  NMR was performed on the crude reaction solution after calibration to an  $\text{H}_3\text{PO}_4$  standard (0 ppm). Again, the broad peak centred about 0 ppm was found to be the only signal observed by  $^{31}\text{P}$  NMR.

*6.1.8 The Unexpected Effect of  $[\text{PPh}_3]$  on Stereoretention*

**Effect of [PPh<sub>3</sub>] on Stereoretention: Study performed in Anhydrous DME.** Cross-coupling experiments were performed on a 0.1 mmol scale between 4-iodoacetophenone and (*R*)-pinacol(1-phenylethyl)boronate (**(*R*)-2-5**, e.r. = 98.5:1.5) in anhydrous DME. The PPh<sub>3</sub> loading was systematically increased over the range of 2-12 equivalents of phosphorous to Pd for five distinct replicates (2, 4, 6, 8 and 12 equivalents PPh<sub>3</sub> to Pd). For example, 4-iodoacetophenone (25.95 mg, 245.9 g/mol, 0.106 mmol), (*R*)-pinacol(1-phenylethyl)boronate (34.27 mg, 232 g/mol, 0.148 mmol, er = 98.5:1.5, 1.4 equiv.) Ag<sub>2</sub>O (35.56 mg, 234 g/mol, 0.152 mmol, 1.4 equiv.), Pd<sub>2</sub>(dba)<sub>3</sub> (3.57 mg, 915 g/mol, 0.0039 mmol, 7.4 mol% Pd), PPh<sub>3</sub> (26.17 mg, 262 g/mol, 0.099 mmol, 0.94 equiv, 12.6 P:Pd) and an internal GC standard (octadecane, 25.95 mg, 254 g/mol, 0.102 mmol) were taken up in DME (1.9 g). The reaction was sealed and stirred at 85 °C for 24 h. Once cooled, the crude reaction solution was filtered through celite, and an aliquot was taken to determine the GC yield of the reaction (42%) The product was isolated by column chromatography (20:1 hexanes: ethyl acetate for 1 column volume, switching to 10:1 hexanes:ethyl acetate) in 40% yield. The enantiomeric ratio was determined by SFC analysis (OJ-H Column, 5% MeOH, 2 mL, 200 bar) to be 90.6:9.4, a 92% retention of e.r.

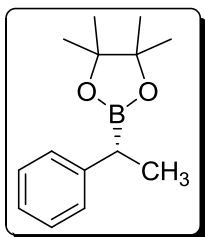
**The Effect of [H<sub>2</sub>O] on Yield and Stereoretention of the Suzuki-Miyaura Cross-Coupling.** The effect of water concentration on the yield and stereoretention of the standard cross-coupling reaction was examined. Individual experiments (0.05 mmol scale) were performed in anhydrous DME and in the presence of 100-8000 ppm of added water. The concentration of PPh<sub>3</sub> was held constant at 8 equivalents per Pd for all

replicates. To achieve low (sub 1000 ppm) concentrations of water, a weighed amount of water was taken up in a separate vial containing a known mass of DME solvent. A weighed amount of this solution was then added to the reaction already taken up in a known weight of anhydrous DME. As an example, 4-iodoacetophenone (12.94 mg, 245.9 g/mol, 0.053 mmol), (*R*)-pinacol(1-phenylethyl)boronate (**(*R*)-2-5**, 18.68 mg, 232 g/mol, 0.081 mmol, er = 98.5:1.5, 1.5 equiv.) Ag<sub>2</sub>O (18.13 mg, 234 g/mol, 0.077 mmol, 1.45 equiv.), Pd(PPh<sub>3</sub>)<sub>4</sub> (4.56 mg, 1155.6 g/mol, 0.0039 mmol, 7.4 mol% Pd), PPh<sub>3</sub> (4.17 mg, 262 g/mol, 0.016 mmol, 0.30 equiv, 8.1:1 P:Pd), K<sub>2</sub>CO<sub>3</sub> (10.80 mg, 138 g/mol, 0.078 mmol, 1.56 equiv.) and an internal GC standard (octadecane, 20.90 mg, 254 g/mol, 0.082 mmol) were taken up in anhydrous DME (1.00 g). In a separate vial, 6.46 mg of H<sub>2</sub>O was added to 0.541 g of anhydrous DME. 9.15 mg of this last H<sub>2</sub>O/DME solution were added to the reaction solution *via* syringe through the septum-containing Teflon cap, resulting in an H<sub>2</sub>O concentration of 108 ppm in the reaction solution. The septum was covered with Teflon tape and the cap was sealed with a generous amount of parafilm before being put in an 85 °C oil bath for 24 h. Once cooled, the reaction solution was passed through a celite plug and the GC yield of the reaction was determined to be 49%. The cross-coupled product was purified by silica gel chromatography (20:1 hexanes:ethyl acetate). The enantiomeric ratio was determined by SFC analysis (OJ-H Column, 5% MeOH, 2 mL, 200 bar) to be 95.3:4.7, a 97% retention of er.

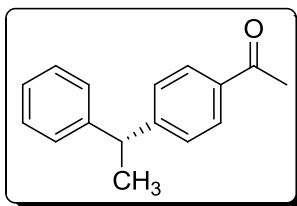
**The effect of [PPh<sub>3</sub>] on yield and stereoretention of the Suzuki-Miyaura Cross-Coupling at 1000 ppm of H<sub>2</sub>O.** The effect of varying the ratio of PPh<sub>3</sub>:Pd at a relatively

constant, yet non-zero concentration of added water as examined. Water concentrations on the order of 6500-8500 ppm were chosen due to the maximum yield output, though water concentrations nearing 500 ppm should be employed to obtain high yields and more acceptable levels of stereoretention. Ultimately, the trends observed in anhydrous DME, namely an increasing yield and decreasing stereoretention as the ratio of PPh<sub>3</sub>:Pd was increased, carried over to the DME:H<sub>2</sub>O solvent system. As an example, 4-iodoacetophenone (12.75 mg, 245.9 g/mol, 0.052 mmol), (*R*)-pinacol(1-phenylethyl)boronate (**(R)-2-5**, 18.32 mg, 232 g/mol, 0.079 mmol, er = 98.5:1.5, 1.52 equiv.) Ag<sub>2</sub>O (17.67 mg, 234 g/mol, 0.076 mmol, 1.45 equiv.), Pd<sub>2</sub>(dba)<sub>3</sub> (1.95 mg, 915 g/mol, 0.0021 mmol, 8.2 mol% Pd), PPh<sub>3</sub> (2.12 mg, 262 g/mol, 0.008 mmol, 0.16 equiv, 1.9:1 P:Pd), K<sub>2</sub>CO<sub>3</sub> (10.43 mg, 138 g/mol, 0.076 mmol, 1.45 equiv.) and an internal GC standard (octadecane, 20.89 mg, 254 g/mol, 0.082 mmol) were taken up in anhydrous DME (0.998 g). Once removed from the glovebox, 8.0 mg of H<sub>2</sub>O were added to the reaction solution *via* syringe through the septum-containing Teflon cap, resulting in an H<sub>2</sub>O concentration of 8000 ppm in the reaction solution. The septum was covered with Teflon tape and the cap was sealed with a generous amount of parafilm before being put in an 85 °C oil bath for 24 h. Once cooled, the reaction solution was passed through a celite plug and the GC yield of the reaction was determined to be 47%. The cross-coupled product was purified by silica gel chromatography (20:1 hexanes:ethyl acetate). The enantiomeric ratio was determined by SFC analysis (OJ-H Column, 5% MeOH, 2 mL, 200 bar) to be 97.4:2.6, a 99% retention of er.

### 6.1.9 Towards a Mechanistic Understanding of the Reaction

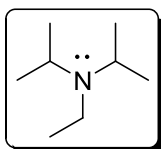


**Effect of the Reaction Conditions on the Enantiopurity of Starting Benzylic Boronic Ester (*R*)-2-5.** In a nitrogen-filled glovebox, (*R*)-pinacol(1-phenylethyl)boronate ((*R*)-2-5, 35.70 mg, 232 g/mol, 0.154 mmol, er = 98.5:1.5, 1.5 equiv.), Ag<sub>2</sub>O (35.12 mg, 234 g/mol, 0.150 mmol), Pd<sub>2</sub>(dba)<sub>3</sub> (3.27 mg, 915 g/mol, 0.0036 mmol), PPh<sub>3</sub> (25.24 mg, 262 g/mol, 0.016 mmol, 0.96 equiv), and K<sub>2</sub>CO<sub>3</sub> (21.07 mg, 138 g/mol, 0.152 mmol) were taken up in anhydrous DME (1.90 g). Once removed from the glovebox, 11.9 mg of H<sub>2</sub>O were added to the reaction solution *via* syringe through the septum-containing Teflon cap, resulting in an H<sub>2</sub>O concentration of 6200 ppm in the reaction solution. The septum was covered with Teflon tape and the cap was sealed with a generous amount of parafilm before being put in an 85 °C oil bath for 24 h. Once cooled, the crude reaction was filtered through celite twice and washed with copious amounts of diethyl ether. The boronic ester was oxidized without prior purification with a pre-made 2:1 1M NaOH<sub>(aq.)</sub>:H<sub>2</sub>O<sub>2</sub> solution under air-free conditions. The resultant alcohol (*sec*-phenethanol) was isolated by silica gel chromatography (10:1 hexanes:ethyl acetate) and the enantiomeric ratio was determined by SFC analysis (OJ-H Column, 5% MeOH, 2 mL, 200 bar) to be 96.2:3.8 from an initial er = 98.5:1.5.



**Effect of the Suzuki-Miyaura Reaction Conditions on the Enantiopurity of (*R*)-1-phenyl-1-(4-acetylphenyl)ethane**

**(*R*)-2-6**. Cross-coupled product (*R*)-2-6 with initial e.r. of 97.4:2.3 was resubjected to the the harshest reaction conditions (in the absence of benzylic boronic ester) and analyzed for any possible loss of enantiopurity. (*R*)-1-phenyl, 1-(4-acetylphenyl)ethane (synthesized with a  $\text{PPh}_3:\text{Pd} = 2$ , er = 97.4:2.3), 4-iodoacetophenone (12.50 mg, 245.9, 0.051 mmol),  $\text{Ag}_2\text{O}$  (18.06 mg, 234 g/mol, 0.077 mmol),  $\text{Pd}_2(\text{dba})_3$  (1.74 mg, 915.7 g/mol, 0.0019 mmol) and  $\text{K}_2\text{CO}_3$  (12.49 mg, 138 g/mol, 0.091 mmol) were taken up in 1.09 g of anhydrous DME. Once removed from the glovebox, 6.7 mg of  $\text{H}_2\text{O}$  were added to the reaction solution *via* syringe through the septum-containing Teflon cap, resulting in an  $\text{H}_2\text{O}$  concentration of 6100 ppm in the reaction solution. The septum was covered with Teflon tape and the cap was sealed with a generous amount of parafilm before being put in an 85 °C oil bath for 24 h. Once cooled, the crude reaction was filtered through celite twice and washed with copious amounts of diethyl ether. The diarylethane was isolated by silica gel chromatography (20:1 hexanes:ethyl acetate) and the enantiomeric ratio was determined by SFC analysis (OJ-H Column, 5% MeOH, 2 mL, 200 bar) to be 97.3:2.7 from an initial er = 97.4:2.3.



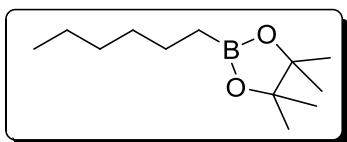
**Higher Observed Stereoretention for the Suzuki-Miyaura Cross-Coupling with Hünig's Base.**

In a nitrogen-filled glovebox, 4-iodoacetophenone (12.40 mg, 245.9 g/mol, 0.050 mmol), (*R*)-pinacol(1-phenylethyl)boronate (**(*R*)-2-5**, 17.89 mg, 232 g/mol, 0.077 mmol, er = 98.5:1.5, 1.54

equiv.), Ag<sub>2</sub>O (17.46 mg, 234 g/mol, 0.075 mmol, 1.5 equiv.), Pd<sub>2</sub>(dba)<sub>3</sub> (1.76 mg, 915 g/mol, 0.0019 mmol, 7.7 mol% Pd), PPh<sub>3</sub> (12.36 mg, 262 g/mol, 0.047 mmol, 0.94 equiv, 12.4 P:Pd) and an internal GC standard (octadecane, 20.03 mg, 254 g/mol, 0.079 mmol) were taken up in DME (1.05 g). The reaction was sealed, and stirred at 85 °C for 24 h. Once cooled, the crude reaction solution was filtered through celite, and an aliquot was taken to determine the GC yield of the reaction (45%) The product was isolated by column chromatography (20:1 hexanes: ethyl acetate) and the enantiomeric ratio was determined by SFC analysis (OJ-H Column, 5% MeOH, 2 mL, 200 bar) to be 89.8:10.2, a 91% retention of er. Under similar conditions (anhydrous DME and 12 equivalents of PPh<sub>3</sub> per Pd), reactions performed with K<sub>2</sub>CO<sub>3</sub> were found to have an e.r. = 86.4:13.6.

## 6.2 Lithiation-Borylation to Synthesize Novel Asymmetric Boronic Ester Cross-Coupling Partners

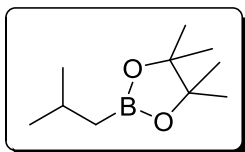
### 6.2.1 Synthesis of Racemic Secondary Allylic Boronic Esters



**1-hexylboronic acid pinacolate ester (3-9).** 1.514 g of 1-hexylboronic acid (130 g/mol, 11.64 mmol, 1.0 equiv.) and 1.374 g of pinacol (118 g/mol, 11.64 mmol, 1.0 equiv.) were taken up in 10 mL of diethyl ether. Once dissolved, 1.415 g of MgSO<sub>4</sub> (120 g/mol, 11.8 mmol, 1.0 equiv.) was dispersed in the solution, which was stirred at 25 °C for 24 h. The dispersion was filtered by vacuum and washed with copious amounts of diethyl ether. The homogeneous

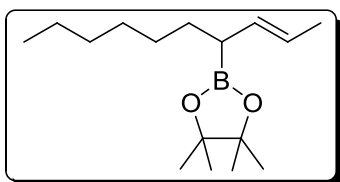


solution was then concentrated *in vacuo* to yield the pure boronic ester in 98% isolated yield. **<sup>1</sup>H NMR:** (400 MHz, CDCl<sub>3</sub>) δ 1.37-1.28 (m, 2 H), 1.23-1.19 (m, 6 H), 1.17 (s, 12H), 0.80 (m, 3 H), 0.69 (t, *J* = 7.6 Hz, 2 H) **<sup>11</sup>B NMR:** (160 MHz, CDCl<sub>3</sub>): δ 34.1. **<sup>13</sup>C NMR:** (100 MHz, CDCl<sub>3</sub>) δ 82.8, 32.1, 31.6, 24.8, 23.9, 22.5, 14.0 12-11 (br.). **HRMS (EI-TOF):** calcd for [M]<sup>+</sup> (C<sub>12</sub>H<sub>25</sub>O<sub>2</sub>B) *m/z* 212.1948; found 212.1956.



**1-(2-methylpropyl)-boronic acid pinacolate ester.** Prepared by same procedure as alkyl boronic ester **3-9**. *iso*-butylboronic acid (510.8 mg, 102 g/mol, 5.01 mmol, 1.0 equiv), pinacol (591.8 mg,

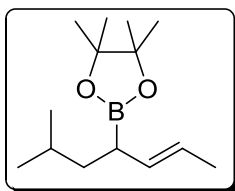
118 g/mol, 5.01 mmol, 1.0 equiv.) and MgSO<sub>4</sub> (595 mg, 120 g/mol, 4.96 mmol, 1.0 equiv.) were added to 25 mL Et<sub>2</sub>O and stirred at 25 °C for 22 h. Vacuum filtration and concentration of the ethereal solution *in vacuo* yielded 838 mg of clear oil, representing a 91% isolated yield. **<sup>1</sup>H NMR:** (400 MHz, CDCl<sub>3</sub>) δ 1.79 (heptuplet, *J* = 6.8 Hz, 1 H), 1.18 (s, 12 H), 0.85 (d, *J* = 6.8 Hz, 6 H), 0.66 (d, *J* = 7.2 Hz, 2 H). **<sup>11</sup>B NMR:** (160 MHz, CDCl<sub>3</sub>): δ 33.9. **<sup>13</sup>C NMR:** (100 MHz, CDCl<sub>3</sub>) δ 82.8, 25.2, 24.8, 24.8



**4-(Boronic acid pinacolate ester)-2-decene (3-10a).**

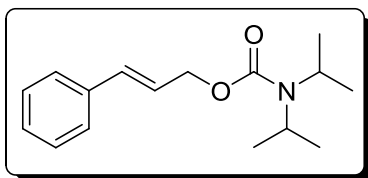
Drisolv dichloromethane (0.9 mL, 14.2 mmol, 15 equiv.), stored under Ar<sub>(g)</sub>, was added to 3.5 mL of freshly distilled THF. While under Ar<sub>(g)</sub>, the solution was dropped to an internal temperature of -90 °C by cooling in an N<sub>2</sub>/MeOH bath. *s*-butyllithium (1.1 mL, 1.3 M, 1.4 equiv.) was added

dropwise to the stirring solution, with care given to keep the internal temperature below -85 °C. Lithiation was allowed to proceed at -90 °C for 60 min prior to the dropwise addition of the 1-hexyboronic acid pinacolate ester solution (161.6 mg, 0.762 mmol, 0.8 equiv., 1 mL THF). The solution was kept at -90 °C for 30 min to ensure complete borylation before addition of ZnCl<sub>2</sub> (0.95 mL, 1.0 M, 0.95 mmol, 1 equiv.). After addition of ZnCl<sub>2</sub>, the solution was slowly warmed to 0 °C at which point the reaction was quenched with 2x 5 mL sat. NH<sub>4</sub>Cl<sub>(aq.)</sub> aliquots. The aqueous layers were washed with 3 x 10 mL Et<sub>2</sub>O. The organic layers were combined and dried with anhydrous MgSO<sub>4</sub> and filtered by vacuum. The ethereal solution was concentrated *in vacuo* to yield a slightly yellow crude oil. This oil was then taken up in 4 mL of freshly distilled Et<sub>2</sub>O and cooled to 0 °C. To this solution was added 1-propenylmagnesium bromide (2.3 mL, 0.5 M, 1.22 equiv.). The solution was allowed to warm to 25 °C before aqueous quench and workup. The resultant yellow oil was purified by silica gel chromatography (80:1 hexanes:ethyl acetate, R<sub>f</sub> = 7/20) to give 104.0 mg (51% isolated yield) of a clear, viscous oil. <sup>1</sup>H NMR (400 MHz, CDCl<sub>3</sub>) δ 5.41-5.20 (m, 2 H), 2.04-1.95 (m, 1 H), 1.57-1.52 (dd, J = 6.6 Hz, 1.4 Hz, 3 H), 1.19-1.16 (m, 22 H), 0.82-0.78 (m, 3 H) <sup>11</sup>B NMR: (160 MHz, CDCl<sub>3</sub>): δ 33.1 <sup>13</sup>C NMR: (100 MHz, CDCl<sub>3</sub>): δ 131.8, 122.9, 82.9, 65.9, 31.8, 31.2, 29.4, 29.2, 24.8, 24.7, 24.6, 24.5, 22.6, 15.3, 14.1, 13.1.



**Synthesis of 4-(Boronic acid pinacolate ester)-6-methyl-2-heptene (3-10b).** Drisolv dichloromethane (1.0 mL, 16.3 mmol, 15 equiv.) was added to 5.0 mL of freshly distilled THF. While under

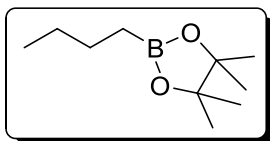
Ar<sub>(g)</sub>, the solution was dropped to an internal temperature of -90 °C by cooling in an N<sub>2</sub>/MeOH bath. *s*-butyllithium (1.2 mL, 1.22 M, 1.4 mmol, 1.3 equiv.) was added dropwise to the stirring solution, with care given to keep the internal temperature below -85 °C. Lithiation was allowed to proceed at -90 °C for 75 min. prior to the dropwise addition of the 1-(2-methylpropyl)-boronic acid pinacolate ester solution (200 mg, 1.09 mmol, 1.0 equiv., 2 mL THF). The solution was kept at -90 °C for 45 min to ensure complete borylation before addition of ZnCl<sub>2</sub> (1.2 mL, 1.0 M, 1.2 mmol, 1.1 equiv.). After addition of ZnCl<sub>2</sub>, the solution was slowly warmed to 0 °C overnight at which point the reaction was quenched with 2x 5 mL sat. NH<sub>4</sub>Cl<sub>(aq.)</sub> aliquots. The aqueous layers were washed with 3x 10 mL Et<sub>2</sub>O. The organic layers were combined and dried with anhydrous MgSO<sub>4</sub> and filtered by vacuum. The ethereal solution was concentrated *in vacuo* to yield a slightly yellow crude oil. This oil was then taken up in 4 mL of freshly distilled Et<sub>2</sub>O and cooled to 0 °C. To this solution was added 1-propenylmagnesium bromide (2.3 mL, 0.5 M, 1.22 equiv.). The solution was kept at 0 °C for 2 h before being allowed to warm to 25 °C. Aqueous workup (as above) preceded purification by silica gel chromatography (80:1 hexanes: ethyl acetate, 1 inch column). Incomplete borylation led to contamination of the product by starting alkyl boronic ester. Distillation under high vacuum, aided by heat source, led to pure product but in very reduced yield (9% isolated, overall). NMR Characterization complicated by the presence of an isomeric mixture of products. **LRMS:** 238.2 *m/z* (expected = 238).



***N,N*-Diisopropyl carbamic acid cinnamyl ester (3-**

**11).** *N,N*-Diisopropylcarbamoyl chloride (1.953 g, 163.65 g/mol, 11.94 mmol, 1.05 equiv.) and freshly distilled

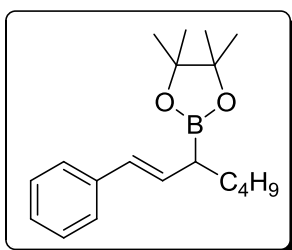
triethylamine (1.6 mL, 0.726 g/mL, 101.2 g/mol, 11.5 mmol, 1.0 equiv.) were taken up in 20 mL of CH<sub>2</sub>Cl<sub>2</sub>. Cinnamyl alcohol (semi-solid, 1.57 g, 134.2 g/mol, 11.7 mmol, 1 equiv.) was added and the solution was stirred under refluxing conditions for 21 h, with salts eventually precipitating out of solution. The solution was washed with sat. NH<sub>4</sub>Cl<sub>(aq.)</sub> and the aqueous layer was extracted with 3 x 25 mL CH<sub>2</sub>Cl<sub>2</sub>. The crude oil was purified by silica gel chromatography (Load 20:1 hexanes:ethyl acetate, elute 10:1 hexanes:ethyl acetate, 2 inch by 5 inch column) to yield 1.928 g of the desired carbamate, or 63% isolated yield. **<sup>1</sup>H NMR** (400 MHz, CDCl<sub>3</sub>) δ 7.31 (d, *J* = 7.6 Hz, 2 H), 7.25-7.15 (m, 5 H), 6.55 (d, *J* = 16 Hz, 1 H), 6.25 (dt, *J* = 15.6 Hz, 6.4 Hz, 1 H), 4.67 (dd, *J* = 6.8 Hz, 1.2 Hz, 2 H), 4.0-3.6 (d, br, 2 H), 1.14 (d, *J* = 6.8 Hz, 12 H). **<sup>13</sup>C NMR:** (100 MHz, CDCl<sub>3</sub>): δ 155.4, 136.6, 133.0, 128.6, 127.8, 126.6, 124.7, 65.2, 46 (br), 21.0 (br). **HRMS (EI-TOF):** calcd for [M]<sup>+</sup> (C<sub>16</sub>H<sub>23</sub>O<sub>2</sub>N) *m/z* 261.1729; found 261.1733.



**Synthesis of 1-butylboronic acid pinacolate ester .** 1.519 g of 1-

hexylboronic acid (101.8 g/mol, 14.9 mmol, 1.0 equiv.) and 1.763 g of pinacol (118 g/mol, 14.9 mmol, 1.0 equiv.) were taken up in 15 mL of diethyl ether. Once dissolved, 1.783 g of MgSO<sub>4</sub> (120 g/mol, 14.9 mmol, 1.0 equiv.) was dispersed in the solution, which was stirred at 25 °C for 24 h. The dispersion was filtered by vacuum and washed with copious amounts of diethyl ether. The homogeneous solution was then

concentrated *in vacuo* to yield 2.105 g of the pure boronic ester, or 77% isolated yield.  $^1\text{H}$  NMR (400 MHz,  $\text{CDCl}_3$ )  $\delta$  1.36 (m, 4 H), 1.25 (s, 12 H), 0.89 (t,  $J = 9.6$  Hz, 3 H), 0.78 (m, 2 H).  $^{11}\text{B}$  NMR: (160 MHz,  $\text{CDCl}_3$ ):  $\delta$  21.  $^{13}\text{C}$  NMR: (100 MHz,  $\text{CDCl}_3$ ):  $\delta$  82.8, 26.2, 25.4, 24.8, 13.9, 10 (br). HRMS (EI-TOF): calcd for  $[\text{M}]^+$  ( $\text{C}_{10}\text{H}_{21}\text{O}_2\text{B}$ )  $m/z$  184.1635; found 184.1642.



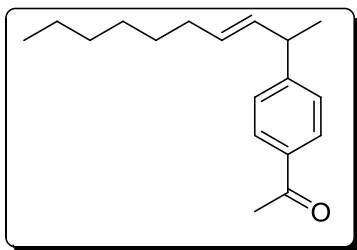
**3-(boronic acid pinacolate ester)-1-phenyl-1-heptene (3-**

**10c).** *N,N*-Diisopropyl carbamic acid cinnamyl ester **3-11** (282.7 mg, 261 g/mol, 1.083 mmol, 1.15 equiv.) and (-)-sparteine (0.3 mL, 1.02 g/mL, 234.4 g/mol, 1.4 mmol, 1.45 equiv.) were taken

up in diethyl ether and cooled to  $-78$  °C in a dry ice/acetone bath. *s*-Butyllithium (1.1 mL, 1.3 M, 1.4 mmol, 1.45 equiv.) was added dropwise to the cold solution, creating a bright yellow solution, which eventually turned to dark green. After 4 h of lithiation, an ethereal solution of 1-butylboronic acid pinacolate ester (177.1 mg, 184 g/mol, 0.94 mmol, 1.0 equiv., 1 mL  $\text{Et}_2\text{O}$ ) was added dropwise. No colour change was observed. After 5 h borylation, freshly prepared  $\text{MgBr}_2$  diethyl etherate (3.0 equiv.) was added to the cold solution as an ethereal solution.  $\text{MgBr}_2$  diethyl etherate is prepared by adding a necessary amount of 1,2-dibromoethane, in this case, 3 equivalents per boronic ester to an excess of Mg turnings in dry ether. The contents of the dense layer that dissociates from the ether are added to the reaction solution *via* syringe. After addition of the  $\text{MgBr}_2$ , the solution is allowed to warm slowly before being heated to reflux overnight. After aqueous workup, two silica gel chromatography steps (20:1 hexanes:ethyl acetate) were required and only

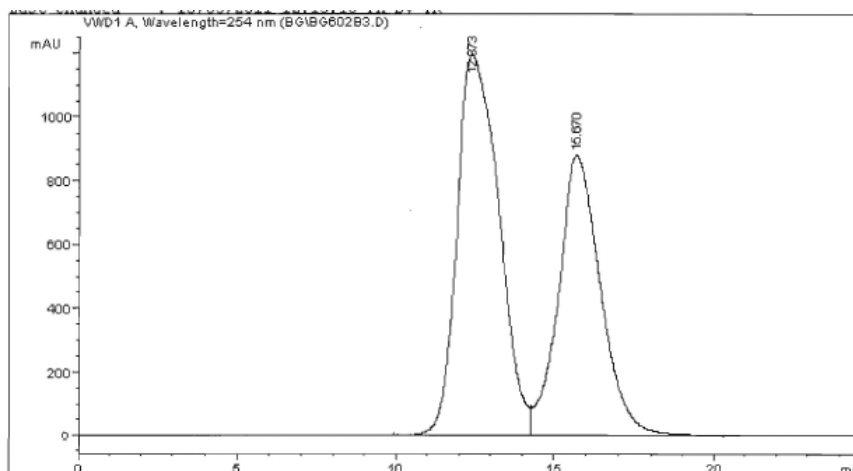
50.3 mg (18% yield) of white solid was isolated. The process was also performed with the achiral TMEDA ligand and gave similar yields. In the interest of obtaining a useable amount of product, the two batches were combined.  $^1\text{H NMR}$  (400 MHz,  $\text{CDCl}_3$ )  $\delta$  7.27 (d,  $J = 7.2$  Hz, 2 H), 7.20 (t,  $J = 7.6$  Hz, 2 H), 7.09 (m, 1 H), 6.28 (d,  $J = 15.6$  Hz, 1 H), 6.13 (dd,  $J = 16.0$  Hz, 9.2 Hz, 1 H), 1.89 (q,  $J = 8.0$  Hz, 1 H), 1.56 (m, 1 H), 1.44 (m, 1 H), 1.25 (m, 4 H), 1.17 (s, 12 H), 0.81 (t,  $J = 6.8$  Hz, 3 H).  $^{13}\text{C NMR}$ : (100 MHz,  $\text{CDCl}_3$ ):  $\delta$  138.3, 132.2, 128.9, 128.4, 126.5, 125.9, 83.3, 31.5, 30.5, 24.6, 14.1.

### 6.2.2 Cross-Coupling of Racemic Secondary Allylic Boronic Esters



**Synthesis of 2-(4-acetylphenyl)-3-decene (3-12aa).** In a nitrogen-atmosphere glovebox, 4-iodoacetophenone (12.68 mg, 245.9 g/mol, 0.052 mmol, 1.0 equiv.), 4-(boronic acid pinacolate ester)-2-decene (**3-10a**, 22.65 mg, 266 g/mol, 0.085 mmol, 1.6 equiv.),  $\text{Ag}_2\text{O}$  (18.80 mg, 234 g/mol, 0.081 mmol, 1.6 equiv.),  $\text{Pd}(\text{PPh}_3)_4$  (4.55 mg, 1155.6 g/mol, 0.004 mmol, 7.6 mol% Pd),  $\text{PPh}_3$  (5.03 mg, 262 g/mol, 0.019 mmol, 0.37 equiv., 8.75:1 P: Pd) and  $\text{K}_2\text{CO}_3$  (12.65 mg, 138 g/mol, 0.092 mmol, 1.76 equiv.) were added to a tared 1 dram vial and taken up in 980 mg of DME. The reaction solution was sealed in the glovebox, removed, and placed in an 85 °C oil bath for 24 h. Once cooled, the reaction solution was passed through a celite plug and washed with copious amounts of diethyl ether. The solution was concentrated *in vacuo* to dryness and

an NMR internal standard was added (hexamethylbenzene, HMB, 6.68 mg). NMR yield of the major isomer was determined to be 78% and the ratio of major ( $\gamma$ ) to minor ( $\alpha$ ) isomers was 92:8 prior to isolation. Peak assignments for major and minor isomers were performed using 2D COSY-NMR correlations. The crude mixture was purified by silica gel chromatography (20:1 hexanes:ethyl acetate) and 11.2 mg of a mixture of isomers ( $\gamma$ : $\alpha$  = 87:13) was obtained, representing an 84% isolated yield.  **$^1\text{H}$  NMR** (400 MHz,  $\text{CDCl}_3$ )  $\delta$  7.82 (d,  $J$  = 8.4 Hz, 2 H), 7.22 (d,  $J$  = 8.4 Hz, 2 H), 5.48-5.40 (m, 2 H), 3.42-3.39 (m, inc.  $J$  = 7.2 Hz, 1 H), 2.51 (s, 3 H), 1.96-1.91 (m, 2 H), 1.28 (d,  $J$  = 7.2 Hz, 3 H), 1.22-1.14 (m, 8 H), 0.82-0.80 (m, 3 H)  **$^{13}\text{C}$  NMR** (100 MHz,  $\text{CDCl}_3$ )  $\delta$  197.8, 152.3, 135.2, 133.9, 130.3, 128.6, 127.4, 42.4, 32.5, 31.7, 29.4, 28.8, 26.6, 22.6, 21.3, 14.1. (13.1) **HRMS (EI-TOF)**: calcd for  $[\text{M}]^+$  ( $\text{C}_{18}\text{H}_{26}\text{O}$ )  $m/z$  258.1984; found 258.1977. **Chiral HPLC**: Column = AD-H, 99.8:0.2 hexanes: *i*-PrOH, 0.6 mL/min, Detector  $\lambda$  = 254 nm.



```

=====
                          Area Percent Report
=====
Sorted By      :      Signal
Multiplier    :      1.0000
Dilution      :      1.0000
Sample Amount  :      1.00000 [ng/ul] (not used in calc.)
Use Multiplier & Dilution Factor with ISTDs

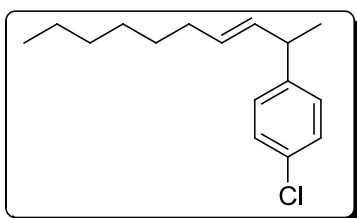
Signal 1: VWD1 A, Wavelength=254 nm

Peak RetTime Type Width Area Height Area
# [min] [min] mAU *s [mAU] l %
-----|-----|-----|-----|-----|-----
1 12.373 BV 1.4731 1.09123e5 1193.28735 57.8302
2 15.670 VB 1.3341 7.95723e4 876.72577 42.1698

Totals : 1.88695e5 2070.01312

Results obtained with enhanced integrator!
=====
*** End of Report ***

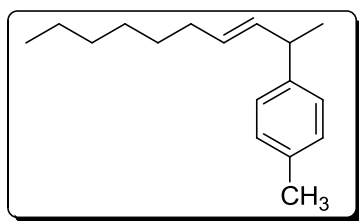
```



**Synthesis of 2-(4-chlorophenyl)-3-decene (3-12ab).** In a nitrogen-atmosphere glovebox, 4-chloriodobenzene (12.62 mg, 238.4 g/mol, 0.053 mmol, 1.0 equiv.), 4-(boronic acid pinacolate ester)-2-decene (**3-10a**, 23.35 mg, 266 g/mol, 0.088 mmol, 1.67 equiv.), Ag<sub>2</sub>O (18.60 mg, 234 g/mol, 0.080 mmol, 1.50 equiv.), Pd(PPh<sub>3</sub>)<sub>4</sub> (4.50 mg, 1155.6 g/mol, 0.0039 mmol, 7.3 mol% Pd), PPh<sub>3</sub> (4.23 mg, 262 g/mol, 0.016 mmol, 0.30 equiv., 8.10:1 P: Pd) and K<sub>2</sub>CO<sub>3</sub> (10.66 mg, 138 g/mol, 0.077 mmol, 1.46 equiv.) were added to a tared 1 dram vial and taken up in 1.10 g of DME. The reaction solution was

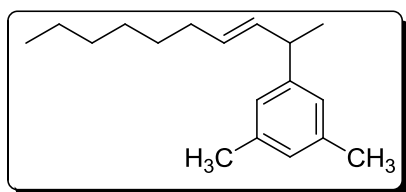


sealed in the glovebox, removed, and placed in an 85 °C oil bath for 24 h. Once cooled, the reaction solution was passed through a celite plug and washed with copious amounts of diethyl ether. The solution was concentrated *in vacuo* to dryness and an NMR internal standard was added (*p*- dimethoxybenzene, DMB, 10.42 mg). The NMR yield of the major isomer was determined to be 72% and the ratio of major ( $\gamma$ ) to minor ( $\alpha$ ) isomers (assigned by 2D-COSY NMR correlations) was 83:17 prior to isolation. The crude mixture was purified by silica gel chromatography (20:1 hexanes:ethyl acetate) and 13.25 mg of a mixture of isomers ( $\gamma$ : $\alpha$  = 79:21) was obtained, representing an 83% isolated yield. **<sup>1</sup>H NMR** (400 MHz, CDCl<sub>3</sub>)  $\delta$  7.18 (d, *J* = 6 Hz, 2 H), 7.06 (d, *J* = 8.4 Hz, 2 H), 5.50-5.40 (m, 1 H), 5.40-5.28 (m, 1 H), 3.32 (dq, *J* = 6.8 Hz, 1 H), 1.93 (m, 2 H), 1.3-1.15 (m, 8 H), 1.23 (d, *J* = 6.8 Hz, 3 H), 0.81 (m, 3 H). **<sup>13</sup>C NMR** (100 MHz, CDCl<sub>3</sub>)  $\delta$  145.0, 134.4, 129.8, 128.6, 128.4, 124.9, 41.7, 32.5, 31.7, 29.4, 28.8, 22.6, 21.5, 14.1. **HRMS (EI-TOF)**: calcd for [M]<sup>+</sup> (C<sub>16</sub>H<sub>23</sub>Cl) *m/z* 250.1488; found 250.1483.



**Synthesis of 2-(4-tolyl)-3-decene (3-12ac).** In a nitrogen-atmosphere glovebox, 4-iodotoluene (11.80 mg, 217.9 g/mol, 0.054 mmol, 1.0 equiv.), 4-(boronic acid pinacolate ester)-2-decene (**3-10a**, 20.14 mg, 266 g/mol, 0.076 mmol, 1.41 equiv.), Ag<sub>2</sub>O (17.50 mg, 234 g/mol, 0.075 mmol, 1.38 equiv.), Pd(PPh<sub>3</sub>)<sub>4</sub> (4.52 mg, 1155.6 g/mol, 0.0039 mmol, 7.2 mol% Pd), PPh<sub>3</sub> (4.52 mg, 262 g/mol, 0.017 mmol, 0.32 equiv., 8.36:1 P:Pd) and K<sub>2</sub>CO<sub>3</sub> (11.97 mg, 138 g/mol, 0.087 mmol, 1.61 equiv.) were added to a tared 1 dram vial and taken up in 1.0 g of DME. The reaction solution was sealed in the glovebox,

removed, and placed in an 85 °C oil bath for 24 h. Once cooled, the reaction solution was passed through a celite plug and washed with copious amounts of diethyl ether. The solution was concentrated *in vacuo* to dryness. The crude mixture ( $\gamma$ : $\alpha$  = 90:10, assigned by 2D-COSY NMR correlation) was purified by silica gel chromatography (20:1 hexanes:ethyl acetate) and 8.7 mg of a mixture of isomers was obtained, representing an 70% isolated yield. The ratio of the major ( $\gamma$ ) and minor ( $\alpha$ ) products after isolation was determined to be 86:14 by  $^1\text{H}$  NMR.  $^1\text{H}$  NMR (400 MHz,  $\text{CDCl}_3$ )  $\delta$  7.02 (m, 4 H), 5.47 (dd,  $J$  = 6.8 Hz, 1 H), 5.38 (m, inc.  $J$  = 6.8 Hz, 1 H), 3.31 (dq,  $J$  = 14 Hz, 6.8 Hz, 1 H), 2.24 (s, 3 H), 1.92 (dt,  $J$  = 14 Hz, 6.8 Hz, 2 H), 1.32-1.14 (m, 8 H), 1.24 (d,  $J$  = 7.2 Hz, 3 H).  $^{13}\text{C}$  NMR (100 MHz,  $\text{CDCl}_3$ )  $\delta$  143.6, 135.7, 135.1, 129.1, 129.0, 127.0, 41.9, 32.6, 31.8, 29.5, 28.9, 22.6, 21.6, 21.0, 14.1. **HRMS (EI-TOF):** calcd for  $[\text{M}]^+$  ( $\text{C}_{17}\text{H}_{26}$ )  $m/z$  230.2035; found 230.2036.

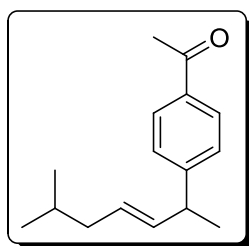


#### Synthesis of 2-(3,5-dimethylphenyl)-3-decene (3-

**12ad).** In a nitrogen-atmosphere glovebox, 3,5-

dimethyliodobenzene (**3-10a**, 13.73 mg, 232.9 g/mol, 0.059 mmol, 1.0 equiv.), 4-(boronic acid pinacolate ester)-2-decene (24.94 mg, 266 g/mol, 0.094 mmol, 1.59 equiv.),  $\text{Ag}_2\text{O}$  (23.88 mg, 234 g/mol, 0.10 mmol, 1.73 equiv.),  $\text{Pd}(\text{PPh}_3)_4$  (5.68 mg, 1155.6 g/mol, 0.0049 mmol, 8.3 mol% Pd),  $\text{PPh}_3$  (5.85 mg, 262 g/mol, 0.022 mmol, 0.38 equiv., 8.49:1 P:Pd) and  $\text{K}_2\text{CO}_3$  (12.00 mg, 138 g/mol, 0.087 mmol, 1.47 equiv.) were added to a tared 1 dram vial and taken up in 1.05 g of DME. The reaction solution was sealed in the glovebox, removed, and placed in an 85 °C oil bath

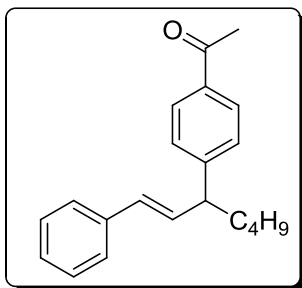
for 24 h. Once cooled, the reaction solution was passed through a celite plug and washed with copious amounts of diethyl ether. The solution was concentrated *in vacuo* to dryness and an NMR internal standard was added (*p*- dimethoxybenzene, DMB, 7.90 mg). NMR yield of the major isomer was determined to be 78% and the ratio of major ( $\gamma$ ) to minor ( $\alpha$ ) isomers (assigned by 2D-COSY-NMR correlations) was 91:9 prior to isolation. The crude mixture was purified by silica gel chromatography (20:1 hexanes:ethyl acetate) and 10.4 mg of a mixture of isomers ( $\gamma$ : $\alpha$  = 90:10) was obtained, representing an 72% isolated yield.  **$^1\text{H}$  NMR** (400 MHz,  $\text{CDCl}_3$ )  $\delta$  6.75 (s, 3 H), 5.49 (dd,  $J$  = 6.8 Hz, 1 H), 5.38 (m, inc  $J$  = 6.8 Hz, 1 H), 3.26 (dq,  $J$  = 6.8 Hz, 1 H), 2.22 (s, 6 H), 1.93 (dt,  $J$  = 14 Hz, 6.8 Hz, 2 H), 1.32-1.15 (m, 8 H), 1.25 (d,  $J$  = 6.8 Hz, 3 H), 0.80 (m, 3 H).  **$^{13}\text{C}$  NMR** (100 MHz,  $\text{CDCl}_3$ )  $\delta$  146.6, 137.8, 135.6, 129.1, 127.5, 125.0, 42.2, 32.6, 31.8, 29.3, 28.9, 22.7, 21.7, 21.4, 14.1. **HRMS (EI-TOF)**: calcd for  $[\text{M}]^+$  ( $\text{C}_{18}\text{H}_{28}$ )  $m/z$  244.2191; found 244.2199.



**Synthesis of 2-(4-acetylphenyl)-6-methyl-3-heptene (3-12ba).** In

a nitrogen-atmosphere glovebox, 4-iodoacetophenone (14.86 mg, 245.9 g/mol, 0.060 mmol, 1.0 equiv.), 4-(boronic acid pinacolate ester)-6-methyl-2-heptene (**3-10b**, 21 mg, 238 g/mol, 0.088 mmol, 1.51 equiv.),  $\text{Ag}_2\text{O}$  (22.00 mg, 234 g/mol, 0.088 mmol, 1.51 equiv.),  $\text{Pd}(\text{PPh}_3)_4$  (5.29 mg, 1155.6 g/mol, 0.0046 mmol, 7.6 mol% Pd),  $\text{PPh}_3$  (5.51 mg, 262 g/mol, 0.021 mmol, 0.35 equiv., 8.56:1 P:Pd) and  $\text{K}_2\text{CO}_3$  (14.77 mg, 138 g/mol, 0.11 mmol, 1.77 equiv.) were added to a tared 1 dram vial and taken up in 1.08 g of DME. The reaction solution was

sealed in the glovebox, removed, and placed in an 85 °C oil bath for 24 h. Once cooled, the reaction solution was passed through a celite plug and washed with copious amounts of diethyl ether. The solution was concentrated *in vacuo* to dryness and an NMR internal standard was added (*p*-dimethoxybenzene, DMB, 7.51 mg). The NMR yield of the major isomer was determined to be 76% and the ratio of major ( $\gamma$ ) to minor ( $\alpha$ ) isomers (assigned by 2D-COSY-NMR correlations) was 88:12 prior to isolation. The crude mixture was purified by silica gel chromatography (50:1 hexanes:ethyl acetate load and first 8 fractions, followed by 20:1 hexanes:ethyl acetate for the remainder) and 10.3 mg of a mixture of isomers ( $\gamma$ : $\alpha$  = 86:14) was obtained, representing an 74% isolated yield. **<sup>1</sup>H NMR** (400 MHz, CDCl<sub>3</sub>)  $\delta$  7.82 (d,  $J$  = 8.4 Hz, 2 H), 7.23 (d,  $J$  = 8 Hz, 2 H), 5.48 (dd,  $J$  = 6.4 Hz, 1 H), 5.39 (m, inc  $J$  = 6.8 Hz, 0.8 Hz, 1 H), 3.42 (dq,  $J$  = 6.8 Hz, 1 H), 2.51 (s, 3 H), 1.83 (dd,  $J$  = 6.4 Hz, 6 Hz, 2 H), 1.54 (m, inc.  $J$  = 6.8 Hz, 1 H), 1.29 (d,  $J$  = 7.2 Hz, 3 H), 0.81 (d,  $J$  = 6.4 Hz, 3 H), 0.79 (d,  $J$  = 6.8 Hz, 3 H). **<sup>13</sup>C NMR** (100 MHz, CDCl<sub>3</sub>)  $\delta$  197.9, 152.3, 135.1, 128.9, 128.6, 128.6, 127.4, 42.4, 41.8, 28.4, 26.6, 22.3, 22.2, 21.3. **HRMS (EI-TOF)**: calcd for [M]<sup>+</sup> (C<sub>16</sub>H<sub>22</sub>O)  $m/z$  230.1671; found 230.1677.



**Synthesis of 3-(4-acetylphenyl)-1-phenylheptene (3-12ca).** In a nitrogen-atmosphere glovebox, 4-iodoacetophenone (6.00 mg, 245.9 g/mol, 0.0244 mmol, 1.0 equiv.), 3-(boronic acid pinacolate ester)-1-phenylheptene (**3-10c**, 12 mg, 300 g/mol, 0.04 mmol, 1.64 equiv.), Ag<sub>2</sub>O (9.30 mg, 234 g/mol, 0.04 mmol, 1.62 equiv.), Pd(PPh<sub>3</sub>)<sub>4</sub> (2.17 mg, 1155.6 g/mol, 0.0018 mmol, 7.7 mol% Pd), PPh<sub>3</sub> (2.09 mg, 262 g/mol, 0.008

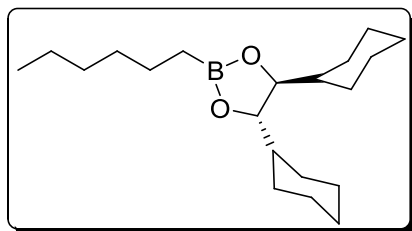
mmol, 0.33 equiv., 8.44:1 P:Pd) and  $K_2CO_3$  (5.94 mg, 138 g/mol, 0.043 mmol, 1.76 equiv.) were added to a tared 1 dram vial and taken up in 0.6 g of DME. The reaction solution was sealed in the glovebox, removed, and placed in an 85 °C oil bath for 24 h. Once cooled, the reaction solution was passed through a celite plug and washed with copious amounts of diethyl ether. The solution was concentrated *in vacuo* to dryness. The crude mixture ( $\alpha : \gamma = 88:12$ , assigned by 2D-COSY NMR correlations) was then purified by silica gel chromatography (20:1 hexanes:ethyl acetate) and 4.1 mg of a mixture of isomers ( $\alpha : \gamma = 92:8$ ) was obtained, representing an 58% isolated yield.  **$^1H$  NMR** (400 MHz,  $CDCl_3$ )  $\delta$  7.84 (d,  $J = 8.4$  Hz, 2 H), 7.30-7.10 (m, 7 H), 6.32 (d,  $J = 16$  Hz, 1 H), 6.23 (dd,  $J = 15.6$  Hz, 7.6 Hz, 1 H), 3.40 (m, inc.  $J = 7.6$  Hz, 1 H), 2.52 (s, 3 H), 1.80-1.70 (m, 2 H), 1.33-1.10 (m, 4 H), 0.85-0.75 (m, 3 H).  **$^{13}C$  NMR** (100 MHz,  $CDCl_3$ )  $\delta$  150.5, 137.3, 135.4, 133.3, 130.0, 128.7, 128.5, 127.9, 127.3, 126.2, 49.2, 35.5, 29.8, 26.6, 22.6, 14.0, (Carbonyl peak not assigned). **HRMS (EI-TOF)**: calcd for  $[M]^+$  ( $C_{21}H_{24}O$ )  $m/z$  292.1827; found 292.1819.

### 6.2.3 Attempted Ligand-based Regioselectivity Switch for Allyl Coupling

In a nitrogen-atmosphere glovebox, 4-iodoacetophenone (12.29 mg, 245.9 g/mol, 0.050 mmol, 1.0 equiv.), 3-(boronic acid pinacolate ester)-2-decene (19.43 mg, 266 g/mol, 0.073 mmol, 1.46 equiv.),  $Ag_2O$  (17.55 mg, 234 g/mol, 0.075 mmol, 1.50 equiv.),  $Pd_2dba_3$  (1.95 mg, 915.7 g/mol, 0.0021 mmol, 8.5 mol% Pd), dppp (diphenylphosphine

propane, 5.38 mg, 262 g/mol, 0.013 mmol, 0.26 equiv., 6.2:1 P:Pd) and  $K_2CO_3$  (11.55 mg, 138 g/mol, 0.084 mmol, 1.67 equiv.) were added to a tared 1 dram vial and taken up in 1.1 g of DME. The reaction solution was sealed in the glovebox, removed, and placed in an 85 °C oil bath for 21 h. Once cooled, the reaction solution was passed through a celite plug and washed with copious amounts of diethyl ether. Analysis by GC-MS indicates that the boronic ester was the major species present in solution, with only trace amounts of arylated product detected.

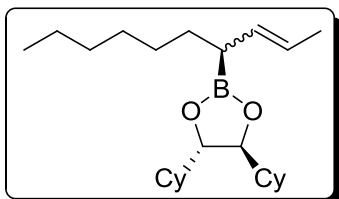
#### 6.2.4 Synthesis of Non-Racemic Secondary Allylic Boronic Esters



**Synthesis of (4*S*,5*S*)-4,5-dicyclohexyl-2-hexyl-1,3,2-dioxaborolane.** 0.7862 g of 1-hexylboronic acid (130 g/mol, 6.04 mmol, 1.0 equiv.) and 1.366 g of (1*S*,2*S*)-1,2-dicyclohexylethane-1,2-diol (226 g/mol, 6.04

mmol, 1.0 equiv.) were taken up in 20 mL of diethyl ether. Once dissolved, 0.721 g of  $MgSO_4$  (120 g/mol, 6.03 mmol, 1.0 equiv.) was dispersed in the solution, which was stirred at 25 °C for 16 h. The dispersion was filtered by vacuum and washed with copious amounts of diethyl ether. The homogeneous solution was then concentrated *in vacuo* to yield the pure boronic ester in quantitative isolated yield.  $^1H$  NMR (400 MHz,  $CDCl_3$ )  $\delta$  3.77-3.74 (m, inc.  $J = 4.8$  Hz, 2 H), 1.75-1.64 (m, 6 H), 1.63-1.57 (m, 2 H), 1.55-1.48 (m, 2 H), 1.39-1.30 (m, 2 H), 1.29-1.07 (m, 14 H), 1.08-0.85 (m, 5 H), 0.84-0.76 (m, 3 H),

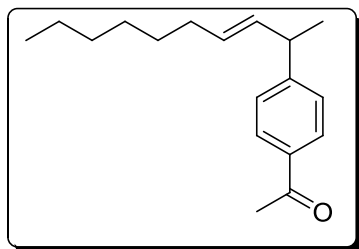
0.729 (t,  $J = 7.6$  Hz, 2 H)  $^{11}\text{B}$  NMR: (160 MHz,  $\text{CDCl}_3$ ):  $\delta$  33.5  $^{13}\text{C}$  NMR (400 MHz,  $\text{CDCl}_3$ )  $\delta$  83.2, 43.1, 32.1, 31.7, 28.4, 27.4, 26.5, 26.1, 25.9, 24.1, 22.6.



**Synthesis of 4-((4S,5S)-4,5-dicyclohexyl-1,3,2-dioxaborolane)-2-decene (3-13).** Dissolve dichloromethane (1.0 mL, 15.6 mmol, 15 equiv.), stored under  $\text{Ar}_{(\text{g})}$ , was added to 4.0 mL of freshly distilled THF. While under  $\text{Ar}_{(\text{g})}$ , the solution was dropped to an internal temperature of  $-90$  °C by cooling in an  $\text{N}_2/\text{MeOH}$  bath. *s*-butyllithium (1.6 mL, 1.3 M, 2.0 equiv.) was added dropwise to the stirring solution, with care given to keep the internal temperature below  $-85$  °C. Lithiation was allowed to proceed at  $-90$  °C for 60 min prior to the dropwise addition of the (4S,5S)-4,5-dicyclohexyl-2-hexyl-1,3,2-dioxaborolane solution (328.3 mg, 1.03 mmol, 1.0 equiv., 2 mL THF). The solution was kept at  $-90$  °C for 20 min to ensure complete borylation before addition of  $\text{ZnCl}_2$  (2.0 mL, 1.0 M, 2.0 mmol, 2 equiv.). After addition of  $\text{ZnCl}_2$ , the solution was slowly warmed to  $0$  °C at which point the reaction was quenched with 2 x 5 mL sat.  $\text{NH}_4\text{Cl}_{(\text{aq})}$  aliquots. The aqueous layers were washed with 3x 10 mL  $\text{Et}_2\text{O}$ . The organic layers were combined and dried with anhydrous  $\text{MgSO}_4$  and filtered by vacuum. The ethereal solution was concentrated *in vacuo* to yield a clear crude oil. This oil was then taken up in 6 mL of freshly distilled  $\text{Et}_2\text{O}$  and cooled to  $0$  °C. To this solution was added 1-propenylmagnesium bromide (3.8 mL, 0.5 M, 2.0 equiv.). The solution was kept at  $0$  °C for 4 h and then was allowed to warm to  $25$  °C before aqueous quench and workup. The resultant yellow, viscous oil was purified by silica gel chromatography (80:1

hexanes:ethyl acetate,  $R_f = 7/20$ ), though some fractions were contaminated with starting boronic ester. These fractions (containing ~90% product) were oxidized for SFC analysis of the enantioexcess and did not figure in the overall yield recorded. After a second purification step (as above), 95.2 mg of the clear product oil was isolated in 98:2 dr.  $^1\text{H}$  NMR (400 MHz,  $\text{CDCl}_3$ )  $\delta$  5.40-5.22 (m, 2 H), 3.76 (d,  $J = 4.8$  Hz, 2 H), 2.10-2.01 (m, inc.  $J = 8.8$  Hz, 1 H), 1.80-1.65 (d,  $J = 7.6$  Hz, 6 H), 1.63-1.44 (m, 8 H; inc. dd,  $J = 6.8$  Hz, 1.4 Hz), 1.33-1.15 (m, 12 H), 1.14-1.06 (m, 5 H), 1.03-0.83 (m, 4 H), 0.80 (t,  $J = 6.8$  Hz, 3 H).  $^{11}\text{B}$  NMR: (160 MHz,  $\text{CDCl}_3$ ):  $\delta$  32.9.  $^{13}\text{C}$  NMR (400 MHz,  $\text{CDCl}_3$ )  $\delta$  132.1, 122.7, 83.2, 43.1, 31.9, 31.5, 29.4, 29.2, 28.3, 27.4, 26.5, 26.0, 25.9, 22.6, 14.1.

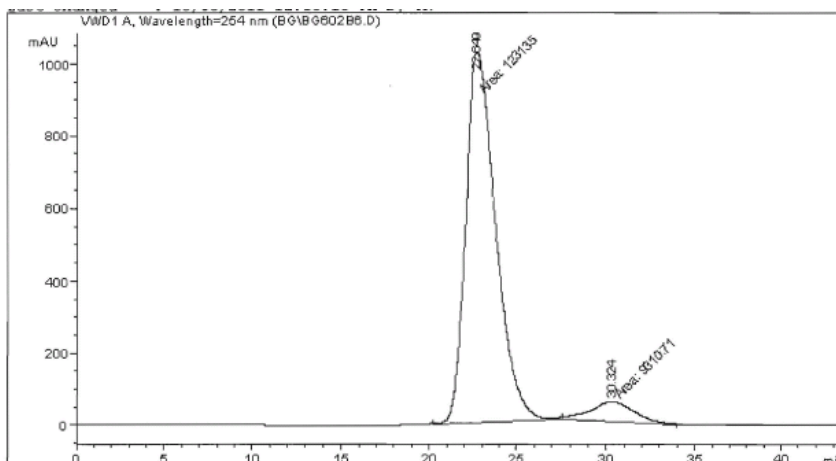
### 6.2.5 Cross-Coupling of Non-Racemic Secondary Allylic Boronic Esters



**Synthesis of 2-(4-acetylphenyl)-3-decene (3-14a).** In a nitrogen-atmosphere glovebox, 4-iodoacetophenone (12.46 mg, 245.9 g/mol, 0.051 mmol, 1.0 equiv.), 4-((4*S*,5*S*)-4,5-dicyclohexyl-1,3,2-dioxaborolane)-2-decene (**3-13**, 28.87 mg, 374 g/mol, 0.077 mmol, 1.51 equiv.),  $\text{Ag}_2\text{O}$  (18.54 mg, 234 g/mol, 0.079 mmol, 1.55 equiv.),  $\text{Pd}(\text{PPh}_3)_4$  (4.87 mg, 1155.6 g/mol, 0.0042 mmol, 8.3 mol% Pd),  $\text{PPh}_3$  (4.64 mg, 262 g/mol, 0.018 mmol, 0.35 equiv., 8.3:1 P:Pd) and  $\text{K}_2\text{CO}_3$  (12.15 mg, 138 g/mol, 0.088 mmol, 1.72 equiv.) were added to a tared 1 dram vial and taken up in 940 mg of DME. The reaction solution was sealed in the glovebox, removed, and placed in an 85 °C oil



bath for 24 h. Once cooled, the reaction solution was passed through a celite plug and washed with copious amounts of diethyl ether. The solution was concentrated *in vacuo* to dryness and an NMR internal standard was added (hexamethylbenzene, HMB, 4.89 mg). NMR yield of the major isomer was determined to be 78% and the ratio of major ( $\gamma$ ) to minor ( $\alpha$ ) isomers (assigned by 2D-COSY NMR correlations) was 88:12 prior to isolation. The crude mixture was purified by silica gel chromatography (20:1 hexanes:ethyl acetate) and 10.78 mg of a mixture of isomers ( $\gamma$ : $\alpha$  = 88:12) was obtained, representing an 83% isolated yield. **Chiral HPLC:** Column = AD-H, 99.8:0.2 hexanes : *i*-PrOH , 0.6 mL/min, Detector  $\lambda$  = 254 nm.



```

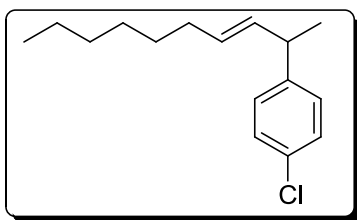
=====
                          Area Percent Report
=====
Sorted By      :      Signal
Multiplier    :      1.0000
Dilution      :      1.0000
Sample Amount :      1.00000 [ng/ul] (not used in calc.)
Use Multiplier & Dilution Factor with ISTDs

Signal 1: VWD1 A, Wavelength=254 nm

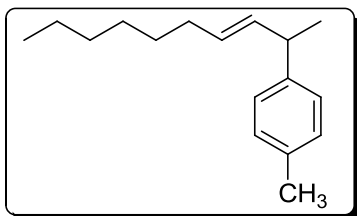
Peak RetTime Type Width Area Height Area
# [min] [min] [min] mAU *s [mAU ] %
-----|-----|-----|-----|-----|-----
 1 22.649 NM 1.9995 1.23135e5 1026.35352 92.9701
 2 30.324 NM 2.8196 9310.71094 55.03490 7.0299
Totals :                      1.32445e5 1081.38841

Results obtained with enhanced integrator!
=====
*** End of Report ***

```

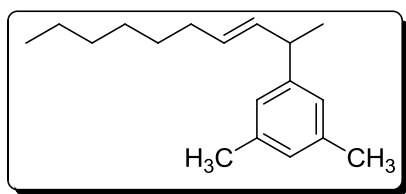


**Synthesis of 2-(4-chlorophenyl)-3-decene (3-14b).** In a nitrogen-atmosphere glovebox, 4-chloriodobenzene (**3-13**, 12.16 mg, 238.4 g/mol, 0.051 mmol, 1.0 equiv.), 4-((4*S*,5*S*)-4,5-dicyclohexyl-1,3,2-dioxaborolane)-2-decene (29.59 mg, 374 g/mol, 0.079 mmol, 1.55 equiv.), Ag<sub>2</sub>O (19.08 mg, 234 g/mol, 0.082 mmol, 1.57 equiv.), Pd(PPh<sub>3</sub>)<sub>4</sub> (4.74 mg, 1155.6 g/mol, 0.0041 mmol, 8.0 mol% Pd), PPh<sub>3</sub> (4.07 mg, 262 g/mol, 0.016 mmol, 0.30 equiv., 7.9:1 P:Pd) and K<sub>2</sub>CO<sub>3</sub> (10.70 mg, 138 g/mol, 0.078 mmol, 1.53 equiv.) were added to a tared 1 dram vial and taken up in 1.1 g of DME. The reaction solution was sealed in the glovebox, removed, and placed in an 85 °C oil bath for 24 h. Once cooled, the reaction solution was passed through a celite plug and washed with copious amounts of diethyl ether. The solution was concentrated *in vacuo* to dryness and an NMR internal standard was added (*p*-dimethoxybenzene, DMB, 9.98 mg). NMR yield of the major isomer was determined to be 75% and the ratio of major ( $\gamma$ ) to minor ( $\alpha$ ) isomers (assigned by 2D-COSY NMR correlations) was 82:18 prior to isolation. The crude mixture was purified by silica gel chromatography (pentane) and 9.2 mg of a mixture of isomers ( $\gamma$  :  $\alpha$  = 80:20) was obtained, representing an 72% isolated yield.



**Synthesis of 2-(4-tolyl)-3-decene (3-14c).** In a nitrogen-atmosphere glovebox, 4-iodotoluene (11.37 mg, 217.9 g/mol, 0.052 mmol, 1.0 equiv.), 4-((4*S*,5*S*)-4,5-

dicyclohexyl-1,3,2-dioxaborolane)-2-decene (**3-13**, 28.88 mg, 374 g/mol, 0.077 mmol, 1.51 equiv.), Ag<sub>2</sub>O (18.12 mg, 234 g/mol, 0.077 mmol, 1.51 equiv.), Pd(PPh<sub>3</sub>)<sub>4</sub> (4.52 mg, 1155.6 g/mol, 0.0039 mmol, 7.6 mol% Pd), PPh<sub>3</sub> (4.96 mg, 262 g/mol, 0.019 mmol, 0.37 equiv., 8.87:1 P:Pd) and K<sub>2</sub>CO<sub>3</sub> (10.1 mg, 138 g/mol, 0.073 mmol, 1.43 equiv.) were added to a tared 1 dram vial and taken up in 1.05 g of DME. The reaction solution was sealed in the glovebox, removed, and placed in an 85 °C oil bath for 24 h. Once cooled, the reaction solution was passed through a celite plug and washed with copious amounts of diethyl ether. The solution was concentrated *in vacuo* to dryness. The crude mixture ( $\gamma$ : $\alpha$  = 90:10, assigned by 2D-COSY NMR correlations) was purified by silica gel chromatography (20:1 hexanes:ethyl acetate) and 8.7 mg of a mixture of isomers was obtained, representing an 70% isolated yield. The ratio of the major ( $\gamma$ ) and minor ( $\alpha$ ) products after isolation was determined to be 88:12 by <sup>1</sup>H NMR.

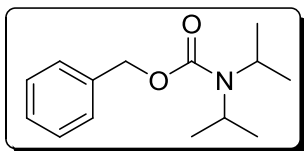


**Synthesis of 2-(3,5-dimethylphenyl)-3-decene (3-14d).** In a nitrogen-atmosphere glovebox, 3,5-dimethyliodobenzene (12.31 mg, 232.9 g/mol, 0.053

mmol, 1.0 equiv.), 4-((4*S*,5*S*)-4,5-dicyclohexyl-1,3,2-dioxaborolane)-2-decene (**3-13**, 28 mg, 374 g/mol, 0.075 mmol, 1.4 equiv.), Ag<sub>2</sub>O (18.23 mg, 234 g/mol, 0.78 mmol, 1.47 equiv.), Pd(PPh<sub>3</sub>)<sub>4</sub> (4.72 mg, 1155.6 g/mol, 0.0041 mmol, 7.7 mol% Pd), PPh<sub>3</sub> (4.30 mg, 262 g/mol, 0.016 mmol, 0.31 equiv., 7.90:1 P:Pd) and K<sub>2</sub>CO<sub>3</sub> (11.35 mg, 138 g/mol, 0.082 mmol, 1.55 equiv.) were added to a tared 1 dram vial and taken up in 1.1 g of DME. The reaction solution was sealed in the glovebox, removed, and placed in an 85 °C

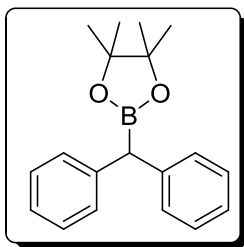
oil bath for 22 h. Once cooled, the reaction solution was passed through a celite plug and washed with copious amounts of diethyl ether. The solution was concentrated *in vacuo* to dryness and an NMR internal standard was added (*p*- dimethoxybenzene, DMB, 7.14 mg). NMR yield of the major isomer was determined to be 71% and the ratio of major ( $\gamma$ ) to minor ( $\alpha$ ) isomers (assigned by 2D-COSY NMR correlations) was 92:8 prior to isolation. The crude mixture was purified by silica gel chromatography (pentane) and 10.7 mg of a mixture of isomers ( $\gamma$ : $\alpha$  = 91:9) was obtained, representing an 83% isolated yield..

#### 6.2.6 Synthesis of Symmetrical Triarylmethanes by Suzuki-Miyaura Cross-Coupling



***N,N*-Diisopropyl carbamic acid benzyl ester (3-15).** *N,N*-diisopropylcarbonyl chloride (1.646 g, 163.65 g/mol, 10.1 mmol, 1.05 equiv.) and freshly distilled triethylamine (1.4 mL, 0.726 g/mL, 101.2 g/mol, 10.1 mmol, 1.05 equiv.) were taken up in 20 mL of CH<sub>2</sub>Cl<sub>2</sub>. Benzyl alcohol (1.025 g, 108 g/mol, 0.094 mmol, 1 equiv.) was added and the solution was stirred under refluxing conditions for 24 h, with salts eventually precipitating out of solution. The solution was washed with sat. NH<sub>4</sub>Cl<sub>(aq.)</sub> and the aqueous layer was extracted with 3 x 25 mL CH<sub>2</sub>Cl<sub>2</sub>. The crude oil was purified by silica gel chromatography (10:1 hexanes:ethyl acetate, 2 inch by 5 inch column) to yield 1.996 g of the desired carbamate, or 90% isolated yield. <sup>1</sup>H NMR (400 MHz, CDCl<sub>3</sub>)  $\delta$  7.40-7.15

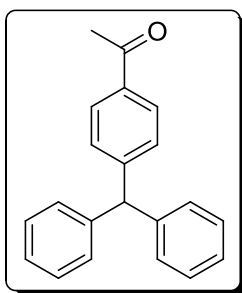
(m, 5 H), 5.06 (s, 2 H), 4.1-3.5 (br, 2 H), 1.14 (d,  $J = 6.8$  Hz, 12 H).  $^{13}\text{C}$  NMR (400 MHz,  $\text{CDCl}_3$ )  $\delta$  155.5, 137.2, 128.4, 127.9, 127.8, 66.5, 46.2 (br), 21.1 (br).



**Synthesis of Dibenzyl boronic acid pinacolate ester (3-16).** *N,N*-

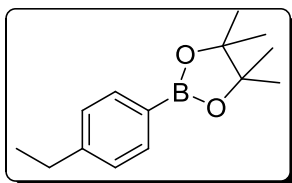
diisopropyl benzyl carbamate (74.41 mg, 235 g/mol, 0.317 mmol, 1.0 equiv.) and *N,N,N,N*-tetramethylethylenediamine (TMEDA, 0.07 mL, 0.78 g/mL, 116 g/mol, 0.45 mmol, 1.3 equiv.) were taken

up in diethyl ether and cooled to  $-78$  °C in a dry ice/acetone bath. *s*-Butyllithium (0.3 mL, 1.4 M, 0.42 mmol, 1.3 equiv.) was added dropwise to the cold solution, creating a slightly brown solution. After 2 h of lithiation, an ethereal solution of phenylboronic acid pinacolate ester (92.0 mg, 204 g/mol, 0.44 mmol, 1.4 equiv., 1.2 mL  $\text{Et}_2\text{O}$ ) was added dropwise. After 3 h of borylation, freshly prepared  $\text{MgBr}_2$  diethyl etherate (2.0 equiv.) was added to the cold solution as an ethereal solution.  $\text{MgBr}_2$  diethyl etherate is prepared by adding a necessary amount of 1,2-dibromoethane, in this case, two equivalents per boronic ester to an excess of Mg turnings in dry ether. The contents of the dense layer that dissociates from the ether are added to the reaction solution *via* syringe. After addition of the  $\text{MgBr}_2$ , the solution is allowed to warm slowly before being heated to reflux overnight. After aqueous workup, two silica gel chromatography steps (40:1 hexanes:ethyl acetate) were required and 50.3 mg (54% yield) of white solid was isolated.  $^1\text{H}$  NMR (400 MHz,  $\text{CDCl}_3$ )  $\delta$  7.19-7.07 (m, 10 H), 3.79 (s, 1 H), 1.16 (s, 12 H).  $^{11}\text{B}$  NMR: (160 MHz,  $\text{CDCl}_3$ ):  $\delta$  32.6.  $^{13}\text{C}$  NMR (400 MHz,  $\text{CDCl}_3$ )  $\delta$  129.1, 128.4, 125.6, 24.6.



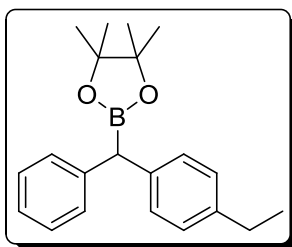
**Synthesis of (4-acetylphenyl)-diphenylmethane (3-17).** In a nitrogen-atmosphere glovebox, 4-iodoacetophenone (20.66 mg, 245.9 g/mol, 0.084 mmol, 1.0 equiv.), dibenzylboronic acid pinacolate ester (33.31 mg, 294 g/mol, 0.11 mmol, 1.35 equiv.), Ag<sub>2</sub>O (27.78 mg, 234 g/mol, 0.119 mmol, 1.4 equiv.), Pd<sub>2</sub>dba<sub>3</sub> (2.85 mg, 915 g/mol, 0.0031 mmol, 7.4 mol% Pd), PPh<sub>3</sub> (14.70 mg, 262 g/mol, 0.056 mmol, 0.67 equiv., 9.0:1 P:Pd) and K<sub>2</sub>CO<sub>3</sub> (18.39 mg, 138 g/mol, 0.13 mmol, 1.60 equiv.) were added to a tared 4 dram vial and taken up in 1.1 g of diethyl ether. The reaction solution was sealed in the glovebox, removed, and placed in a 65 °C oil bath for 16 h. Once cooled, the reaction solution was passed through a celite plug and washed with copious amounts of diethyl ether. The solution was concentrated *in vacuo* to dryness and an NMR internal standard was added (hexamethylbenzene, HMB, 6.2 mg). NMR yield of the product was determined to be 52%. The crude mixture was purified by silica gel chromatography (Packed with 50:1 hexanes:ethyl acetate, crude oil loaded and eluted with 40:1 hexanes:ethyl acetate until separation of layers visible on the column. Elution completed with 20:1 hexanes:ethyl acetate) to yield 11.5 mg of a slightly yellow oil, or a 48% isolated yield. **<sup>1</sup>H NMR** (300 MHz, CDCl<sub>3</sub>) δ 7.91 (d, *J* = 8.1 Hz, 2 H), 7.4-7.2 (m, 8 H), 7.12 (dd, *J* = 7.2 Hz, 0.3 Hz, 4 H), 5.62 (s, 1 H), 2.60 (s, 3 H). **<sup>13</sup>C NMR** (400 MHz, CDCl<sub>3</sub>) δ 197.8, 149.6, 143.0, 135.4, 129.7, 129.4, 128.5, 128.5, 126.7, 56.8, 26.6. **HRMS (EI-TOF):** calcd for [M]<sup>+</sup> (C<sub>21</sub>H<sub>18</sub>O) *m/z* 286.1358; found 286.1369.

### 6.2.7 Synthesis of Unsymmetrical Triarylmethanes by Suzuki-Miyaura Cross-Coupling



#### Synthesis of 4-Ethylphenylboronic acid pinacolate ester.

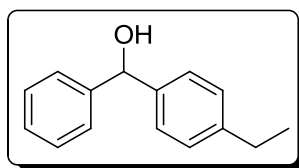
1.004 g of 4-ethylphenylboronic acid (150 g/mol, 6.69 mmol, 1.0 equiv.) and 0.791 g of pinacol (118 g/mol, 6.69 mmol, 1.0 equiv.) were taken up in 10 mL of diethyl ether. Once dissolved, 0.808 g of  $\text{MgSO}_4$  (120 g/mol, 6.69 mmol, 1.0 equiv.) was dispersed in the solution, which was stirred at 25 °C for 18 h. The dispersion was filtered by vacuum and washed with copious amounts of diethyl ether. The homogeneous solution was then concentrated *in vacuo* to yield the pure boronic ester in 95% isolated yield.  $^1\text{H NMR}$  (400 MHz,  $\text{CDCl}_3$ )  $\delta$  7.66 (d,  $J = 7.6$  Hz, 2 H), 7.14 (d,  $J = 8$ , 2 H), 2.59 (q,  $J = 7.6$  Hz, 2 H), 1.27 (s, 12 H), 1.16 (t,  $J = 7.6$  Hz, 3 H).  $^{11}\text{B NMR}$ : (160 MHz,  $\text{CDCl}_3$ ):  $\delta$  31.1.  $^{13}\text{C NMR}$  (100 MHz,  $\text{CDCl}_3$ )  $\delta$  147.7, 134.9, 127.4, 83.6, 29.1, 24.9, 15.5. **HRMS (EI-TOF)**: calcd for  $[\text{M}]^+$  ( $\text{C}_{14}\text{H}_{21}\text{O}_2\text{B}$ )  $m/z$  232.1635; found 232.1643.



#### Synthesis of *rac*-(4-Ethylphenyl)phenyl methane boronic acid pinacolate ester (3-18). *N,N*-Diisopropyl carbamic acid

benzyl ester (477.4 mg, 235 g/mol, 2.03 mmol, 1.0 equiv.) and *N,N,N,N*-tetramethylethylenediamine (TMEDA, 0.26 mL, 0.78 g/mL, 116 g/mol, 2.84 mmol, 1.4 equiv.) were taken up in 10 mL of diethyl ether and cooled to -78 °C in a dry ice/acetone bath. *s*-Butyllithium (3.0 mL, 1.4 M, 3.05 mmol, 1.5

equiv.) was added dropwise to the cold solution, creating a creamy orange solution. After 2 h of lithiation, an ethereal solution of 4-ethylphenylboronic acid pinacolate ester (494.7 mg, 232 g/mol, 2.13 mmol, 1.1 equiv., 2.5 mL Et<sub>2</sub>O) was added dropwise. After 3 h borylation, freshly prepared MgBr<sub>2</sub> diethyl etherate (3.0 equiv.) was added to the cold solution as an ethereal solution. MgBr<sub>2</sub> diethyl etherate is prepared by adding a necessary amount of 1,2-dibromoethane, in this case, 3 equivalents per boronic ester to an excess of Mg turnings in dry ether. The contents of the dense layer that dissociates from the ether are added to the reaction solution *via* syringe. After addition of the MgBr<sub>2</sub>, the solution is allowed to warm slowly before being heated to reflux overnight. After aqueous workup, two silica gel chromatography steps (40:1 hexanes:ethyl acetate) were performed to ensure purity and 376 mg (57% yield) of white solid was isolated. **<sup>1</sup>H NMR** (400 MHz, CDCl<sub>3</sub>) δ 7.18 (m, 4 H), 7.10-6.95 (m, 5 H), 3.75 (s, 1 H), 2.52 (q, *J* = 7.6 Hz, 2H), 1.15 (s, 12 H). **<sup>11</sup>B NMR:** (160 MHz, CDCl<sub>3</sub>): δ 32.9. **<sup>13</sup>C NMR** (100 MHz, CDCl<sub>3</sub>) δ 142.4, 141.3, 139.2, 129.1, 129.0, 128.4, 127.9, 125.5, 83.7, 28.4, 24.6, 15.5.

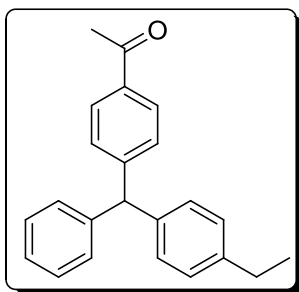


**Synthesis of *rac*-(4-ethylphenyl)phenylmethanol (*rac*-3-26).**

23.4 mg of pure *rac*-(4-ethylphenyl)phenyl methane boronic acid pinacolate ester (322 g/mol, 0.073 mmol) were taken up in 2 mL of diethyl ether and cooled to 0 °C. Separately, 1.5 mL of 30% H<sub>2</sub>O<sub>2</sub>(aq.) and 1.5 mL of 1 M NaOH<sub>(aq.)</sub> were combined under flowing Ar<sub>(g)</sub>. 1.5 mL of this solution was added slowly to the ethereal solution of boronic ester. TLC analysis of the reaction progress (10:1 hexanes:ethyl acetate) indicated that the reaction was nearly complete



after 2 h. The reaction was quenched with an excess of 1 M NaOH<sub>(aq.)</sub> and worked up with a saturated solution of NH<sub>4</sub>Cl<sub>(aq.)</sub>. The aqueous layers were washed thrice with diethyl ether, and the combined organic layers were dried over MgSO<sub>4</sub>. Purification of the product alcohol was achieved by silica gel chromatography (10:1 hexanes:ethyl acetate) to yield 10.0 mg of a clear oil (65% isolated). Chromatographic Separation of Enantiomers: SFC OD-H 5% MeOH, 2 mL, 200 bar. er = 50.0:50.0. <sup>1</sup>H NMR (400 MHz, CDCl<sub>3</sub>) δ 7.31 (d, *J* = 7.2 Hz, 2 H), 7.23 (m, 5 H), 7.10 (d, *J* = 8.4 Hz, 2 H), 5.75 (s, 1 H), 2.55 (q, *J* = 7.6 Hz, 2 H), 2.1 (s, br), 1.15 (t, *J* = 7.6 Hz, 3 H). <sup>13</sup>C NMR (100 MHz, CDCl<sub>3</sub>) δ 144.0, 143.7, 128.5, 128.0, 127.5, 126.6, 126.5, 76.2, 28.5, 15.5. **HRMS (EI-TOF)**: calcd for [M]<sup>+</sup> (C<sub>15</sub>H<sub>16</sub>O) *m/z* 212.1201; found 212.1209.



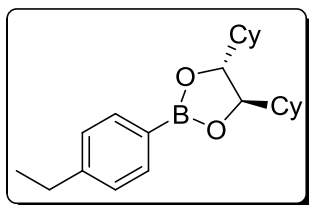
**Synthesis of (4-Acetylphenyl)-(4-ethylphenyl)phenylmethane (3-19).**

In a nitrogen-atmosphere glovebox, 4-iodoacetophenone (25.88 mg, 245.9 g/mol, 0.105 mmol, 1.0 equiv.), *rac*-(4-ethylphenyl)phenyl methane boronic acid pinacolate ester (53.0 mg, 322 g/mol, 0.165 mmol, 1.57 equiv.), Ag<sub>2</sub>O (35.43 mg, 234 g/mol, 0.151 mmol, 1.44 equiv.), Pd<sub>2</sub>dba<sub>3</sub> (3.86 mg, 915 g/mol, 0.0042 mmol, 8.0 mol% Pd), PPh<sub>3</sub> (17.97 mg, 262 g/mol, 0.069 mmol, 0.65 equiv., 8.2:1 P:Pd) and K<sub>2</sub>CO<sub>3</sub> (21.9 mg, 138 g/mol, 0.159 mmol, 1.51 equiv.) were added to a tared 4 dram vial and taken up in 1.5 g of diethyl ether. The reaction solution was sealed in the glovebox, removed, and placed in a 65 °C oil bath for 16 h. Once cooled, the reaction solution was passed through a celite plug and washed with copious amounts of diethyl ether. The

solution was concentrated *in vacuo* to dryness and an NMR internal standard was added (hexamethylbenzene, HMB, 6.85 mg). NMR yield of the product was determined to be 74%. The crude mixture was purified by silica gel chromatography (Packed with 50:1 hexanes:ethyl acetate, crude oil loaded and eluted with 40:1 hexanes:ethyl acetate until separation of layers visible on the column. Elution completed with 20:1 hexanes:ethyl acetate) to yield 18.5 mg of a clear oil, or a 56% isolated yield. Chromatographic Separation of Enantiomers: SFC AD-H 5% MeOH, 2 mL, 300 bar. er = 51:49. **<sup>1</sup>H NMR** (400 MHz, CDCl<sub>3</sub>) δ 7.80 (d, *J* = 8.4 Hz, 2 H), 7.20 (m, 5 H), 7.0 (m, 4 H), 6.93 (d, *J* = 8 Hz, 2 H), 5.48 (s, 1 H), 2.55 (q, *J* = 7.6 Hz, 2 H), 2.50 (s, 3 H), 1.15 (t, *J* = 7.6 Hz, 3 H). **<sup>13</sup>C NMR** (100 MHz, CDCl<sub>3</sub>) δ 197.8, 149.8, 143.2, 142.6, 140.2, 135.3, 129.7, 129.4, 129.3, 128.5, 128.4, 128.0, 126.6, 56.5, 28.4, 26.6, 15.5. **HRMS (EI-TOF)**: calcd for [M]<sup>+</sup> (C<sub>23</sub>H<sub>22</sub>O) *m/z* 314.1671; found 314.1682.

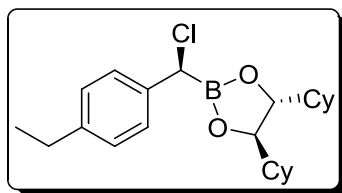
### 6.2.8 Synthesis of Enantiomerically Enriched Dibenzyl boronic esters by Matteson

#### Homologation



**Synthesis of (4*R*,5*R*)-4,5-dicyclohexyl-2-(4-ethylphenyl)-1,3,2-dioxaborolane (3-20).** 0.2088 g of 4-ethylphenylboronic acid (150 g/mol, 1.391 mmol, 1.0 equiv.) and 0.3144 g of pinacol (118 g/mol, 1.391 mmol, 1.0 equiv.) were taken up in 15 mL of diethyl ether. Once dissolved, 0.1703 g of MgSO<sub>4</sub> (120 g/mol, 1.4 mmol, 1.05 equiv.) was dispersed in

the solution, which was stirred at 25 °C for 20 h. The suspension was filtered by vacuum and washed with copious amounts of diethyl ether. The homogeneous solution was then concentrated *in vacuo* to yield the pure boronic ester in quantitative isolated yield. **<sup>1</sup>H NMR** (400 MHz, CDCl<sub>3</sub>) δ 7.68 (d, *J* = 8.0 Hz, 2 H), 7.14 (d, *J* = 8.0 Hz, 2 H), 3.94 (d, *J* = 7.2 Hz, 2 H), 2.58 (q, *J* = 7.6 Hz, 2 H), 1.78 (d, *J* = 12.8 Hz, 2 H), 1.68 (d, *J* = 12.0 Hz, 4 H), 1.59 (m, 4 H), 1.34 (m, inc. *J* = 3.6 Hz, 2 H), 1.17 (m, 2 H), 1.16 (t, *J* = 7.6 Hz, 2 H), 1.11 (t, *J* = 8.0 Hz, 2 H), 1.13-0.95 (dt, inc. *J* = 12.4 Hz, 3.2 Hz, 7 H). **<sup>11</sup>B NMR:** (160 MHz, CDCl<sub>3</sub>): δ 30.7. **<sup>13</sup>C NMR** (100 MHz, CDCl<sub>3</sub>) δ 147.7, 135.1, 127.4, 83.8, 43.2, 29.15, 28.4, 27.5, 26.5, 26.1, 25.9. **HRMS (EI-TOF):** calcd for [M]<sup>+</sup> (C<sub>22</sub>H<sub>33</sub>O<sub>2</sub>B) *m/z* 340.2574; found 340.2586.

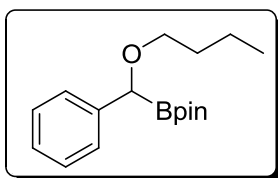


**Attempted Synthesis of (4*R*,5*R*)-4,5-dicyclohexyl-2-(4-ethylphenyl)chloromethane-1,3,2-dioxaborolane using *s*-butyllithium (3-21).** 163.8 mg of the diastereomerically

enriched boronic ester (4*R*,5*R*)-4,5-dicyclohexyl-2-(4-ethylphenyl)-1,3,2-dioxaborolane (340 g/mol, 0.482 mmol) and dichloromethane (0.1 mL, 1.327 g/mL, 85 g/mol, 1.445 mmol, 3 equiv.) were taken up in freshly distilled THF. The solution was cooled to -78 °C and *s*-butyllithium (0.4 mL, 1.45 M, 0.578 mmol, 1.2 equiv.) was added dropwise, such that the internal temperature never exceeded -70 °C. After 10 m of stirring at -78 °C, ZnCl<sub>2</sub> (1 mL, 1 M in diethyl ether, 1 mmol) was added dropwise. After stirring for 30 mins, the reaction solution was warmed to 25 °C and stirred at this temperature for 2 h.

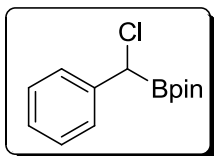
An aliquot was taken *via* syringe and given an aqueous workup. GC-MS analysis indicated that no  $\alpha$ -chlorobenzyl boronic ester was produced.

**Attempted Synthesis of (4*R*,5*R*)-4,5-dicyclohexyl-2-(4-ethylphenyl)chloromethane-1,3,2-dioxaborolane (3-21) using LDA.** 74.2 mg of the diastereomerically enriched boronic ester (4*R*,5*R*)-4,5-dicyclohexyl-2-(4-ethylphenyl)-1,3,2-dioxaborolane (340 g/mol, 0.218 mmol) and dichloromethane (0.08 mL, 1.327 g/mL, 85 g/mol, 1.09 mmol, 5 equiv.) were taken up in freshly distilled THF. The solution was cooled to -42 °C (with an acetonitrile/dry ice bath) and lithium diisopropylamide (LDA, 0.65 mL, 0.51 M, 0.578 mmol, 1.4 equiv.) was added dropwise, such that the internal temperature never exceeded -40 °C. After 10 min of stirring at -40 °C, ZnCl<sub>2</sub> (0.44 mL, 1 M in diethyl ether, 0.44 mmol, 2 equiv.) was added dropwise. After stirring for 30 mins, the reaction solution was warmed to 25 °C and stirred at this temperature for 3 h. An aliquot was taken *via* syringe and given an aqueous workup. GC-MS analysis indicated that the starting phenyl boronic ester was the main species present.



**Attempted Synthesis of 1-phenyl-1-chloromethylboronic acid pinacolate ester (3-22) Leading to an Unexpected Side Product.** 0.7 mL Dichloromethane (1.327 g/mL, 85 g/mol, 11 mmol, 19 equiv.) was taken up in freshly distilled THF and cooled to -100 °C with an 95% EtOH / N<sub>2</sub>(liq.) bath. *n*-butyllithium (1 mL, 1.3 M, 1.3 mmol, 1.7 equiv.) was added

down the sides of the flask so that the internal temperature never exceeded -100 °C. A solution of phenyl boronic acid pinacol ester (PhBPin, 0.160 g, 204 g/mol, 0.76 mmol, 1 equiv) in 1 mL THF was added quickly to the cold reaction solution; temperatures reached -90 °C. ZnCl<sub>2</sub> (0.76 mL, 1 M, 0.76 mmol, 1 equiv.) added quickly along sides of flask causing the temperature of the reaction to reach -80 °C, after which the reaction was allowed to slowly warm to room temperature. GC-MS analysis indicated the presence of a new, unexpected product which was isolated by silica gel chromatography (25:1 hexanes, ethyl acetate) and assigned as the ring-opened THF product by NMR **LRMS**: 290.1 (*m/z* for  $\alpha$ -borylether **3-21**: 290), major fragment loss = 57 (assigned to -CH<sub>2</sub>CH<sub>2</sub>CH<sub>2</sub>CH<sub>3</sub>). **Crude** <sup>1</sup>H NMR contains 4.25 (s, 1 H), AB splitting of diastereotopic protons (1 H, 1 H, -O-CH<sub>2</sub>CH<sub>2</sub>-).

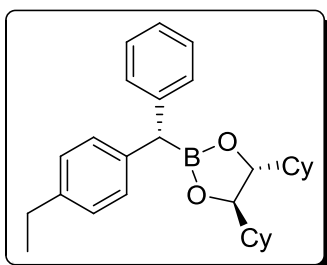


**Synthesis of 1-chloro-1-phenylmethylboronic acid pinacolate ester in the absence of ZnCl<sub>2</sub>.** ZnCl<sub>2</sub> was omitted from the homologation procedure to disfavor any product arising from ring-opened THF. 0.08 mL of dichloromethane (1.327 g/mL, 85 g/mol, 1.2 mmol, 1.6 equiv.) was taken up in freshly distilled THF and cooled to -100 °C with an 95% EtOH / N<sub>2</sub>(liq.) bath. *n*-butyllithium (0.85 mL, 1.3 M, 1.1 mmol, 1.5 equiv.) was added down the sides of the flask so that the internal temperature never exceeded -100 °C. After 30 min, a solution of phenyl boronic acid pinacol ester (PhBPin, 0.157 g, 204 g/mol, 0.76 mmol, 1 equiv) in 1 mL THF was added quickly to the cold reaction solution; temperatures reached -85 °C. A white precipitate was observed which redissolved only after the

internal temperature of the reaction reached  $-45\text{ }^{\circ}\text{C}$ . After warming to room temperature overnight, a dark, but translucent, solution was observed. Analysis of a crude aliquot indicated that, although the undesired benzylic ether product is still produced, the desired  $\alpha$ -chlorobenzyl boronic ester is the major species observed in solution when  $\text{ZnCl}_2$  is omitted.

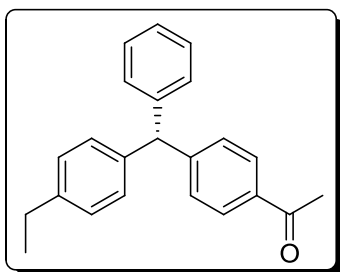
**Synthesis of 1-chloro-1-phenylmethylboronic acid pinacolate ester in the presence of  $\text{ZnCl}_2$ : An Examination of Reaction Temperature.**  $\text{ZnCl}_2$  was reincorporated into the reaction procedure, with aliquots taken during the warming step to determine point at which the desired  $\alpha$ -chlorobenzyl boronic ester is consumed by secondary reactions. In the event, 0.08 mL dichloromethane (1.327 g/mL, 85 g/mol, 1.2 mmol, 1.6 equiv.) was taken up in 1 mL of freshly distilled THF and cooled to  $-100\text{ }^{\circ}\text{C}$  with an 95% EtOH /  $\text{N}_2(\text{liq.})$  bath. *n*-butyllithium (0.85 mL, 1.3 M, 1.1 mmol, 1.5 equiv.) was added down the sides of the flask so that the internal temperature never exceeded  $-100\text{ }^{\circ}\text{C}$ . After 30 min, a solution of phenyl boronic acid pinacol ester (PhBPIn, 0.155 g, 204 g/mol, 0.76 mmol, 1 equiv) in 1 mL THF was added quickly to the cloudy reaction slurry; temperatures reached  $-85\text{ }^{\circ}\text{C}$  though dissolution of the precipitate did not occur. After 5 min,  $\text{ZnCl}_2$  (0.75 mL, 1 M, 0.75 mmol, 1 equiv.) was added portion-wise. Aliquots were taken at various temperatures throughout the warming process and quenched by aqueous workup prior to GC-MS analysis. Migration (in the presence of  $\text{ZnCl}_2$ ) begins at  $-40\text{ }^{\circ}\text{C}$ , though starting PhBpin is still the major species observed. By  $-20\text{ }^{\circ}\text{C}$ , the desired  $\alpha$ -chlorobenzyl boronic ester is the major species observed, though the benzyl ether is also observed in

small amounts. By 0 °C, an approximately equimolar amount of product and undesired ether are observed.



**In situ Grignard Quench to Synthesize (S)-(4R,5R)-4,5-dicyclohexyl-2-(1-phenyl-1-(4-ethylphenyl)methyl)-1,3,2-dioxaborolane (3-23).** 0.04 mL Dichloromethane (1.327 g/mL, 85 g/mol, 0.6 mmol, 1.5 equiv.) was taken up in 1 mL of freshly distilled THF and cooled to -100 °C with an 95% EtOH / N<sub>2</sub>(liq.) bath. *n*-Butyllithium (0.27 mL, 1.45 M, 0.368 mmol, 1.3 equiv.) was added down the sides of the flask so that the internal temperature never exceeded -100 °C. After 30 min, a solution of (4R,5R)-4,5-dicyclohexyl-2-(4-ethylphenyl)-1,3,2-dioxaborolane (96.2 mg, 340 g/mol, 0.283 mmol, 1.0 equiv.) in 1 mL diethyl ether was added quickly to the cloudy reaction slurry; temperatures reached -78 °C and the murky precipitate temporarily disappears. After 5 min, ZnCl<sub>2</sub> (0.75 mL, 1 M, 0.75 mmol, 1 equiv.) was added portion-wise and the precipitate is reformed. The reaction solution was slowly warmed to -20 °C over the course of two hours, after which PhMgBr (0.3 mL, 1 M, 0.3 mmol, 1 equiv.) was added dropwise. Despite being the major product observed by GC-MS (after warming to room temperature overnight), the desired dibenzylic boronic ester was isolated in only 13% yield after aqueous workup and silica gel chromatography (5:1 hexanes: ethyl acetate). Product is suspected to be unstable under aqueous conditions. <sup>1</sup>H NMR (400 MHz, CDCl<sub>3</sub>) δ 7.20 (m, 4 H), 7.13 (m, 2 H), 7.06 (m, 1 H), 7.01 (d, 2 H, *J* = 8.0 Hz), 3.81 (d, 2 H, overlapping with singlet at 3.80 ppm), 3.80 (s, 1 H), 2.51 (t, *J* = 7.6 Hz, 2 H), 1.65 (m,

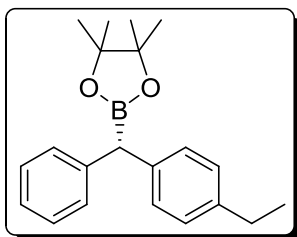
br, 6 H), 1.57 (m, 2 H), 1.45 (m, 2 H), 1.23 (m, 2 H), 1.12 (t,  $J = 7.6$  Hz, 3 H), 1.05 (m, 5 H), 0.93 (m, 3 H), 0.81 (m, 2 H)  $^{13}\text{C}$  NMR (400 MHz,  $\text{CDCl}_3$ )  $\delta$  142.6, 141.4, 139.4, 129.1, 128.3, 127.9, 125.5, 83.8, 43.0, 28.3, 27.5, 26.5, 26.0, 25.9, 15.6. **LRMS:**  $m/z$  430.3.



**Attempted Synthesis of non-racemic (4-Acetylphenyl)-(4-ethylphenyl)phenylmethane.** In a nitrogen-atmosphere glovebox, 4-iodoacetophenone (5.98 mg, 245.9 g/mol, 0.024 mmol, 1.0 equiv.), (S)-(4*R*,5*R*)-4,5-dicyclohexyl-2-(1-phenyl-1-(4-ethylphenyl)methyl)-1,3,2-dioxaborolane (15.5 mg, 430 g/mol, 0.035 mmol, 1.49 equiv.),  $\text{Ag}_2\text{O}$  (8.67 mg, 234 g/mol, 0.037 mmol, 1.54 equiv.),  $\text{Pd}(\text{PPh}_3)_4$  (3.67 mg, 1155.6 g/mol, 0.0032 mmol, 13.0 mol% Pd),  $\text{PPh}_3$  (3.23 mg, 262 g/mol, 0.012 mmol, 0.51 equiv., 7.8:1 P:Pd) and  $\text{K}_2\text{CO}_3$  (5.41 mg, 138 g/mol, 0.039 mmol, 1.63 equiv.) were added to a tared 4 dram vial and taken up in 0.5 g of DME. The reaction solution was sealed in the glovebox, removed, and placed in a 85 °C oil bath for 16 h. Once cooled, the reaction solution was passed through a celite plug and washed with copious amounts of diethyl ether. GC-MS analysis revealed that the dibenzylic boronic ester was completely consumed and that the protodeboronated 1,1-(4-ethylphenyl)phenylmethane was the major product in solution. No cross-coupling product was observed.

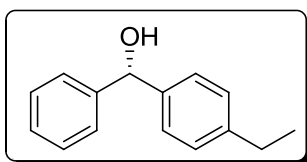


### 6.2.9 Synthesis of Asymmetric Dibenzyl boronic esters by Lithiation-Borylation



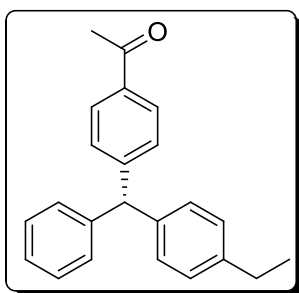
**Synthesis of (S)-(4-Ethylphenyl)phenyl methane boronic acid pinacolate ester ((S)-3-18).** *N,N*-diisopropyl benzyl carbamate (261.67 mg, 235 g/mol, 1.113 mmol, 1.0 equiv.) and (-)-sparteine (0.35 mL, 1.02 g/mL, 234.4 g/mol, 1.448 mmol,

1.3 equiv.) were taken up in 5 mL of hexanes and cooled to -78 °C in a dry ice/acetone bath. *s*-Butyllithium (1.1 mL, 1.4 M, 1.54 mmol, 1.4 equiv.) was added dropwise to the cold solution, to give a bright yellow solution which eventually turned orange. After 2 h of lithiation, an ethereal solution of 4-ethylphenylboronic acid pinacolate ester (256.8 mg, 232 g/mol, 1.10 mmol, 1.0 equiv., in 1.2 mL hexanes) was added dropwise. After 3 h borylation, freshly prepared MgBr<sub>2</sub> diethyl etherate (2.0 equiv.) was added to the cold solution as an ethereal solution. MgBr<sub>2</sub> diethyl etherate is prepared by adding a necessary amount of 1,2-dibromoethane, in this case, 2 equivalents per boronic ester to an excess of Mg turnings in dry ether. The contents of the dense layer that dissociates from the ether are added to the reaction solution *via* syringe. After addition of the MgBr<sub>2</sub>, the solution is allowed to warm slowly before being heated to reflux overnight. After aqueous workup, two silica gel chromatography steps (40:1 hexanes:ethyl acetate) were performed to ensure purity and 114 mg (33% yield) of white solid was isolated.



### Synthesis of (S)-(4-ethylphenyl)phenylmethanol (3-26).

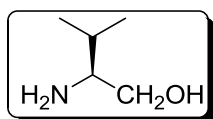
19.5 mg of non-racemic (4-ethylphenyl)phenyl methane boronic acid pinacolate ester (322 g/mol, 0.061 mmol) (**S**)-**3-18** were taken up in 2 mL of diethyl ether and cooled to 0 °C. Separately, 1.5 mL of 30% H<sub>2</sub>O<sub>2</sub>(aq.) and 1.5 mL of 1 M NaOH<sub>(aq.)</sub> were combined under flowing Ar<sub>(g)</sub>. 1.5 mL of this solution was added slowly to the ethereal solution of boronic ester. TLC analysis of the reaction progress (10:1 hexanes:ethyl acetate) indicated that the reaction was nearly complete after 1 h. The reaction was quenched with an excess of 1 M NaOH<sub>(aq.)</sub> and worked up with a saturated solution of NH<sub>4</sub>Cl<sub>(aq.)</sub>. The aqueous layers were washed thrice with diethyl ether, and the combined organic layers were dried over MgSO<sub>4</sub>. GC-MS analysis of the crude mixture indicated that the alcohol had been formed cleanly and so its enantiopurity was determined by SFC separation (Column = OD, 5% MeOH, 2 mL, 300 bar) without prior purification. The er of the alcohol was determined to be 66.5:33.5



### Synthesis of non-racemic (4-Acetylphenyl)-(4-

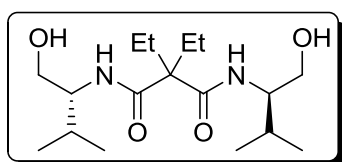
**ethylphenyl)phenylmethane ((S)-3-19)**. In a nitrogen-atmosphere glovebox, 4-iodoacetophenone (8.60 mg, 245.9 g/mol, 0.035 mmol, 1.0 equiv.), (4-ethylphenyl)phenyl methane boronic acid pinacolate ester (**S**)-**3-18**, 16.0 mg, 322 g/mol, 0.53 mmol, 1.42 equiv.er = 66.5:33.5), Ag<sub>2</sub>O (12.3 mg, 234 g/mol, 0.151 mmol, 1.50 equiv.), Pd<sub>2</sub>dba<sub>3</sub> (1.52 mg, 915 g/mol, 0.0017 mmol, 9.5 mol% Pd), PPh<sub>3</sub> (5.97 mg, 262

g/mol, 0.023 mmol, 0.65 equiv., 6.8:1 P:Pd) and  $K_2CO_3$  (8.00 mg, 138 g/mol, 0.058 mmol, 1.66 equiv.) were added to a tared 4 dram vial and taken up in 0.36 g of diethyl ether. The reaction solution was sealed in the glovebox, removed, and placed in a 65 °C oil bath. After 12 h, the reaction solution was found to be concentrated to the point of near dryness; the vial was thus removed from heat at this point. Once cooled, supplemental diethyl ether was added and the reaction solution was passed through a celite plug. The solution was then concentrated *in vacuo* to dryness and an NMR internal standard was added (hexamethylbenzene, HMB, 6.50 mg). NMR yield of the product was determined to be 89%. The crude mixture was purified by silica gel chromatography (column packed with 40:1 hexanes:ethyl acetate before eluting with 20:1 hexanes:ethyl acetate) to yield 6.5 mg of a clear oil, or a 59% isolated yield. Analysis by SFC (Column = AD-H, 5% MeOH, 2 mL, 300 bar) indicated that the product was formed in 61:39 er, or a 92% retention of stereochemistry.



**Synthesis of L-valinol.** 3.90 g  $NaBH_4$  (38 g/mol, 102.4 mmol, 2.4 equiv.) was added to a flame-dried three-neck RBF equipped with a condenser. The two remaining joints were sealed with rubber septa and 125 mL of freshly distilled THF were added *via* syringe. The dispersion was then cooled to 0 °C in an ice bath. While stirring at 0 °C, a solution of  $I_2$  (10.92 g, 253.8 g/mol, 42.68 mmol, 1.0 equiv.) in 25 mL of THF was added dropwise in a highly exothermic reaction. During the first half of the addition, the red-orange colour of the iodine solution quickly dissipated in the reaction flask, after which the orange colour began to persist. Once the iodine solution

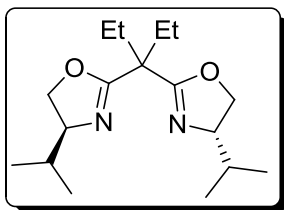
was completely added, the orange, chalky suspension was raised to room temperature before being heated to reflux (oil bath = 70 °C) for 18 h. After cooling, 400 mL of MeOH was added to dissolve the chalky precipitate and the solution was stirred at room temperature for 20 min. before being concentrated *in vacuo* to yield a creamy yellow paste. A 20% KOH<sub>(aq.)</sub> (14.7 g KOH in 75 mL H<sub>2</sub>O) was added to the paste, dissolving most of it, and stirred at room temperature for 5 h. The aqueous solution was extracted with 3 portions of dichloromethane and the combined organic layers were dried over MgSO<sub>4</sub> overnight. After filtration of the MgSO<sub>4</sub> and evaporation of the CH<sub>2</sub>Cl<sub>2</sub> *in vacuo*, 4.41 g of an off-white paste were obtained, representing an 81% crude yield.



**Synthesis of non-racemic (S)-N,N'-Bis[1-(hydroxymethyl)-2-methylpropyl]-2,2'-diethyl-1,3-propanediamide.** 402.8 mg of crude L-valinol (103 g/mol,

3.911 mmol, 1 equiv.) was added to a flame-dried RBF and purged with Ar<sub>(g)</sub>. The L-valinol was taken up in 8 mL of CH<sub>2</sub>Cl<sub>2</sub>, followed by the addition of 1.4 mL of freshly-distilled NEt<sub>3</sub> (0.726 g/mL, 101.2 g/mol, 10.0 mmol, 2.6 equiv.). The solution was cooled to 0°C in an ice bath. Diethylmalonyl dichloride (0.37 mL, 1.145 g/mL, 197.06 g/mol, 2.15 mmol, 0.55 equiv.) was added dropwise to the reaction solution, which was stirred at 0 °C for 5 min before warming slowly to room temperature over the course of an hour. Addition of 6 mL of supplemental CH<sub>2</sub>Cl<sub>2</sub> causes the precipitate which had formed to redissolve. The reaction solution was then quenched with 20 mL of saturated NH<sub>4</sub>Cl<sub>(aq.)</sub> and the aqueous layer was washed with 3 x 20 mL of CH<sub>2</sub>Cl<sub>2</sub>. The combined organic

layers were washed with 40 mL of 1 M HCl<sub>(aq.)</sub>, NaHCO<sub>3(sat. aq.)</sub>, and brine. After each wash, the aqueous layers were extracted with CH<sub>2</sub>Cl<sub>2</sub>, which, once combined, was dried over MgSO<sub>4</sub>. The CH<sub>2</sub>Cl<sub>2</sub> was evaporated *in vacuo* to give 541.7 mg of a sticky white semi-solid, representing an 84% crude yield.



**Mesylation and Ring Closing to Form 3,3-Bis[2-[4(S)-iso-propyl-1,3-oxazoliny]]pentane (3-25).** 997.0 mg of the non-racemic dihydroxydiamide was dispersed in 20 mL of CH<sub>2</sub>Cl<sub>2</sub>. 1.85 mL of freshly-distilled NEt<sub>3</sub> (0.726 g/mL, 101.2 g/mol, 13.3 mmol, 4.4 equiv.) was added and the solution was cooled to 0 °C. The dihydroxydiamide was not fully soluble in CH<sub>2</sub>Cl<sub>2</sub>, even after the addition of NEt<sub>3</sub>, so a further 10 mL of CH<sub>2</sub>Cl<sub>2</sub> were added. To the cooled solution was added 0.56 mL of mesitylchloride (MsCl, 1.480 g/mL, 114.5 g/mol, 7.25 mmol, 2.4 equiv.) causing all remaining solids to solubilize. The solution was warmed to room temperature before being worked up with NH<sub>4</sub>Cl<sub>(sat., aq.)</sub>, and brine. The combined organic layers were dried over MgSO<sub>4</sub> before being filtered and concentrated *in vacuo* to yield 1.477 g of an orange oil, representing a quantitative conversion to the desired dimesitylated product. Without purification, the orange oil was taken up in 12 mL of a 0.5 M NaOH H<sub>2</sub>O/MeOH solution, though the dimesitylated product was initially not fully soluble. The dispersion was heated to reflux with a condenser for 3 h before being cooled and diluted with 10 mL of MeOH to fully solubilize everything. The aqueous solution was then extracted with 3 x 20 mL CH<sub>2</sub>Cl<sub>2</sub>

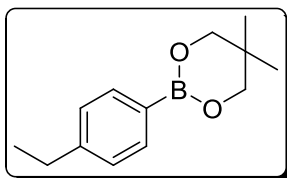
and the combined organic layers were washed with brine and dried over  $\text{MgSO}_4$ . Filtration and concentration yielded 938 mg of crude oil. The crude oil was purified by silica gel chromatography (10:1  $\text{CHCl}_3$ :Acetone) to give 763.7 mg of clear oil, representing an 86% isolated yield over two steps.  $^1\text{H NMR}$  (400 MHz,  $\text{CDCl}_3$ )  $\delta$  4.15-4.05 (m, 2 H), 3.95-3.85 (m, 4 H), 1.91 (m, 4 H), 1.73 (m, 2 H), 0.86 (d,  $J = 7.2$  Hz, 6 H), 0.76 (m, 12 H).  $^{13}\text{C NMR}$  (100 MHz,  $\text{CDCl}_3$ )  $\delta$  167.2, 71.7, 69.5, 46.6, 32.3, 25.2, 18.8, 18.2, 17.7, 8.3. **HRMS**: calcd for  $[\text{M}+\text{H}]^+$  ( $\text{C}_{21}\text{H}_{24}\text{O}$ )  $m/z$  341.2804; found 341.2800.

**Synthesis of (S)-(4-Ethylphenyl)phenyl methane boronic acid pinacolate ester (S)-3-18 with Bis(oxazoline) ligand 3-25.** *N,N*-Diisopropyl carbamic acid benzyl ester (82.7 mg, 235 g/mol, 0.352 mmol, 1.0 equiv.) and chiral bis(oxazoline) ligand **3-25** (131.5 mg, 294 g/mol, 0.422 mmol, 1.2 equiv.) were taken up in 4 mL of hexanes and cooled to  $-78$  °C in a dry ice/acetone bath. *s*-Butyllithium (0.32 mL, 1.2 M, 0.422 mmol, 1.2 equiv.) was added dropwise to the cold solution. After 0.5 h of lithiation, a hexanes solution of 4-ethylphenylboronic acid pinacolate ester (98.2 mg, 232 g/mol, 0.528 mmol, 1.2 equiv., in 1 mL hexanes) was added dropwise. After 1 h borylation, freshly prepared  $\text{MgBr}_2$  diethyl etherate (2.0 equiv.) was added to the cold solution as an ethereal solution.  $\text{MgBr}_2$  diethyl etherate is prepared by adding a necessary amount of 1,2-dibromoethane, in this case, 2 equivalents per boronic ester to an excess of Mg turnings in dry ether. The contents of the dense layer that dissociates from the ether are added to the reaction solution *via* syringe. After addition of the  $\text{MgBr}_2$ , the solution is allowed to warm slowly before being heated to reflux overnight. After an aqueous workup ( $\text{NH}_4\text{Cl}_{(\text{sat.})}$ ), the combined organic layers

were concentrated *in vacuo* and then taken up in 5 mL of diethyl ether and cooled to 0 °C. 3 mL of a pre-prepared solution of NaOH/H<sub>2</sub>O<sub>2</sub> (3 mL 1 M NaOH, 1.5 mL H<sub>2</sub>O<sub>2</sub>) were added under air-free conditions and the oxidation was allowed to proceed at 0 °C for 2 h. The reaction was quenched with an excess of 1 M NaOH<sub>(aq.)</sub> and washed with NH<sub>4</sub>Cl<sub>(sat.)</sub>. The combined organic layers were dried over MgSO<sub>4</sub>, filtered and concentrated *in vacuo*. The resultant crude oil was purified by silica gel chromatography (10:1 hexanes:ethyl acetate) and submitted to SFC analysis (Column = OD, 7% MeOH, 100 bar, 2 mL) which revealed that the dibenzylic alcohol was synthesized with an er = 52:48.

**Lithiation-borylation with chiral bis(oxazoline) ligand 3-25 and MeOH.** *N,N*-Diisopropyl carbamic acid benzyl ester (81.4 mg, 235 g/mol, 0.346 mmol, 1.0 equiv.) and chiral bis(oxazoline) ligand **3-25** (135.5 mg, 294 g/mol, 0.46 mmol, 1.2 equiv.) were taken up in 4 mL of hexanes and cooled to -78 °C in a dry ice/acetone bath. *s*-Butyllithium (0.32 mL, 1.2 M, 0.422 mmol, 1.2 equiv.) was added dropwise to the cold solution. After 0.5 h of lithiation, a hexanes solution of 4-ethylphenylboronic acid pinacolate ester (162.3 mg, 232 g/mol, 0.693 mmol, 2.0 equiv., in 1 mL hexanes) was added dropwise. After 1 h borylation, commercially available MgBr<sub>2</sub> dietherate was taken up in 0.5 mL of MeOH and added to the cold reaction solution. After addition of the MgBr<sub>2</sub>/MeOH, the solution was allowed to warm slowly before being heated to reflux overnight. After an aqueous workup (NH<sub>4</sub>Cl<sub>(sat.)</sub>), the combined organic layers were concentrated *in vacuo* and then taken up in 5 mL of diethyl ether and cooled to 0 °C. 3

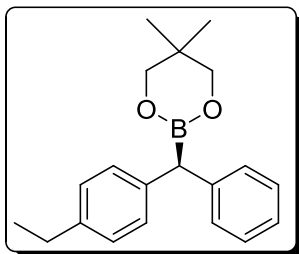
mL of a pre-prepared solution of NaOH/H<sub>2</sub>O<sub>2</sub> (3 mL 1 M NaOH, 1.5 mL H<sub>2</sub>O<sub>2</sub>) were added under air-free conditions and the oxidation was allowed to proceed at 0 °C for 2 h. The reaction was quenched with an excess of 1 M NaOH<sub>(aq.)</sub> and washed with NH<sub>4</sub>Cl<sub>(sat.)</sub>. The combined organic layers were dried over MgSO<sub>4</sub>, filtered and concentrated *in vacuo*. The resultant crude oil was submitted to SFC analysis (Column = OD, 7% MeOH, 100 bar, 2 mL) which revealed that the dibenzylic alcohol was synthesized with an er = 57:43.



**Synthesis of 4-ethylphenylboronic acid (2,2-dimethyl-1,3-**

**propanediol) ester (3-27).** 0.819 g of 4-ethylphenylboronic acid (150 g/mol, 5.46 mmol, 1.0 equiv.) and 0.569 g of 2,2-dimethyl-1,3-propanediol (104 g/mol, 5.46 mmol, 1.0 equiv.) were taken up in 10 mL of diethyl ether. Once dissolved, 0.663 g of MgSO<sub>4</sub> (120 g/mol, 5.48 mmol, 1.0 equiv.) was dispersed in the solution, which was stirred at 25 °C for 21 h. The dispersion was filtered by vacuum and washed with copious amounts of diethyl ether. The homogeneous solution was then concentrated *in vacuo* to yield 1.182 g of the pure boronic ester, representing a 99% isolated yield. **<sup>1</sup>H NMR** (400 MHz, CDCl<sub>3</sub>) δ 7.65 (d, *J* = 7.6 Hz, 2 H), 7.12 (d, *J* = 7.6 Hz, 2 H), 3.68 (s, 4 H), 2.58 (q, *J* = 7.2 Hz, 2 H), 1.16 (t, *J* = 7.6 Hz, 3 H). **<sup>11</sup>B NMR:** (160 MHz, CDCl<sub>3</sub>): δ 26.9. **<sup>13</sup>C NMR** (400 MHz, CDCl<sub>3</sub>) δ 146.6, 133.4, 126.6, 71.7, 31.3, 28.4, 21.3, 14.9. **HRMS (EI-TOF):** calcd for [M]<sup>+</sup> (C<sub>13</sub>H<sub>29</sub>O<sub>2</sub>B) *m/z* 218.1478; found 218.1486.





### Optimization of Dibenzylic boronic neopentyl esters with

**Bis(oxazoline) ligand (3-28).** *N,N*-Diisopropyl carbamic acid

benzyl ester (70.74 mg, 235 g/mol, 0.301 mmol, 1.0 equiv.) and

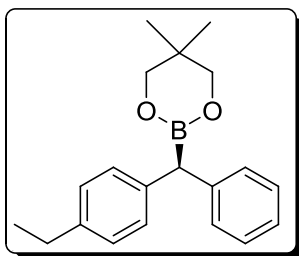
chiral bis(oxazoline) ligand **3-25** (105.6 mg, 294 g/mol, 0.360

mmol, 1.2 equiv.) were taken up in 3.5 mL of hexanes and cooled to  $-78\text{ }^{\circ}\text{C}$  in a dry ice/acetone bath. *s*-Butyllithium (0.28 mL, 1.3 M, 0.361 mmol, 1.2 equiv.) was added dropwise to the cold solution, maintaining an internal temperature of  $-70\text{ }^{\circ}\text{C}$ . After 2 h of lithiation, a hexanes solution of 4-ethylphenylboronic acid (2,2-dimethyl-1,3-propanediol) ester (**3-27**, 131.2 mg, 232 g/mol, 0.602 mmol, 2.0 equiv., in 1 mL hexanes) was added dropwise. After 1 h borylation, freshly prepared  $\text{MgBr}_2$  diethyl etherate (3.0 equiv.) was added to the cold solution as an ethereal solution.  $\text{MgBr}_2$  diethyl etherate is prepared by adding a necessary amount of 1,2-dibromoethane, in this case, 3 equivalents per boronic ester to an excess of Mg turnings in dry ether. The contents of the dense layer that dissociates from the ether are added to the reaction solution *via* syringe. After addition of the  $\text{MgBr}_2$ , the solution is allowed to warm slowly before being heated to reflux overnight ( $50\text{ }^{\circ}\text{C}$  oil bath). After an aqueous workup ( $\text{NH}_4\text{Cl}_{(\text{sat.})}$ ), the combined organic layers were concentrated *in vacuo* and then taken up in 5 mL of diethyl ether and cooled to  $0\text{ }^{\circ}\text{C}$ . 3 mL of a pre-prepared solution of  $\text{NaOH}/\text{H}_2\text{O}_2$  (3 mL 1 M  $\text{NaOH}$ , 1.5 mL  $\text{H}_2\text{O}_2$ ) were added under air-free conditions and the oxidation was allowed to proceed at  $0\text{ }^{\circ}\text{C}$  for 2 h. The reaction was quenched with an excess of 1 M  $\text{NaOH}_{(\text{aq.})}$  and washed with  $\text{NH}_4\text{Cl}_{(\text{sat.})}$ . The combined organic layers were dried over  $\text{MgSO}_4$ , filtered and concentrated *in vacuo*. The resultant crude oil (containing both the dibenzylic alcohol and

the phenol generated from oxidation of the excess starting boronic ester) was submitted to SFC analysis without purification (Column = OD, 7% MeOH, 100 bar, 2 mL). The dibenzylic alcohol (*S*)-(4-ethylphenyl)phenylmethanol, was found to have been synthesized with an e.r. = 99:1. As a means of verifying the veracity of this result, 75 mg of the oil was taken up in 1.5 mL of CHCl<sub>3</sub> and checked for optical rotation; a measured rotation of +0.06° was observed.

**Synthesis of dibenzylic boronic ester 3-28 with a smaller excess of neopentyl boronic ester.** The enantioselectivity of the reaction was determined at a lesser (1.2 equiv.) excess of boronic ester. *N,N*-Diisopropyl carbamic acid benzyl ester (68.0 mg, 235 g/mol, 0.289 mmol, 1.0 equiv.) and chiral bis(oxazoline) ligand **3-25** (105.0 mg, 294 g/mol, 0.357 mmol, 1.2 equiv.) were taken up in 3.5 mL of hexanes and cooled to -78 °C in a dry ice/acetone bath. *s*-butyllithium (0.28 mL, 1.3 M, 0.361 mmol, 1.2 equiv.) was added dropwise to the cold solution, creating a dark brown slurry. After 1.5 h of lithiation, the solution appears yellow. After the requisite 2 h of lithiation, a hexanes solution of 4-ethylphenylboronic acid (2,2-dimethyl-1,3-propanediol) ester (**3-27**, 81.9 mg, 232 g/mol, 0.376 mmol, **1.2 equiv.**, in 1 mL hexanes) was added dropwise. After 1 h borylation, freshly prepared MgBr<sub>2</sub> diethyl etherate (3.0 equiv.) was added to the cold solution as an ethereal solution. MgBr<sub>2</sub> diethyl etherate is prepared by adding a necessary amount of 1,2-dibromoethane, in this case, 3 equivalents per boronic ester to an excess of Mg turnings in dry ether. The contents of the dense layer that dissociates from the ether are added to the reaction solution *via* syringe. After addition of the MgBr<sub>2</sub>, the solution is

allowed to warm slowly before being heated to reflux overnight (50 °C oil bath). After an aqueous workup ( $\text{NH}_4\text{Cl}_{(\text{sat.})}$ ), the combined organic layers were concentrated *in vacuo* and then taken up in 5 mL of diethyl ether and cooled to 0 °C. 3 mL of a pre-prepared solution of  $\text{NaOH}/\text{H}_2\text{O}_2$  (3 mL 1 M  $\text{NaOH}$ , 1.5 mL  $\text{H}_2\text{O}_2$ ) were added under air-free conditions and the oxidation was allowed to proceed at 0 °C for 2 h. The reaction was quenched with an excess of 1 M  $\text{NaOH}_{(\text{aq.})}$  and washed with  $\text{NH}_4\text{Cl}_{(\text{sat.})}$ . The combined organic layers were dried over  $\text{MgSO}_4$ , filtered and concentrated *in vacuo*. The resultant yellow oil (containing both the dibenzylic alcohol and the phenol generated from oxidation of the excess starting boronic ester) was submitted to SFC analysis without purification (Column = OD, 7% MeOH, 100 bar, 2 mL). The dibenzylic alcohol was again found to have been synthesized with an e.r. = 99:1.

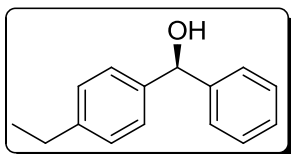


**Synthesis and Isolation of (S)-(4-Ethylphenyl)phenylmethane boronic acid neopentyl ester (3-28).** *N,N*-

Diisopropyl carbamic acid benzyl ester (163.3 mg, 235 g/mol, 0.695 mmol, 1.0 equiv.) and chiral bis(oxazoline) ligand **3-25**

(252.0 mg, 294 g/mol, 0.834 mmol, 1.2 equiv.) were taken up in 7 mL of hexanes and cooled to -78 °C in a dry ice/acetone bath. *s*-butyllithium (0.65 mL, 1.3 M, 0.834 mmol, 1.2 equiv.) was added dropwise to the cold solution, maintaining an internal temperature of -71 °C. After 2 h of lithiation, a hexanes solution of 4-ethylphenylboronic acid (2,2-dimethyl-1,3-propanediol) ester (**3-27**, 167.0 mg, 232 g/mol, 0.765 mmol, 1.1 equiv., in 2 mL hexanes) was added dropwise, keeping the internal temperature between -72 °C and -

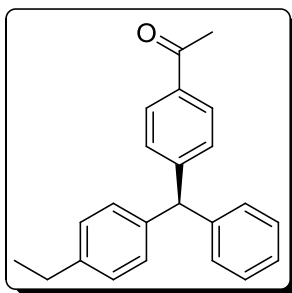
69 °C. After 1 h of borylation, freshly prepared MgBr<sub>2</sub> diethyl etherate (3.0 equiv.) was added to the cold solution as an ethereal solution. MgBr<sub>2</sub> diethyl etherate is prepared by adding a necessary amount of 1,2-dibromoethane, in this case, 3 equivalents per boronic ester to an excess of Mg turnings in dry ether. The contents of the dense layer that dissociates from the ether are added to the reaction solution *via* syringe. After addition of the MgBr<sub>2</sub>, the solution is allowed to warm slowly before being heated to reflux overnight (50 °C oil bath). After an aqueous workup (NH<sub>4</sub>Cl<sub>(sat.)</sub>), the combined organic layers were concentrated *in vacuo* to give a bright yellow oil. Separation of the product from the starting boronic ester proved difficult, ultimately requiring two silica gel chromatography steps (20:1 hexanes:ethyl acetate). Impure fractions containing the desired product were discarded after both chromatography steps, severely affecting the isolated yield. Indeed, the crude yield after the first column was 31%, with an isolated yield of 11% being recorded after the second purification step. <sup>1</sup>H NMR (400 MHz, CDCl<sub>3</sub>) δ 7.19 (m, 4 H), 7.11 (d, *J* = 8 Hz, 2 H), 7.07 (m, 1 H), 7.02 (d, *J* = 8 Hz, 2 H), 3.55 (s, 4 H), 2.52 (q, *J* = 7.6 Hz, 2 H), 1.14 (t, *J* = 7.6 Hz, 3 H), 0.85 (s, 6 H). <sup>11</sup>B NMR: (160 MHz, CDCl<sub>3</sub>): δ 29.3.



**Synthesis of (*S*)-(4-ethylphenyl)phenylmethanol for Analysis of Enantiopurity (3-26).** 29.3 mg of the dibenzylic boronic neopentyl ester (*S*)-**3-28** was taken up in 3 mL of diethyl ether

and cooled to 0 °C. 1.5 mL of a pre-prepared solution of NaOH/H<sub>2</sub>O<sub>2</sub> (2 mL 1 M NaOH,

1 mL H<sub>2</sub>O<sub>2</sub>) was added under air-free conditions and the oxidation was allowed to proceed at 0 °C for 1 h. The reaction was quenched with 2 mL of 1 M NaOH<sub>(aq.)</sub> and washed with NH<sub>4</sub>Cl<sub>(sat.)</sub>. The combined organic layers were dried over MgSO<sub>4</sub>, filtered and concentrated *in vacuo*. The resultant crude oil was purified by silica gel chromatography (10:1 hexanes:ethyl acetate, R<sub>f</sub> = 6/35) to yield 17.0 mg of a white solid, representing an 84% yield. Analysis by SFC (Column = OD, 7% MeOH, 100 bar, 2 mL) indicated that the dibenzylic alcohol, and thus the dibenzylic boronic ester as well, was synthesized with an er = 99.2:0.8.

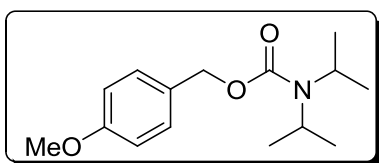


#### Cross-Coupling of Enantioenriched Dibenzylic Boronic

#### Esters: The Synthesis of non-racemic triarylmethane (*R*)-3-

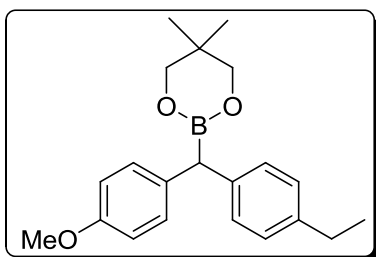
**19.** In a nitrogen-atmosphere glovebox, 4-iodoacetophenone (15.44 mg, 245.9 g/mol, 0.063 mmol, 1.0 equiv.), (4-ethylphenyl)phenyl methane boronic acid (2,2-dimethyl-1,3-propanediol) ester (**3-28**, 29.30 mg, 308 g/mol, 0.095 mmol, 1.51 equiv., er = 99:1), Ag<sub>2</sub>O (21.9 mg, 234 g/mol, 0.095 mmol, 1.51 equiv.), Pd(PPh<sub>3</sub>)<sub>4</sub> (5.84 mg, 1155.6 g/mol, 0.0050 mmol, 7.9 mol% Pd), PPh<sub>3</sub> (6.45 mg, 262 g/mol, 0.025 mmol, 0.39 equiv., 9.0:1 P: Pd) and K<sub>2</sub>CO<sub>3</sub> (14.1 mg, 138 g/mol, 0.102 mmol, 1.62 equiv.) were added to a tared 4 dram vial and taken up in 1.1 g of DME. The reaction solution was sealed in the glovebox, removed, and placed in a 75 °C oil bath. After 22 h, the reaction was removed from the oil bath, and allowed to cool to room temperature. Once cooled, the reaction solution was passed through a

celite plug and washed with copious amounts of diethyl ether. The solution was then concentrated *in vacuo* and the crude oil was purified by silica gel chromatography (40:1 hexanes:ethyl acetate,  $R_f = 5/35$ ) to yield 8.24 mg of a clear oil, or a 42% isolated yield. Analysis by SFC (Column = AD-H, 5% MeOH, 2 mL, 200 bar) indicated that the product was formed with an er = 82.1:17.9, representing an 83% retention of stereochemistry.



**Synthesis of *N,N*-Diisopropyl carbamic acid (4-methoxybenzyl) ester (3-29).** *N,N*-diisopropylcarbonyl chloride (1.703 g, 163.65 g/mol, 10.5 mmol, 1.05 equiv.)

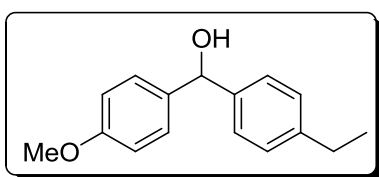
and freshly distilled triethylamine (1.4 mL, 0.726 g/mL, 101.2 g/mol, 10.1 mmol, 1.05 equiv.) were taken up in 20 mL of  $\text{CH}_2\text{Cl}_2$ . (4-methoxy)-benzyl alcohol (1.25 mL, 1.108 g/mL, 138 g/mol, 9.91 mmol, 1 equiv.) was added and the solution was stirred under refluxing conditions (oil bath = 50 °C) for 24 h, with salts eventually precipitating out of solution. The solution was then washed with sat.  $\text{NH}_4\text{Cl}_{(\text{aq})}$  and the aqueous layer was extracted with 3 x 25 mL  $\text{CH}_2\text{Cl}_2$ . The crude oil was purified by silica gel chromatography (10:1 hexanes:ethyl acetate,  $R_f = 1/6$ ) to yield 2.054 g of the desired carbamate, or 78% isolated yield.  **$^1\text{H NMR}$**  (400 MHz,  $\text{CDCl}_3$ )  $\delta$  7.32 (d,  $J = 8.4$  Hz, 2 H), 6.90 (d,  $J = 8.2$  Hz, 2 H), 5.08 (s, 2 H), 4.3-3.9 (br, 2 H), 3.83 (s, 3 H), 1.21 (d,  $J = 6.8$  Hz, 12 H).  **$^{13}\text{C NMR}$**  (400 MHz,  $\text{CDCl}_3$ )  $\delta$  159.3, 155.6, 129.7, 129.3, 113.8, 66.3, 55.3, 45.4 (br), 20.8 (br). **HRMS (EI-TOF):** calcd for  $[\text{M}]^+$  ( $\text{C}_{15}\text{H}_{23}\text{O}_3\text{N}$ )  $m/z$  265.1678; found 265.1672.



**Synthesis of rac-(1-(4-methoxyphenyl), 1-(4-ethylphenyl))methylboronic acid (2,2-dimethyl-1,3-propanediol) ester (3-30).** *N,N*-Diisopropyl carbamic acid (4-methoxybenzyl) ester (**3-29**, 400.4 mg, 265.2

g/mol, 1.51 mmol, 1.0 equiv.) and TMEDA (219.9 mg, 116 g/mol, 1.86 mmol, 1.25 equiv.) were taken up in 10 mL of hexanes and cooled to  $-78\text{ }^{\circ}\text{C}$  in a dry ice/acetone bath. *s*-butyllithium (1.4 mL, 1.3 M, 1.82 mmol, 1.2 equiv.) was added dropwise to the cold solution, maintaining an internal temperature of  $-74\text{ }^{\circ}\text{C}$ . After 2 h of lithiation, a hexanes solution of 4-ethylphenylboronic acid (2,2-dimethyl-1,3-propanediol) ester (**3-27**, 366.5 mg, 232 g/mol, 1.68 mmol, 1.1 equiv., in 1.5 mL hexanes) was added dropwise, keeping internal temperature below  $-71\text{ }^{\circ}\text{C}$ . After 1 h borylation, freshly prepared  $\text{MgBr}_2$  diethyl etherate (3.0 equiv.) was added to the cold solution as an ethereal solution.  $\text{MgBr}_2$  diethyl etherate is prepared by adding a necessary amount of 1,2-dibromoethane, in this case, 3 equivalents per boronic ester to an excess of Mg turnings in dry ether. The contents of the dense layer that dissociates from the ether are added to the reaction solution *via* syringe. After addition of the  $\text{MgBr}_2$ , the solution is allowed to warm slowly before being heated to reflux overnight ( $50\text{ }^{\circ}\text{C}$  oil bath). After an aqueous workup ( $\text{NH}_4\text{Cl}_{(\text{sat.})}$ ), the combined organic layers were concentrated *in vacuo* and the crude oil was purified in one step by silica gel chromatography (20:1 hexanes:ethyl acetate). 292.9 mg of pure product were obtained, representing a 57.4% isolated yield.  $^1\text{H NMR}$  (400 MHz,  $\text{CDCl}_3$ )  $\delta$  7.11 (m, 4H), 7.02 (d,  $J = 8\text{ Hz}$ , 2H), 6.74 (d,  $J = 8.4\text{ Hz}$ , 2H), 3.70 (s, 3H), 3.59 (s, 1H), 3.56 (s,

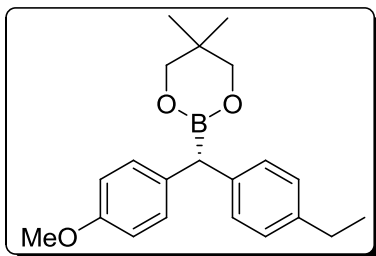
4H), 2.53 (q,  $J = 7.6$  Hz, 2H), 1.14 (t,  $J = 7.6$  Hz, 3H), 0.86 (s, 6H).  **$^{11}\text{B}$  NMR**: (160 MHz,  $\text{CDCl}_3$ ):  $\delta$  29.3.  **$^{13}\text{C}$  NMR** (400 MHz,  $\text{CDCl}_3$ )  $\delta$  157.4, 141.0, 140.6, 135.3, 130.0, 128.8, 127.8, 113.8, 72.3, 55.2, 31.7, 28.4, 21.9, 15.5. **HRMS (EI-TOF)**: calcd for  $[\text{M}]^+$  ( $\text{C}_{21}\text{H}_{27}\text{O}_3\text{B}$ )  $m/z$  338.2053; found 338.2049.



**Synthesis of rac-(4-ethylphenyl)-(4-methoxyphenyl)methanol** 27.5 mg of rac-(1-(4-methoxyphenyl), 1-(4ethylphenyl))methylboronic acid

neopentyl ester (**3-30**) was taken up in 3 mL of diethyl ether and cooled to 0 °C. 1.5 mL of a pre-prepared solution of  $\text{NaOH}/\text{H}_2\text{O}_2$  (2 mL 1 M  $\text{NaOH}$ , 1 mL  $\text{H}_2\text{O}_2$ ) was added under air-free conditions and the oxidation was allowed to proceed at 0 °C for 1 h. The reaction was quenched with 2 mL of 1 M  $\text{NaOH}_{(\text{aq.})}$  and washed with  $\text{NH}_4\text{Cl}_{(\text{sat.})}$ . The combined organic layers were dried over  $\text{MgSO}_4$ , filtered and concentrated *in vacuo*. The resultant crude oil was purified by silica gel chromatography (6:1 hexanes:ethyl acetate,  $R_f = 8/41$ ) to yield 19.7 mg of a white solid, representing an 74% yield. SFC conditions were found that cleanly separated the two enantiomers (OD, 7% MeOH, 2 mL, 100 bar); er = 50.1:49.9.  **$^1\text{H}$  NMR** (400 MHz,  $\text{CDCl}_3$ )  $\delta$  7.21 (m, 4 H), 7.09 (d,  $J = 8$  Hz, 2 H), 6.79 (d,  $J = 8.4$  Hz, 2 H), 5.70 (s, 1 H), 3.71 (s, 3 H), 2.55 (q,  $J = 7.6$  Hz, 2 H), 2.1 (s, br), 1.14 (t,  $J = 7.6$  Hz, 3 H).  **$^{13}\text{C}$  NMR** (400 MHz,  $\text{CDCl}_3$ )  $\delta$  159.0, 143.5, 141.4, 136.3, 128.0, 127.8, 126.5, 113.9, 75.7, 55.3, 31.6, 28.5, 22.7, 15.6, 14.1. **HRMS (EI-TOF)**: calcd for  $[\text{M}]^+$  ( $\text{C}_{16}\text{H}_{18}\text{O}_2$ )  $m/z$  242.1307; found 242.1299.

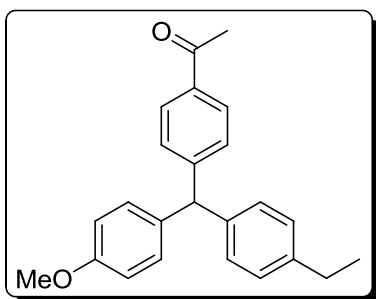




**Synthesis of non-racemic 1,1-(4-methoxyphenyl),(4'-ethylphenyl)-methylboronic acid neopentyl ester ((S)-3-30).** *N,N*-Diisopropyl carbamic acid (4-methoxybenzyl) ester (127.8 mg, 265.2 g/mol, 0.483 mmol, 1.0 equiv.)

and chiral bis(oxazoline) ligand **3-25** (170.5 mg, 294 g/mol, 0.580 mmol, 1.2 equiv.) were taken up in 3.5 mL of hexanes and cooled to  $-78\text{ }^{\circ}\text{C}$  in a dry ice/acetone bath. *s*-butyllithium (0.45 mL, 1.3 M, 0.580 mmol, 1.2 equiv.) was added dropwise to the cold solution, maintaining an internal temperature of  $-73\text{ }^{\circ}\text{C}$ . After 2 h of lithiation, a hexanes solution of 4-ethylphenylboronic acid (2,2-dimethyl-1,3-propanediol) ester (**3-27**, 115.4 mg, 232 g/mol, 0.532 mmol, 1.1 equiv., in 1 mL hexanes) was added dropwise, keeping internal temperature below  $-69\text{ }^{\circ}\text{C}$ . After 1 h borylation, freshly prepared  $\text{MgBr}_2$  diethyl etherate (3.0 equiv.) was added to the cold solution as an ethereal solution.  $\text{MgBr}_2$  diethyl etherate is prepared by adding a necessary amount of 1,2-dibromoethane, in this case, 3 equivalents per boronic ester to an excess of Mg turnings in dry ether. The contents of the dense layer that dissociates from the ether are added to the reaction solution *via* syringe. After addition of the  $\text{MgBr}_2$ , the solution is allowed to warm slowly before being heated to reflux overnight ( $50\text{ }^{\circ}\text{C}$  oil bath). After an aqueous workup (2 x 10 mL  $\text{NH}_4\text{Cl}_{(\text{sat.})}$ ), the combined organic layers were concentrated *in vacuo* and the crude oil was purified in one step by silica gel chromatography (20:1 hexanes:ethyl acetate,  $R_f = 4/38$ ). 29.9 mg of pure product were obtained, representing a 18.4% isolated yield. 8.5 mg of the non-

racemic boronic ester were taken up in 1.5 mL of diethyl ether and cooled to 0 °C. 0.4 mL of a pre-prepared NaOH/H<sub>2</sub>O<sub>2</sub> solution (2 mL 1 M NaOH<sub>(aq.)</sub>, 1 mL H<sub>2</sub>O<sub>2</sub>) was added dropwise to the stirring solution and kept at 0 °C for 15 min before raising to room temperature. After 1.5 h, the reaction was quenched by 2 mL of 1 M NaOH<sub>(aq.)</sub> and worked up with a saturated solution of NH<sub>4</sub>Cl<sub>(aq.)</sub>. SFC analysis (Column = OD, 7% MeOH, 2 mL, 100 bar) indicates an er = 91.5:8.5.



### Synthesis of 1,1-(4-Acetylphenyl),(4'-

**ethylphenyl),(4''-methoxyphenyl)methane (3-31).** In a

nitrogen-atmosphere glovebox, 4-iodoacetophenone

(18.43 mg, 245.9 g/mol, 0.075 mmol, 1.0 equiv.), rac-(1-

(4-methoxyphenyl), 1-(4ethylphenyl))methylboronic acid

(2,2-dimethyl-1,3-propanediol) ester (**3-30**, 36.0 mg, 338 g/mol, 0.106 mmol, 1.4 equiv.),

Ag<sub>2</sub>O (28.4 mg, 234 g/mol, 0.121 mmol, 1.6 equiv.), Pd(PPh<sub>3</sub>)<sub>4</sub> (6.85 mg, 1155.6 g/mol,

0.0059 mmol, 7.9 mol% Pd), PPh<sub>3</sub> (6.84 mg, 262 g/mol, 0.026 mmol, 0.35 equiv., 8.4:1

P:Pd) and K<sub>2</sub>CO<sub>3</sub> (16.23 mg, 138 g/mol, 0.117 mmol, 1.57 equiv.) were added to a tared

4 dram vial and taken up in 1.5 g of DME. The reaction solution was sealed in the

glovebox, removed, and placed in a 75 °C oil bath. After 21 h, the reaction was removed

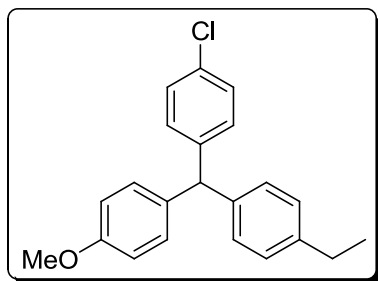
from the oil bath, and allowed to cool to room temperature. Once cooled, the reaction

solution was passed through a celite plug and washed with copious amounts of diethyl

ether. The solution was then concentrated *in vacuo* and the crude oil was purified by

silica gel chromatography (20:1 hexanes:ethyl acetate for one column volume, followed by 10:1 hexanes:ethyl acetate  $R_f = 7/41$  (10:1)) to yield 5.23 mg of a clear oil, or a 20% isolated yield. SFC conditions (Column = OJ, 5% MeOH, 2 mL, 100 bar) were then found that efficiently separated the enantiomer peaks. 4.4 mg of another product with  $R_f = 11/36$  (10:1 hexanes:ethyl acetate) was also isolated and determined by NMR to be the result of boronic ester homocoupling. **Coupling-Product:**  $^1\text{H NMR}$  (400 MHz,  $\text{CDCl}_3$ )  $\delta$  7.80 (d,  $J = 8.4$  Hz, 2 H), 7.14, (d,  $J = 8.0$  Hz, 2 H), 7.05 (d,  $J = 8.4$  Hz, 2 H), 6.93 (d,  $J = 8.4$  Hz, 2 H), 6.92 (d,  $J = 7.6$  Hz, 2 H), 6.75 (d,  $J = 7.2$  Hz, 2 H), 5.44 (s, 1 H), 3.71 (s, 3 H), 2.55 (q,  $J = 7.6$  Hz, 2 H), 2.50 (s, 3 H), 1.15 (t,  $J = 7.6$  Hz, 3 H).  $^{13}\text{C NMR}$  (400 MHz,  $\text{CDCl}_3$ )  $\delta$  150.2, 142.5, 140.6, 138.5, 135.5, 130.3, 129.6, 129.2, 128.4, 127.9, 113.8, 55.7, 55.3, 28.4, 26.6, 15.5. **HRMS (EI-TOF):** calcd for  $[\text{M}]^+$  ( $\text{C}_{24}\text{H}_{24}\text{O}_2$ )  $m/z$  344.1776; found 344.1789.

**Homocoupling Product**  $^1\text{H NMR}$  (400 MHz,  $\text{CDCl}_3$ )  $\delta$  6.98 (d,  $J = 8.0$  Hz, 4 H), 6.96 (d,  $J = 8.4$  Hz, 4 H), 6.85 (d,  $J = 8.0$  Hz, 4 H), 6.56 (d,  $J = 8.8$  Hz, 4 H), 4.56 (s, 2 H), 3.61 (s, 6 H), 2.42 (q,  $J = 7.2$  Hz, 4 H), 1.05 (t,  $J = 7.6$  Hz, 6 H).  $^{13}\text{C NMR}$  (400 MHz,  $\text{CDCl}_3$ )  $\delta$  157.4, 141.2, 136.4, 129.4, 128.2, 127.7, 127.5, 113.5, 55.3, 55.1, 28.3, 15.3.

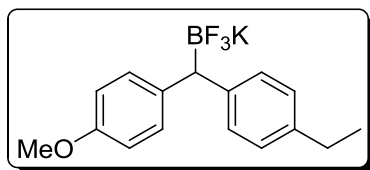


**Synthesis of 1,1-(4-chlorophenyl),(4'-ethoxyphenyl),(4''-ethylphenyl)methane (3-32).** In a nitrogen-atmosphere glovebox, 4-chloriodobenzene

(25.00 mg, 238.4 g/mol, 0.105 mmol, 1.0 equiv.), rac-(1-(4-methoxyphenyl), 1-(4ethylphenyl))methylboronic acid (2,2-dimethyl-1,3-propanediol) ester (**3-30**, 52.3 mg, 338 g/mol, 0.155 mmol, 1.47 equiv.), Ag<sub>2</sub>O (38.5 mg, 234 g/mol, 0.167 mmol, 1.59 equiv.), Pd(PPh<sub>3</sub>)<sub>4</sub> (9.46 mg, 1155.6 g/mol, 0.0082 mmol, 7.8 mol% Pd), PPh<sub>3</sub> (8.80 mg, 262 g/mol, 0.026 mmol, 0.34 equiv., 7.2:1 P:Pd) and K<sub>2</sub>CO<sub>3</sub> (19.7 mg, 138 g/mol, 0.143 mmol, 1.36 equiv.) were added to a tared 4 dram vial and taken up in 1.5 g of DME. The reaction solution was sealed in the glovebox, removed, and placed in a 75 °C oil bath. After 22 h, the reaction was removed from the oil bath, and allowed to cool to room temperature. Once cooled, the reaction solution was passed through a celite plug and washed with copious amounts of diethyl ether. The solution was then concentrated *in vacuo* and the crude oil was purified by silica gel chromatography (50:1 hexanes:ethyl acetate R<sub>f</sub> = 4/39) to yield 9.03 mg of a clear oil, or a 26% isolated yield. A significant amount of boronic ester homocoupling was again observed (R<sub>f</sub> = 6/39), and slightly overlapped with the desired product during separation. <sup>1</sup>H NMR (400 MHz, CDCl<sub>3</sub>) δ 7.16 (d, *J* = 8.4 Hz, 2 H), 7.03 (d, *J* = 8.0 Hz, 2 H), 6.96 (d, *J* = 8.4 Hz, 2 H), 6.93 (m, 4 H), 6.74 (d, *J* = 8.8 Hz, 2 H), 5.35 (s, 1 H), 3.71 (s, 3 H), 2.54 (q, *J* = 7.6 Hz, 2 H), 1.14 (t, *J* = 7.6 Hz, 3 H). <sup>13</sup>C NMR (400 MHz, CDCl<sub>3</sub>) δ 143.1, 142.4, 140.1, 135.8, 132.0, 130.7, 130.3, 129.2, 128.4, 127.9, 113.9, 55.3, 55.0, 28.4, 15.5. HRMS (EI-TOF): calcd for [M]<sup>+</sup> (C<sub>22</sub>H<sub>21</sub>OCl) *m/z* 336.1281; found 336.1293.

**Synthesis of 1,1,1-(4-chlorophenyl),(4'-ethylphenyl),(4''-methoxyphenyl)methane (3-32): Conditions Optimization.** The cross-coupling was performed under more dilute

conditions at lower temperature in an attempt to disfavor homocoupling of the boronic ester. In a nitrogen-atmosphere glovebox, 4-chloriodobenzene (25.6 mg, 238.4 g/mol, 0.107 mmol, 1.0 equiv.), rac-(1-(4-methoxyphenyl), 1-(4ethylphenyl))methylboronic acid (2,2-dimethyl-1,3-propanediol) ester (**3-30**, 50.20 mg, 338 g/mol, 0.149 mmol, 1.40 equiv.), Ag<sub>2</sub>O (37.1 mg, 234 g/mol, 0.161 mmol, 1.50 equiv.), Pd(PPh<sub>3</sub>)<sub>4</sub> (9.76 mg, 1155.6 g/mol, 0.0084 mmol, 7.9 mol% Pd), PPh<sub>3</sub> (9.94 mg, 262 g/mol, 0.034 mmol, 0.32 equiv., 8.0:1 P:Pd) and K<sub>2</sub>CO<sub>3</sub> (22.24 mg, 138 g/mol, 0.161 mmol, 1.51 equiv.) were added to a tared 4 dram vial and taken up in 2.5 g of DME. The reaction solution was sealed in the glovebox, removed, and placed in a 50 °C oil bath. After 48 h, the reaction was removed from the oil bath, and allowed to cool to room temperature. Once cooled, the reaction solution was passed through a celite plug and washed with copious amounts of diethyl ether. The solution was then concentrated *in vacuo* and the crude oil was purified by silica gel chromatography (50:1 hexanes:ethyl acetate R<sub>f</sub> = 5/38) to yield 13.97 mg of a slightly yellow oil, or a 39% isolated yield.



**Synthesis of Potassium 1-(4-methoxyphenyl), 1-(4'ethylphenyl)methyl trifluoroborate (3-33).** 151.1 mg of rac-(1-(4-methoxyphenyl), 1-

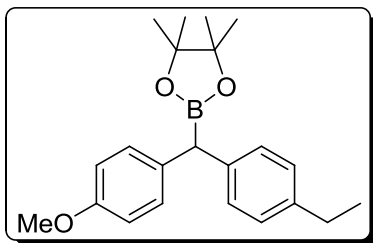
(4ethylphenyl))methylboronic acid (2,2-dimethyl-1,3-propanediol) ester (**3-30**, 338 g/mol, 0.447 mmol, 1.0 equiv.) was dispersed in 2.5 mL of MeOH before addition of 0.45 mL of a saturated solution of KHF<sub>2</sub> (4.5 M, 2.012 mmol, 4.5 equiv.). The solution was

stirred at room temperature for 45 mins, during which time precipitation was observed in the flask. The reaction was concentrated *in vacuo*, before being redissolved in 5 mL of a 1:1 MeOH:H<sub>2</sub>O solution. This dissolution/concentration cycle was repeated 6 times. After the last concentration step, the organics were taken up in acetone to separate them from the excess inorganic salts. After evaporation of the acetone under vacuum, the crude trifluoroborate salt was purified by Kugelrohr distillation; excess 2,2-dimethyl-1,3-pentanediol was removed under high vacuum at 100 °C to leave 121.6 mg of pure trifluoroborate salt, representing a 82% isolated yield. **<sup>1</sup>H NMR** (400 MHz, CD<sub>2</sub>Cl<sub>2</sub>) δ 7.07-7.03 (m, 4 H), 6.97 (d, *J* = 7.6 Hz, 2 H), 6.69 (d, *J* = 8 Hz, 2 H), 3.65 (s, 3 H), 2.98 (d, *J* = 4.0 Hz, 1 H), 2.50 (q, *J* = 7.2 Hz, 2 H), 1.11 (t, *J* = 7.2 Hz, 3 H). **<sup>11</sup>B NMR**: (160 MHz, CD<sub>2</sub>Cl<sub>2</sub>): δ 5.70. **<sup>13</sup>C NMR** (400 MHz, CD<sub>2</sub>Cl<sub>2</sub>) δ 157.6, 144.2, 141.1, 138.6, 130.1, 129.1, 128.1, 114.0, 55.6, 28.7, 16.0.

**Attempted Cross-Coupling of Potassium 1-(4-methoxyphenyl), 1-(4'-ethylphenyl)methyl trifluoroborate (3-33).** In a nitrogen-atmosphere glovebox, 4-iodoacetophenone (19.86 mg, 245.9 g/mol, 0.081 mmol, 1.0 equiv.), potassium 1,1-(4-ethylphenyl-4'-methoxyphenyl) methane trifluoroborate (30.88 mg, 332 g/mol, 0.093 mmol, 1.15 equiv.), Ag<sub>2</sub>O (27.75 mg, 234 g/mol, 0.120 mmol, 1.48 equiv.), Pd(OAc)<sub>2</sub> (3.68 mg, 224.5 g/mol, 0.016 mmol, 20 mol% Pd), XPhos (7.73 mg, 476 g/mol, 0.016 mmol, 0.20 equiv., 2:1 P:Pd) and Cs<sub>2</sub>CO<sub>3</sub> (82.92mg, 325.8 g/mol, 0.25 mmol, 3.1 equiv.) were added to a tared 4 dram vial and taken up in 1.5 g of DME. The reaction solution was sealed in the glovebox, removed, and the Teflon cap was replaced with a rubber

septum. 0.3 mL of degassed H<sub>2</sub>O was added and the vial was placed in an 80 °C oil bath under Ar<sub>(g)</sub> for 24 h. The reaction was then removed from the oil bath, and allowed to cool to room temperature. Once cooled, the reaction solution was passed through a celite plug and washed with copious amounts of diethyl ether. Analysis of the crude reaction solution indicated that no triarylmethane was formed, and the protodeboronated product was the major species in solution. Similar experiments were conducted with RuPhos ligand, with and without Ag<sub>2</sub>O. Again, these experiments yielded reduced product almost exclusively, and the triarylmethane resulting from cross-coupling was not observed.

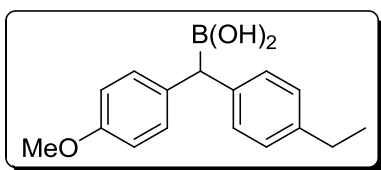
*6.2.10 Transesterification of (2,2-dimethyl-1,3-propanediol) boronic esters to their pinacolate analogues*



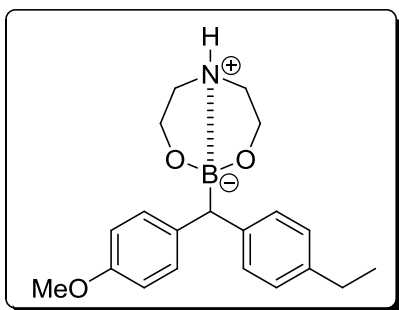
**Attempted conversion from (2,2-dimethyl-1,3-propanediol) boronic ester 3-30 to pinacolate ester with excess pinacol.** 29.4 mg of 1-(4ethylphenyl)methylboronic acid (2,2-dimethyl-1,3-

propanediol) ester (**3-30**, 338 g/mol, 0.087 mmol, 1.0 equiv.) and 102 mg of pinacol (118 g/mol, 0.870 mmol, 10 equiv.) were taken up in 3 mL of hexanes and refluxed (oil bath = 50 °C) for 16 h. GC-MS analysis of the crude reaction mixture indicates that less than 10% of the boronic ester was transesterified to the pinacolate.

**Attempted conversion from (2,2-dimethyl-1,3-propanediol) boronic ester 3-30 to pinacolate ester with a Lewis Acid and excess pinacol.** 21.9 mg of 1-(4ethylphenyl)methylboronic acid (2,2-dimethyl-1,3-propanediol) ester (**3-30**, 338 g/mol, 0.065 mmol, 1.0 equiv.) and 66.9 mg of pinacol (118 g/mol, 0.57 mmol, 8.8 equiv.) were taken up in 3 mL of either hexanes or diethyl ether. To these solutions was added 6.0 equiv. of freshly-prepared  $\text{MgBr}_2$ . The reaction solutions were refluxed (oil bath = 50 °C) for 16 h, though in neither case did significant transesterification occur.



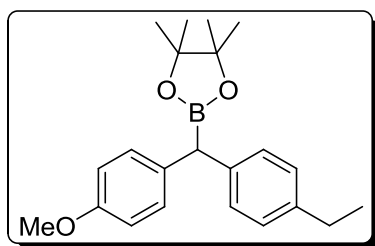
**Attempted conversion hydrolysis of (2,2-dimethyl-1,3-propanediol) ester 3-30 to boronic acid.** 30.3 mg of 1-(4ethylphenyl)methylboronic acid (2,2-dimethyl-1,3-propanediol) ester (**3-30**, 338 g/mol, 0.090 mmol, 1.0 equiv.) was dispersed in 3 N  $\text{HCl}_{(\text{aq})}$  and heated to reflux for 12 h. Once cooled to room temperature and extracted with  $\text{CH}_2\text{Cl}_2$ , analysis by GC-MS indicates that the major product is the over-oxidized benzophenone analogue.



**Conversion of the (2,2-dimethyl-1,3-propanediol) boronic ester 3-30 to analogous zwitterionic salt (3-36).** 750 mg of crude 1-(4ethylphenyl)methylboronic acid (2,2-dimethyl-1,3-propanediol) ester (**3-30**, 338



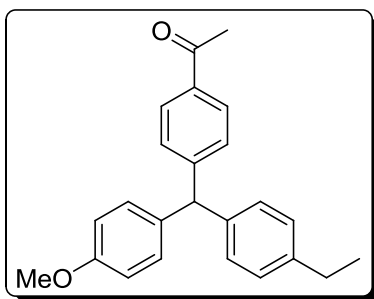
g/mol, 2.21 mmol, 1.0 equiv.) was taken up in 1.5 mL of degassed isopropanol and cooled to 0 °C in an ice bath. In a separate flask, 0.953 g of diethanolamine (105 g/mol, 9.08 mmol) was taken up in 4 mL of degassed isopropanol and added dropwise to the solution of boronic ester. Within 5 min, a custard-yellow precipitate is observed and after 75 mins, a large amount of precipitate was observed. 20 mL of freshly-distilled diethyl ether was added to complete the precipitation, and then the solution was filtered and washed with cold diethyl ether to yield 408.7 mg of a white powder, representing a 68% crude yield. **MPt** = 142-145 °C. **<sup>1</sup>H NMR** (400 MHz, CD<sub>2</sub>Cl<sub>2</sub>) δ 7.33 (d, *J* = 8.4 Hz, 2 H), 7.28 (d, *J* = 8.0 Hz, 2 H), 7.07 (d, *J* = 7.6 Hz, 2 H), 6.80 (d, *J* = 8.8 Hz, 2 H), 3.98 (m, 2 H), 3.86 (m, 2 H), 3.77 (s, 3 H), 3.24 (s, 1 H), 2.92 (m, 2 H), 2.67 (m, 2 H), 2.60 (q, *J* = 7.6 Hz, 2 H), 1.6 (s, br), 1.22 (t, *J* = 7.6 Hz, 3 H). **<sup>11</sup>B NMR**: (160 MHz, CD<sub>2</sub>Cl<sub>2</sub>): δ 12.9. **<sup>13</sup>C NMR** (400 MHz, CD<sub>2</sub>Cl<sub>2</sub>) δ 157.5, 144.6, 140.8, 139.2, 130.3, 129.1, 127.9, 113.8, 63.4, 55.53, 51.9, 28.7, 16.0.



**Synthesis of rac-(1-(4-methoxyphenyl), 1-(4ethylphenyl))methylboronic acid pinacolate ester (3-37): Hydrolysis of Zwitterionic Salt (3-36) and Pinacol Esterification.** 204.25 mg of the dibenzylic zwitterionic

salt (**3-36**, 339 g/mol, 0.603 mmol) were dispersed in 10 mL of diethyl ether. While stirring at room temperature, 6 mL of 1 M HCl<sub>(aq.)</sub> was added, dropwise. After five minutes, 355.5 mg of pinacol (118 g/mol, 3.013 mmol, 5 equiv.) in 3 mL of diethyl ether was added, solubilizing the precipitate and rendering the solution biphasic. GC-MS of

aliquots taken from the reaction indicate that the transesterification is nearly complete after 15 mins, though the reaction was allowed to continue for 3 h. The reaction solution was then extracted with 3x20 mL of diethyl ether and the combined organic portions were dried over MgSO<sub>4</sub>. Filtration and concentration of the crude reaction solution was followed by silica gel chromatography (20:1 hexanes:ethyl acetate, R<sub>f</sub> = 12/39) to yield 198.1 mg of a clear oil which solidified upon cooling to -20 °C, representing an 93% isolated yield. <sup>1</sup>H NMR (400 MHz, CDCl<sub>3</sub>) δ 7.11 (d, *J* = 8.4 Hz, 2 H), 7.07 (d, *J* = 8.0 Hz, 2 H), 7.01 (d, *J* = 8.4 Hz, 2 H), 6.73 (d, *J* = 8.4 Hz, 2 H), 3.69 (s, 3 H), 3.69 (s, 1 H), 2.52 (q, *J* = 7.6 Hz, 2 H), 1.15 (s, 12 H), 1.13 (t, *J* = 7.6 Hz, 3 H). <sup>11</sup>B NMR: (160 MHz, CDCl<sub>3</sub>): δ 32.8. <sup>13</sup>C NMR (400 MHz, CDCl<sub>3</sub>) δ 157.6, 141.2, 139.7, 134.4, 130.1, 128.8, 127.9, 113.8, 83.6, 55.2, 28.4, 24.6, 15.5.

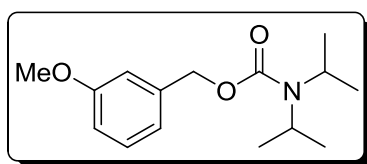


**Synthesis of 1,1,1-(4-acetylphenyl),(4'-ethoxyphenyl),(4''-methoxyphenyl)methane (3-31).** In a nitrogen-atmosphere glovebox, 4-iodoacetophenone (25.51 mg, 245.9 g/mol, 0.103 mmol, 1.0 equiv.), 1,1-(4-ethylphenyl-4'-methoxyphenyl) methane boronic acid

pinacolate ester (**3-37**, 52.79 mg, 352 g/mol, 0.150 mmol, 1.46 equiv.), Ag<sub>2</sub>O (36.67 mg, 234 g/mol, 0.158 mmol, 1.53 equiv.), Pd<sub>2</sub>(dba)<sub>3</sub> (3.48 mg, 915.7 g/mol, 0.0038 mmol, 7.4 mol% Pd), PPh<sub>3</sub> (18.29 mg, 262 g/mol, 0.070 mmol, 0.67 equiv., 9.2:1 P:Pd) and K<sub>2</sub>CO<sub>3</sub> (22.50 mg, 138 g/mol, 0.163 mmol, 1.58 equiv.) were added to a tared 4 dram vial and taken up in 1.9 g of DME. The reaction solution was sealed in the glovebox, removed,

and placed in a 65 °C oil bath. After 24 h, the reaction was removed from the oil bath, and allowed to cool to room temperature. Once cooled, the reaction solution was passed through a celite plug and washed with copious amounts of diethyl ether. The solution was then concentrated *in vacuo* and an NMR internal standard was added (hexamethylbenzene, HMB, 12.29 mg). The NMR yield for the unsymmetrical triarylmethane was determined to be 30%. The crude oil was purified by silica gel chromatography (20:1 hexanes:ethyl acetate for one column volume, followed by 10:1 hexanes:ethyl acetate  $R_f = 7/41$  (10:1)) to yield 6.5 mg of a clear oil, or a 18% isolated yield, indicating that the low yield is likely due to the strongly electron donating *para*-substituent, and not the nature of the boronic ester.

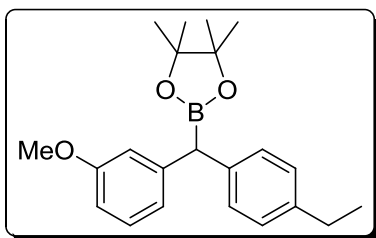
#### 6.2.11 Synthesis of Unsymmetrical Triarylmethanes



**Synthesis of *N,N*-Diisopropyl carbamic acid (3-methoxybenzyl) ester (3-38).** *N,N*-diisopropylcarbonyl chloride (1.857 g, 163.65 g/mol, 11.4 mmol, 1.05 equiv.)

and freshly distilled triethylamine (1.75 mL, 0.726 g/mL, 101.2 g/mol, 12.5 mmol, 1.16 equiv.) were taken up in 20 mL of  $\text{CH}_2\text{Cl}_2$ . (4-methoxy)-benzyl alcohol (1.25 mL, 1.108 g/mL, 138 g/mol, 9.91 mmol, 1 equiv.) was added and the solution was stirred under refluxing conditions (oil bath = 50 °C) for 24 h, with salts eventually precipitating out of solution. The solution was then washed with sat.  $\text{NH}_4\text{Cl}_{(\text{aq.})}$  and the aqueous layer was

extracted with 3 x 25 mL CH<sub>2</sub>Cl<sub>2</sub>. The crude oil was purified by silica gel chromatography (20:1 hexanes:ethyl acetate for one column volume, 10:1 hexanes:ethyl acetate, R<sub>f</sub> = 8/38 (10:1)) to yield 1.794 g of the desired carbamate, or 63% isolated yield. **<sup>1</sup>H NMR** (400 MHz, CDCl<sub>3</sub>) δ 7.18 (t, *J* = 8.0 Hz, 1 H), 6.85 (m, 2 H), 6.75 (dd, *J* = 8.0 Hz, 2.0 Hz, 1 H), 5.03 (s, 2 H), 4.1-3.7 (br, 2 H), 3.72 (s, 3 H), 1.14 (d, *J* = 7.2 Hz, 12 H). **<sup>13</sup>C NMR** (400 MHz, CDCl<sub>3</sub>) δ 159.7, 155.4, 138.8, 129.5, 120.0, 113.3, 113.2, 66.3, 55.2, 45 (br), 21.1 (br). **HRMS (EI-TOF)**: calcd for [M]<sup>+</sup> (C<sub>15</sub>H<sub>23</sub>O<sub>3</sub>N) *m/z* 265.1678; found 265.1686.

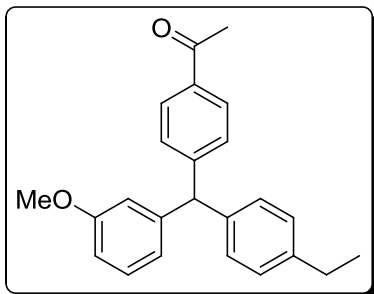


**Synthesis of rac-(1-(3-methoxyphenyl), 1-(4-ethylphenyl))methylboronic acid pinacolate ester (3-39)** *N,N*-Diisopropyl carbamic acid (3-methoxybenzyl) ester (473.8 mg, 265.2 g/mol, 1.788 mmol, 1.0 equiv.)

and TMEDA (250.7 mg, 116 g/mol, 2.146 mmol, 1.2 equiv.) were taken up in 10 mL of hexanes and cooled to -78 °C in a dry ice/acetone bath. *s*-butyllithium (1.7 mL, 1.3 M, 2.21 mmol, 1.23 equiv.) was added dropwise to the cold solution, creating a bright red / orange solution. After 2 h of lithiation, a hexanes solution of 4-ethylphenylboronic acid neopentylate ester (EtC<sub>6</sub>H<sub>4</sub>Bneop, 477.3 mg, 232 g/mol, 2.05 mmol, 1.15 equiv., in 2 mL hexanes) was added dropwise, keeping internal temperature below -70 °C. After 1 h borylation, freshly prepared MgBr<sub>2</sub> diethyl etherate (3.0 equiv.) was added to the cold solution as an ethereal solution. MgBr<sub>2</sub> diethyl etherate is prepared by adding a necessary amount of 1,2-dibromoethane, in this case, 3 equivalents per boronic ester to an excess of

Mg turnings in dry ether. The contents of the dense layer that dissociates from the ether are added to the reaction solution *via* syringe. After addition of the  $\text{MgBr}_2$ , the solution is allowed to warm slowly before being heated to reflux for 16 h (50 °C oil bath). After an aqueous workup ( $\text{NH}_4\text{Cl}_{(\text{sat.})}$ ), the combined organic layers were dried over  $\text{MgSO}_4$ , filtered and concentrated *in vacuo* to yield 758 mg of yellow oil. The crude oil was taken up in 2 mL of degassed isopropanol and cooled to 0 °C with an ice bath. In a separate flask, 0.95 g diethanolamine (105 g/mol, 9 mmol, 5 equiv.) were taken up in 4 mL of degassed isopropanol and added dropwise to the cooled solution of crude boronic ester. Within 5 mins, the solution became a brown foam, and required the addition of 3 mL of supplemental isopropanol. After 45 mins, 10 mL of diethyl ether was added to complete the precipitation of the zwitterionic salt. The dispersion was then filtered and washed with chilled diethyl ether to yield 396 mg of white powder, or 65% crude yield. 240.8 mg of the dibenzylic zwitterionic salt (339 g/mol, 0.710 mmol) were then dispersed in 10 mL of diethyl ether. 21.8 mg Hexamethylbenzene was added as a qualitative internal standard to aid in assessing when reaction had gone to completion by GC-MS, as neither the zwitterionic salt, nor the hydrolyzed boronic acid were expected to be visible; an exclusive product peak in this case would therefore be without meaning. The ethereal dispersion was stirred at room temperature and 6 mL of 1 M  $\text{HCl}_{(\text{aq.})}$  was added, dropwise. After five minutes, 425.4 mg of pinacol (118 g/mol, 3.60 mmol, 5.1 equiv.) in 3 mL of diethyl ether was added, solubilizing the precipitate and rendering the solution biphasic. After 3.5 hours, the reaction solution was then extracted with water and 3x20 mL of diethyl ether. The combined organic portions were dried over  $\text{MgSO}_4$ . Filtration

and concentration of the crude reaction solution yielded 446 mg of crude oil. The crude oil was purified by silica gel chromatography (20:1 hexanes:ethyl acetate,  $R_f = 7/40$ ) to yield 195.0 mg of a clear oil, representing a 78% yield. The clear oil did not solidify after 24 h at  $-30\text{ }^\circ\text{C}$ .  **$^1\text{H NMR}$**  (400 MHz,  $\text{CDCl}_3$ )  $\delta$  7.10 (m, 3 H), 7.01 (d,  $J = 8.0$  Hz, 2 H), 6.76 (m, 2 H), 6.60 (m, 1 H), 3.68 (s, 3 H), 2.52 (q,  $J = 7.6$  Hz, 2 H), 1.16 (s, 12 H), 1.12 (t,  $J = 8.0$  Hz, 3H).  **$^{11}\text{B NMR}$** : (160 MHz,  $\text{CDCl}_3$ ):  $\delta$  32.7.  **$^{13}\text{C NMR}$**  (400 MHz,  $\text{CDCl}_3$ )  $\delta$  159.6, 144.0, 141.4, 139.0, 129.2, 129.0, 127.9, 121.6, 114.8, 110.9, 83.7, 55.1, 28.4, 24.7, 15.5. **HRMS (EI-TOF)**: calcd for  $[\text{M}]^+$  ( $\text{C}_{22}\text{H}_{29}\text{O}_3\text{B}$ )  $m/z$ . 352.2210; found 352.2219.

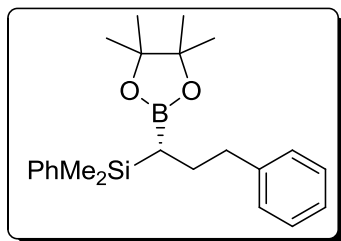


**Synthesis of racemic 1,1-(4-acetylphenyl),(4'-ethylphenyl),(3''-methoxyphenyl)methane (3-41).** In

a nitrogen-atmosphere glovebox, 4-iodoacetophenone (24.37 mg, 245.9 g/mol, 0.996 mmol, 1.0 equiv.), 1,1-(4-ethylphenyl-3'-methoxyphenyl) methane boronic acid pinacolate ester (52.50 mg, 352 g/mol, 0.149 mmol, 1.5 equiv.),  $\text{Ag}_2\text{O}$  (34.69 mg, 234 g/mol, 0.150 mmol, 1.51 equiv.),  $\text{Pd}(\text{PPh}_3)_4$  (9.22 mg, 1155.6 g/mol, 0.0080 mmol, 8.0 mol% Pd),  $\text{PPh}_3$  (8.42 mg, 262 g/mol, 0.070 mmol, 0.32 equiv., 8.75:1 P:Pd) and  $\text{K}_2\text{CO}_3$  (22.53 mg, 138 g/mol, 0.163 mmol, 1.63 equiv.) were added to a tared 4 dram vial and taken up in 1.9 g of DME. The reaction solution was sealed in the glovebox, removed, and placed in an  $80\text{ }^\circ\text{C}$  oil bath. After 25 h, the reaction was removed from the oil bath, and allowed to cool to room temperature. Once cooled, the reaction solution was passed through a celite plug and washed with copious amounts of diethyl ether. The solution was

then concentrated *in vacuo* and an NMR internal standard was added (hexamethylbenzene, HMB, 12.29 mg), indicating an NMR yield of 60%. The crude oil was purified by silica gel chromatography (20:1 hexanes:ethyl acetate) to yield 16.1 mg of a clear oil, or a 47% isolated yield. **<sup>1</sup>H NMR** (400 MHz, CDCl<sub>3</sub>) δ 7.80 (d, *J* = 7.6 Hz, 2 H), 7.16 (m, 3 H), 7.05 (d, *J* = 8.0 Hz, 2 H), 6.94 (d, *J* = 8.0 Hz, 2 H), 6.70 (dd, *J* = 8.0 Hz, *J* = 2.0 Hz, 1 H), 6.59 (d, *J* = 8.0 Hz, 1 H), 6.57 (d, *J* = 2 Hz, 1 H), 5.45 (s, 1 H), 3.66 (s, 3 H), 2.55 (q, *J* = 7.6 Hz, 2 H), 2.50 (s, 3 H), 1.15 (t, *J* = 7.6 Hz, 3 H). **<sup>13</sup>C NMR** (400 MHz, CDCl<sub>3</sub>) δ 197.8, 159.7, 149.7, 144.9, 142.6, 140.0, 135.3, 129.6, 129.4, 129.3, 128.4, 128.0, 121.9, 115.6, 111.5, 28.4, 26.6, 15.5. **HRMS (EI-TOF)**: calcd for [M]<sup>+</sup> (C<sub>24</sub>H<sub>24</sub>O<sub>2</sub>) *m/z* 344.1776; found 334.1788.

### 6.2.12 The Synthesis of Non-Racemic $\alpha$ -Silyl Boronic Esters as Intermediates for Chiral Allyl Silanes



#### Synthesis of (*R*)-Dimethyl(phenyl)(3-phenyl-1-(4,4,5,5-tetramethyl-1,3,2-dioxaborolan-2-yl)propyl)silane (3-44).

*N,N*-Diisopropyl carbamic acid (3-phenylpropyl) ester was synthesized following procedure outlined for carbamate **3-15**. Once isolated, 3-Phenylpropyl diisopropylcarbamate (0.50 mL, 1.89 mmol) and (–)-sparteine (0.45 mL, 1.89 mmol) were dissolved in diethyl ether (8 mL) and cooled to –78 °C. *s*-Butyllithium (1.4 mL, 1.3 M solution in cyclohexane/hexane (92:8), 1.89 mmol) was added dropwise and the mixture was stirred at –78 °C for 5 hours.

Dimethylphenylsilyl boronic acid pinacolate ester (Sigma-Aldrich, 0.35 mL, 1.32 mmol) was added dropwise and the resulting mixture was stirred at  $-78\text{ }^{\circ}\text{C}$  for 1 hour, allowed to warm to  $23\text{ }^{\circ}\text{C}$  and stirred for an additional 18 hours. Water was added, the phases were separated, the aqueous phase was extracted with diethyl ether and the combined organic phases were washed with brine, dried ( $\text{Na}_2\text{SO}_4$ ), filtered and concentrated. Column chromatography (silica gel, 5 % diethyl ether in petroleum ether,  $R_f = 0.2$ ) gave boronic ester **3-42** (344 mg, 69 %) as a colourless oil. The racemate was obtained using TMEDA instead of (–)-sparteine.  $^1\text{H NMR}$  (500 MHz,  $\text{CDCl}_3$ ):  $\delta$  7.49–7.45 (m, 2 H), 7.34–7.28 (m, 3 H), 7.25–7.20 (m, 2 H), 7.16–7.07 (m, 3 H), 2.68 (ddd,  $J = 13.4, 9.8, 4.8$  Hz, 1 H), 2.43 (ddd,  $J = 13.4, 9.8, 6.8$  Hz, 1 H), 1.89 (dddd,  $J = 13.1, 12.0, 9.8, 4.8$  Hz, 1 H), 1.64 (dddd,  $J = 13.1, 9.8, 6.8, 2.8$  Hz, 1 H), 1.23 (s, 6 H), 1.20 (s, 6 H), 0.71 (dd,  $J = 12.0, 2.8$  Hz, 1 H), 0.32 (s, 3H), 0.31 (s, 3 H).  $^{13}\text{C NMR}$  (125 MHz,  $\text{CDCl}_3$ ):  $\delta$  142.6, 138.8, 133.8, 128.8, 128.5, 128.2, 127.6, 125.6, 82.8, 39.4, 28.0, 25.2, 24.7,  $-2.3, -3.4$ .  $^{11}\text{B NMR}$  ( $\text{CDCl}_3$ , 96 MHz):  $\delta$  33.7. **HRMS** (ESI): calc'd for  $\text{C}_{23}\text{H}_{33}\text{BO}_2\text{Si}$  ( $[\text{M}^+\text{Na}]^+$ ):  $m/z = 403.2235$ , found:  $m/z = 403.2224$ .

### 6.3 Material Stability and the Protective Effect of the Suzuki-Miyaura Reaction

#### 6.3.1 Material Synthesis

**MCM-41.** 2.407 g of cetyltrimethylammonium bromide (CTAB) surfactant and 10.5 mL of  $\text{NH}_4\text{OH}_{(\text{aq})}$  were added to 120 mL of deionized  $\text{H}_2\text{O}$  in a 1 L glass jar with a plastic, screw-on lid. To this stirring suspension, was added 10 mL of tetraethylorthosilicate



(TEOS) over the course of 15 mins. The suspension was then allowed to stir at 25 °C for 1 h, after which a layer of white foam was observed. The slurry was filtered under vacuum to yield a substantial amount of white gel, which was broken apart to facilitate drying. The white gel was then placed in a 90 °C oven for 16 h to produce 4.465 g of a clumpy white powder. At this point, the batch was split in two to explore both the extraction and calcination methods of templating surfactant removal. An acidic extraction was carried out on 1.504 g of surfactant-loaded silica, whereby the silica was dispersed in 150 mL of anhydrous ethanol containing 5 mL of 9 M HCl<sub>(aq.)</sub>. After 4.5 h, 0.932 g of solid white powder were collected by vacuum filtration. The white powder was washed with H<sub>2</sub>O, MeOH and diethyl ether, consecutively. Nitrogen porosimetry indicates that a porous material with pore sizes of 25 Å was synthesized. Surfactant extraction of the other batch occurred by calcination for 5 h at 823 K, following a 1 K/min heating ramp from 298 K.

**H<sub>x</sub> MCM-41.** MCM-41 was synthesized in an adapted procedure that included a hydrothermal treatment step, more typical of thicker-walled SBA-15-type materials. In the event, 2.406 g of CTAB surfactant were stirred in 120 mL of deionized H<sub>2</sub>O until the solution turned clear, indicating that micelle formation was complete. 1.0 mL of decane (a pore-swelling agent) was added dropwise, before 10 mL of NH<sub>4</sub>OH<sub>(aq.)</sub> were added slowly. 10 mL of TEOS was then added over the course of the next 15 mins, and the dispersion was allowed to stir at 43 °C for 1 h. The stir bar was then removed and the sealed solution was statically heated to 80 °C for 48 h. The resultant gel was filtered and

washed with copious amounts of deionized H<sub>2</sub>O and dried under vacuum. The pseudo-dry gel was then placed in an 80 °C vacuum oven for 14 h. The white, clumpy powder was then crushed and submitted to surfactant removal *via* calcination (823 K for 5 h). After calcination, 2.537 g of white powder were recovered.

**SBA-15.** 2 g of Pluronic 123 (P123, surfactant, EO<sub>20</sub>PO<sub>70</sub>EO<sub>20</sub>) was weighed into a tared glass jar and dispersed in 15 mL of deionized H<sub>2</sub>O. The dispersion was stirred at 35 °C for 3 h, after which a further 55 mL of deionized H<sub>2</sub>O and 10 mL of conc. HCl<sub>(aq.)</sub> were added and stirred for 22 h. 4.5 mL of TEOS were then added and stirred (at 35 °C) for 20 h. The stir bar was then removed and the gel was hydrothermally treated at 80 °C in the sealed glass jar for 48 h. After filtration and washing with copious amount of deionized H<sub>2</sub>O, 1.00 g of the polymer-containing silica network was dispersed in 120 mL of absolute ethanol containing 5 mL of conc. HCl<sub>(aq.)</sub> and stirred for 6 h. Vacuum filtration led to the recovery of 0.528 g of a white solid which was then washed with copious amounts of water, methanol and diethyl ether. After drying, 0.223 g of SBA-15 were recovered.

**SBA-15-NaCl.** A mesoporous silica with intermediate stability (between MCM-41 and standard SBA-15) was synthesized by way of an NaCl doping procedure.<sup>3</sup> 2.0 g of P123 were weighed into a glass jar. Separately, 2.0 g of NaCl were dissolved in 20 mL of deionized H<sub>2</sub>O, which, along with 10 mL of conc. HCl<sub>(aq.)</sub>, was added to the jar containing the P123 surfactant. The dispersion was stirred at 40 °C for 20 h. 4.5 mL of TEOS was then added and the warmed dispersion was stirred for a further 20 h. The stir

bar was then removed from the white solution and the sealed glass jar was heated to 90 °C for 48 h. The resultant gel was filtered and washed with copious amounts of water, before being dried in a 100 °C vacuum oven for 4 h. High temperature calcination (823 K, 5h, 1 K/min ramp) removed the templating surfactant to yield 1.07 g of NaCl-SBA-15.

**Al-SBA-15.** Initially, Al-SBA-15 was synthesized in the presence of NaCl to provide a valid comparison to the NaCl-SBA-15 material. 4.0 g of P123 surfactant and 30 mL of deionized H<sub>2</sub>O were added to a tared glass jar. After stirring at 25 °C for 1.5 h, the solution turned clear. After 2 h, both 5.00 g of NaCl in 60 mL of deionized H<sub>2</sub>O and 20 mL of conc. HCl<sub>(aq.)</sub> in another 20 mL of H<sub>2</sub>O were added and stirred for 16 h. 8.4 mL of TEOS was then added, and the solution turned opaque within 45 mins. In a separate flask, 0.153 g of NaAlO<sub>2</sub> and 1 mL of conc. HCl<sub>(aq.)</sub> were added to 30 mL of deionized H<sub>2</sub>O and sonicated to break down the large clumps. The aluminum-containing solution was then added to the silicate solution and stirred at room temperature for 24 h. Static hydrothermal treatment was then carried out at 100 °C for 46 h. The pH of the solution was then adjusted to between 5-7 by addition of NH<sub>4</sub>OH<sub>(aq.)</sub> aliquots and then the silicate gel was treated at 100 °C for a further 24 h. The glass jar was then removed from heat and allowed to cool to room temperature before the silica gel was filtered and washed with copious amounts of H<sub>2</sub>O. The white gel was dried in a 90 °C vacuum oven for 6 h prior to high temperature calcination (823 K, 5 h, 1 K/min ramp). 2.25 g of Al-SBA-15 were recovered.

**Al-SBA-15 (Post-Synthetic Aluminum Doping).** Alumina-doped mesoporous silicas were also synthesized by incorporating aluminum into purely siliceous SBA-15. 0.321 g

of NaCl-SBA-15 and 0.016 g of NaAlO<sub>2</sub> (for an Si/Al ratio ~ 14) were dispersed in 40 mL of deionized H<sub>2</sub>O and stirred at room temperature for 18 h. The dispersion was then filtered and dried in air for 4 h prior to high temperature calcination (823 K, 5 h, 1 K/min ramp).

**Al-SBA-15 (Increased Stability).** The following represents an optimized procedure for Al-SBA-15 which showed reproducible stability when subjected to the *pseudo*-reaction conditions. 1.0 g of P123 was stirred in 7.5 mL of deionized H<sub>2</sub>O. After 4 h, 5 mL of conc. HCl<sub>(aq.)</sub> in 30 mL of H<sub>2</sub>O was added and the dispersion was stirred at 35 °C for 12 h. 2.1 mL of TEOS were then added whilst the temperature was increased slightly to 40 °C. The dispersion turns opaque white within 45 mins of TEOS addition. After 4 h, 38 mg of NaAlO<sub>2</sub> was added directly as a solid and the dispersion was then stirred at 40 °C for a further 20 h. The stir bar was then removed and the white gel was hydrothermally treated at 90 °C for 30 h. The pH of the solution was then adjusted to ~5 by an initial addition of 5 mL of NH<sub>4</sub>OH<sub>(aq.)</sub>, followed by shimming with a 7:1 H<sub>2</sub>O:NH<sub>4</sub>OH<sub>(aq.)</sub> solution to obtain the desired pH. The glass jar was resealed and the hydrothermal treatment was continued at 90 °C for another 29 h. After the second hydrothermal treatment, the pH of the solution was found to still be ~5. The gel was filtered and dried for 11h in an 80 °C vacuum oven prior to high-temperature calcination (823 K, 5 h, 1 K/min ramp).

### 6.3.2 *Pseudo Studies on Mesoporous Supports*

**MCM-41.** 79.8 mg of MCM-41 and 539 mg of  $K_2CO_3$  were dispersed in 21 mL of a 20:1 DMF:H<sub>2</sub>O solution. The dispersion was stirred under Ar<sub>(g.)</sub> at 80 °C for 4 h, before being filtered and washed with copious amounts of water. After being dried, the white silica powder was examined for mesoprosity by nitrogen porosimetry.

**SBA-15.** 70.6 mg of extracted SBA-15 and 548 mg of  $K_2CO_3$  were dispersed in 21 mL of a 20:1 DMF:H<sub>2</sub>O solution. The dispersion was stirred under Ar<sub>(g.)</sub> at 80 °C for 8 h, before being filtered and washed with copious amounts of water. After being dried, the white silica powder was examined for mesoprosity by nitrogen porosimetry.

**NaCl-SBA-15.** 76.6 mg of NaCl-SBA-15 and 537 mg of  $K_2CO_3$  were dispersed in 21 mL of a 20:1 DMF:H<sub>2</sub>O solution. The dispersion was stirred under Ar<sub>(g.)</sub> at 80 °C for 8 h, before being filtered and washed with copious amounts of water. After being dried, the white silica powder was examined for mesoprosity by nitrogen porosimetry.

**Al-SBA-15 (4 h).** 76.3 mg Al-SBA-15 (pH adjusted) and 485 mg of  $K_2CO_3$  were dispersed in 21 mL of a 20:1 DMF:H<sub>2</sub>O solution. The dispersion was stirred under Ar<sub>(g.)</sub> at 80 °C for 8 h, before being filtered and washed with copious amounts of water. After being dried, the white silica powder was examined for mesoprosity by nitrogen porosimetry.

**Al-SBA-15 (8 h).** 82.2 mg of Al-SBA-15 (pH adjusted) and 524 mg of  $K_2CO_3$  were dispersed in 21 mL of a 20:1 DMF:H<sub>2</sub>O solution. The dispersion was stirred under Ar<sub>(g.)</sub>

at 80 °C for 8 h, before being filtered and washed with copious amounts of water. After being dried, the white silica powder was examined for mesoprosity by nitrogen porosimetry.

### *6.3.3 Effect of base on Mesoporous Silica Stability*

**NaCl-SBA-15 (Full Pseudo Conditions).** 70.0 mg of NaCl-SBA-15 and 523 mg of  $K_2CO_3$  were dispersed in 21 mL of a 20:1 DMF:H<sub>2</sub>O solution. The dispersion was stirred under Ar<sub>(g.)</sub> at 80 °C for 8 h, before being filtered and washed with copious amounts of water. After being dried, the white silica powder was examined for mesoprosity by nitrogen porosimetry.

**NaCl-SBA-15 (Full Pseudo Conditions).** 70.0 mg of NaCl-SBA-15 and 523 mg of  $K_2CO_3$  were dispersed in 21 mL of a 20:1 DMF:H<sub>2</sub>O solution. The dispersion was stirred under Ar<sub>(g.)</sub> at 80 °C for 8 h, before being filtered and washed with copious amounts of water. After being dried, the white silica powder was examined for mesoprosity by nitrogen porosimetry.

**NaCl-SBA-15 (Pseudo Conditions, No Base).** 47 mg of NaCl-SBA-15 were dispersed in 16 mL of a 20:1 DMF:H<sub>2</sub>O solution. The dispersion was stirred under Ar<sub>(g.)</sub> at 80 °C for 8 h, before being filtered and washed with copious amounts of water. After being dried, the white silica powder was examined for mesoprosity by nitrogen porosimetry.

**NaCl-SBA-15 (Pseudo Conditions, No Water).** 71 mg of NaCl-SBA-15 and 526 mg of  $K_2CO_3$  were dispersed in 20 mL of DMF. The dispersion was stirred under  $Ar_{(g)}$  at 80 °C for 8 h, before being filtered and washed with copious amounts of water. After being dried, the white silica powder was examined for mesoprosity by nitrogen porosimetry.

#### *6.3.4 Protective Effect of the Suzuki-Miyaura Reaction on Material Stability*

**Stability Test in High-Converting Reaction Filtrate.** 80 mg of NaCl-SBA-15 and 544 mg of  $K_2CO_3$  were dispersed in 20 mL of the filtrate from a heterogeneously catalyzed Suzuki-Miyaura reaction that attained > 90% conversion. The dispersion was stirred under  $Ar_{(g)}$  at 80 °C for 8 h, before being filtered and washed with copious amounts of water. After being dried, the white silica powder was examined for mesoprosity by nitrogen porosimetry.

**Effect of Side-Products (KBr).** 80 mg of NaCl-SBA-15, 548 mg of  $K_2CO_3$  and 473 mg of IR grade KBr were dispersed in 21 mL of a 20:1 DMF:H<sub>2</sub>O solution. The dispersion was stirred at 80 °C for 8 h, before being filtered and washed with copious amounts of water. After being dried, the white silica powder was examined for mesoporosity by nitrogen porosimetry.

**Effect of Side-Products (B(OH)<sub>3</sub>).** 80 mg of NaCl-SBA-15, 550 mg of  $K_2CO_3$  and 246 mg of B(OH)<sub>3</sub> (representing approximately an equimolar amount of boric acid to

potassium carbonate, being a representative situation at reaction completion) were dispersed in 21 mL of a 20:1 DMF:H<sub>2</sub>O solution. The dispersion was stirred at 80 °C for 8 h, before being filtered and washed with copious amounts of water. After being dried, the white silica powder was examined for mesoporosity by nitrogen porosimetry.

**Effect of B(OH)<sub>3</sub> Concentration on Material Stability.** The effect of having 0 equivalents (a standard *pseudo* reaction) and 2 equivalents (*vide supra*) of B(OH)<sub>3</sub> relative to a typical amount of PhBpin used in a reaction are known. Intermediate concentrations of B(OH)<sub>3</sub> (0.5 and 1 equivalent) are tested for their stabilizing effect on a mesoporous silica material, representing the early stages of the reaction. As an example, 69.2 mg of NaCl-SBA-15, 546 mg of K<sub>2</sub>CO<sub>3</sub> and 63.2 mg of B(OH)<sub>3</sub> (0.5 equivalents) were dispersed in 21 mL of a 20:1 DMF:H<sub>2</sub>O solution. The dispersion was stirred at 80 °C for 8 h, before being filtered and washed with copious amounts of water. After being dried, the white silica powder was examined for mesoporosity by nitrogen porosimetry.

#### 6.3.5 Effect of B(OH)<sub>3</sub> on the pH of the Reaction Solution

**Evolving pH of the Pseudo Reaction.** 60.8 mg of NaCl-SBA-15 and 410 mg of K<sub>2</sub>CO<sub>3</sub> were dispersed in 16 mL of a 20:1 DMF:H<sub>2</sub>O solution. The dispersion was stirred under Ar<sub>(g.)</sub> at 80 °C. A 0.5 mL aliquot was taken from the dispersion after 10 min of heating, and diluted in 4.5 mL of deionized H<sub>2</sub>O. pH was determined by calibrated pH probe (10.2) followed by back calculation (9.2) to account for the dilution step. The process was repeated for aliquots taken at 0.5, 2, 3 and 4 h. After 4 h, the dispersion was filtered



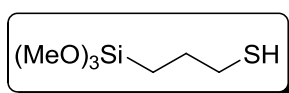
and washed with copious amounts of water. After being dried, the white silica powder was examined for mesoporosity by nitrogen porosimetry.

**Evolving pH of the Pseudo Reaction with B(OH)<sub>3</sub>.** 80.1 mg of NaCl-SBA-15, 545 mg of K<sub>2</sub>CO<sub>3</sub> and 247.2 mg B(OH)<sub>3</sub> were dispersed in 21 mL of a 20:1 DMF:H<sub>2</sub>O solution. The dispersion was stirred under Ar<sub>(g.)</sub> at 80 °C. A 0.5 mL aliquot was taken from the dispersion after 0.5 h of heating, and diluted in 4.5 mL of deionized H<sub>2</sub>O. pH was determined by calibrated pH probe (8.5) followed by back calculation (7.5) to account for the dilution step. The process was repeated for aliquots taken at 1, 2, 3 and 4 h. After 4 h, the dispersion was filtered and washed with copious amounts of water. After being dried, the white silica powder was examined for mesoporosity by nitrogen porosimetry.

**Second Pseudo Study on Material Preserved by B(OH)<sub>3</sub>: A Potential Carry-Over Effect.** NaCl-SBA-15 maintained its porosity over the course of a 4 h *pseudo* reaction in the presence of B(OH)<sub>3</sub>. In an effort to distinguish between the pH lowering effect of boric acid, and a possible incorporation into the silica structure, the NaCl-SBA-15 sample was resubjected to the *pseudo* reaction conditions, this time in the absence of the protective boric acid. In the event, 56.4 mg of the intact NaCl-SBA-15 and 384.7 mg of K<sub>2</sub>CO<sub>3</sub> were dispersed in 16 mL of a 20:1 DMF:H<sub>2</sub>O solution. The dispersion was stirred under Ar<sub>(g.)</sub> at 80 °C. A 0.5 mL aliquot was taken from the dispersion after 0.5 h of heating, and diluted in 4.5 mL of deionized H<sub>2</sub>O. pH was determined by calibrated pH probe (8.0) followed by back calculation (7.0) to account for the dilution step. The process was repeated for aliquots taken at 1, 2, 3 and 4 h. After 4 h, the dispersion was

filtered and washed with copious amounts of water. After being dried, the white silica powder was examined for mesoporosity by nitrogen porosimetry.

### 6.3.6 Thiol-functionalization of Mesoporous Silica and Pd Loading



**Standard Mercaptopropyltrimethoxysilane (MPTMS)**

**Grafting.** 135.5 mg of SBA-15 were dispersed in 20 mL of toluene. 0.5 mL of mercaptopropyltrimethoxysilane (MPTMS) was added and the suspension was heated to 110 °C for 24 h. Once cooled, the solvent was evaporated *in vacuo* to yield an oil-like substance which was redispersed in toluene and filtered by vacuum filtration. Under vacuum, the white powder was washed with copious amounts of methanol, acetone and diethyl ether, to ensure that all non-grafted thiol was removed from the surface of the material. Once dried, a sample of the white powder was sent for external Elemental Analysis; a composition of 3.44% S was reported.

**Higher Thiol-Loadings from Rehydrated Silanol Surface.** Water was added to the grafting solvent with the aim of hydrolyzing surface siloxanes to create more silanols to condense MPTMS to the pore (and exterior) surface. In the event, 499 mg of MCM-41 and 0.8 mL of H<sub>2</sub>O were dispersed in 30 mL of toluene. Rather than dispersing freely as usual, the white silica powder clumped and precipitated to the bottom of the flask. The would-be dispersion was stirred at 90 °C for 1 h prior to addition of 2.3 mL of MPTMS. In an attempt to fully disperse the mesoporous silica, the walls of the flask were washed

with excess toluene, and the flask was sonicated briefly before heating to 114 °C with a condenser. Once the reaction reached the desired temperature, it turned translucent, indicating that the dispersion had finally formed. After 18 h, the flask was removed from the oil bath and the reaction was allowed to cool. Once cooled, the suspension was filtered and washed with toluene, methanol, acetone and finally diethyl ether. To ensure that none of the large excess of MPTMS remained (ungrafted) on the surface of the silica, the white powder was washed by continuous Soxhlet extraction with absolute ethanol for 24 h. A sample of the functionalized mesoporous silica was sent for external Elemental Analysis; a composition of 4.99% S was reported.

**Loading Pd onto Thiol-Functionalized Mesoporous Silica.** From the thiol composition obtained by Elemental Analysis, a suitable amount of Pd can be added to ensure the optimal S: Pd ratio of 2:1. In the event, 76 mg of thiol-functionalized SBA-15-SH (1.78% S) were dispersed in 30 mL of THF. 4.69 mg of Pd(OAc)<sub>2</sub> were then added to the dispersion, which was then stirred at room temperature for 1 h. Addition of Pd(OAc)<sub>2</sub> imparted a rusty brown colour on the reaction. The silica was then filtered and washed with THF to reveal a newly orange-red silica material. The remarkably clear filtrate indicates that all the Pd added was captured by the thiol-functionalized silica.

### *6.3.7 Catalysis with Pd-Loaded Thiol-Functionalized Mesoporous Silica*

**MCM-41-SH Pd.** In a 100 mL RBF, 0.422 g of 4-bromoacetophenone (198.9 g/mol, 2.12 mmol), 0.144 g *p*-dimethoxybenzene (138 g/mol, 1.04 mmol), 0.577 g K<sub>2</sub>CO<sub>3</sub> (138 g/mol, 4.18 mmol), 0.720 g phenylboronic acid pinacolate ester (PhBpin, 204 g/mol, 3.53 mmol) and 59.9 mg of MCM-41-SH Pd (2:1 S:Pd, 1 mol% Pd with respect to Aryl Bromide) were taken up in 22 mL of degassed 20:1 DMF:H<sub>2</sub>O. While under Ar<sub>(g.)</sub>, the reaction was heated to 80 °C. Aliquots were taken at regular intervals over the course of 4 h to determine the reaction profile by GC analysis and calibration curve. At 2 h, the reaction had reached completion and was removed from the heat. The mesoporous silica supported catalyst was isolated by simple vacuum filtration, and, after washing with copious amounts of ethyl acetate and water, 46.6 mg of the material were recovered. Recycling studies were performed by scaling the subsequent reactions to the amount of catalyst recovered. In the case of MCM-41-SH Pd, catalysis ceased during the third replicate, concomitant with loss of mesoporosity.

**Al-SBA-15-SH Pd.** In a 100 mL RBF, 1.41 g of 4-bromoacetophenone (198.9 g/mol, 7.08 mmol), 0.490 g *p*-dimethoxybenzene (138 g/mol, 3.55 mmol), 1.95 g K<sub>2</sub>CO<sub>3</sub> (138 g/mol, 14.1 mmol), 2.327 g phenylboronic acid pinacolate ester (PhBpin, 204 g/mol, 11.4 mmol) and 79.3 mg of Al-SBA-15-SH Pd (2:1 S:Pd, 1 mol% Pd with respect to Aryl Bromide) were taken up in 70 mL of degassed 20:1 DMF:H<sub>2</sub>O. While under Ar<sub>(g.)</sub>, the reaction was heated to 80 °C. Aliquots were taken at regular intervals over the course of 4 h to determine the reaction profile by GC analysis and calibration curve. At 4 h, the reaction had reached 87% conversion to product and was removed from the heat. The

mesoporous silica supported catalyst was isolated by simple vacuum filtration, and, after washing with copious amounts of ethyl acetate and water, 78 mg of the material were recovered. The Al-SBA-15-SH Pd catalyst retained its mesoporosity (and catalytic activity) for 3 subsequent uses, totaling 20 h of reaction time.

#### 6.4 References

- (1) Armarego, W. L. F.; Perrin, D. D. *Purification of Laboratory Chemicals*; Butterworth Heinemann: 1996; pp 529.
- (2) Dutheuil, G.; Selander, N.; Szabo, K. J.; Aggarwal, V. K. Direct Synthesis of Functionalized Allylic Boronic Esters from Allylic Alcohols and Inexpensive Reagents and Catalysts. *Synthesis* **2008**, 2297.
- (3) Li, C.; Wang, Y.; Guo, Y.; Liu, X.; Guo, Y.; Zhang, Z.; Wang, Y.; Lu, G. Synthesis of Highly Ordered, Extremely Hydrothermal stable SBA-15/Al-SBA-15 under the Assistance of Sodium Chloride. *Chem. Mater.* **2007**, 19, 173-178.

## Chapter 7

### Conclusions and Perspectives

The results presented in the previous chapters have addressed two pertinent issues in the field of Pd catalysis, namely the cross-coupling of previously inert secondary boronic esters and the factors that affect the lifetime of mesoporous silicas used as supports for functionally heterogeneous Pd. In the case of the former, the use of a stoichiometric amount of Ag<sub>2</sub>O and a high loading of PPh<sub>3</sub>, coupled with a catalytic amount of Pd, were sufficient to affect the cross-coupling of benzylic and allylic secondary boronic esters. The benzylic boronic esters, easily synthesized by way of the asymmetric hydroboration reaction, were found to cross-couple with high levels of stereoretention. Though preliminary evidence obtained for the cross-coupling of non-racemic secondary *allylic* boronic esters suggests strongly that they too proceed without significant loss of stereochemical information, systems with defined olefin geometry are needed to truly understand the stereochemical outcome of this reaction.

A strong understanding of the chemoselective nature of the silver-mediated cross-coupling protocol has also been grasped. The complementary reactivities of primary and secondary boronic esters is currently being used to develop a step-wise cross-coupling paradigm whereby 1,1,2-triarylethanes can be synthesized with easily varied aryl groups. The asymmetric diboration of styrene derivatives is also being used to pursue non-racemic targets of this kind. Interestingly, terminal alkenes were shown to be left untouched during both inter- and intramolecular competition studies between potential

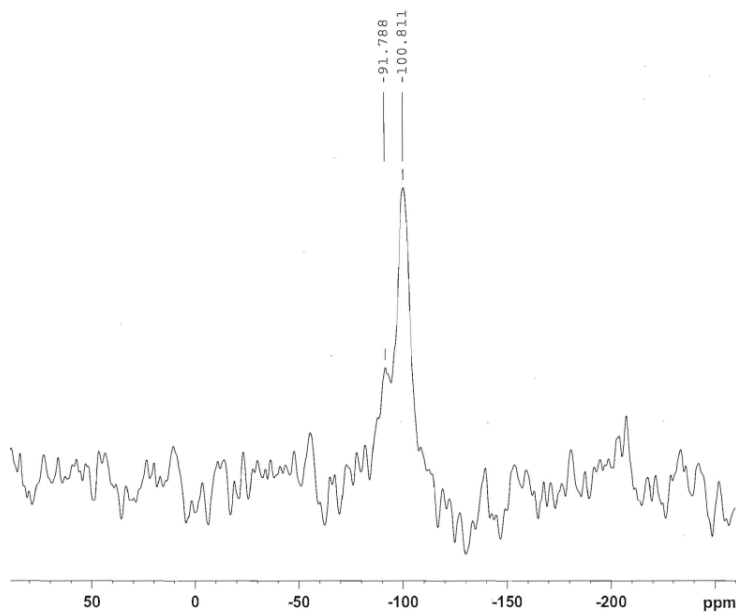
Mizoroki-Heck reactions and the cross-coupling of benzylic boronic esters. Subsequent studies will focus on elaborating the alkene after successful arylation at the benzylic site.

Non-racemic triarylmethanes were also synthesized to display the power of this newly developed cross-coupling protocol. Despite providing access to this interesting molecular motif, the cross-coupling of enantioenriched dibenzlic boronic esters proceeds with lower stereoretentions than their benzylic boronic ester counterparts. Though decent enantioexcesses are observed in the triarylmethane product, the source of the small amount of stereochemical scrambling must be determined and addressed.

Lastly, the effect of the Suzuki-Miyaura reaction conditions on mesoporous silica was examined in detail. The boric acid produced during a Suzuki-Miyaura cross-coupling reaction helps to mitigate the deleterious effect of aqueous base on the ordered silica framework. Alumina-doped materials were synthesized to improve heterogeneous catalyst recyclability and, ultimately, materials were prepared that remained mesoporous (and therefore catalytically active) over the course of multiple uses.

## Appendix

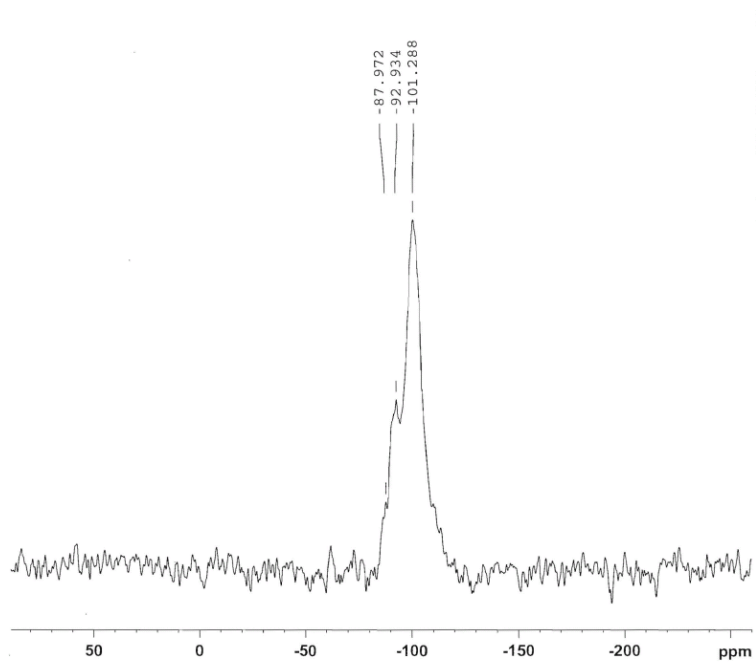
### SBA-15 NaCl Solid State NMR



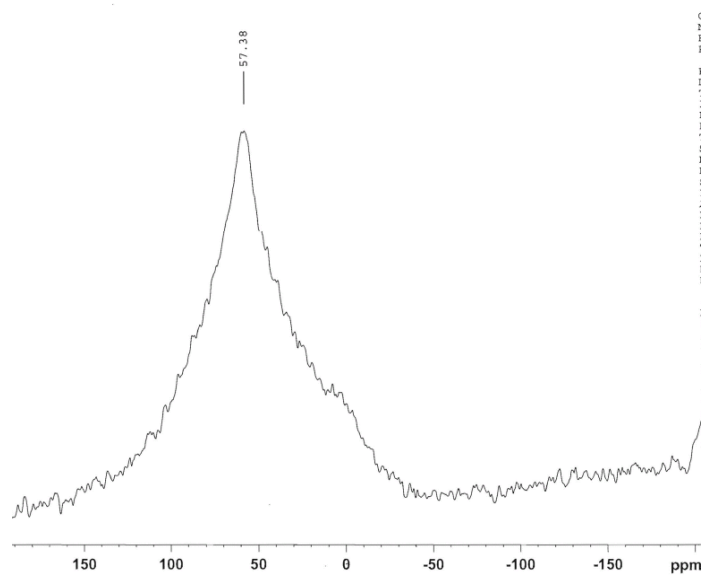
$^{29}\text{Si}$  CP-MAS NMR of SBA-15-NaCl after 8 h exposure to pseudo conditions in the presence of 2 eq. of  $\text{B}(\text{OH})_3$ . Rotation = 11050 Hz, D1 = 2 s.

### Al-SBA-15 Solid State NMR

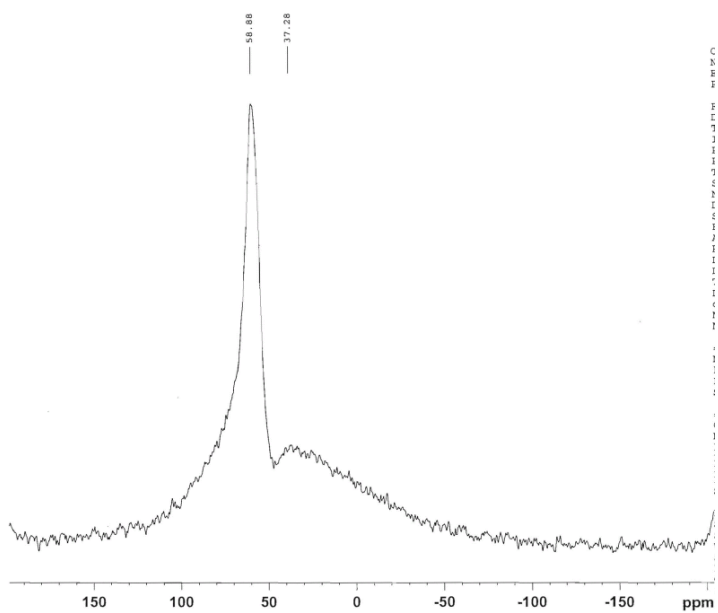




$^{29}\text{Si}$  CP-MAS NMR of Al-SBA-15. Rotation = 11050 Hz, D1 = 5 s.



$^{27}\text{Al}$  MAS NMR of Al-SBA-15. Rotation = 11050 Hz, D1 = 1s.



$^{27}\text{Al}$  MAS NMR of Al-SBA-15 after 4 h of exposure to *pseudo* conditions. Rotation = 11050 Hz, D1 = 1s.